DOTTORATO DI RICERCA IN

Scienze biomediche

XXXVI CICLO

Design of a new methodology applicable on non-implantable devices capable of detecting basal parameters with high accuracy, evaluated with Sigma score.

Candidata:

Ing. Terenzia Natale

Matricola n. 50044251

Relatore:

Prof. Andrea Fausto Piana

Tutor:

Ing. Leonardo Fiore

Questo lavoro è dedicato a Gianluca Ara.

Grazie per averci insegnato quanto
possa essere importante sorridere.

Summary

Introduction

The healthcare scenario has changed significantly in recent times due to a greater autonomy in the use of IT systems by people in general and by patients in managing their health.

The latest challenges that the health system has faced, due to the spread of Covid-19, have highlighted the need to re-evaluate the importance of telemedicine.

OMS has defined telemedicine "The supply of care and assistance, in situations where distance is a critical factor, through information and communication technologies, for exchanging useful information for diagnosis, treatment, prevention, research, evaluation and continuous training of healthcare personnel".

"The future of telemedicine for the management of heart failure patients: a Consensus Document of the Italian Association of Hospital Cardiologists (A.N.M.C.O), the Italian Society of Cardiology (S.I.C.) and the Italian Society for Telemedicine and eHealth (Digital S.I.T.), Eur Heart Journal Suppl. 2017 May"- Andrea Di Lenarda, Giancarlo Casolo, Michele Massimo Gulizia, Nadia Aspromonte, Simonetta Scalvini, Andrea Mortara, Gianfranco Alunni, Renato Pietro Ricci, Roberto Mantovan, Giancarmine Russo, Gian Franco Gensini, and Francesco Romeo[1].

This study demonstrates that cardiopathic patients found a lot of benefits in the remote monitoring of vital parameters such as blood pressure, heart rhythm and blood oxygenation less access to hospitals as well as more precise observance of the therapies.

The introduction of telemedicine in health management could help in developing of Hub and Spoke centers health reorganization.

In this scenario many devices were developed with different aims and functions.

Many companies investigated these kinds of technologies for commercial purposes and their solutions are customized for monitoring personal performance in the sport medicine field. However, these technologies, user-friendly and commercially appealing, are not comparable in terms of accuracy to the ones used in the ambulatory monitoring.

A significant starting point in exploring new solutions with a major medical accuracy, that can help at the same time physicians and patients, is to have a clear state of the art of the most important available wearable

1 A. Di Lenarda *et al.*, "The future of telemedicine for the management of heart failure patients: A Consensus Document of the Italian Association of Hospital Cardiologists (A.N.M.C.O), the Italian Society of Cardiology (S.I.C.) and the Italian Society for Telemedicine and eHealth (Digital S.I.T.)," *Eur. Hear. Journal, Suppl.*, vol. 19, pp. D113–D129, 2017, doi: 10.1093/eurheartj/sux024.

technologies. This analysis will involve smartwatch devices, able to detect the most important patient's basal parameters such as ECG, BP, SPO_2 and IG.

ECG: State of the art

The wearable ECG recording systems have different goals, considering the patient or the physician's point of view. Patients want to monitor their health parameters, beginning aware of their medical conditions, physicians need to have a more specific device with a maximum level of accuracy, able to detect the most common indicators of a pathological condition. So, the different point of view is reflected on the different level of accuracy that these two types of users need. Patients could be satisfied with a more accurate system; physicians cannot accept a not accurate device!

Nowadays, an extensive diversity of ECG monitoring systems with challenging technologies such as IoT and edge computing are used in different environment and conditions and their classification and comparison can be approach from different points of view.

The first classification can be approached looking at the way the devices interact with the body: portable, handheld and patch.

This group of devices can be further divided in single lead and multiple lead monitoring system.

A single lead device **EKO DUO** is an ECG monitor that combines heart sounds and ECG, providing a fast and complete diagnosis. A peculiarity of this device is to be easy portable thanks to its dimensions and to capture ECG and systolic time intervals. This aspect is fundamental for AF and heart failure detection. This device can be used both in clinical and home environment and represents a valid solution to monitor the vital parameters without more invasive methods.

Another portable single-lead device is **Nuubo** suited both for mid and long-term ECG monitoring. The system is placed on the patient's chest and the simplicity of its texture is a key aspect that improves portability and wearability. In fact, the property of the elastic tissue guarantees adaptability to the patients' movements, following them in the daily physical activities without cables and the necessity of clinicians to supervise.

Moreover, **Omron Heartscan** is a light, single-lead, wireless, user-friendly ECG monitoring system with electrodes positioned on the finger and on the chest of the patient. This device has a high-resolution screen for the visualization of the signals, but the battery must be recharged frequently. One of the applications of this device is the atrial fibrillation detection (AF). The study of **Marazzi et al**.[2] showed 100% sensitivity,

[2] G. Marazzi, F. Iellamo, M. Volterrani, and M. Lombardo, "Erratum to: Comparison of Microlife BP A200 Plus and Omron M6 Blood Pressure Monitors to Detect Atrial Fibrillation in Hypertensive

92% specificity, and 95% accuracy in detection of atrial fibrillation. Different results were the ones found by **Kearley et al.**[3] (a sensitivity of 98.7% and specificity of 76.2%) and by Gerrit **Kaleschke et al.**[4] (sensitivity of 99% and specificity of 96%). Finally, **De Asmundis et al.**[5] compared the output of this system with the traditional Holter monitor and they discovered a relevant higher symptom detection with the Omron HeartScan. A minus of this system is the absence of a built-in rechargeable battery and that it is a stand-alone gadget.

Considering instead the multi lead portable devices **Qardio Core** is an ECG, FDA approved, monitoring device positioned on the chest of the subject. This system has an interesting clinical application in the field of the arrhythmia detection. This is a multiparameter device so it can simultaneously monitor body temperature, respiratory rate, stress levels and activity. It has also the ability to interact with the smartphone and to send data to a remote server.

Another multiple lead portable device is **Spyder ECG**, that consists in a small and wireless ECG sensor placed on the patient's chest. Designed by Singaporean medical companies, it can send the ECG signal to the smartphone where it is showed on the display. Furthermore, all the data are delivered to a specific cloud server. A remarkable clinical application is the one demonstrated by **Lukito et al.**[6] that have used this sensor to validate the best techniques for the detection of silent atrial fibrillation.

To the category of the handhelde device belongs **MyDiagnostick**, a simple and efficient ECG monitoring system, shaped like a stick and with electrode on both ends. To record single-lead electrocardiogram (iECG) the device is hold by the handles with both hands for 1 min.

Another handhelde device is **Alivecor Kardia**, an FDA certified monitor system that can be used in free-living condition thanks to his shape and the absence of cables. This toll gives the possibility to check the recorded cardiac measurement during the day and it found a clinical application also in the detection of atrial fibrillation which takes just 30 s (sensitivity of 98% and specificity of 97% according to the study of **Lau et al.**[6] and sensitivity of 98.5% and specificity of 91.4% as demonstrated by **Lowers et al.**[6]). The

Patients(Advances in Therapy, (2012) 29(1):64–70, 10.1007/s12325-011-0087-0)," *Adv. Ther.*, vol. 31, no. 12, p. 1317, 2014, doi: 10.1007/s12325-014-0172-2.

3 K. Kearley *et al.*, "Triage tests for identifying atrial fibrillation in primary care: A diagnostic accuracy study comparing single-lead ECG and modified BP monitors," *BMJ Open*, vol. 4, no. 5, 2014, doi: 10.1136/bmjopen-2013-004565.

4 G. Kaleschke *et al.*, "Prospective, multicentre validation of a simple, patient-operated electrocardiographic system for the detection of arrhythmias and electrocardiographic changes," *Europace*, vol. 11, no. 10, pp. 1362–1368, 2009, doi: 10.1093/europace/eup262.

5 C. De Asmundis *et al.*, "Comparison of the patient-activated event recording system vs. traditional 24 h Holter electrocardiography in individuals with paroxysmal palpitations or dizziness," *Europace*, vol. 16, no. 8, pp. 1231–1235, 2014, doi: 10.1093/europace/eut411.

6 R. Jaafar and A. S. Abdul Salam, "Portable electrocardiography with cloud based features: A review of current technologies," *2019 Int. Biomed. Instrum. Technol. Conf. IBITeC 2019*, pp. 118–122, 2019, doi: 10.1109/IBITeC46597.2019.9091683.

possibility of receiving an email with the updates about the heart condition is a key feature for the tacking the track of the ECG modulation. A limitation of this system is the necessity to use an Android /Iphone.

A further device in this category is **Zenicor ECG**, an efficient finger sensor that communicate with a smartphone and that has the capacity to store a large amount of recorded data. The most relevant applications of this system are the AF detection (**Doliwa et al.** [6] found a sensitivity of 96% and specificity of 92%) and supraventricular tachycardia and in general abnormal ECG (**Usadel et al**.[6] demonstrated a 92% sensitivity in diagnosing supraventricular tachycardia and 77% sensitivity and 92% specificity for abnormal ECG detection). A weakness of this device is that it cannot display the data on the monitor.

Moreover, there is **Reka Health,** a light handheld device that can record the signal when the subject put the thumb on the electrode. The device is connected to a cloud-service to store the recorded ECG signals even if it has the limit to not display them. This system is user-friendly, and it has a good wearability.

Another device is **CALM-M Actigraph** that combines a single lead ECG and 3-axis accelerometer. This device has different applications like activity analysis, movement tracking, posture monitoring, sleep analysis and sleep disorder screening. This tool is very comfortable to wear thanks to its dimensions and its shape and it is very easy to use thanks to its interactive monitor.

Another system is **AfibAlert**, a small FDA approved, two-finger recording device. Its peculiarities are the possibility of instantaneously analyse the recorded data and to be user-friendly. The main disadvantage is instead the absence of a display to visualize the ECG data. The most important clinical application of this home monitoring system is the AF detection (94.6% of accuracy).

To this category belong also **InstantCheck** and **ReadMyHeart** two FDA approved 1-lead handled ECG recorders that can simply be used positioning the thumbs on the electrodes. The first device has the advantage of a user-friendly display and the possibility of storing data but the disadvantages of not having a built-in rechargeable battery and a short auto turn-off time. The second one has comparable characteristics, but it has not a display to visualize the data.

Other two handheld device are two FDA approved monitoring system: **HeartCheck pen** and **ECG Check**. The remarkable characteristics of these device are the compact size that make these systems portable everywhere, the display and the ergonomic configuration that makes them intuitive to use and the speed of the results' generation. However, they do not have a built-in rechargeable battery and the ECG Check needs to be used necessarily with a phone.

Finally, the category of patches involves for example **VitalPatch,** that can be used in different environment from the hospital to the home setting and so it helps reducing costs and improving the quality of the patient

treatment. One of the clinical applications is the QRS detection with a result of 99% positive predictive value on real ECG databases (**Selvaraj et al.** [6]**)**

Another device of this group is **Zio patch**, an ambulatory ECG monitoring adhesive patch positioned on the chest of the patient. This 3-lead system is waterproof, wireless and it is worn by the subject for 14 days without the need of battery change or to be recharged. Many different studies showed the clinical relevance of this device in comparison to the traditional Holter. For example, **Rosenberg et al.** [6] demonstrated that during 24-hour the signals of the atrial fibrillation detection on this device and a 24-hour Holter was comparable ($P < .0001$). A key role of this device is played especially after 48 hours of monitoring when, according to the study of **Tung et al.**[6], 15% of first paroxysmal atrial fibrillation occur. In fact, the conventional Holter monitor cannot detect this arrhythmia because it has a shorter period of observation. Finally, with a study of 146 patients, **Barrett et al.** [6] compared the Zio patch and the Holter monitoring in the detection of six different types of arrhythmia: supraventricular tachycardia, atrial fibrillation/flutter, atrioventricular block, ventricular tachycardia, or polymorphic ventricular tachycardia/ventricular fibrillation. The **McNemar's** tests demonstrated that the Zio patch detected more arrhythmia than the Holter (96 versus 61 respectively), so this device is a valid alternative for ambulatory monitoring.

To this category belongs also **J. IRyhthm**, a waterproof ECG monitor, with a good wearability (it can be worn up to 14 days even during activities like showering and exercising) and usability. These peculiarities and the algorithm of the device allow a high accuracy. The raw data acquired by the sensors are processed by a central monitoring station where they are analysed. A specific report is provided to the clinicians.

Furthermore, there is **Zephyr Bioharness BH3**, a reliable ECG monitoring system specific designed for monitoring adults in the home setting. The electronics module that (used as a patch) can be attached to a strap or a shirt with integrated textile electrodes. The ECG signal are transmitted and received by Bluetooth and then stored. This is a multiple parameter device that can also measure respiration rate, body orientation and activity.

Another system is **Biostamp,** a wearable and waterproof sensor that can be worn in different part of the body. The main characteristic of this device is to be flexible enough to conform to the shape of the body. It also communicates with a cloud server where the processed signals are sent.

To this category belongs also the family of **CardioLeaf** that comprehends **3 wireless 3-lead multilead products: CardioLeaf FIT, CardioLeaf PRO and CardioLeaf ULTRA.** The peculiarities of all these devices are the thickness (just nine millimetres), the wearability and the ergonomic design. Moreover, these products are waterproof and positioned on the chest so the patient has freedom of movement and he can wear them during the daily activities. The low power consumption allows to collect data up to seven days

and the multi-channel architecture gives the possibility to acquire other vital signals like EMG, EEG, and body temperature. In addition, the three-Lead CardioLeaf consent a more powerful analysis of the heart condition because more data are acquired in comparison to a single-lead monitor. This aspect became fundamental in the detection of complex arrhythmias.

Another ground-breaking technology that overcome the offline analysis of Zio patch is **NUVANT Mobile Cardiac Telemetry (MCT)** (Corventis, San Jose, California), a wireless, 3 lead real and time ECG monitoring patch. The system is portable, and it consist also a magnet used as a trigger when the patient has an arrythmia. The con of this technology is the long application of the device necessary to reach valid values.

Moreover**, Shao et al.**[7] presented a wearable ECG monitoring system composed by a wearable patch for the acquisition of the signals that transmit them to an Android smartphone via Bluetooth. The signals are showed on the display and transmitted every 30s to a remote server. One of the applications of this device is FA detection thanks to the machine learning algorithm CatBoost that using 17 selected features reached a sensitivity of 99.61%, a specificity of 99.64% and an overall accuracy of 99.62 %.

Finally, a lot of different kind of sensors were explored to a potential incorporation inside different monitoring system.

For example, **Voiculescu et al.**[8] presented a flexible generator fabricated on PDMS sheet positioned on the skin and that can transform the movement of the human body in energy. The device is constituted of two flexible golden electrodes with a piezoelectric thin film of ZnO in the middle. This is a groundbreaking technology for this application. The results showed that a 8% strain can produce 2 V and 160 W power as output.

Another classification can be made **looking at the environment in which the device will be used**.

In fact, it can be used inside the hospital, in the ambulatory, at home, or in the remote setting.

The first category is the oldest one and it involves **intensive care unit (ICU) clinical setting, non-ICU clinical setting, or a Holter monitoring setting**.

The second category can be further divided into **cardiac/telemetry monitoring and Wearable ECG monitoring.** In fact, to assist the patients outside the hospital environment a wide range of free-living conditions solutions were explored with numerous applications in various clinical field like sports or

7 M. Shao, Z. Zhou, G. Bin, Y. Bai, and S. Wu, "A wearable electrocardiogram telemonitoring system for atrial fibrillation detection," *Sensors (Switzerland)*, vol. 20, no. 3, 2020, doi: 10.3390/s20030606.

8 I. Voiculescu, F. Li, G. Kowach, K. L. Lee, N. Mistou, and R. Kastberg, "Stretchable piezoelectric power generators based on ZnO thin films on elastic substrates," *Micromachines*, vol. 10, no. 10, 2019, doi: 10.3390/mi10100661.

arrhythmia detection. These devices were primarily design to guarantee home assistance for patients with chronic disease but in the recent years the spectrum became larger and involves different kind of clinical subjects. For this purpose, the last two categories were implemented. **In particular, the home monitoring comprehends telemonitoring, wearable continuous monitoring and monitoring specifically designed for the elderly people**.

The last category is specifically designed **for distant patients with a lively lifestyle that makes them move frequently during the day**, so the presence at home is not required. This group of monitoring system can be further split into textile-based systems and contactless based systems and can detect different heart clinical conditions. Their main advantage is to be comfortable because they are flexible and non-adhesive and to be environmentally friendly because they are reusable. Moreover, they overcome the disadvantages in terms of stability and environmental sustainability of the conventional electrodes.

Many studies were conducted to test their performances in comparison to the standard electrodes used inside the hospital and to correlate how different factors can affect those performances.

Tong et al.[9] investigated the sensitivity of textile-based ECG evaluating those four factors: contact pressure, textile placement, user's activity, and muscle activity. The analysis compares the signal recorded with the standard electrodes gel and the signals acquired with the textile sensor and it showed that the area of the placement influenced the signal quality and that the best area is the one with fewer muscles.

A similar analysis was conducted by **Castrillón et al.**[10] that compared PEDOT: PSS treated fabrics based on cotton, cotton–polyester, lycra and polyester, a commercial fabric made of silver-plated nylon Shielde® Med-Tex P130 and commercial Ag/AgCl electrodes looking at four electrical characteristics: contact impedance, electrodepolarization, noise, and long-term performance. The results showed the feasibility of the PEDOT: PSS fabrics with an error lower than 2% and good performances after 36h of no-stop use.

An et al.[11] explored the performances of the textile electrode and particularly the different performances with different configuration of electrodes position, size and holding pressure. The results showed that the output of this kind of sensor is comparable to the one of the wet electrodes when all the parameters are optimized.

---

9 W. Tong, C. Kan, and H. Yang, "Sensitivity analysis of wearable textiles for ECG sensing," *2018 IEEE EMBS Int. Conf. Biomed. Heal. Informatics, BHI 2018*, vol. 2018-Janua, no. March, pp. 157–160, 2018, doi: 10.1109/BHI.2018.8333393.

10 R. Castrillón, J. J. Pérez, and H. Andrade-Caicedo, "Electrical performance of PEDOT: PSS-based textile electrodes for wearable ECG monitoring: A comparative study," *Biomed. Eng. Online*, vol. 17, no. 1, pp. 1–23, 2018, doi: 10.1186/s12938-018-0469-5.

11 X. An, O. Tangsirinaruenart, and G. K. Stylios, "Investigating the performance of dry textile electrodes for wearable end-uses," *J. Text. Inst.*, vol. 110, no. 1, pp. 151–158, 2019, doi: 10.1080/00405000.2018.1508799.

Another study was the one of **Arquilla et al.**[12] that introduced a sewn textile silver-coated electrode with a zig zag pattern. The study, that involved 8 subjects, showed that the detection of the R-R peak with these sensors was comparable to the one with the traditional sensor. This result combined with the resistance to different kind of stress (stretch, bend, or wash testing) showed a potential further implementation inside a wearable device.

Tsukada et al.[13] introduced a highly conductive textile sensor constituted of nano-fibers coated with the PEDOT-PSS polymer and tested his response to different kind of stress with a study that involved 66 subjects. The results demonstrated that the electrical conductivity of the textile electrode stopped to be functional after 50 machine washes and that the ECG patterns of P, QRS, and T waves were comparable between traditional and textile electrodes in supine rest, seated rest, upright trunk rotation and stepping movement is but that the signal-to-artifact-and/or-noise ratio (SAR) during twisting was larger in the textile electrodes than in the conventional ones.

An et al.[14] presented two sensors embedded in one device: a textile electrode for ECG sensing, and a motion sensor for activity tracking. In this study the assessment of the performances leads to two major factor that influence the output: the properties of the material and the dimensions of the electrodes. Therefore, the selected electrode was a 20mm-40mm silver plated electrode and made of a high stitch density.

Wu et al.[15] proposed a flexible sensor made of graphene as active layer and polyvinyl alcohol film as flexible electrode substrate. This combination guaranteed excellent performances both from the mechanical and electrical point of view with a Young's modulus of 8.598 MPa, a maximum strain of 135% a resistivity of 35.88Ω·m and a resistance that fluctuated within 20% strain.

Villegas et al.[16] presented a wearable arm-ECG sensor system (WAMECG1) for continuous, long-term and non-invasive heart rhythm monitoring integrated into an ergonomically designed arm-band ECG sensor system. An Ag–AgCl based dry electrode pair detect the bipolar signal from the arm-ECG. The comparison between this technology and the traditional electrodes showed a cross-correlation value of 99.7% and an error of less than 0.75%. The test of the motion artifacts in different positions and activities showed that the R-peak detection average sensibilities were 99.66% and 94.64%, while the positive predictive values

12 K. Arquilla, A. K. Webb, and A. P. Anderson, "Textile electrocardiogram (Ecg) electrodes for wearable health monitoring," *Sensors (Switzerland)*, vol. 20, no. 4, pp. 1–13, 2020, doi: 10.3390/s20041013.

13 Y. T. Tsukada *et al.*, "Validation of wearable textile electrodes for ECG monitoring," *Heart Vessels*, vol. 34, no. 7, pp. 1203–1211, 2019, doi: 10.1007/s00380-019-01347-8.

14 X. An and G. K. Stylios, "A hybrid textile electrode for electrocardiogram (ECG) measurement and motion tracking," *Materials (Basel).*, vol. 11, no. 10, 2018, doi: 10.3390/ma11101887.

15 N. Wu, H. Liu, S. Wan, S. Su, H. Huang, and L. Sun, "Ultrahigh Skin-Conformal and Biodegradable Graphene-based Flexible Sensor for Measuring ECG Signal," *Int. J. Inf. Electron. Eng.*, vol. 10, no. 2, pp. 52–56, 2020, doi: 10.18178/ijiee.2020.10.2.720.

16 A. Villegas, D. McEneaney, and O. Escalona, "Arm-ECG wireless sensor system for wearable long-term surveillance of heart arrhythmias," *Electron.*, vol. 8, no. 11, pp. 1–26, 2019, doi: 10.3390/electronics8111300.

achieved 99.1% and 92.68%, respectively. Furthermore, the average signal-to-noise ratio (SNR) values were 21.71 for resting in a chair and 18.25 for doing physical activities.

Nowadays the wearable devices became an effective solution for different clinical applications.

For instance**, Ahn et al.**[17] introduced a device worn on both the ears that can continuously measure electrocardiograms (ECG) and EEG with the purpose to evaluate daily stress. The advantages of this device are the weight just (42.5 g) et the reduced noise (0.12 microVrms). For the study 14 young subjects were enrolled and the classification with a support vector machine technique led to an accuracy of 87.5%.

Huda et al.[18] propose a cost-effective, power-saving and wireless ECG monitoring system for automatic arrhythmia detection using Convolutional Neural Network (CNN) based deep learning model. The results showed an accuracy of 94.03% in the arrhythmia classification on the MIT-BIH Arrhythmia Database.

Làzaro et al.[19] showed that the performances of this device during a day of continuous monitoring. This system collects signals from 3 channels, and it can be easily worn because of his dry electrodes that overcome the issues of skin irritation caused by the traditional wet ones. The results of the device's linear classifier were evaluated using as a standard goal an Holter monitoring system and they showed a relative error less than 10%.

Tada et al.[20] presented a smart shirt for ECG monitoring with 6 electrodes on the chest that can acquire unipolar precordial leads. The material of the electrodes and the wires of the shirt is conductive ink, and this property gives to the device flexibility and wearability for everybody shape. The main issue of this technology is the gap between the tissue and the body that is critical for the stability of the electrodes V1 and V2, but this problem was solved thanks to a conductive foam block.

Boehm et al.[21] developed instead an ECG monitoring T-shirt with integrated patches of conductive textile into the ECG T-shirt and to improve the signal quality the circuits were attached outside the T-shirt. The results showed a mean relative error of the RR intervals of 0.96% and mean coverage of 96.6%. Another analysis investigated the correlation between the ECG signal: a correlation of 0.703 was found for the P-wave for walking subjects and higher than 0.9 for other activities.

---

17 J. W. Ahn, Y. Ku, and H. C. Kim, "A novel wearable EEG and ECG recording system for stress assessment," *Sensors (Switzerland)*, vol. 19, no. 9, 2019, doi: 10.3390/s19091991.

18 N. Huda, S. Khan, R. Abid, S. B. Shuvo, M. M. Labib, and T. Hasan, "A Low-cost, Low-energy Wearable ECG System with Cloud-Based Arrhythmia Detection," *2020 IEEE Reg. 10 Symp. TENSYMP 2020*, pp. 1840–1843, 2020, doi: 10.1109/TENSYMP50017.2020.9230619.

19 J. Lazaro, N. Reljin, Y. Noh, P. Laguna, and K. H. Chon, "Feasibility of Long-Term Daily Life Electrocardiogram Monitoring Based on a Wearable Armband Device," *Proc. Annu. Int. Conf. IEEE Eng. Med. Biol. Soc. EMBS*, pp. 4314–4317, 2019, doi: 10.1109/EMBC.2019.8857219.

20 Y. Tada, Y. Amano, T. Sato, S. Saito, and M. Inoue, "A smart shirt made with conductive ink and conductive foam for the measurement of electrocardiogram signals with unipolar precordial leads," *Fibers*, vol. 3, no. 4, pp. 463–477, 2015, doi: 10.3390/fib3040463.

21 A. Boehm, X. Yu, W. Neu, S. Leonhardt, and D. Teichmann, "A novel 12-lead ECG T-shirt with active electrodes," *Electron.*, vol. 5, no. 4, 2016, doi: 10.3390/electronics5040075.

Steinberg et al.[22] assessed the signal quality and R-R of the OMgaments, a wearable ECG sensor system compared to a standard 3-lead Holter. The focus of the analysis was on the P-QRS-T distinction and was performed by three electrophysiologists that studied without knowing the source of the acquisition the recorded signals. The results showed that the signal quality and accuracy of the OMgaments was equivalent to Holter-monitoring (84% vs. 93% electrophysiologists rating, $p = 0.06$). **Lin et al.**[23] developed a wearable smart clothing system with a multi-channel mechanocardiogram (MCG) with the purpose to predict the myo-cardiac left ventricular ejection fraction (LVEF) function. The result of the CHAMP (Cardiac Health Assessment and Monitoring Platform) system was compared with actual heart failure (HF) patients showing a consistency.

Even considering all the potential application of this cutting-edge cluster of monitoring system the accuracy of these sensors is still not competing with the traditional Holter technology in terms of accuracy. In fact, the output is strictly related with external factors such as sensor placement and contact pressure. For this reason, a new branch of devices conquered the market: the wearable watches.

One of the most used and accurate wearable watch devices is the **Apple Watch**. A lot of different studies has been conducted to assess his accuracy and his potential application in many medical fields.

The widest (419,093 participants) and most relevant study in making a turning point in the field of wearable watch was the Apple Watch study (**Turakhia et al.**[24]). This study demonstrates the ability of the Apple watch algorithm to identify irregular pulse in the participants and, as a secondary goal, to compare the detection by the Apple Watch to the simultaneously recorded ambulatory ECGs. After this one a lot of different studies were conducted.

For example, **Fuller et al.**[25] implemented a machine learning algorithm for activities classification. To the 49 participants (23 men and 26 women) of the study was asked to wear an **Apple Watch Series 2, a Fitbit Charge HR2, and an iPhone 6S** and to perform a 65-minute protocol (40 minutes of total treadmill time and 25 minutes of sitting or lying time). Four different machine learning models were tested (decision trees, support vector machines, random forest, and rotation forest models) and the highest accuracy was reached

22 C. Steinberg *et al.*, "A novelwearable device for continuous ambulatory ECG recording: Proof of concept and assessment of signal quality," *Biosensors*, vol. 9, no. 1, pp. 1–13, 2019, doi: 10.3390/bios9010017.

23 W. Y. Lin, H. L. Ke, W. C. Chou, P. C. Chang, T. H. Tsai, and M. Y. Lee, "Realization and technology acceptance test of a wearable cardiac health monitoring and early warning system with multi-channel MCGs and ECG," *Sensors (Switzerland)*, vol. 18, no. 10, 2018, doi: 10.3390/s18103538.

24 M. P. Turakhia *et al.*, "Rationale and design of a large-scale, app-based study to identify cardiac arrhythmias using a smartwatch: The Apple Heart Study," *Am. Heart J.*, vol. 207, pp. 66–75, 2019, doi: 10.1016/j.ahj.2018.09.002.

25 D. Fuller *et al.*, "Using machine learning methods to predict physical activity types with Apple Watch and Fitbit data using indirect calorimetry as the criterion.," pp. 1–16, 2020, doi: 10.21203/rs.3.rs-17022/v1.

by Rotation Forest (82.6% for Apple Watch and 89.3% for Fitbit). Therefore, they demonstrated that, thanks to their accuracy, these devices can be used for activities detection in the free-living environment combing the continuous acquisition and the selected machine learning method.

Another interesting study is the one of **Samol et al.**[26] that recruited 50 healthy subjects and recorded a 12-lead ECG and three bipolar ECGs using the **Apple Watch Series 4** to evaluate its accuracy in comparison to a three lead ECG recording. Einthoven I was recorded with the watch on the left wrist and the right index finger on the crown, Einthoven II with the watch on the left lower abdomen and the right index finger on the crown, Einthoven III with the watch on the left lower abdomen and the left index finger on the crown. After that, four cardiologists assigned the measurements acquired with the Apple watch to Einthoven leads for each subject. An accuracy of 91% was shown, so the study demonstrates the reliability of this wearable device and its interchangeability with all the ambulatory ECG recording systems.

An innovative implementation of the **Apple Watch Series 4** was to give the possibility to the patients to record the rhythm and to be assisted in the detection of their atrial fibrillation (**Isakadze et al**.[27])

A key element of this feature is the app that, thanks to its algorithm, shows the classification of the recorded heart rhythm. In particular, the strength in the atrial fibrillation detection made this device obtain the Food and Drug Administration clearance. Furthermore, **Strik et al.**[28] explored the accuracy of the Apple watch in the QT measurement in different positions (85% accuracy on the left wrist).

Another device for the arrhythmia detection in free-living conditions is the **AliveCor Kardia Mobile (KM)**. **Selder et al.** the rhythm was acquired by 233 patients and the output of the classification was 59% SR, 22% possible AF, 17% unclassified and 2% unreadable. Even the device has a high NPV, the limitation of this study is the low PPV that make necessary the integration with a cardiologist evaluation. Furthermore, the absence of the 12-lead ECGs as a reference can cause an overestimated specificity. **Goldenthal et al.**[29] demonstrated, thanks to a multivariate Cox model, that the use of this devices is fundamental for earlier detection of AF/AFL recurrence.

In a study that enrolled 285 children, **Karacan et al.**[30] showed another application of AliveCor in the detection of long QT syndrome in children. In particular, they tested the accuracy of the device using as a reference a 12-lead ECG and the evaluation of two electrophysiologists and they found out a correlation of

---

26 A. Samol, K. Bischoff, B. Luani, D. Pascut, M. Wiemer, and S. Kaese, "Recording of bipolar multichannel ECGs by a smartwatch: Modern ECG diagnostic 100 years after Einthoven," *Sensors (Switzerland)*, vol. 19, no. 13, 2019, doi: 10.3390/s19132894.

27 N. Isakadze and S. S. Martin, "How useful is the smartwatch ECG?," *Trends Cardiovasc. Med.*, vol. 30, no. 7, pp. 442–448, 2020, doi: 10.1016/j.tcm.2019.10.010.

28 M. Strik *et al.*, "Validating QT-Interval measurement using the apple watch ecg to enable remote monitoring during the COVID-19 pandemic," *Circulation*, vol. 142, no. 4, pp. 416–418, 2020, doi: 10.1161/CIRCULATIONAHA.120.048253.

29 I. L. Goldenthal *et al.*, "Recurrent atrial fibrillation/flutter detection after ablation or cardioversion using the AliveCor KardiaMobile device: iHEART results," *J. Cardiovasc. Electrophysiol.*, vol. 30, no. 11, pp. 2220–2228, 2019, doi: 10.1111/jce.14160.

30 M. Karacan, "Validation of a smartphone based electrocardiography in the screening of QT intervals in children," *North. Clin. Istanbul*, vol. 6, no. 1, pp. 48–52, 2018, doi: 10.14744/nci.2018.44452.

0.83 [p<0.001] between the measurement of the QT interval obtained with a 12-lead ECG compared to the one obtained with AliveCor.

Bumgarner et al.[31] introduced the smartwatch **AliveCor Kardia Band** and evaluated his signal's accuracy in comparison to a standard 12-lead ECG. Furthermore, the study explored the smartwatch AF detection ability enrolling 100 patients with AF. The evaluation was done by clinicians that evaluated both the 169 signals obtained from the smartwatch and the 169 recorded by the traditional technology. The results showed a 93% sensitivity, 84% specificity, and a K coefficient of 0.77 in comparison to the standard ECG in the detection of AF. This value changed adding the clinician's interpretation: 99% sensitivity, 83% specificity, and a K coefficient of 0.83. This output demonstrated the potential of this device in the AF detection. However, the limitation of this study were the small sample size and the specific kind of patients selected in terms of gender, clinical conditions, and absence of implantable devices so with a different set of subjects the performances would be lower. Moreover, the patients were instructed for the utilization of the device so this bias was eliminated.

A novel device is the one proposed by **Randazzo et al.**[32]: **VITAL-ECG"**, a low-cost smartwatch commissioned by two Italian healthcare facilities for a continuous monitoring of critical vital parameters like ECG, SpO2 and skin temperature. This wearable device is connected to a mobile app that can show the changes of the recorded signals during the day. For assessing the signals quality in comparison to a standard ECG device used inside the hospital an experiment was conducted recording signals from 36 participants while they were seating. The quality of the ECG signal was assessed at different level. First, thanks to the Bland–Altman Plot, a data variation around the maximum of less than 5% was showed. This output demonstrated that there was no significance difference between the two system. After that, the investigation of the power spectral density and the cumulative spectral power exhibited a similar signals' distribution. Then the analysis in the time domain showed a mean difference around 1%, and a standard deviation slightly above 12% between the two signals. A limitation of this study is the acquisition of the signal only in a steady condition, so the accuracy of the measurement can be overestimated. Furthermore, the design of the smartwatch can be improved with a user-friendly monitor.

Thomas et al.[33] presented **Biowatch**, a smartwatch for the measurement of electrocardiogram and photoplethysmogram and combining both these acquisitions to calculate the pulse transit time (PTT). This system can potentially facilitate continuous and ubiquitous monitoring of ECG, PPG, heart rate, blood

31 J. M. Bumgarner *et al.*, "Smartwatch Algorithm for Automated Detection of Atrial Fibrillation," *J. Am. Coll. Cardiol.*, vol. 71, no. 21, pp. 2381–2388, 2018, doi: 10.1016/j.jacc.2018.03.003.

32 V. Randazzo, J. Ferretti, and E. Pasero, "A wearable smart device to monitor multiple vital parameters—VITAL ECG," *Electron.*, vol. 9, no. 2, pp. 1–13, 2020, doi: 10.3390/electronics9020300.

33 S. S. Thomas *et al.*, "BioWatch - A wrist watch based signal acquisition system for physiological signals including blood pressure," *2014 36th Annu. Int. Conf. IEEE Eng. Med. Biol. Soc. EMBC 2014*, pp. 2286–2289, 2014, doi: 10.1109/EMBC.2014.6944076.

oxygenation and BP. The aim of this study, that includes 4 participants is to find a fitting function to convert the PTT value to its corresponding systolic BP and to validate the results on different postures. A significant limitation of this study is the number of the participants.

Lee et al.[34] present a **smartwatch** for ECG continuous and convenient monitoring of the patient's cardiovascular system. For comprehensive monitoring of the patient's cardiovascular system, the concurrent electrocardiogram (ECG) and arterial pulse wave (APW) sensor front-end are fabricated in 0.18 mm CMOS technology. The ECG sensor frontend achieves 84.6-dB CMRR and 2.3-mVrms-input referred noise with 30-mW power consumption. The APW sensor front-end achieves 3.2-V/W sensitivity with accurate bio-impedance measurement lesser than 1% error, consuming only 984-mW. The ECG and APW sensor front-end are combined with power management unit, micro controller unit (MCU), display and Bluetooth transceiver so that concurrently measured ECG and APW can be transmitted into smartphone, showing patient's cardiovascular state in real time. In order to verify operation of the cardiovascular monitoring system, cardiovascular indicator is extracted from the healthy volunteer. As a result, 5.74 m/second-pulse wave velocity (PWV), 79.1 beats/minute-heart rate (HR) and positive slope of b-d peak-accelerated arterial pulse wave (AAPW) are achieved, showing the volunteer's healthy cardiovascular state.

Furthermore, another device for continuous monitoring and with different clinical applications is the **Verily Study Watch. Bloem et al.**[35] presented a prospective, longitudinal, single-centre cohort study of 650 subjects with a Parkinson's disease for more than 5 years and older than 18 years. The data were collected over 2 years and stored maintaining the subject privacy. The aim of the study was to evaluate the progression of the disease.

Finally, **Hernandez et al.**[36] introduced a wrist-worn ECG monitor composed by an accelerometer and a gyroscope. Twelve participants were enrolled, and they were asked to stay in a standing up, sitting down and lying down position, a mean absolute error of 1.27 beats per minute in comparison to the standard ECG was reached.

Most of the devices measure multiple parameters like heart rate (HR), body temperature (BT), calories burned (CB), distance (D), body posture (BP) and skin temperature (ST). C.

There are still a lot of issues to solve in terms of portability and accuracy.

---

34 H. Lee *et al.*, "Toward all-day wearable health monitoring: An ultralow-power, reflective organic pulse oximetry sensing patch," *Sci. Adv.*, vol. 4, no. 11, pp. 1–9, 2018, doi: 10.1126/sciadv.aas9530.

35 B. R. Bloem *et al.*, "The Personalized Parkinson Project: Examining disease progression through broad biomarkers in early Parkinson's disease," *BMC Neurol.*, vol. 19, no. 1, 2019, doi: 10.1186/s12883-019-1394-3.

36 J. Hernandez, D. McDuff, and R. W. Picard, "Biowatch: Estimation of heart and breathing rates from wrist motions," *Proc. 2015 9th Int. Conf. Pervasive Comput. Technol. Heal. PervasiveHealth 2015*, pp. 169–176, 2015, doi: 10.4108/icst.pervasivehealth.2015.259064.

BP: State of the art

Blood pressure (BP) is a bio-physiological signal that can provide useful information about human's general health. High or low blood pressure or its rapid fluctuations can be associated to various diseases or clinical conditions. High blood pressure or hypertension is the most common cause of death and disability in the world, and a major risk factor for aneurysms of the arteries, strokes, and peripheral arterial disease.

Blood pressure is usually represented with three values: systolic (SBP), diastolic (DBP) and mean arterial pressure (MAP).

- *Systolic pressure*: the blood pressure made on the wall of blood vessels while the ventricles squeeze pushing blood out to the rest of the body. The SBP is the maximum pressure that occurs when the blood is pumped from the left ventricle into the aorta.
- *Diastolic pressure*: the pressure made on the blood vessel walls as the heart relaxes. The DBP is the minimum pressure that occurs when the blood flows from the atria to the ventricles.
- *Mean arterial pressure*: the average pressure in arteries during one cardiac cycle.

Accurate blood pressure measurement and monitoring play fundamental role in diagnosis, prevention, and treatment of these diseases. Blood pressure is usually measured in the hospitals, as a part of a standard medical routine. However, there is an increasing demand for methodologies, systems as well as accurate and unobtrusive devices that will permit continuous blood pressure measurement and monitoring for a wide variety of patients, allowing them to perform their daily activities without any disturbance.

Nowadays there are different approaches for measuring blood pressure depending on the environment.

1. **Traditional methods for measuring BP in the hospital**

- *The invasive method*: it uses a catheter, which is a thin flexible tube inserted into the artery. Measuring BP invasively requires experts such as physicians and doctors to conduct the measurement and monitoring. It is very accurate, but is usually restricted to hospital settings, for monitoring a high-risk surgical patients and patients in the Intensive Care Unit.
- *The non-invasive method*: there are various techniques that provides either intermittent or continuous readings. The standard way for arterial BP measurement is using mercury sphygmomanometer. It uses an air-cuff, placed on upper arm of the patient, which is slowly inflating in order to occlude the blood flow in the artery.

2. **Methods for measuring BP at home**

- *Oscillometry:* The current standard methodology for measuring blood pressure (BP) at home is using an automated BP cuff based on oscillometry. It's a non-invasive intermittent BP measurement technique that uses an inflatable cuff placed on the arm or wrist of the patient to occlude the blood flow. This uses a pressure transducer to record the pressure oscillation, during the progressive deflation of the cuff. The pressure at which a maximum oscillation is detected corresponds to MAP, while the SBP and DBP are estimated from the MAP and oscillation pattern.[37]
- *HeartGuide:* wearable cuff method: it has an extra-stiff band that inflates to take an oscillometric measurement like a normal doctor's blood pressure cuff. The watch takes manual readings and spot heart rate measurements but can also be programmed to take night readings to test for hypertension and risk of stroke while sleeping.[37]
- *Oscillometric finger-pressing method:* cuff-less BP monitoring device using a smartphone. As the user presses her/his finger against the smartphone, the external pressure of the underlying artery is steadily increased while the phone measures the applied pressure and resulting variable amplitude blood volume oscillations. A smartphone application provides visual feedback to guide the amount of pressure applied over time via the finger pressing and computes systolic and diastolic BP from the measurements.[38]

3. Methodologies for continuous cuff-less BP measurement

While widely accepted as the gold-standard of BP monitoring, at home oscillometric cuff measurements are inconvenient, have limited portability, and require the user to follow strict guidelines to obtain an accurate reading. An effort to decrease obtrusiveness and increase portability, wrist-worn devices have been developed that currently still use oscillometry to acquire BP, thereby falling into the same obstacle as their uncomfortable upper-arm counterparts.

With advances in computing power and digital signal processing as well as the growing need for personal health monitoring products, computer-based blood pressure assessment and wearable sensors for continuous non-invasive BP measurement have received significant attention. These trends have also incited development of new methods that not only support the popular oscillometric technique but, also provide BP estimation from electrocardiogram (ECG) signals, photoplethysmogram (PPG) signals, or their combination in order to obtain more precise results.[37]

37 A. Stojanova, S. Koceski, and N. Koceska, "Continuous Blood Pressure Monitoring as a Basis for Ambient Assisted Living (AAL) – Review of Methodologies and Devices," *J. Med. Syst.*, vol. 43, no. 2, 2019, doi: 10.1007/s10916-018-1138-8.

38 A. Chandrasekhar, C. S. Kim, M. Naji, K. Natarajan, J. O. Hahn, and R. Mukkamala, "Smartphone-based blood pressure monitoring via the oscillometric finger-pressing method," *Sci. Transl. Med.*, vol. 10, no. 431, pp. 1–12, 2018, doi: 10.1126/scitranslmed.aap8674.

- *Photoplethysmography (PPG)* is optical technique used to estimate the skin blood flow using infrared light. This is non-invasive technique that measures relative blood volume changes in the blood vessels close to the skin. The changes in blood flow can be detected by PPG sensors as changes in the intensity of light because the light is more absorbed by blood than the other surrounding tissues. PPG is a simple, low-cost, and portable optical technique that can be used in detecting blood volume changes in tissue. This technique can be used for developing portable real-time unobtrusive systems capable of continuously monitoring patients for a long period of time in static and dynamic conditions. The reflective sensor should be placed either on a top of the radial or ulnar artery near the wrist, depending on the emerging signal quality.[37]

Cuff-less non-invasive BP estimation methods are intensively researched in the last decade. Several research groups have developed cuff-less wearable BP monitoring devices that allow patients to continuously monitor BP without interfering with their daily activities.

Depending on the input signals used for BP derivation these methodologies can be classified in different categories:

a) **BP estimation from Pulse Transit Time (PTT):** the most employed technique for cuff-less BP measurement. When the heart beats, it pumps blood to all parts of the body. The speed of heart beating is directly proportional to BP. The time it takes for blood to reach the certain location in the human body is inversely proportional to BP and is called pulse transit time (PTT). The speed of this travel corresponds to the pulse wave velocity (PWV). By continuously measuring PTT, SBP and DBP can be estimated. PTT can also be described as the time needed for the arterial pulse pressure-wave to propagate through a length of the arterial tree. [37]

There are two typical methods used to calculate PTT:

- BP estimation from PTT calculated by ECG and PPG signals: uses the time delay between the peak of the R-wave in ECG and the fingertip PPG to calculate the PTT.
- Wearable cuff-less electrocardiography (ECG) and photoplethysmogram (PPG)-based SBP and HR monitoring system: ECG and PPG sensors are integrated into a single-arm band to provide a super wearability. A highly convenient but challenging single-lead configuration is proposed for weak single-arm-ECG acquisition instead of placing the electrodes on the chest, or two wrists. To identify heartbeats and estimate HR from the motion artifacts-sensitive weak arm-ECG, a machine learning-

enabled framework is applied. Then ECG-PPG heartbeat pairs are determined for pulse transit time (PTT) measurement.[39]

- ***InBodyWATCH:*** is a wearable activity tracker that provides activity tracking functions such as step counts, sleep tracking, and heart rate measurement. Two bottom electrodes and one top electrode are used to obtain ECG signals by measuring the voltage difference between the left wrist (bottom electrodes) and the right arm (top electrode). A PPG sensor (with green LED) placed on the base is used to measure volumetric changes in blood vessels by alternating current (AC) modulation in reflected LED light, as blood behaves as an absorber of LED light.[40]
- ***Wearable Body Sensor Networks****:* a wristband is worn to collect plethysmogram (PPG) signals, and a heart rate (HR) belt is worn at the chest to collect electrocardiogram (ECG) signals.[41]
- ***Ear-ECG/PPG:*** electrocardiogram (ECG) and photoplethysmography (PPG) sensors behind two ears to achieve a super wearability, and successfully acquire weak ear-ECG/PPG signals using a semi-customized platform.[42]

b) <u>BP estimation from PTT calculated by PPG signals: measures the delay of different PPGs acquired from different parts of the body.</u>

- ***SeismoWatch:*** a wrist-watch BP monitor was developed to measure BP through a simple maneuver: holding the watch against the sternum to detect micro-vibrations of the chest wall associated with the heartbeat. As a pulse wave propagates from the heart to the wrist, an accelerometer and optical sensor on the watch measure the travel time - pulse transit time (PTT) - to estimate BP. An accelerometer inside the watch measures thoracic vibrations associated with the heartbeat, or the seismocardiogram (SCG) signal, to obtain the proximal timing indicating the ejection of blood from the left ventricle into the aorta. Optical sensors on the watch measure the blood volume pulse, or photoplethysmogram (PPG) signal, to obtain the distal timing associated with the arrival of the pulse wave at the radial artery (on the wrist). The time delay calculated between fiducial points on these two measurements then provides the PTT, and is then used with subject specific parameters (obtained using an initial calibration step) to calculate an estimate for BP.[43]

---

39 Q. Zhang, D. Zhou, and X. Zeng, "Highly wearable cuff-less blood pressure and heart rate monitoring with single-arm electrocardiogram and photoplethysmogram signals," *Biomed. Eng. Online*, vol. 16, no. 1, pp. 1–20, 2017, doi: 10.1186/s12938-017-0317-z.

40 J. H. Moon, M. K. Kang, C. E. Choi, J. Min, H. Y. Lee, and S. Lim, "Validation of a wearable cuff-less wristwatch-type blood pressure monitoring device," *Sci. Rep.*, vol. 10, no. 1, pp. 1–9, 2020, doi: 10.1038/s41598-020-75892-y.

41 H. Lin, W. Xu, N. Guan, D. Ji, Y. Wei, and W. Yi, "Continuous Blood."

42 Q. Zhang, X. Zeng, W. Hu, and D. Zhou, "A Machine Learning-Empowered System for Long-Term Motion-Tolerant Wearable Monitoring of Blood Pressure and Heart Rate with Ear-ECG/PPG," *IEEE Access*, vol. 5, pp. 10547–10561, 2017, doi: 10.1109/ACCESS.2017.2707472.

43 A. M. Carek, J. Conant, A. Joshi, H. Kang, and O. T. Inan, "SeismoWatch," *Proc. ACM Interactive, Mobile, Wearable Ubiquitous Technol.*, vol. 1, no. 3, pp. 1–16, 2017, doi: 10.1145/3130905.

- ***BioWatch:*** the wristwatch-based system we developed can measure electrocardiogram and photoplethysmogram. From these two signals, we measure pulse transit time through which we can obtain systolic and diastolic blood pressure through regression techniques.[44]
- ***Multiwavelength photoplethysmography (MWPPG) device***: utilising multiple different wavelengths of light allows the studying of blood vessels at different depths. The developed device uses five wavelengths to study the different blood vessels with the goal of assessing microvasculature. The device proved to produce good quality signal making it possible to compute the small-time differences between the pulses measured at different wavelengths, and hence enabling the computation of pulse transit times in the skin microvasculature (PTTM)[45]

c) <u>BP estimation from PTT calculated by other signals: a combination of ECG, PPG and others acquired from different part of the body.</u>

- ***Wearable Limb Ballistocardiogram in Blood Pressure Monitoring via Pulse Transit Time:*** wearable limb ballistocardiography (BCG) to enable cuff-less blood pressure (BP) monitoring, by investigating the association between wearable limb BCG-based pulse transit time (PTT) and BP. A wearable BCG-based PTT was calculated using the BCG and photoplethysmogram (PPG) signals acquired by a wristband as proximal and distal timing reference (called the wrist PTT).[46]
- ***Multimodal Wrist Biosensor for Wearable Cuff-less BP Monitoring System***: enables a fully non-intrusive system that is cuff-less, also utilize a single measurement site for maximum wearability and convenience of the patients. It measures BP with chest electrocardiogram (ECG), wrist PPG, and wrist IPG collected simultaneously.[47]
- ***Cuffless BP Monitoring from an Array of Wrist Bio-Impedance Sensors:*** this method uses an array of wrist-worn bio-impedance sensors placed on the radial and the ulnar arteries of the wrist to monitor the arterial pressure pulse from the blood volume changes at each sensor site. The Bio-Z signal provides a more accurate measurement of arterial blood volume changes since it can reach deep arterial sites.[48]

---

44 S. S. Thomas, V. Nathan, C. Zong, K. Soundarapandian, X. Shi, and R. Jafari, "BioWatch: A Noninvasive Wrist-Based Blood Pressure Monitor That Incorporates Training Techniques for Posture and Subject Variability," *IEEE J. Biomed. Heal. Informatics*, vol. 20, no. 5, pp. 1291–1300, 2016, doi: 10.1109/JBHI.2015.2458779.

45 J. P. Sirkia, T. Panula, and M. Kaisti, "Multi-Wavelength Photoplethysmography Device for the Measurement of Pulse Transit Time in the Skin Microvasculature," *Comput. Cardiol. (2010).*, vol. 2020-Septe, 2020, doi: 10.22489/CinC.2020.179.

46 P. Yousefian *et al.*, "The Potential of Wearable Limb Ballistocardiogram in Blood Pressure Monitoring via Pulse Transit Time," *Sci. Rep.*, vol. 9, no. 1, pp. 1–11, 2019, doi: 10.1038/s41598-019-46936-9.

47 V. P. Rachim and W. Y. Chung, "Multimodal Wrist Biosensor for Wearable Cuff-less Blood Pressure Monitoring System," *Sci. Rep.*, vol. 9, no. 1, pp. 1–9, 2019, doi: 10.1038/s41598-019-44348-3.

48 B. Ibrahim and R. Jafari, "Cuffless Blood Pressure Monitoring from an Array of Wrist Bio-impedance Sensors using Subject-Specific Regression Models: Proof of Concept," *IEEE Trans. Biomed. Circuits Syst.*, vol. 13, no. 6, pp. 1723–1735, 2019, doi: 10.1109/TBCAS.2019.2946661.

- ***BP estimation only from ECG signals (ECG):*** this method is generally based on the detection of HR, which can be estimated by dividing the RR interval from ECG signal into 60. This number is marked as BPM (Beats per Minute). Due to the fact that HR is directly proportional to the cardiac output, the increase in HR will increase BP, and vice versa, the decrease of HR will also decrease BP. [37]
- ***Galaxy Watch Active 2:*** measures blood pressure through pulse wave analysis, which is tracked with the Heart Rate Monitoring sensors. It needs to be initially calibrated with a traditional cuff, the program then analyses the relationship between the calibration value and the blood pressure change to determine the blood pressure.
- ***Wearable Piezoelectric-Based System:*** uses the sum of the initial blood pressure by an oscillometric method and pressure change by a piezoelectric sensor to obtain the beat-to-beat SBP and DBP. The continuous PPW signals extracted from the radial artery by a piezoelectric sensor directly reveals the arterial behaviors of expansion and contraction. The beat-to-beat pressure change was obtained by the pressure sensitivity of the piezoelectric sensor.[49]

d) Other methods

- ***Blood Pressure Monitor by EchoLabs****:* this technology leverages spectroscopy to analyse blood, using transmitters to send light and other electromagnetic frequencies to the skin and measuring the light that reflects. The light is reflected from every element it hits: the arteries, skin, bone, and muscle. By the reading of the reflectance with a receiver, it can analyse how exactly the blood flow is functioning. In addition to heart rate, it can measure things like blood gas concentrations and blood pressure.[50]

SPO_2: State of the art

Considered the fifth vital sign, the Oxygen saturation in the blood represents a crucial parameter for patients that suffer from a critical heart condition (heart failure), a pathology of the lungs (lung cancer, pneumonia), sleep apnoea and in general for fragile subjects like the elders and the infants.

49 T. W. Wang and S. F. Lin, "Wearable piezoelectric-based system for continuous beat-to-beat blood pressure measurement," *Sensors (Switzerland)*, vol. 20, no. 3, pp. 1–12, 2020, doi: 10.3390/s20030851.

50 T. Arakawa, "Recent research and developing trends of wearable sensors for detecting blood pressure," *Sensors (Switzerland)*, vol. 18, no. 9, 2018, doi: 10.3390/s18092772.

Moreover, beside the clinical applications, the Oxygen saturation in the blood is a very important measurement in the sport field for high energy activities and especially for the ones that are perform in environments with low oxygen levels like diving and mountaineering.

Multiple strategies are adopted for an efficient and continuous monitor of this parameter.
Therefore, in the last decades a lot of different Oxygen saturation monitoring systems were implemented.
To efficiently explore this wide group of devices, it can be useful to divide them in different categories considering different aspects of these systems:

The technology for the detection of the oxygen saturation:

a) *The blood- Arterial Blood Gas (ABG):* consists in analysing a sample of blood to characterize its pH, the oxygen concentration, the carbon dioxide concentration, and the bicarbonate concentration. This test measures the SaO2 (the Arterial Oxygen Saturation of Haemoglobin) and PAO2 (Partial Pressure of Oxygen) that represents the capacity of oxygen transfer between the lungs and the blood. Although this technology is mainly applied for devices used inside the hospital environment, the portable applications have a consistent output in comparison to the stationary one, like demonstrated by **Nawrocki et al**.[51] that confronted a portable BGA (EPOC, Siemens Healthcare) and a stationary BGA (Rapidpoint500, Siemens Healthcare) within a 105 participant's study. The results showed a comparable output between the two devices in terms of Bias: pH 0.007 (0.029 to 0.044), PaCO2 0.3 mmHg (4.8 to 4.2), and PaO2 0.2 mmHg (9.1 to 4.7). The main advantage of this method is the possibility of also reading the metabolic condition but on the other hand it is very invasive.

b) *The Pulse Oximetry*: this technique overcomes this issue using the property of the Haemoglobin to absorb a certain wavelength of light that varies depending on how much oxygen is carried by this protein. Thanks to this fast, easy, and non-invasive method the Peripheral Oxygen saturation of Haemoglobin (SPO2), which is an estimate of the SaO2 levels, is measured. The Calibration between the SPO2 and the SaO2 readings from ABGs guarantee the accuracy of this method for clinical applications. Furthermore, the levels of SPO2 are proportional to the levels of PAO2 but this correlation varies depending on the pH and on the temperature of the body. In particular, the dissociation curve shows that when the SPO2 goes under 90% (Hypoxemia) the PAO2 drops dramatically.

The ergonomic, looking at the different sites of the body, on which these devices can be placed:

51 J. Nawrocki *et al.*, "Validation of a Portable Blood Gas Analyzer for Use in Challenging Field Conditions at High Altitude," *Front. Physiol.*, vol. 11, no. January, pp. 1–6, 2021, doi: 10.3389/fphys.2020.600551.

- **Kramer et al.**[52] enrolled 42 healthy participants that wore the prototype wearable oximeters on the torso, the arms, and legs. The results showed an ARMS (root-mean-square difference) of 1.7% for the calf; 3.1% for the bicep; 3.4% for forearm; 2.9% for the pectoral and 2.9% for the sternum. The acceptable value for further development was less than 3.5% so the study demonstrated the possible application of the pulsi oximeter in different body sites.
- **Singh et al.**[53] investigated as potential location of the pulse oximeter three different locations: the finger, the forehead, and the chest. The experiments give as output the space just above the Angle of Lewis (the bony protuberance where the body of sternum joins the Manubrium) as the best location for the SpO_2 sensor and they also showed that the accuracy of the measurement for this location is comparable to the finger.
- **Zhang et al.**[54] introduced SensEcho, a wearable multi-sensor vest. The system consists in three electrode patches for single-lead ECG signal monitoring at a 200 Hz sampling rate, and two sensing wires for the chest and abdomen breathing monitoring at a sampling rate of 25 Hz. Moreover, there is a sensor collocated on the wrist that communicates with the device via Bluetooth (1 Hz sampling rate) and an ultra-low power, 3-axis digital accelerometer component ADXL345 with a 25 Hz sampling rate embedded in the vest. The storage of the data is possible both local and into a cloud database. A key element of the system is the Apnoea Hypopnea Index (AHI), used to indicate patients' apnoea levels. The sum of the AHI during the breathing disorder events is the AHI score, which is divided in four levels. [No apnoea: AHI < 5; Mild: 5 _ AHI < 15; Medium: 15 < AHI _ 30; and Severe: AHI > 30]. The prediction model of the AHI, tested on 110 patients at Department of Respiration in Chinese PLA General Hospital has an accuracy of 90.0%, therefore the possible clinical application of this wearable device is demonstrated.
- **Peng et al.**[55] demonstrated a strong correlation (r=0.82) between this neck device and the traditional ones. To acquire signals from this unconventional location, a completely new wearable hardware with low power consumption was designed. Furthermore, this location can be used for monitoring the breathing and heart rates. On the contrary there is an error of 1.4% mainly due to movement artefacts and to distance between the LEDs and the photodiode as well as the duty cycle and pulsing frequency for LEDs that were not optimised for the neck region. Therefore, future improvements

52 M. Kramer, A. Lobbestael, E. Barten, J. Eian, and G. Rausch, "Wearable pulse oximetry measurements on the torso, arms, and legs: A proof of concept," *Mil. Med.*, vol. 182, pp. 92–98, 2017, doi: 10.7205/MILMED-D-16-00129.

53 P. Singh, F. Shaik, P. Eunice, I. Luther, R. S. Deepthi, and Y. A. Nath, "A Novel Method for Monitoring SpO2 in Wearable Health Monitoring Applications," *Int. J. Eng. Adv. Technol.*, vol. 9, no. 1S5, pp. 272–274, 2019, doi: 10.35940/ijeat.a1043.1291s52019.

54 Y. Zhang *et al.*, "Poster abstract: Breathing disorder detection using wearable electrocardiogram and oxygen saturation," *SenSys 2018 - Proc. 16th Conf. Embed. Networked Sens. Syst.*, pp. 313–314, 2018, doi: 10.1145/3274783.3275159.

55 M. Peng, S. A. Imtiaz, and E. Rodriguez-Villegas, "Pulse oximetry in the neck - A proof of concept," *Proc. Annu. Int. Conf. IEEE Eng. Med. Biol. Soc. EMBS*, pp. 877–880, 2017, doi: 10.1109/EMBC.2017.8036964.

can be made like for example MORE acquisition for a better calibration and artefact rejection algorithms. However, despite the current limitations, this location is a reliable and accurate (98.6%).

- **Morey et al.**[56] evaluated the nasal location that is indicated for example in paediatric applications and for patients with finger deformities This is an interesting site because of the perfusion by branches of the external and internal carotid arteries. The Bland–Altman method for the comparison with a traditional fingertip device showed Bias, precision, and accuracy root mean square error (ARMS) over a range of 70–100% significantly better for the nasal device: the mean bias for the alar and finger probes was 0.73% and 1.90% (P,0.001), respectively, the precision values of 1.65 and 1.83 and the ARMS values of 1.78% and 2.72%. Therefore, the feasibility and reliability of the nasal location is demonstrated.
- **Seifi et. al**[57] proposed as a possible site the earlobe, specifically indicated after heart surgery because of the perfusion and the deviation of SpO2 (Oxyhaemoglobin Saturation) and SaO2 (Arterial Oxygen Saturation). They confronted this location with the finger, the toe and the forehead in 67 patients admitted to intensive care units for coronary artery bypass surgery. The results obtained with the Bland-Altman statistical analyses showed the application of earlobe probes in patients admitted to the intensive care unit for coronary artery bypass surgery.
- **Senn et al.**[58] evaluated the accuracy of a novel earlobe device, TOSCA by Linde Medical Sensors, with the feature of monitor both ventilation and oxygenation by a single transcutaneous sensor and demonstrated its clinical application in a study with eighteen critically ill adult patients with acute respiratory failure or heart failure, and 12 patients with sleep apnoea. They compared this new technology with the standard fingertip device, and they showed comparable results between the two technologies with a faster response and a more accurate desaturation's detection for the earlobe device in sleep apnoea patients.
- **Tajkia et al.**[59] examined the accuracy of pulse oximeter oxygen saturation (SpO_2) for the infants on the wrist and ankle in comparison to the traditional location on the palm. The study, with 169 neonates (birth weight 2530.8±772.2 g, gestational age 36.7±3.9 weeks, mean age 7.7 days and age range 1-27 days), was conducted with two pulse oximeters and the SpO_2 was measured at 0 sec, then at 30 sec and at 1 min over the palm and ipsilateral wrist. After that the same procedure was repeated for assessing the ankle accuracy. The results presented a good correlation between SpO2

56 T. E. Morey, M. J. Rice, T. Vasilopoulos, D. M. Dennis, and R. J. Melker, "Feasibility and accuracy of nasal alar pulse oximetry," *Br. J. Anaesth.*, vol. 112, no. 6, pp. 1109–1114, 2014, doi: 10.1093/bja/aeu095.

57 S. Seifi, A. Khatony, G. Moradi, A. Abdi, and F. Najafi, "Accuracy of pulse oximetry in detection of oxygen saturation in patients admitted to the intensive care unit of heart surgery: Comparison of finger, toe, forehead and earlobe probes," *BMC Nurs.*, vol. 17, no. 1, pp. 1–8, 2018, doi: 10.1186/s12912-018-0283-1.

58 O. Senn, C. F. Clarenbach, V. Kaplan, M. Maggiorini, and K. E. Bloch, "Monitoring carbon dioxide tension and arterial oxygen saturation by a single earlobe sensor in patients with critical illness or sleep apnea," *Chest*, vol. 128, no. 3, pp. 1291–1296, 2005, doi: 10.1378/chest.128.3.1291.

59 G. Tajkia, M. Shirin, M. M. Hossain, and M. A. A. Mamun, "Accuracy of SpO2 measurements by placing probes on newborns' wrist and ankle," *Bangladesh Med. Res. Counc. Bull.*, vol. 45, no. 3, pp. 191–196, 2019, doi: 10.3329/BMRCB.V45I3.44651.

measured at the palm versus the wrist (r= 0.92, p<0.0001 (right); r= 0.88, p< 0.0001 (left)) and between SpO2 measured at the sole versus the ankle (r=0.90, p<0.0001 (right); r= 0.98, p<0.0001 (left)). The bias and precision for SpO2 at the right palm and right wrist was 0.08 ± 0.65% and for the left palm and left wrist 0.05 ± 0.79%. Similar results were obtained for SpO2 at the right sole and right ankle (0.11 ± 0.63%) and for the left sole and left ankle (0.56 ± 0.32%). Therefore, the study demonstrated that for infants SpO_2 can be clinically measure also on the wrist and ankle.

The main site remains the fingertip:

- **Adiptura et al**.[60] presented a light, wearable device for measuring oxygen saturation (SpO_2) with an error rate of ± 1.5%. The device is linked to a data processor and a cloud in which the data can be stored for further analysis. The consists of the hardware part of the finger sensor, the oximeter module for the measurement of the heart rate and oxygen saturation (SpO_2) and the MCU that allow to send the data via the internet both to the doctors and to the patients.
- **Ayance et al.[61]** designed and developed a wireless oxygen saturation monitor using low-cost microcontrollers using as a standard goal the commercial pulse oximeter MD300C2. The Bland-Altman method was used for the comparison between the measurements obtained from the two devices: the output showed a standard deviation of 0.0187%.
- **Banik et al.[62]** developed a wearable PO with a novel electronic circuit with an analogy filter that can separate red and green photoplethysmography (PPG) signals, acquire clean PPG signals, and estimate the pulse rate (PR) and peripheral capillary oxygen saturation (SpO_2). Two different algorithms were tested. One that does not consider the motion artifact and one that does. In the first case the mean absolute percentage error (MAPE) was 2.81%, the mean absolute error (MAE) 2.08, and reference closeness factor (RCF) was 0.97. In the second scenario instead with a finger the results were an average 4.5% MAPE,3.66 bpm MAE, 0.96 RCF, and 96.88% SpO_2 accuracy. Moreover, the comparison with the commercial devices showed better performances under motion condition of this novel technology that has many different possible applications as a wearable or hand-held device.
- **Niswar et al.[63]** introduced a low-cost wearable pulse oximeter connected to a smartphone to monitor the signals real time. This device is composed by two biomedical sensors (airflow thermal sensor and pulse oximeter sensor), a microcontroller (ATMEGA 328p), a wireless module (IEEE802.11)

60 R. R. Adiputra, S. Hadiyoso, and Y. Sun Hariyani, "Internet of things: Low cost and wearable SpO2 device for health monitoring," *Int. J. Electr. Comput. Eng.*, vol. 8, no. 2, pp. 939–945, 2018, doi: 10.11591/ijece.v8i2.pp939-945.

61 A. T. Ayance, H. S. Ramírez, J. M. R. Pérez, and C. G. T. Palacios, "Wireless heart rate and oxygen saturation monitor," *AIP Conf. Proc.*, vol. 2090, no. April, pp. 1–5, 2019, doi: 10.1063/1.5095913.

62 P. P. Banik, S. Hossain, T. H. Kwon, H. Kim, and K. D. Kim, "Development of a wearable reflection-type pulse oximeter system to acquire clean ppg signals and measure pulse rate and spo2 with and without finger motion," *Electron.*, vol. 9, no. 11, pp. 1–26, 2020, doi: 10.3390/electronics9111905.

63 M. Niswar, M. Nur, A. A. Ilham, and I. Mappangara, "A low cost wearable medical device for vital signs monitoring in low-resource settings," *Int. J. Electr. Comput. Eng.*, vol. 9, no. 4, pp. 2321–2327, 2019, doi: 10.11591/ijece.v9i4.pp2321-2327.

and a power supply. The system can measure heart rate, SpO_2 level, and respiratory rate of patient and determine the severity level of patient based on vital signs condition. A Wi-Fi module allows the transfer of the data between the device and a smartphone; therefore, the remote monitoring is possible. The evaluation of the accuracy in comparison to the standard SpO_2 of Nellcor OxiMax in Penlon SP M5 showed similar results, so the clinical application of this method was validated.

The most recently investigated location is the wrist:

- **Phillips et al.**[64] explored the reliability of SpO_2 sensing on this location with WristO2, a custom build device with an innovative algorithm specific designed for the wrist that considers for the output even the skin tone. The error is highly reduced, and the device provide a continuous monitoring of the Oxyhaemoglobin Saturation
- **Aleixo et al.**[65] presented BLOO2D, an ABS plastic bracelet that has a high resistance to fracture and water thanks to the properties of this material, therefore this system can be used in different situations. The activation of the device happens when it is near to the smartphone and this allow low consumption of battery. Future improvements can be on the ergonomic of the bracelet to better fix it on the wrist and on the wearability testing different materials.
- **Guber et al.**[66] compared the accuracy of the wrist pulsi oximeter Oxitone-1000 by Oxitone Medical with a traditional fingertip device. The study included Fifteen healthy volunteers and 23 patients with pulmonary disease (COPD) (N = 8), asthma (N = 6), sarcoidosis (N = 5) and others and the recordings were performed in sitting and standing positions. The results were comparable between the two devices: the mean SpO2 was 96.45% and the mean pulse was 74.64 for Oxitone-1000 and the mean SpO2 was 97.18% and the mean pulse was 74.64 for the fingertip sensor. Therefore, the Arms -Root mean-square-error was < 3% and they demonstrated the clinical application of the device which has also the property to have a high wearability and a user-friendly interface.
- **Pang et al.**[67] proposed a new technology that can be wear throughout the day without the inconveniences of the fingertip devices. The peculiar feature of this prototype is the unique design with a concave structure for housing the optical source and sensor. Furthermore, the device has a wireless communication with a smartphone.
- **Lee et al.**[34] explored an organic solution: a flexible patch composed by light-emitting diodes and organic photodiodes designed via an optical simulation of colour-sensitive light propagation within

64 C. Phillips, D. Liaqat, M. Gabel, and E. De Lara, "WristO2: Reliable Peripheral Oxygen Saturation Readings from Wrist-Worn Pulse Oximeters," *2021 IEEE Int. Conf. Pervasive Comput. Commun. Work. other Affil. Events, PerCom Work. 2021*, pp. 623–629, 2021, doi: 10.1109/PerComWorkshops51409.2021.9430986.

65 A. F. P. Aleixo, E. G. Lima, É. C. Leite, A. V. M. Inocêncio, L. T. Lins, and M. A. B. Rodrigues, *Wearable device for acquisition of spo2 and Heart Rate*, vol. 70, no. 1. Springer Singapore, 2019.

66 A. Guber, G. Epstein Shochet, S. Kohn, and D. Shitrit, "Wrist-Sensor Pulse Oximeter Enables Prolonged Patient Monitoring in Chronic Lung Diseases," *J. Med. Syst.*, vol. 43, no. 7, 2019, doi: 10.1007/s10916-019-1317-2.

67 G. Pang and C. Ma, "A Neo-Reflective Wrist Pulse Oximeter," *IEEE Access*, vol. 2, pp. 1562–1567, 2014, doi: 10.1109/ACCESS.2014.2382179.

human skin. The main advantage is the ultralow power consumption (24 mW on average) and this aspect can have an important impact for all-day wearable health monitoring technology.

- **Jarchi et al.**[68] We describe an evaluation of photoplethysmography (PPG) signals with two wavelengths channels (infrared and red) using a wrist-worn sensor for the estimation of heart rate variability (HRV) and oxygen saturation (SpO_2). Five healthy subjects were equipped with a commercial wrist-worn pulse oximeter (Wavelet Health, USA) on the right hand, and both a commercial smart watch for fitness use (Huawei Watch, Series 2) and a clinically validated transmission-mode pulse oximeter (Creative Medical PC-68B) on their left hand as a reference. Synchronised PPG signals from the Wavelet Health, the Huawei watch, and the PC-68B were recorded for approximately 10 minutes. Subjects were asked to leave the left hand in a resting state, while moving the right hand with two types of movement (periodic and random). A method is proposed to incorporate coupling information between the two wavelengths of PPGs based on the bivariate empirical mode decomposition algorithm. Our method is shown to improve the quality of red PPG allowing improved estimation of SpO_2. A comparison of average heart rate (HR), HRV, and SpO_2 from all devices is provided.

Finally, these devices can be divided based on the portability: Tabletop, Handheld, wearable depending on the different application of the technologies.

Figure 1 SPO2 monitoring systems

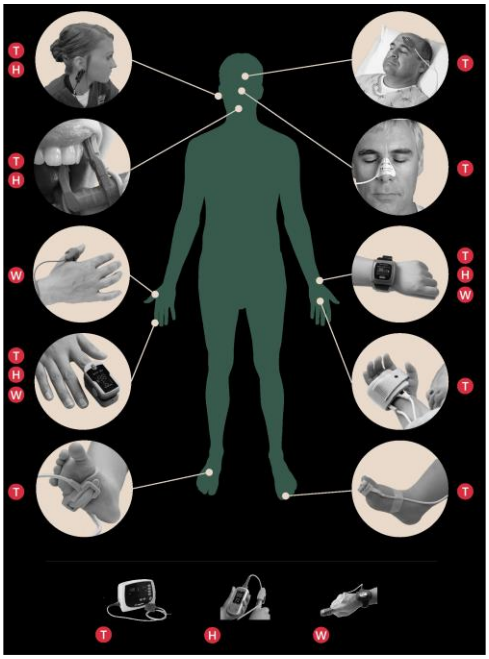

[68] D. Jarchi, D. Salvi, C. Velardo, A. Mahdi, L. Tarassenko, and D. A. Clifton, "Estimation of HRV and SpO2 from wrist-worn commercial sensors for clinical settings," *2018 IEEE 15th Int. Conf. Wearable Implant. Body Sens. Networks, BSN 2018*, vol. 2018-Janua, no. March, pp. 144–147, 2018, doi: 10.1109/BSN.2018.8329679.

Purpose of the work

This study has as its main objective the development of a methodology applicable to most devices for the detection of vital parameters. The first objective is to be able to interconnect devices of the same type so that they provide simultaneous data in particular for ECG detection. This would allow the possibility of interconnecting multiple devices of the same type, providing more information on the patient's health status. Furthermore, this approach could also be applied to devices that detect different parameters.

The second objective is to demonstrate the accuracy of the results obtained and, if the tested device is accurate from the outset, the use of several devices of the same type simultaneously must also be accurate.

The third objective is the validation of the methodology using typically industrial statistical techniques, such as the sigma score, in order to make the analysis projected towards production.

The application of this methodology would allow the simultaneous use of devices already on the market or the design of new devices and their interconnection as well as their connection to telemedicine platforms for the remote evaluation of patients' vital parameters.

From this point of view, it is not necessary to design new and more complex devices but having available those already present in hospitals or simply at home, provided they are validated as accurate at an outpatient level, it would be possible to monitor more parameters and make them available to physicians.

This methodology gives the chance to evaluate different types of devices for different scope and use those that are most in line with the patient's needs, making the results available in real time.

Methods and Materials

Sensors tested: ECG

BMD101 CardioChip - NeuroSky

BMD101 is a bio-signal detection and processing System on Chip (SoC) device containing an analog front-end (AFE) circuitry and a digital signal processing structure. The AFE measures a differential analog input signal, from the electrodes, and processes it using a high pass filter (0.5 Hz) and a low noise amplifier. This output is converted to bits using a 16-bits ADC.

The digital signal processing receives the digital bits stream from the ADC, applies two filters: notch filter (50-60Hz reject electrical network noise) and low pass filter (100Hz). The filtered bits stream is formatted and sent through a serial communication interface (UART).

Figure 2 Neurosky Cardiochip (BMD101 Module)

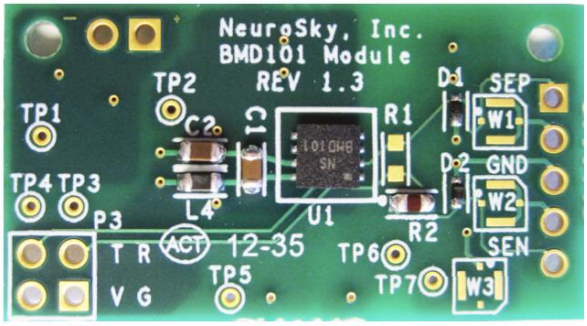

Figure 3 I/O Pins configuration

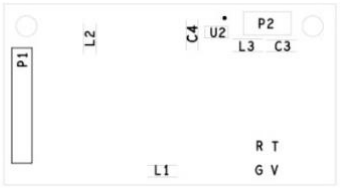

VIEWED FROM TOP SIDE

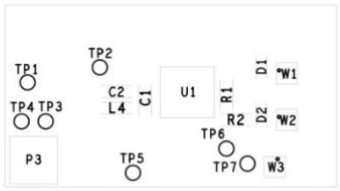

VIEWED FROM BOTTOM SIDE

Sensor Connections (Micro-Coaxial Receptables)

W1: ECG Sensor “SEP”
W2: Reference Sensor “SEN”
W3: Ground Sensor (not populated) GND

Sensor Connections (Thru-hole)

P1

Header P2 (Battery input)

Pin1: VCC “+”
Pin2: GND “-”

Header P3 (U1 Power/serial)

Pin1: RXD “R”
Pin2: TXD “T”
Pin3: GND “G”
Pin4: VCC “V”

Outputs:
There are 2 outputs that can be obtained from the module. Both outputs use standard UART serial protocol, which uses the following settings:
Baud rate: 57,600
Data Bits: 8
Parity: None
Start Bits: 1

Tested configurations:
The configuration of the cardiochip, based on the electrical datasheet, requires fixing in place 2 electrodes to measure the differential signal between them. The three limb leads were recorded each at a time, the image below corresponds to DI.

Figure 4 D1 lead

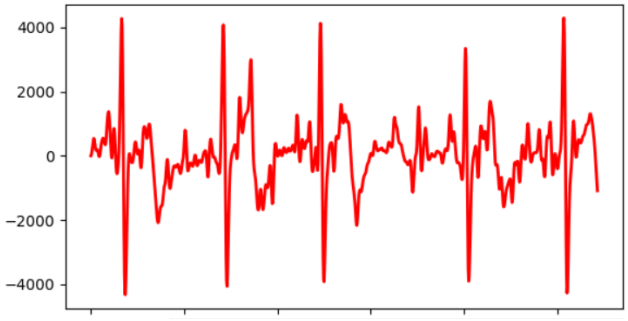

The output values for the peripheral's derivations are good but need some additional filtering to obtain a clear signal for each one. The main disadvantage of this configurations is that it will require three different BMD101 chips and each one will need a microcontroller or serial interface to extract the data, moreover, the wiring between the tree modules is not easy to manage and can generate external noise due to bad contact of the electrodes.

The second configuration corresponds to the connection of the module in two near points for each limb, to obtain the augmented limb leads (aVR, aVL, aVF). In this case, the distance between the electrodes affects the measurement of the augmented limb leads. The image below shows the different configurations to measure the aVL, the first one correctly measures the lead, but for configurations 2 and 3 the signal is too weak and the BMD101 is not able to measure it. Moreover, the first configuration is still uncomfortable due to wiring between the electrodes and the module.

Figure 5 Different configurations

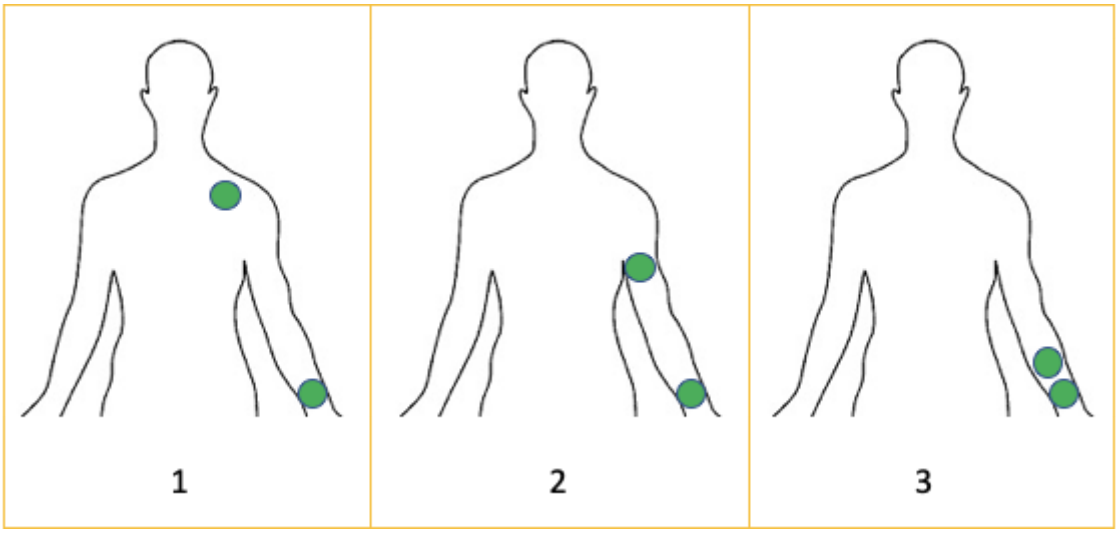

Prototype

After analyzing different types of devices, it was decided to test an outdated commercially available battery powered device.

The device is applied to the chest to acquire, register, and transmit physiological parameters by using a wireless connection on the Bluetooth protocol. Dedicated software is included with the device to gather the acquired signals and filtering them in the desired way.

Figure 6 Device pins configuration

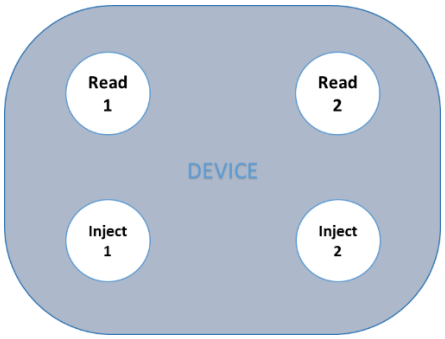

The $read_1$ and $read_2$ pins are connected to the ECG electrodes. The $inject_1$ and $inject_2$ pins are used for bioimpedance measurement.

Pin $inject_2$ provides an internal voltage reference (V_{ref}) that normally is applied to the body and received by $inject_1$, to measure the bioimpedance. In this case, $inject_2$ is used as a voltage reference applied to the body.

Tested configurations:

Using the pulse device's V_{ref}, it is possible to define a voltage reference for all the limb leads. The following image shows the configuration using three different devices, the first devices measure the D_I lead and provides the V_{ref} for all the others leads, meanwhile, two more devices are used to measure the a_{VR} and a_{VF} leads using only the $read_1$ and $read_2$ input from the device, without using a voltage reference.

Figure 7

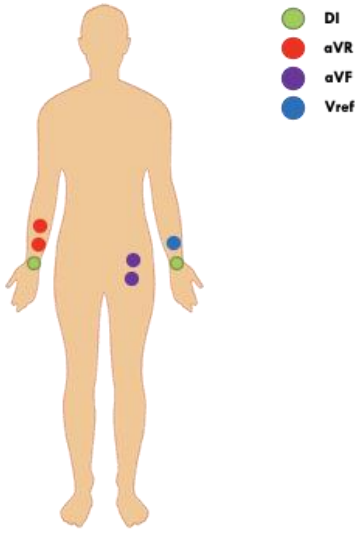

Data extracted from dedicated app:

Figure 8

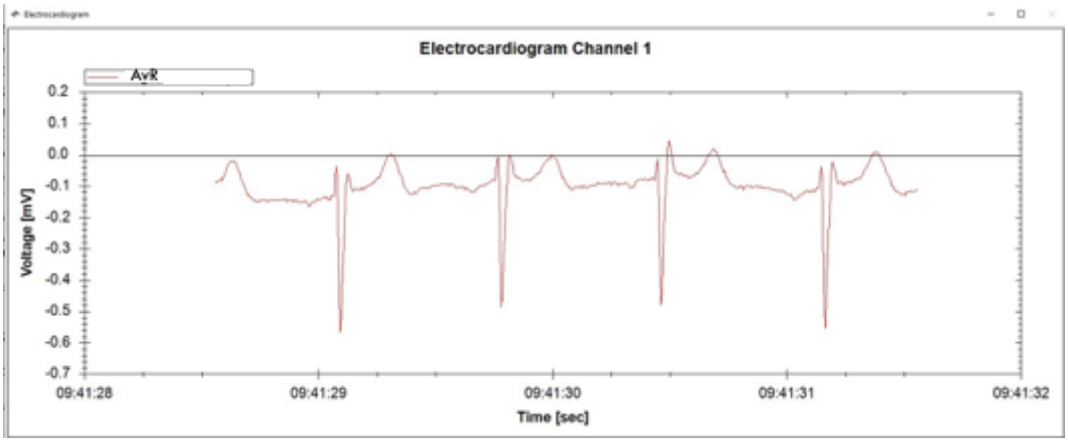

Figure 9

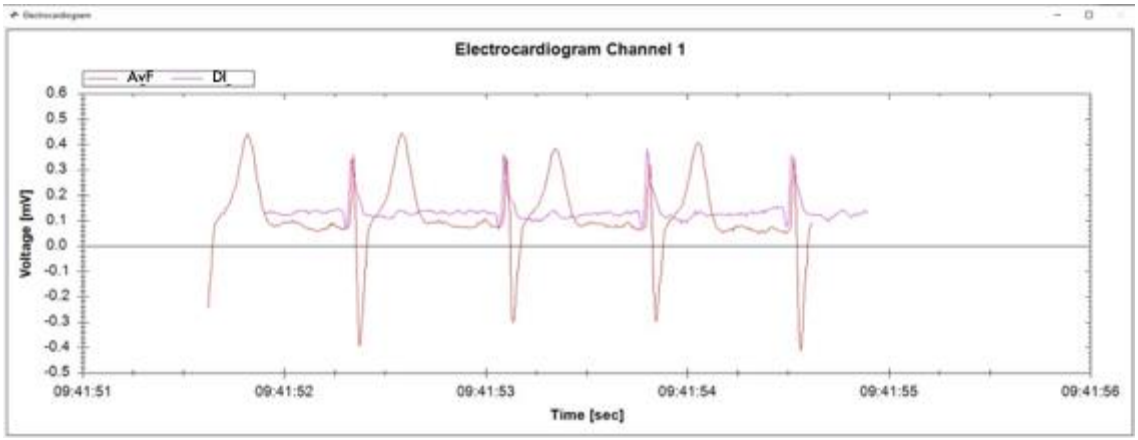

Raw Data extracted:

All the Bluetooth packets, received from the STMicroelectronics app, are stored as raw data. The following images show the raw values, using a sampling frequency of 250Hz.

Figure 10

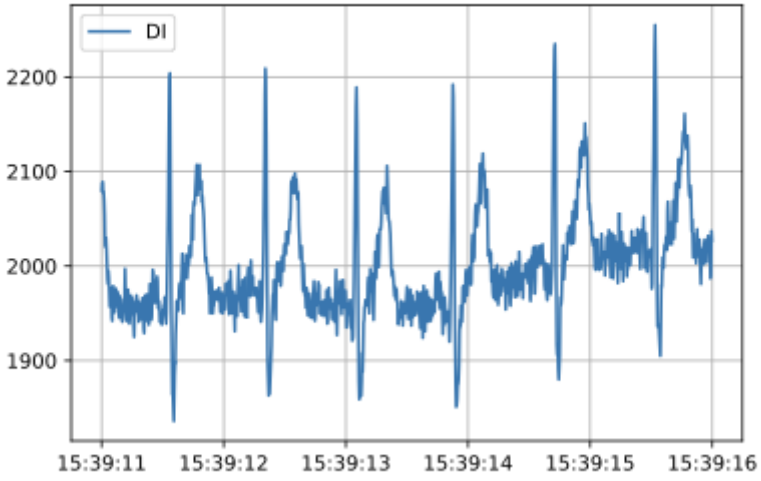

Figure 11

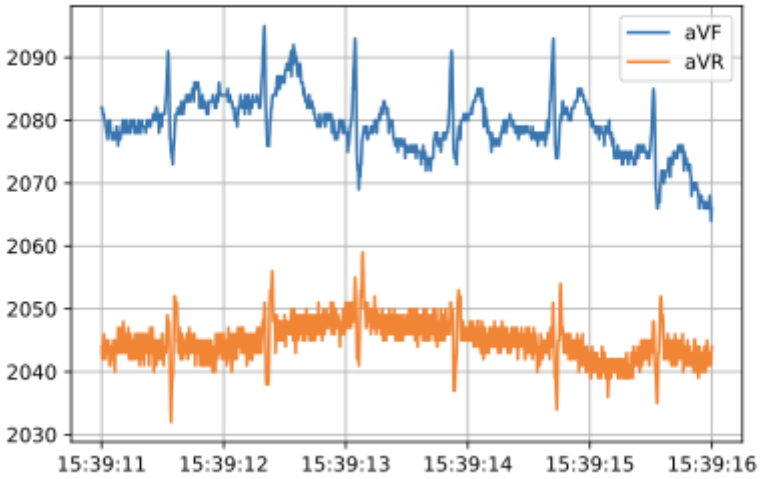

Data extracted and filtered by our filter:

From the raw data, it is possible to apply customized filters to obtain a clean signal. In this case, three different filters were applied: notch filter, low pass filter, and high pass filter.

Figure 12

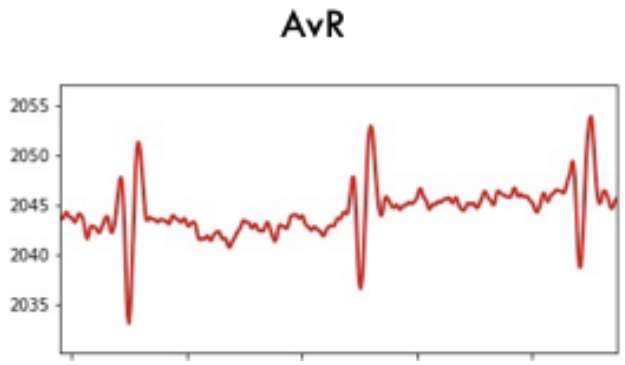

Figure 13

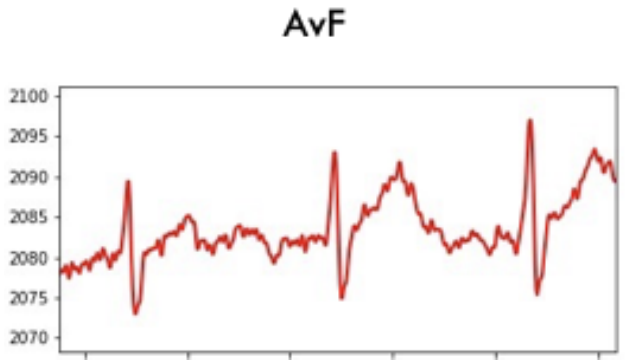

Figure 14

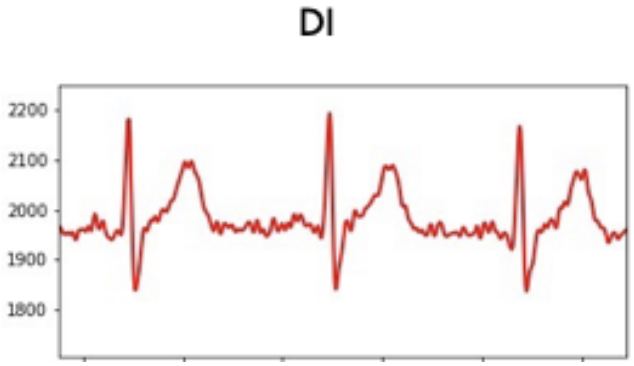

Sensors tested: BP and SpO_2

ADPD1081Z-PPG

ADPD1081Z is a photometric front-end with an optimized discrete optimal design for vital signs monitoring applications. The evaluation board (see Figure 15) is optimized for wrist-based photoplethysmography (PPG) measurements and provides three green light emitting diodes (LEDs) and a 7mm2 photodiode. The reflectance mode is used as shown in Figure 16.

Figure 15 ADPD1081Z evaluation board

Figure 16 Photoplethysmography

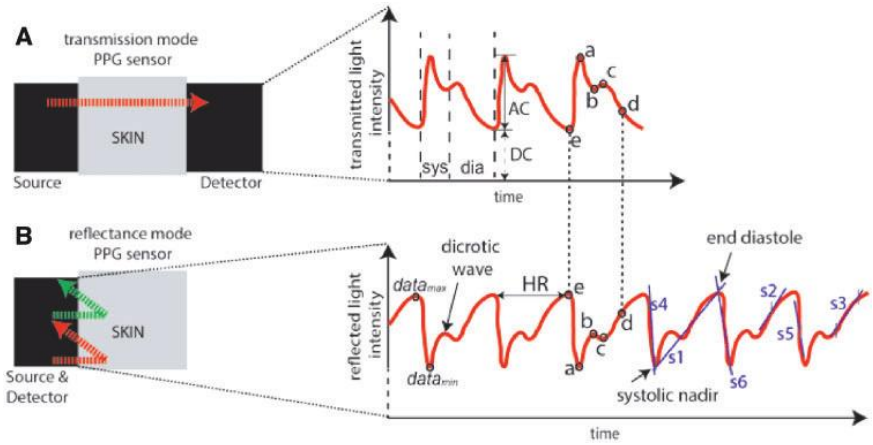

Acquiring data: The APDP1081Z is intended for wrist-based PPG measurements. Figure 17 depicts the raw data acquired by the evaluation board.

Figure 17 Raw data

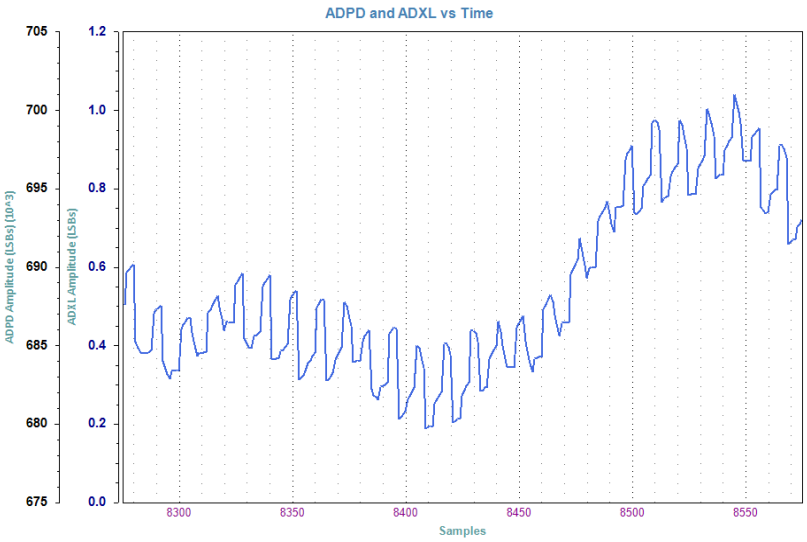

Two different filters can be applied to the raw data. The first one is a filter used to compute the heart rate in beats per minute (BPM). Figure 18 contains the output signal for the PPG_BP filter.

Figure 18 PPG_BP filter

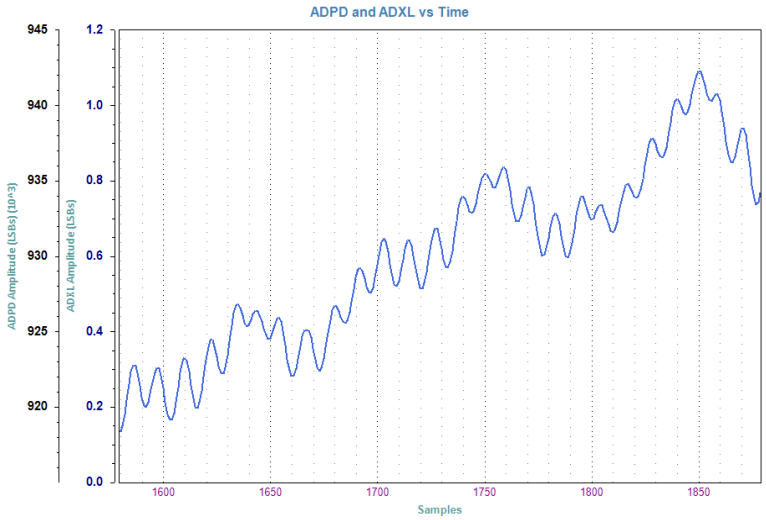

The second one corresponds to a Digital biquad filter, that is a second order recursive linear filter (see Figure 19).

Figure 19 Biquad filter

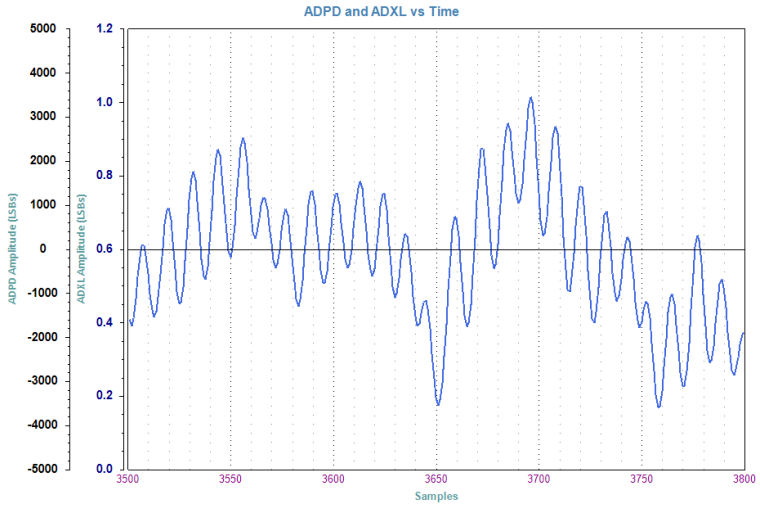

PPG (ADPD1081Z) and ECG (Prototype)

Using the PPG and ECG signals, it is possible to compute the Pulse Transit Time (PTT) that is a Cuff-less method to measure, indirectly, the Blood Pressure (BP).

Figure 20 Pulse Transit Time to measure BP

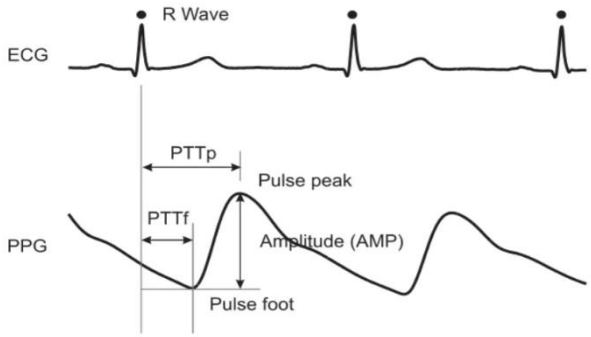

First of all, the R peak is detected in the ECG signal. Using this time as reference, the maximum and minimum are detected from the PPG signal, in this way the PPTp and PTTf times are measured (see Figure 20).

Figura 21 PTT intervals using D1 and PPG raw data

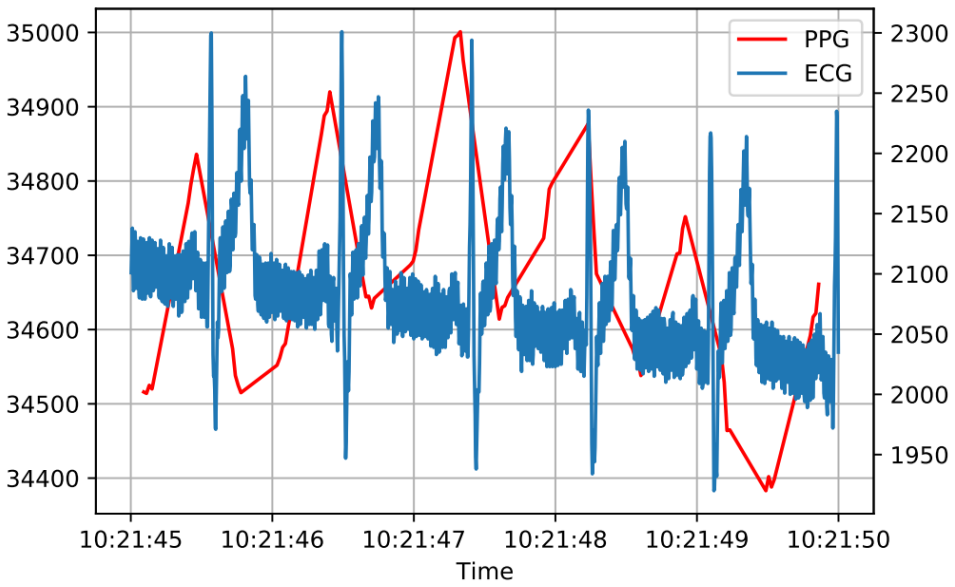

Figure 21 contains the ECG for the D1 derivations obtained by the Pulse Device and the PPG raw data measured by the APDP1081Z.

Peak detection

From the recorded signal, the main task is to detect the peaks. There are different peak detection algorithms that can be implemented, most of them consider parameters such as peak width, peak prominences, periodicity and other parameters that can be tuned to improve the algorithm performance, avoiding false positives.

Figure 8 depicts the peak detected in the ECG signal; in this case the maximum values correspond to the R wave.

Figure 22 ECG peak detection

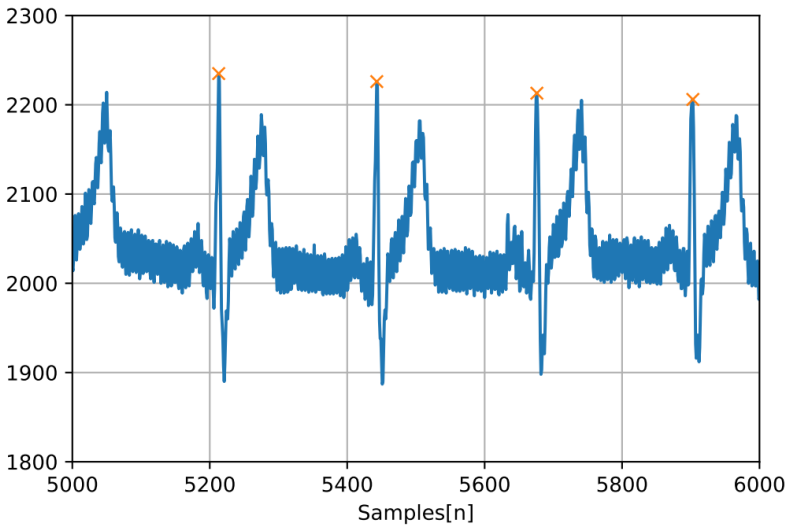

Inverting the PPG signal and implementing the same algorithm, it is possible to detect the minimum values. Figure 23 contains the max and min values in the PPG signal. In this case some max values are not detected properly, and some min values are detected shifted in time. This kind of variation in time or miss detections can generate errors in the blood pressure measurement.

Figure 23 PPG peak detection

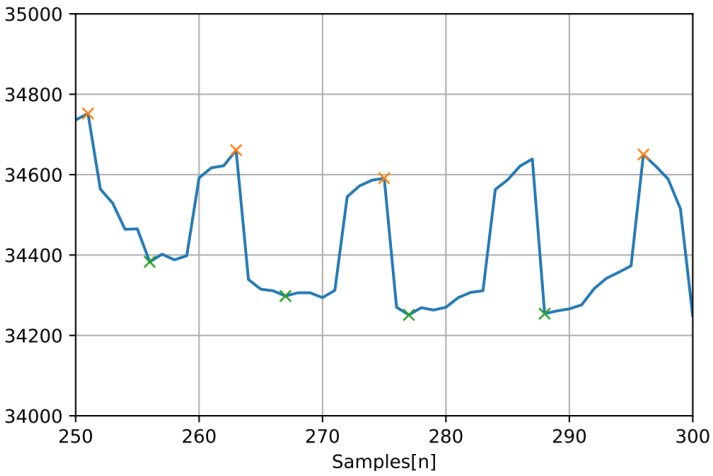

Using the peaks detected in Figure 22 and Figure 23, the PTTp and PTTf times can be computed as shown in Figure 24. These values contain some errors or variations due to wrong peak detection, however these times can be post processed to obtain a stable value. Finally, the characterization of the PTTp and PTTf times can be done in order to obtain the Systolic and Diastolic blood pressure values.

Figure 24 Systolic and diastolic blood pressure

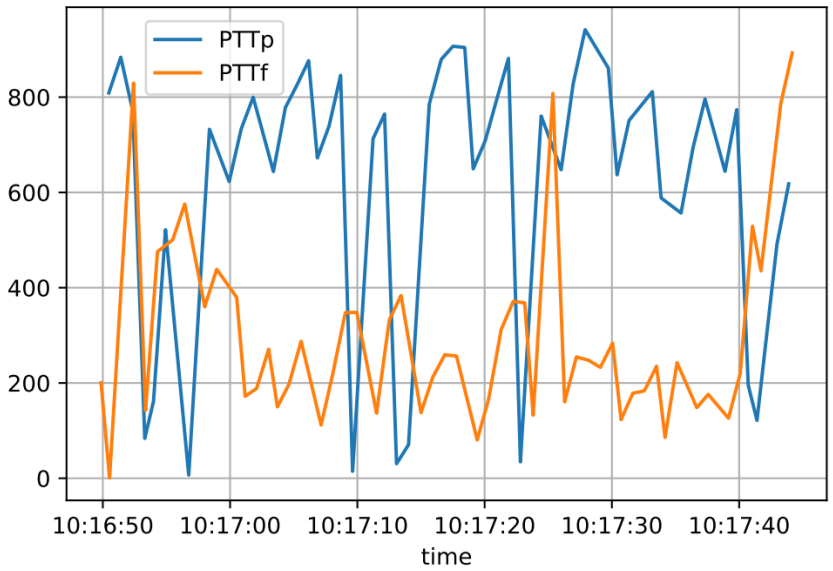

PPG - MAX30102

MAX30102 is a complete pulse oximetry and heart rate sensor system solution module designed for wearable devices. MAX30102 integrates Red and InfraRed LED drivers to modulate LED pulses for PPG measurement in two different wavelengths.

Figure 25 PPG using Red and IR LEDs

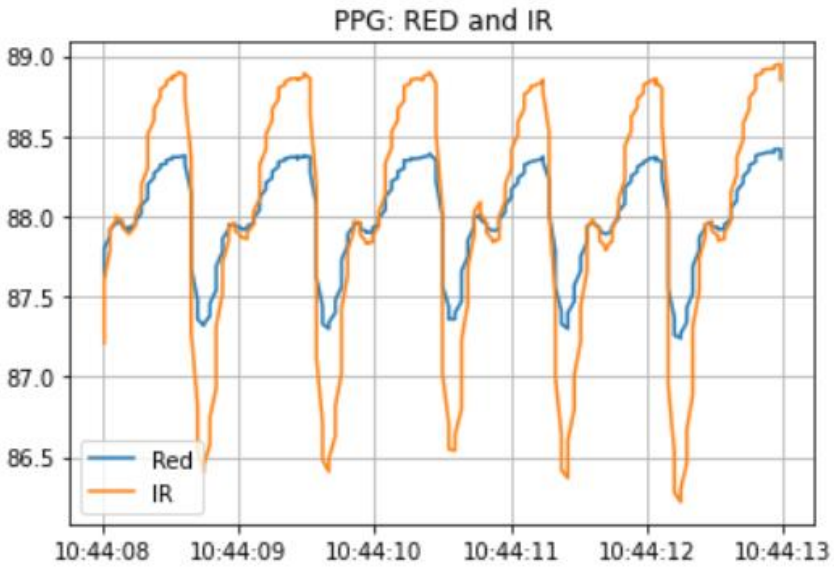

PPG (MAX30102) and ECG (Pulse)

Using the PPG and ECG signals, it is possible to compute the Pulse Transit Time (PTT) which is a Cuff-less method to measure, indirectly, the Blood Pressure (BP).

Figure 26 Pulse Transit Time to measure BP

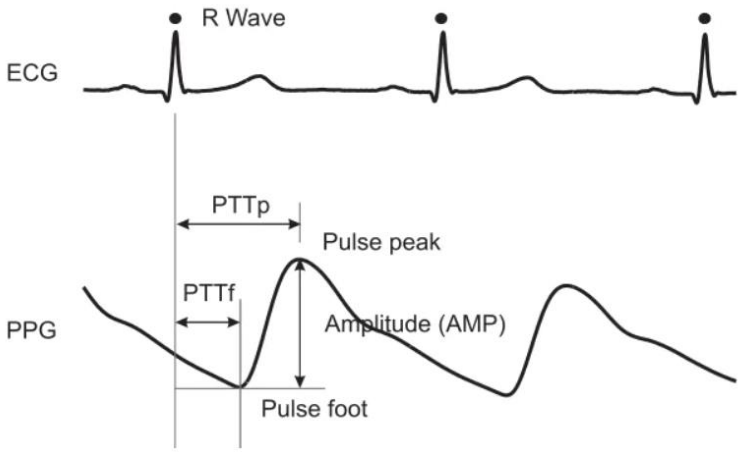

First of all, the R peak is detected in the ECG signal. Using this time as a reference, the maximum and minimum are detected from the PPG signal, in this way the PPTp and PTTf times are measured (see Figure 26).

Figure 27 PTT intervals using D1 and PPG raw data

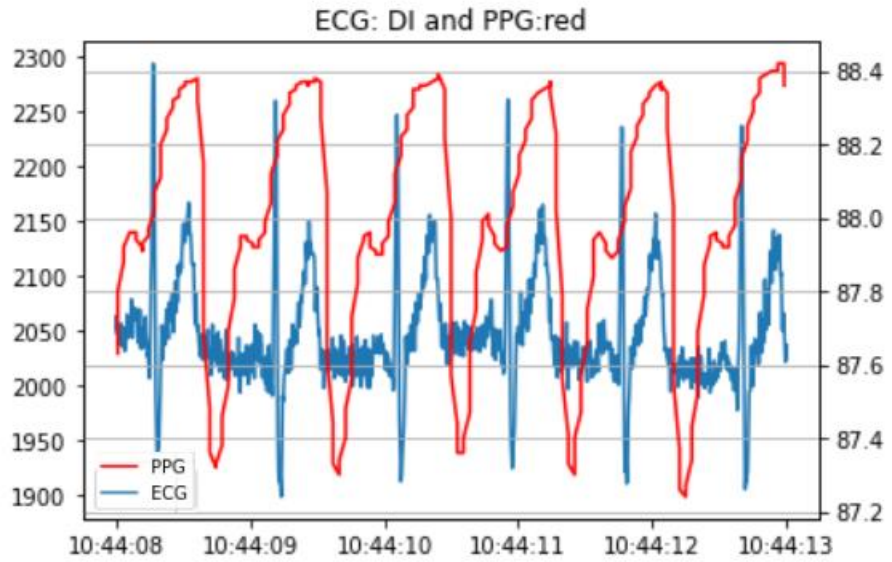

Figure 27 contains the ECG for the D_I derivations obtained by the device and the PPG raw data measured by the MAX30102 using the Red LED.

Peak detection

From the recorded signal, the main task is to detect the peaks. There are different peak detection algorithms that can be implemented, most of them take into account parameters such as peak width, peak prominences, periodicity and other parameters that can be tuned to improve the algorithm performance, avoiding false positives.

Figure 28 depicts the peak detected in the ECG signal, in this case the maximum values correspond to the R wave.

Figure 28 ECG peak detection

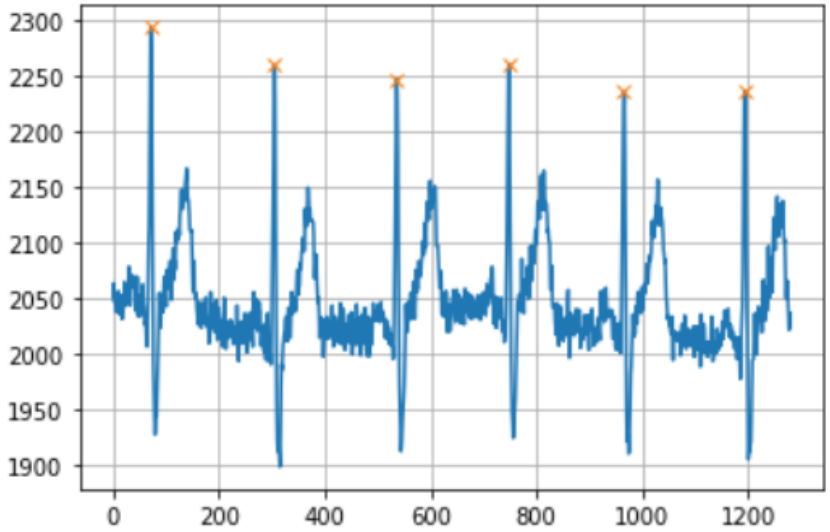

Inverting the PPG signal and implementing the same algorithm, it is possible to detect the minimum values. Figure 8 contains the max and min values in the PPG signal. In this case some max values are not detected properly and some min values are detected shifted in time. This kind of variation in time or miss detections can generate errors in the blood pressure measurement.

Figure 29 PPG peak detection

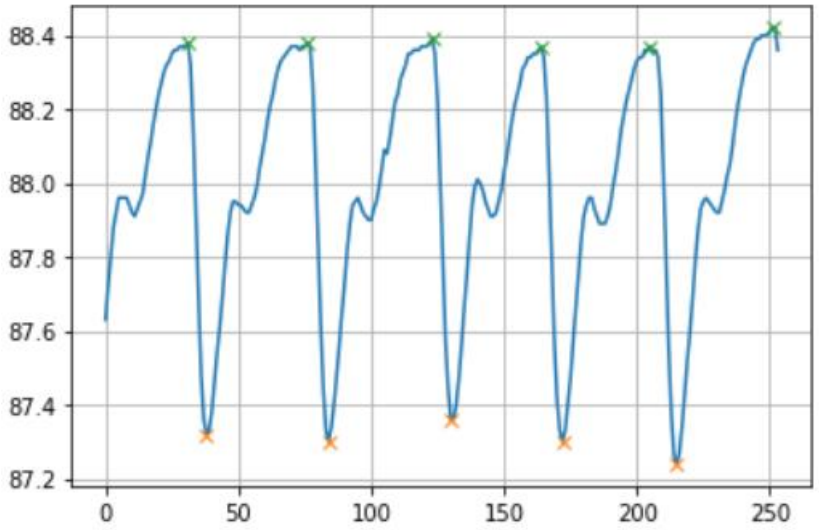

Using the peaks detected in Figure 28 and Figure 29, the PTTp and PTTf times can be computed as shown in Figure 30. These values contain some errors or variations due to wrong peak detection, however, these times can be post-processed to obtain a stable value. Finally, the characterization of the PTTp and PTTf times can be done in order to obtain the Systolic and Diastolic blood pressure values.

Figure 30 PTTp and PTTf times

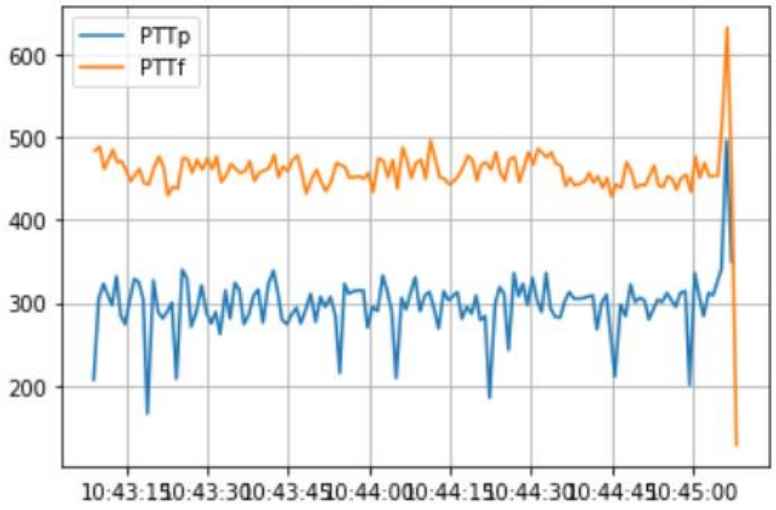

PPG (MAX30102), SpO_2 and Heart Rate

Peripheral oxygen saturation (SpO_2) is an estimation of the oxygen saturation level. SpO_2 estimation is based on the Red light and IR light absorption characteristics of oxygenated hemoglobin (HbO_2) and deoxygenated hemoglobin (Hb). MAX30102 flashes both lights alternately to the finger and measures the non-absorbed light from each LED.

The SpO_2 estimation is given by a look-up table, from empirical values, usually based on calibration curves derived from different measurements of healthy subjects at various SpO_2 levels. In this case, SpO_2 is estimated using the formula:

$$SpO_2 = 100 - 23.3(R-0.4)$$

Where R is a ratio between the PPG measurements from Red and IR LEDs.

$$R=\frac{ACRed/DCRed}{ACIR/DCIR}$$

Where AC corresponds to the Vrms value and DC is the average value, for the Red and IR PPG signals.

Using the PPG signal is also possible to estimate directly the heart rate. Figure 10 depicts the estimated SpO_2 and HR.

Figure 31 SpO_2 and HR

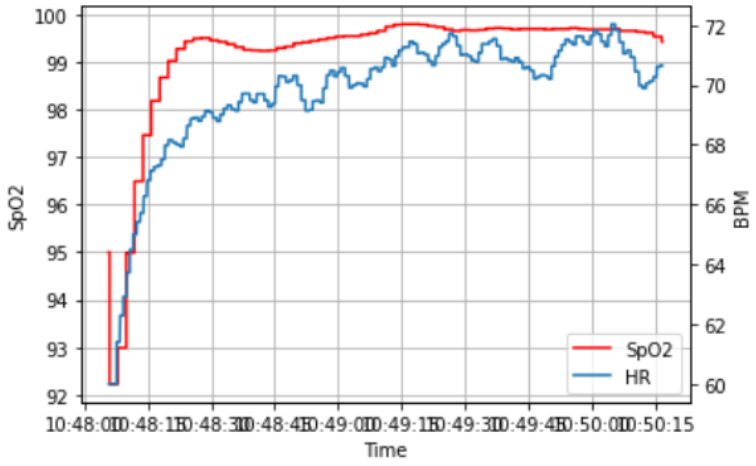

In vitro measurements

Clinical tests were conducted in a controlled environment to evaluate the results by comparing them to measurements obtained with standard detection systems used in the outpatient setting.

The first tests were conducted on a special "EP-David" simulation system. The simulation system consists of an anthropomorphic dummy in which the cardiac anatomy of an adult male in good health and the ribs have been 3D printed starting from the specially redesigned CT images of a real patient.

Figure 32 3D Print of cardiac anatomy and ribs of a real patient

Cardiac conduction was simulated by delivering stimuli using a Phantom 320 ECG pulse generator on the reconstructed heart muscle. The 3D heart was then submerged in a saline solution to better simulate the conduction inside the human body. The case of the prototype was fixed on this system, visible in the following images:

Figure 33 EP-David simulation system

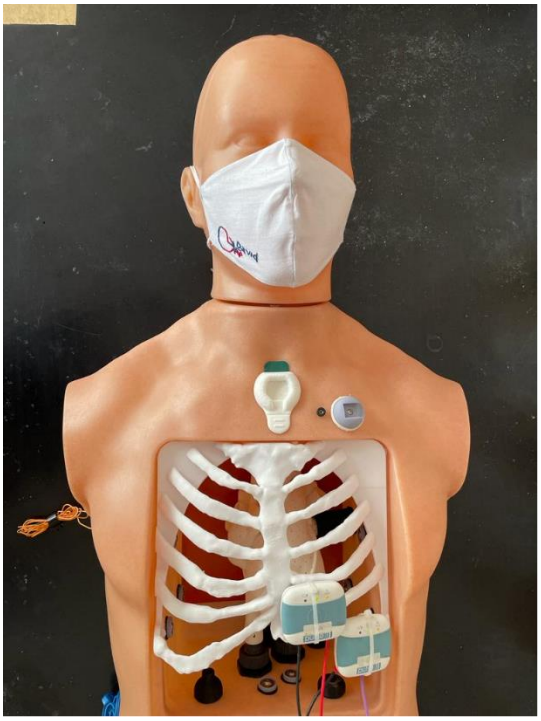

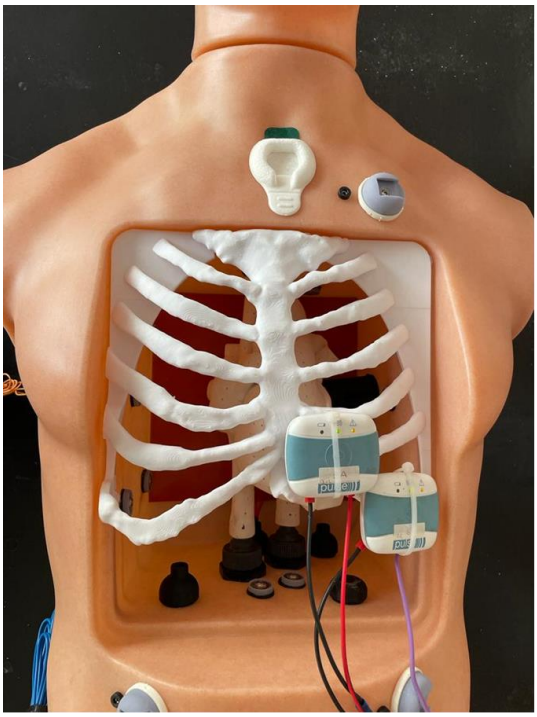

Two different measurements were carried out in order to evaluate the correspondence between the parameters detected with the prototype and the waveforms sent via the Phantom 320 ECG pulse generator. First of all, the Hantek 6022BL oscilloscope was connected to the generator with a Notch filter interposed for the 50-60 Hz frequencies. The oscilloscope detected the ECG tracings referring to three different rhythms, as shown in the images below:

- Sinus Rhythm

Figure 34 Sinus Rhythm

- Atrial Flutter

Figure 35 Atrial Flutter

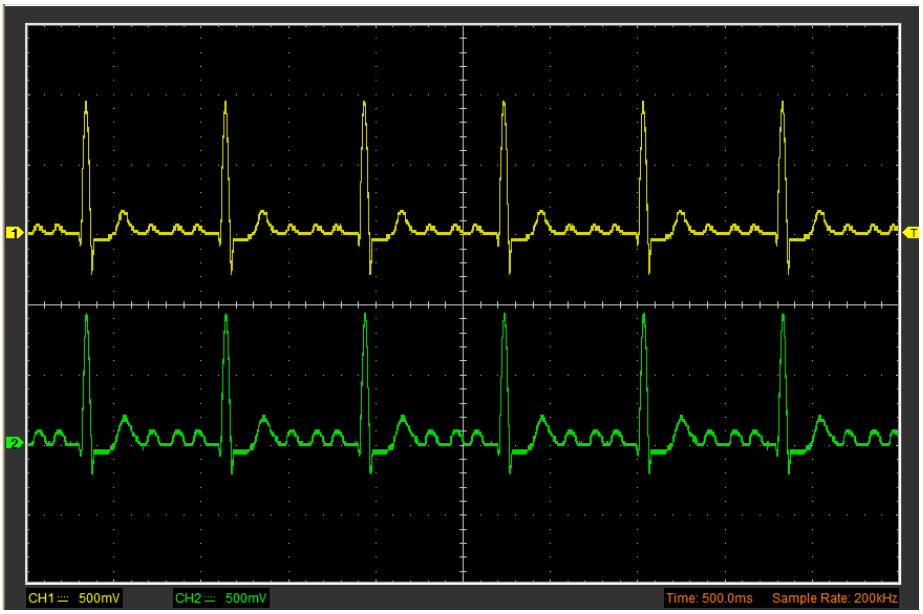

- Atrial Fibrillation

Figure 36 Atrial Fibrillation

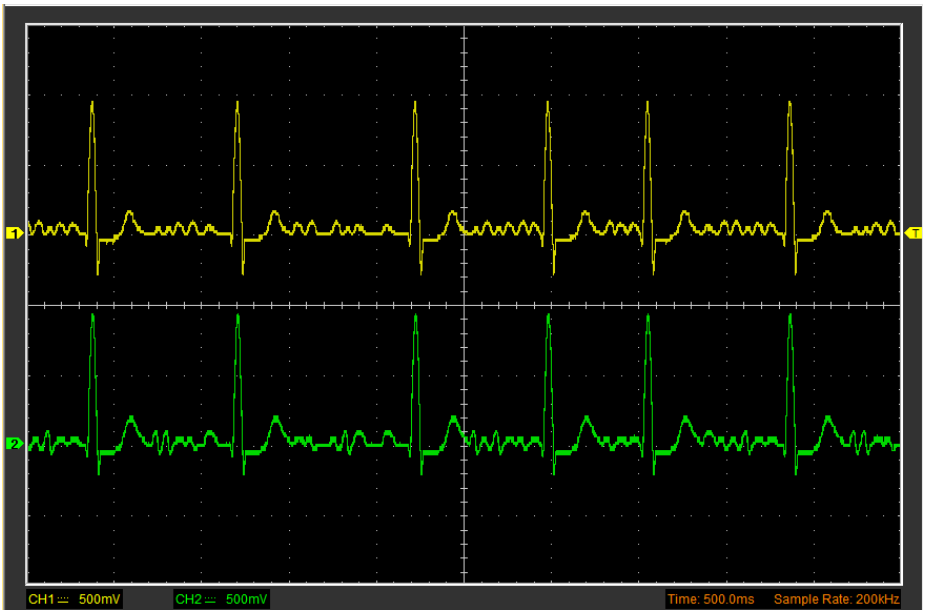

Then the pulse generator was connected to the EP-David Simulator and measurements were carried out using the prototype. The results are shown below:

- Sinus Rhythm

Figure 37 Sinus Rhythm

- Atrial Flutter

Figure 38 Atrial Flutter

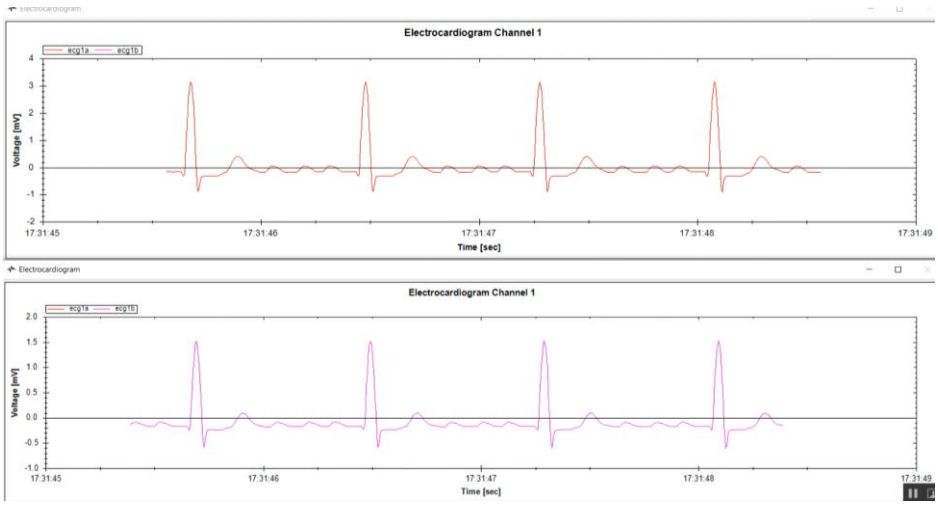

- Atrial Fibrillation

Figure 39 Atrial Fibrillation

The acquired data was considered accurate and identical, in both measurements, to the data sent via the pulse generator. Therefore, the test conducted in a controlled environment was positively evaluated and we moved on to the next phase.

In order to verify the functionality of the system in vivo, a prototype was developed consisting in a case to be applied on the patient's chest in correspondence with leads V_1 and V_2 and a system for detecting lead D_1 containing the chip for simultaneous determination of BP and SpO_2.

Figure 40 First prototype

After having made a specific informed consent form for the management and storage of patients' personal data, a protocol was created to be followed in the phase of acquisition of the parameters (which took place simultaneously with the determination of the same values using traditional methods) and below briefly reported:

Manuale di istruzione per la configurazione dei dispositivi e l'acquisizione dei segnali ECG e SPo2 / PPG.

Materiale:

- **Cartella zip, MCL_EP_SW.zip**

Istruzioni:

1. Decomprimere la cartella MCL_EP_SW. Al suo interno si trovarono 2 cartelle: ***ECG e SOP2_test***.
2. **Collegamento dei sensori:**

   2.1. Pulsometro:

   Collegare la scheda ESP32 mediante il cavo USB

   Considerare:

   Se il dispositivo non viene riconosciuto (Warning), è necessario scaricare il driver ***CP210x USB to UART Bridge VCP Drivers***, mediante il seguente link **https://www.silabs.com/developers/usb-to-uart-bridge-vcp-drivers** .

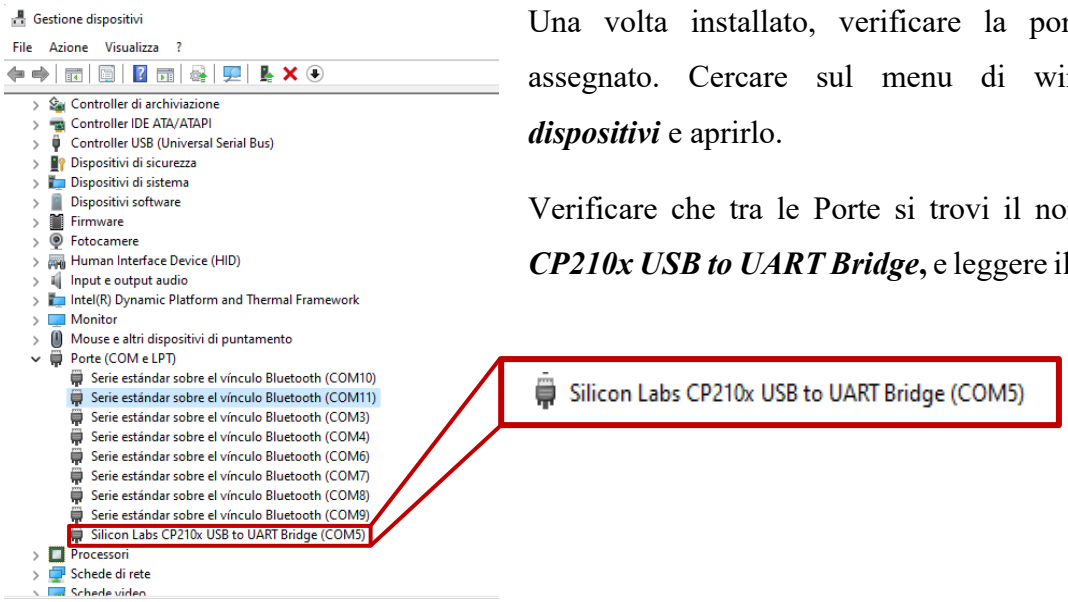

Una volta installato, verificare la porta a cui viene assegnato. Cercare sul menu di windows ***gestione dispositivi*** e aprirlo.

Verificare che tra le Porte si trovi il nome Silicon Labs ***CP210x USB to UART Bridge***, e leggere il numero di porta.

2.2. ECG:

2.2.1. Collegamento bluetooth dei tre dispositivi **"Pulse"**:

Per accendere il dispositivo mantenere premuto il bottone al centro fino a che si accendano dei tre led. Una volta fatto, aprire sul PC l'opzione di Bluetooth per collegarli.

I dispositivi sono chiamati *Pulse Sensor*, per collegarli selezionare la opzioni di ***aggiungi dispositivo***.

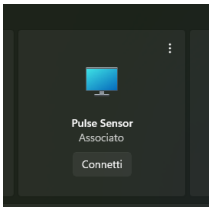

3. Programma:

3.1. ECG: BodyGatewayApp.

Nella cartella ECG aprire l'app *.exe* Lanciare due volte la app al fine di avere due interfacce aperte. Per verificare il corretto collegamento dei dispositivi, nella parte superiore della finestra di programma devono comparire i tre dispositivi.

4. Acquisizione dei dati

4.1. Nella Cartella SPO2_test, aprire il file Excel ***PPG_SPO2_TEMPLATE.*** Una volta aperto, apparirà un'interfaccia chiamata PLX-DAQ.

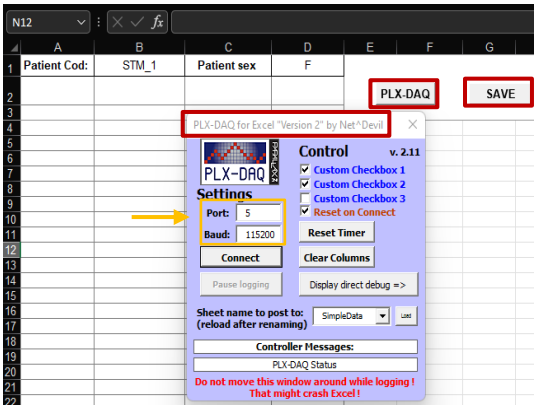

4.2. Spostare la finestra per potere visualizzare i due pulsanti, PLX-DAQ e Save.

4.3. Completare le due richieste di informazione: prima assegnare un codice al paziente **STMxx** (Questo nome non può contenere spazi); e inserire il sesso(F/M).

Nota: È importante la verifica del nome del paziente perché con questo nome viene creata la cartella per salvare la informazione acquisite; se non si cambia il nome, la cartella precedente sarà sovrascritta.

4.4. Nel pannello dell'interfaccia **PLX-DAQ,** inserire il numero della porta verificata nel secondo passo e impostare **115200** come **Baud**.

4.5. Si consiglia di aspettare che i segnali dell'elettrocardiogramma siano in una condizione relativamente stabile per cominciare a prelevare l'informazione.

4.6. Nel Panel dell'ECG, selezionare l'opzione di **Start Session.** Farlo per ciascun sensore e per le due interfacce. Una volta, selezionato nella finestra Electrocardiogram appariranno i segnali ECG.

4.7. Per dare inizio all'acquisizione dei dati nel Panel, premere la opzioni di **Monitoring** per tutti i dispositivi.

Questo fermerà la visualizzazione dei segnali sulla finestra Electrocardiogram.

Acquisire i segnali per il tempo desiderato (si consiglia 30 sec/1 minuto)

Ritornare al file Excel e premere il pulsante ***Connect***. Questo farà sì che il programma inizi a riempire le righe e colonne con l'informazione del pulsometro e del PPG.

4.8. Per finalizzare l'acquisizione **PRIMA** fermare l'acquisizione del pulsometro, premendo il pulsante ***disconnect.*** Dopodiché, ritornare al programma e premere il pulsante **Stop Session.**

5. Salvataggio dei dati:

5.1. Sul file Excel premere il pulsante **SAVE.** Questo creerà una cartella all'interno della cartella. All'interno si troverà il file **.txt** con l'informazione acquisita (tempo, ir_assorbimento, red_assorbimento e SPo2).

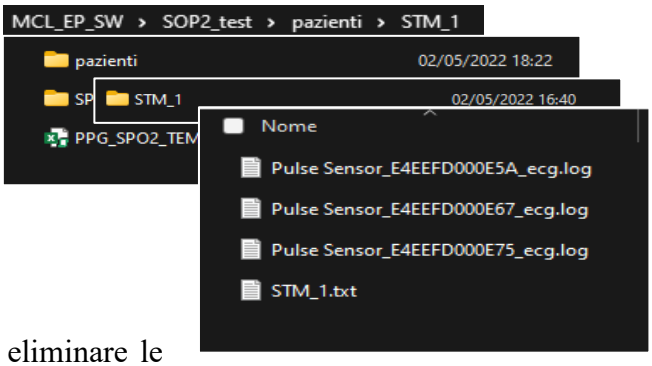

5.2. Salvati i dati, chiudere tutti i programmi ed eliminare le cartelle create all'interno della cartella **log,** e premere il pulsante del **clear columns** nell'interfaccia **PLX-DAQ.**

5.3. Procedere all'acquisizione del nuovo paziente.

In vivo measurements

A trial was conducted to assess the efficiency and the effectiveness in using our prototype.

The measurements (ECG, BP and SpO_2) were conducted using both our system and an outpatient equipment of proven efficiency and accuracy.

The prototype was used on a sample of 16 patients, 9 males and 7 females, without cardiac pathologies.

The prototype has three leads available (V_1, V_2 and D_1) and the ambulatory equipment has 12 leads available (complete ECG). The placement of the electrodes is shown in the figure below (figure 41):

Figure 41 Leads position

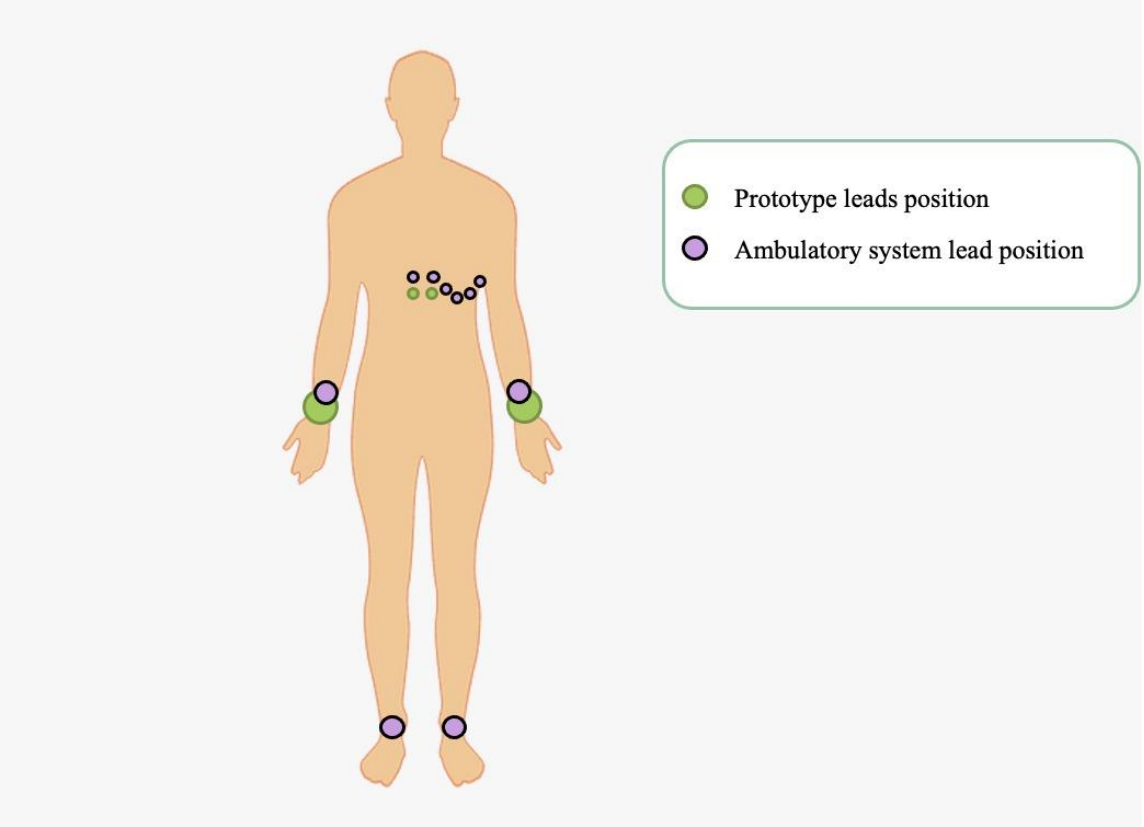

As it is easy to see, it was not possible to overlap the electrodes, therefore, the electrodes of the prototype were positioned about one centimeter below those of the conventional system. This determined a constant and known variation of amplitude that we will find in all the analyzed traces.

For each patient we correlated two data points for each ECG lead:

Prototype

A high pass filter (1-3 Hz) was applied to eliminate the error due to detection tremor and respiratory movements:

```
%%%%%%%%%%%%%%%%%%%%%%%%%%%%%%%%%%%%%%%%%%%%%%%%%%%%%%%%%%%%%%%%%%%%%%%%%%%%
%%%%%%%%%%%%%%%%%%%%    Waveform analysis    %%%%%%%%%%%%%%%%%%%%%%%%%%%%%
%%%%%%%%%%%%%%%%%%%%%%%%%%%%%%%%%%%%%%%%%%%%%%%%%%%%%%%%%%%%%%%%%%%%%%%%%%%%

bpm_teor = 73;                % bpm ECG exam acquired
PR = 220;  PR = PR*1e-3;      % (ms) PR + half of the qrs interval duration
QTc = 430; QTc = QTc*1e-3;    % (ms)

load('DI.mat');
ecg_create = DI;

signal = load("../ecg_d_5A")';

%signal = -signal;   % for v1
freq= 256;           % frequency of data acquisition
```

```
delta_t = 1/freq;

% Acquisition parameter data
n_bit = 12;             %
range_dinamic = 20e-3;  % Dinamic Range +- 10mV
ris = range_dinamic/(2^n_bit-1);

signal = ris*signal;

t =0:delta_t:length(signal)*delta_t - delta_t;

figure(1)
plot(t,(signal-mean(signal))./1e-3)
grid minor, xlabel('Time(s)'), ylabel('Amplitude(mV)')
title('device original signal D_1')   %
```

```
x = signal - mean(signal);      % signal without mean
fc = 1/delta_t;                 % sample frequency
Tw = 5;                         % length in seconds of the considered window
Nw = Tw*fc;                     % Number of samples in the considered window (if not set, =fc/risteor)
risteor = fc/Nw;                % teory resolution (se non imposta, = fc/Nw)
risapp = risteor;               % apparent resolution
NFFT = fc/risapp;               % PSD number of point

[Pxx,f]=pwelch(x, boxcar(length(x)), 0, NFFT, fc);

figure(2)
plot(f,Pxx./max(Pxx))
grid minor, xlabel('(Hz)')
title('Frequency component of the signal')
```

```
fNy = fc/2;
wp = 3/fNy;           % frequenza di taglio
ws = 1/fNy;           % stopband corner frequency
rp = 1;               % ripple (in genere 0.5)
rs = 15;              % attenuation a ws

[n, wn]=buttord(wp, ws, rp, rs);
[b, a]=butter(n, wn, 'high');       % low, bandpass, high, stop

figure()
freqz(b,a,512,fc)

signal_filter = filtfilt(b,a,signal);

figure(3)
plot(t, signal_filter./1e-3)
hold on
plot(t, (signal-mean(signal))./1e-3)
grid minor, xlabel('Time(s)'), ylabel('Amplitude(mV)')
legend('Filter signal', 'signal')
title('device signal compare after High filter')
```

Figure 42 Prototype device original signal

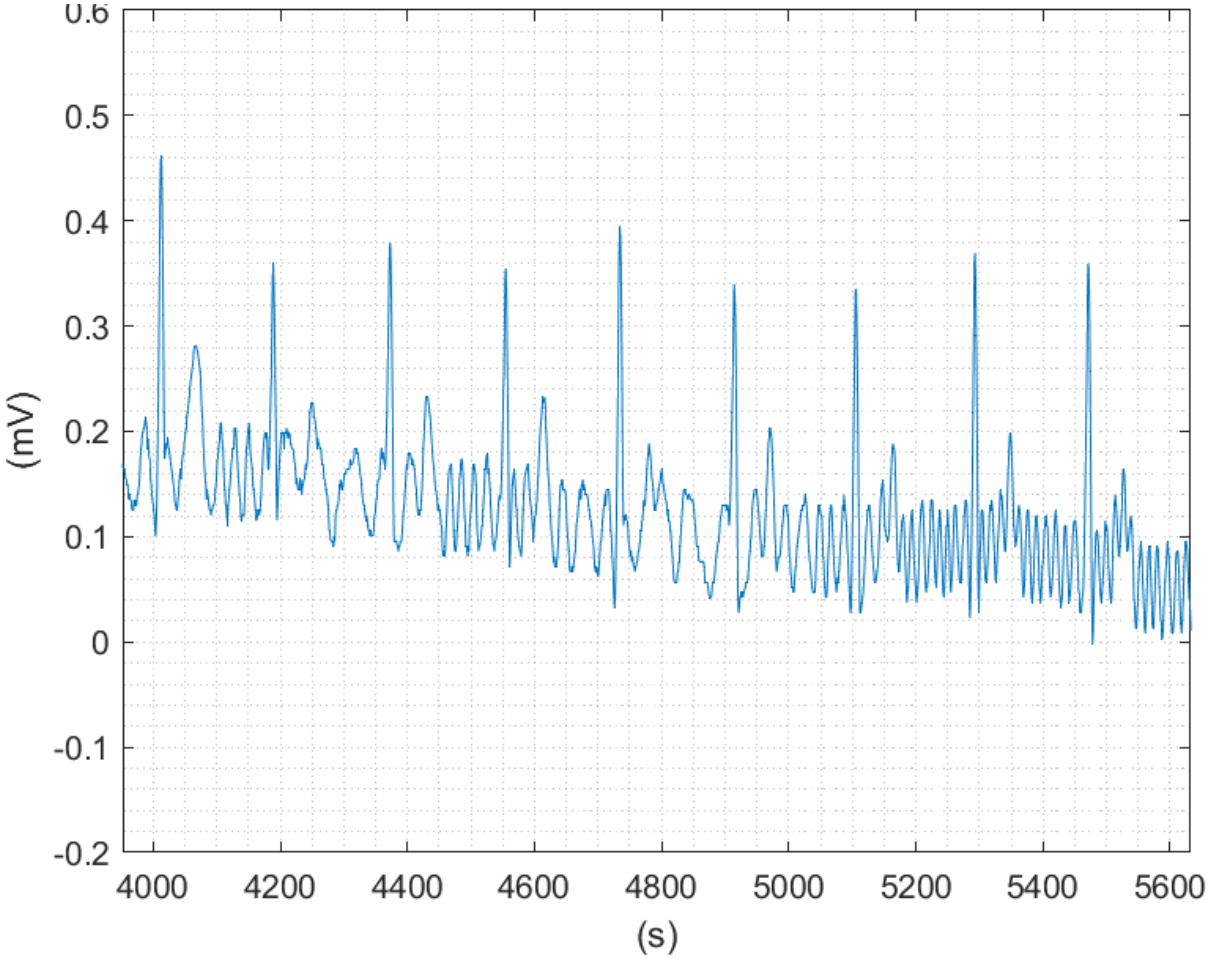

Figure 43 Prototype device original signal after high filter application

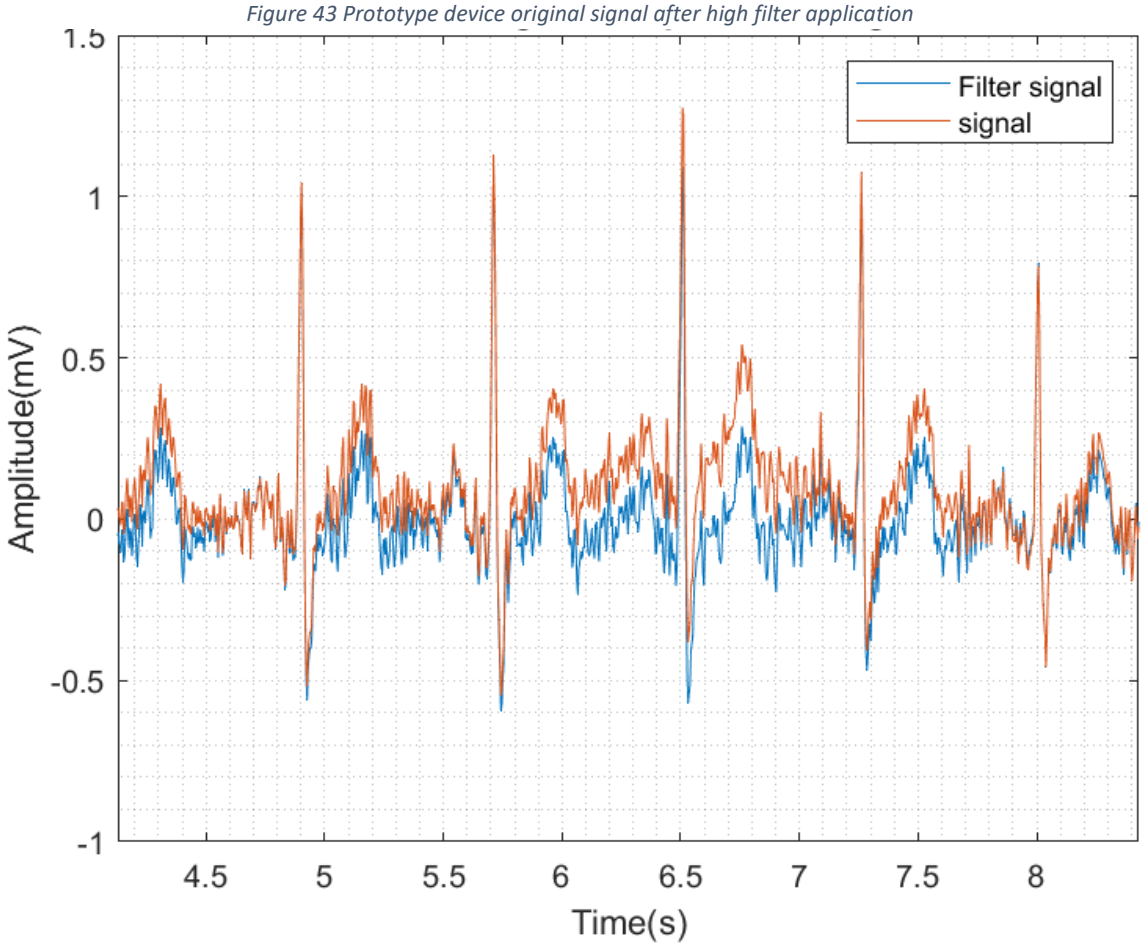

Once the signal has been cleaned up from the basic noise and considering the heartbeat periodicity in sinus rhythm of a healthy patient, the R peaks have been identified because they have a higher amplitude and are easily recognizable:

Figure 44 R-R segment identification

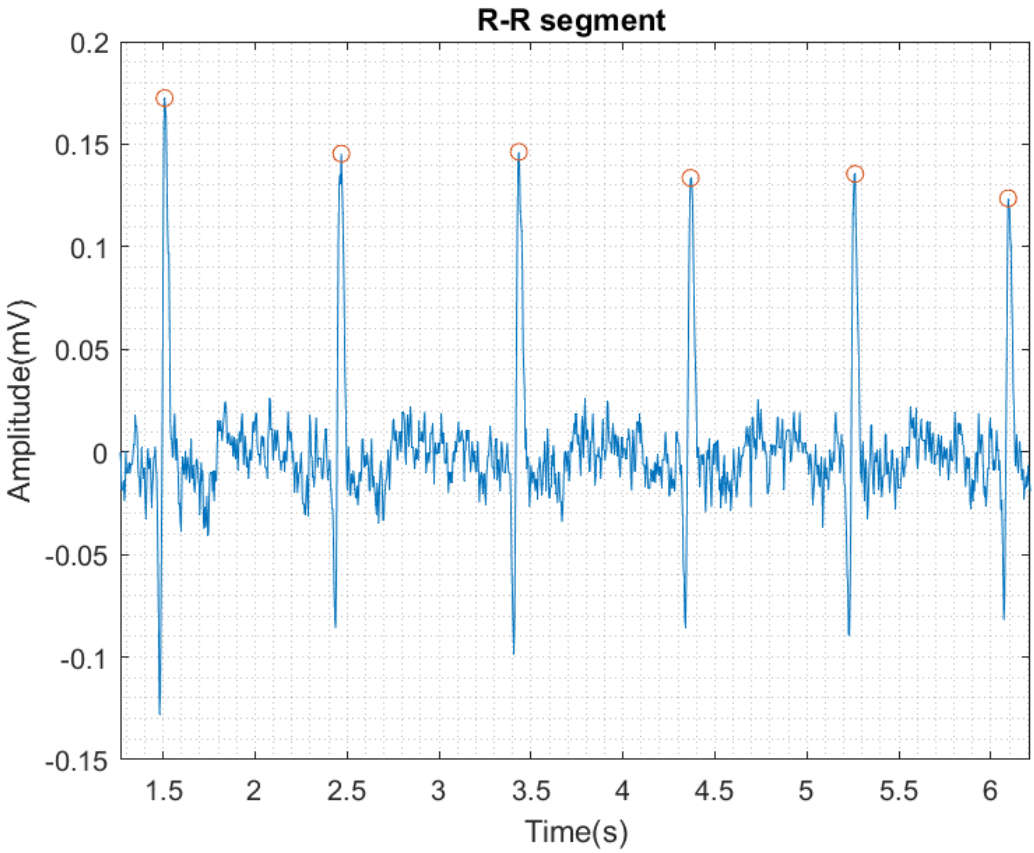

An average filter was applied which, by superimposing the window of identified signals beat by beat, allows to eliminate all the values that are different between beats and therefore to identify the trend of the curve:

```
[pks, locs] = findpeaks(signal_filter,(1/delta_t), 'MinPeakDistance',0.5);

figure(4)
plot(t,signal_filter./1e-3)
hold on
scatter(locs,pks./1e-3)
grid minor, xlabel('Time(s)'), ylabel('Amplitude(mV)')
title('R-R segment ')

duration_period = PR+QTc;   %(s)
signal_average_epoch = [];

for i=1:length(pks)-2
    signal_average_epoch = [signal_average_epoch; ...
        signal_filter(find(t>= locs(i+1)-duration_period/2,1,'first'):...
        find(t>= locs(i+1),1,'first') + round((QTc)/delta_t)-1)];
%
%     plot(mean(signal_average_epoch), LineWidth=1.5)
%     xlabel('s'), grid minor
%     title(['Averaged potential - Epoch ', int2str(i)])
%     figure(5)
%     pause(0.5)
%     drawnow
end
```

```
t_one_heartbeat = 0:delta_t:delta_t*(length(signal_average_epoch) -1);

figure(5)
plot(t_one_heartbeat, (signal_average_epoch./1e-3)')
grid minor
xlabel('(s)')
ylabel('(mV)')
title('ECG signal each epoch acquired')

signal_average = mean(signal_average_epoch,1);
mean_error = std(signal_average_epoch,0,1)./sqrt(i);

curve1 = (signal_average + mean_error);
curve2 = (signal_average - mean_error);

color = [0.1992 0.1602 0.4727];
color_std= [0.5725 0.7098 0.8438];

figure()
plot(t_one_heartbeat, curve1./1e-3, 'color',  color_std)
hold on
plot(t_one_heartbeat, curve2./1e-3, 'color',  color_std)
hold on
t2 = [t_one_heartbeat, fliplr(t_one_heartbeat)];
inBetween = [curve1./1e-3, fliplr(curve2./1e-3)]';
fill(t2', inBetween', color_std, 'Edgecolor',color_std)
hold on
plot(t_one_heartbeat, signal_average./1e-3, 'color', color, 'LineWidth', 0.5)
grid minor
xlabel('(s)')
ylabel('(mV)')
title('Average Heartbeat & error curve')
```

Figure 45 ECG signal each epoch acquired

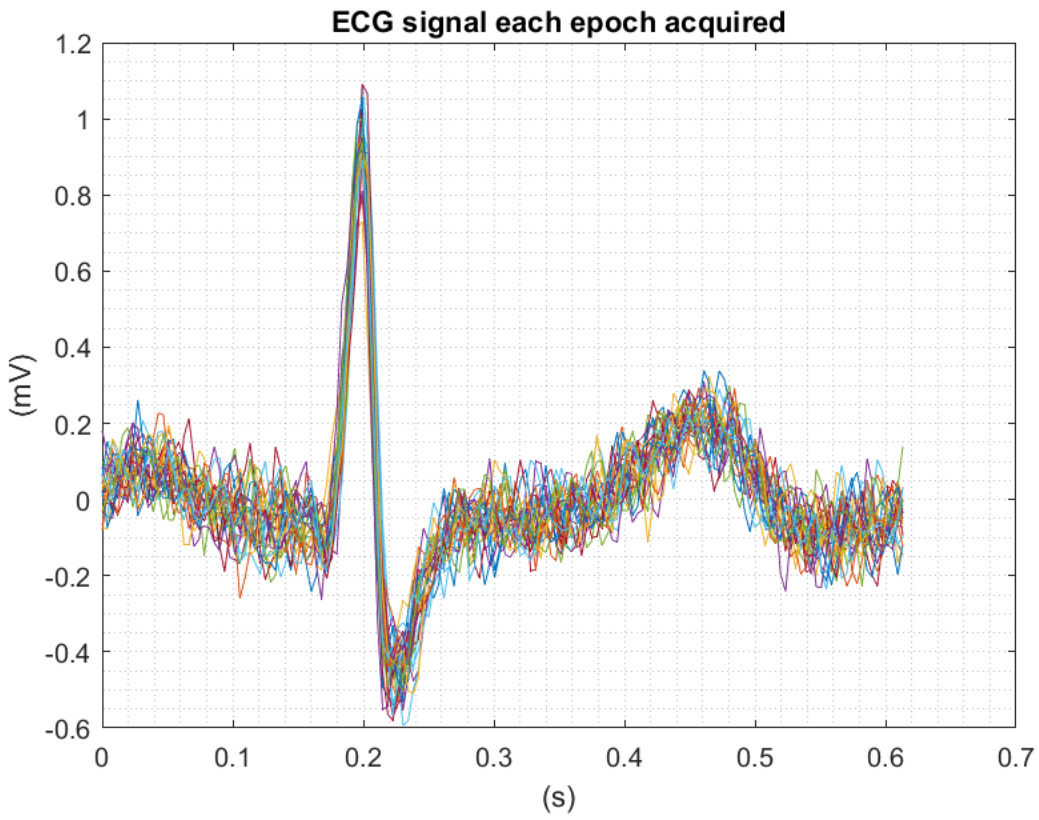

This procedure was applied to all signals recorded by the prototype and to each patient.

Outpatient System

The ECG tracing detected by the outpatient system required manipulation in order to make it comparable with the signal detected by the prototype.

The signals were provided to us in PDF and to make them digital and therefore reproduce a graphical representation we reported the numerical values of the waves and ECG intervals within the code. The counting of the individual points on the track was carried out with a manual technique which introduced a random error which could not be eliminated but which was taken into consideration during the analysis.

Figure 46 Original ECG

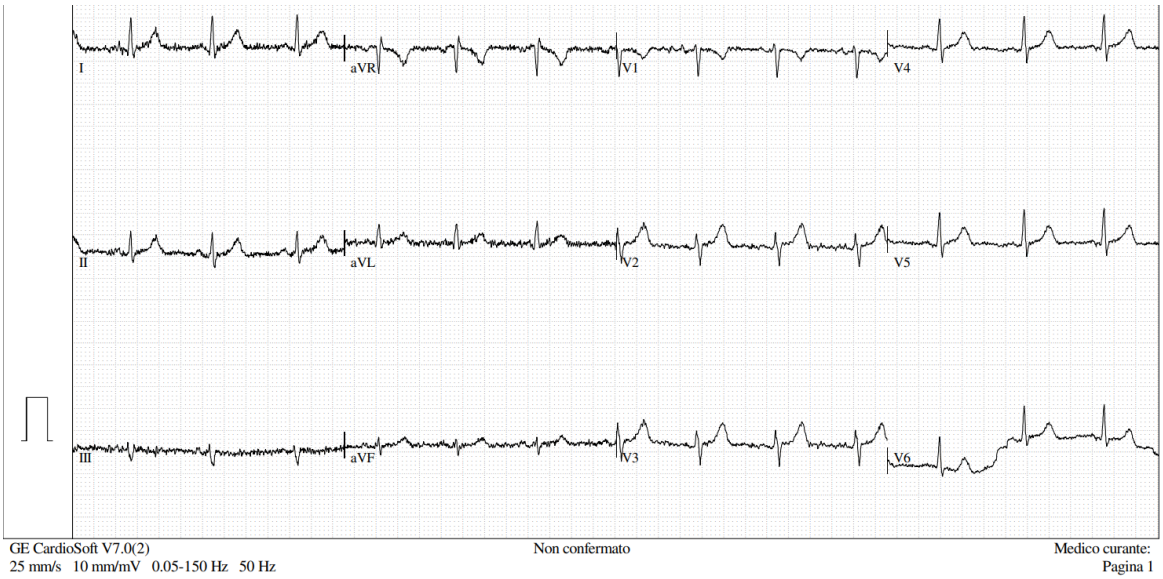

Figure 47 Values calculated from ECG

The amplitude and frequency reproduced are faithful to the measurements taken while the error introduced only concerns the graphic representation of the waveform which could in some cases be similar but not perfectly superimposable.

```
div_sec = 40;        % for mm in seconds  --> 25mm/s = 1mm/40ms (ms)
div_amp = 0.1e-3;    % for mm in mV  --> 10mm/mV = 1mm/0.1mV
```

```
len_signal= 692;     % one second(ms)
delta_T = 4;         % sample time (ms)

P = 104;         %(ms) base onda P
PR = 140;        %(ms) duration PR interval PR
QRS = 98;        %(ms) Complex QRS
QT = 388;        %(ms) base QT / QTc 435
ST = 120;        %(ms) obtained by counting the squares of the ECG

% entered sigma a according to std
sigma_OndaP = 30;
sigma_OndaT = 30;

amp_OndaP = div_amp*(0);
amp_OndaT = div_amp*(-1);
amp_vp_QRS =div_amp*[0.5 -5.5 0];

% Parameters to be entered according to the ECG : V1 - V2 - I
[t,V1] = genSignalecg(div_sec,delta_T, len_signal, P, PR, QRS, QT, ...
    ST,amp_OndaP,amp_OndaT,amp_vp_QRS,sigma_OndaP, sigma_OndaT);

gaussian_rumore = randn(1,length(t))*div_amp./12;

amp_OndaP = div_amp*( 0.5 );
amp_OndaT = div_amp*( 3);
amp_vp_QRS =div_amp*[2 -5 0];

[~,V2] = genSignalecg(div_sec,delta_T, len_signal, P, PR, QRS, QT, ...
    ST,amp_OndaP,amp_OndaT,amp_vp_QRS,sigma_OndaP, sigma_OndaT);

amp_OndaP = div_amp*( 0 );
amp_OndaT = div_amp*( 0 );
amp_vp_QRS =div_amp*[0 1 -1];

[~,DI] = genSignalecg(div_sec,delta_T, len_signal, P, PR, QRS, QT, ...
    ST,amp_OndaP,amp_OndaT,amp_vp_QRS,sigma_OndaP, sigma_OndaT);

save("V1","V1");
save("V2","V2");
save("DI","DI");

figure()
sgtitle('Segnali paramatrice dell''ECG')
subplot(1,3,1), plot(t, V1 + gaussian_rumore + 1e-3, '-r', LineWidth=2)
axis([0 max(t) 0 2e-3]), grid minor,xlabel('time(s)'),ylabel('mV'), legend('V_1')
subplot(1,3,2), plot(t, V2 + gaussian_rumore + 1e-3, '-r', LineWidth=2)
axis([0 max(t) 0 2e-3]), grid minor,xlabel('time(s)'),ylabel('mV'), legend('V_2')
subplot(1,3,3), plot(t, DI + gaussian_rumore + + 1e-3, '-r', LineWidth=2)
axis([0 max(t) 0 2e-3]), grid minor,xlabel('time(s)'),ylabel('mV'), legend('Dv_1')


% repeat ecg  according to the bpm of the patient
bpm = 73;

RR = 60000/bpm;                 % time interval between two R wave
n_samples = floor(RR/delta_T);  % number of samples between to R wave

t_r = 0:delta_T:2500-delta_T;
```

```
DI_r = zeros(1,length(t_r));
V1_r = zeros(1,length(t_r));
V2_r = zeros(1,length(t_r));

DI_r(1:length(DI)) = DI;
DI_r = circshift(DI_r, n_samples);
DI_r(1:length(DI)) = DI;
DI_r = circshift(DI_r, n_samples);
DI_r(1:length(DI)) = DI;

V1_r(1:length(V1)) = V1;
V1_r = circshift(V1_r, n_samples);
V1_r(1:length(V1)) = V1;
V1_r = circshift(V1_r, n_samples);
V1_r(1:length(V1)) = V1;

V2_r(1:length(V2)) = V2;
V2_r = circshift(V2_r, n_samples);
V2_r(1:length(V2)) = V2;
V2_r = circshift(V2_r, n_samples);
V2_r(1:length(V2)) = V2;

figure()
sgtitle('Signals reconstructed')
subplot(3,1,1), plot(t_r, V1_r./1e-3, '-r', LineWidth=1.5)
ylabel('(mV)'),grid minor, legend('V_1')
subplot(3,1,2), plot(t_r, V2_r./1e-3, '-g', LineWidth=1.5)
ylabel('(mV)'),grid minor, legend('V_2')
subplot(3,1,3), plot(t_r, DI_r./1e-3, '-b', LineWidth=1.5)
grid minor, xlabel('time(ms)'),ylabel('mV'), legend('D_1')
```

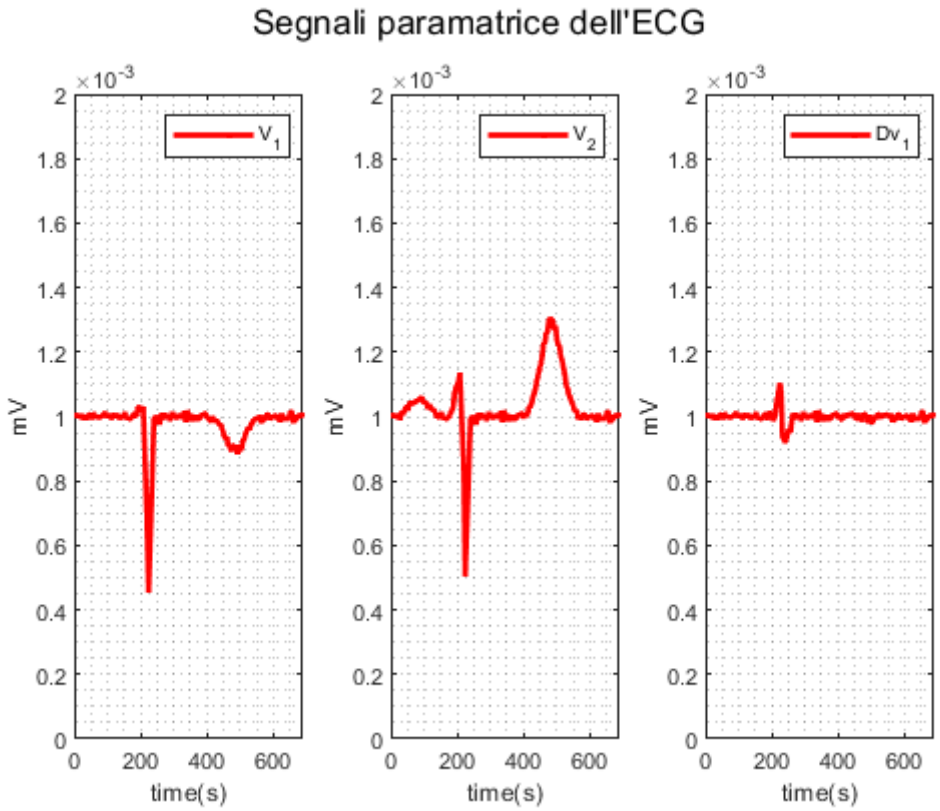

Figure 48 Signals reconstructed

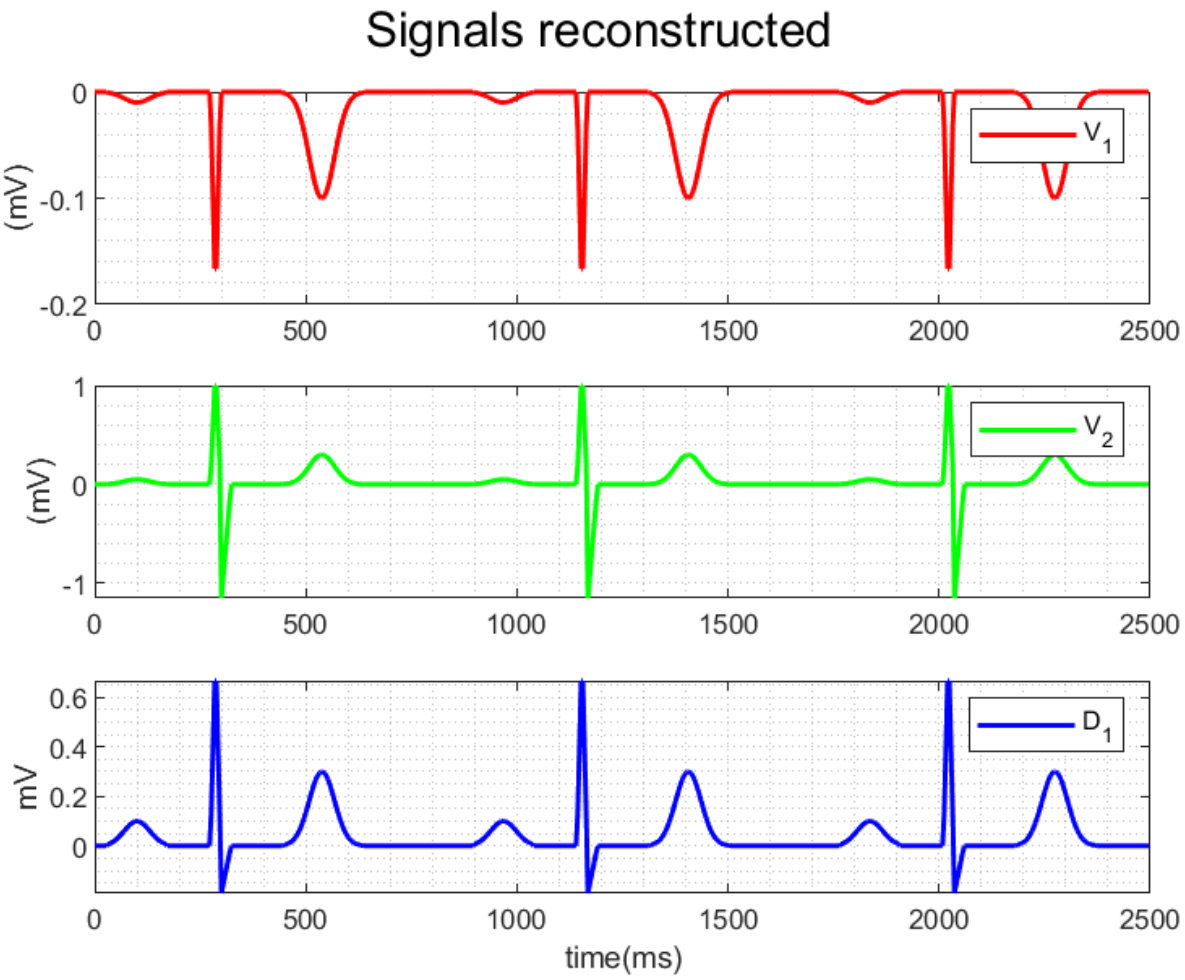

This procedure was applied to all signals recorded by the outpatient system comparable with those of the prototype (V_1, V_2, D_1) and to each patient.

```
figure(6)
subplot(2,1,1), plot(t_one_heartbeat(1:length(ecg_create)), ecg_create./1e-3, 'LineWidth', 1.2), grid
minor, xlabel('(s)'), ylabel('(mV)')
title('parametrical signal ')
subplot(2,1,2), plot(t_one_heartbeat, signal_average./1e-3, 'LineWidth', 1.2),grid minor, xlabel('(s)'),
ylabel('(mV)')
title('Signal acquisition')

ecg_mean_remove = (ecg_create-mean(ecg_create));

ecg1 = (signal_average-mean(signal_average));

ac = xcorr(ecg_mean_remove, ecg1);

[max_value, indmax] = max(ac);

ecg_new_shift = circshift(ecg_mean_remove, (indmax+35));
t1 = 0:delta_t:length(ecg_new_shift)*delta_t-delta_t;

%ecg_new_shift = ecg_new_shift./(max(abs(ecg_new_shift)));
```

```
%ecg1 = ecg1./(max(abs(ecg1)));

figure(7)
plot(t1,ecg_new_shift./1e-3, 'LineWidth', 1)
hold on
plot(t1,ecg1(1:length(ecg_new_shift))./1e-3, 'LineWidth', 1)
xlabel('Time(s)'), ylabel('Amplitude(mV)'), grid minor, axis tight
legend('Ambulatory ecg signal','Prototype ecg signal')
title('Compare signals DI')

bpm = round(60000/((sum(diff(locs))/(length(locs)-1))*1000));

fprintf('The calculated heartbeats is :%d\n',bpm );
fprintf('Ambulatory ECG heartbeat is :%d\n',bpm_teor );
```

Patient #1:

Male 31 years old

BP 138/81

Figure 49 Prototype original signal D1

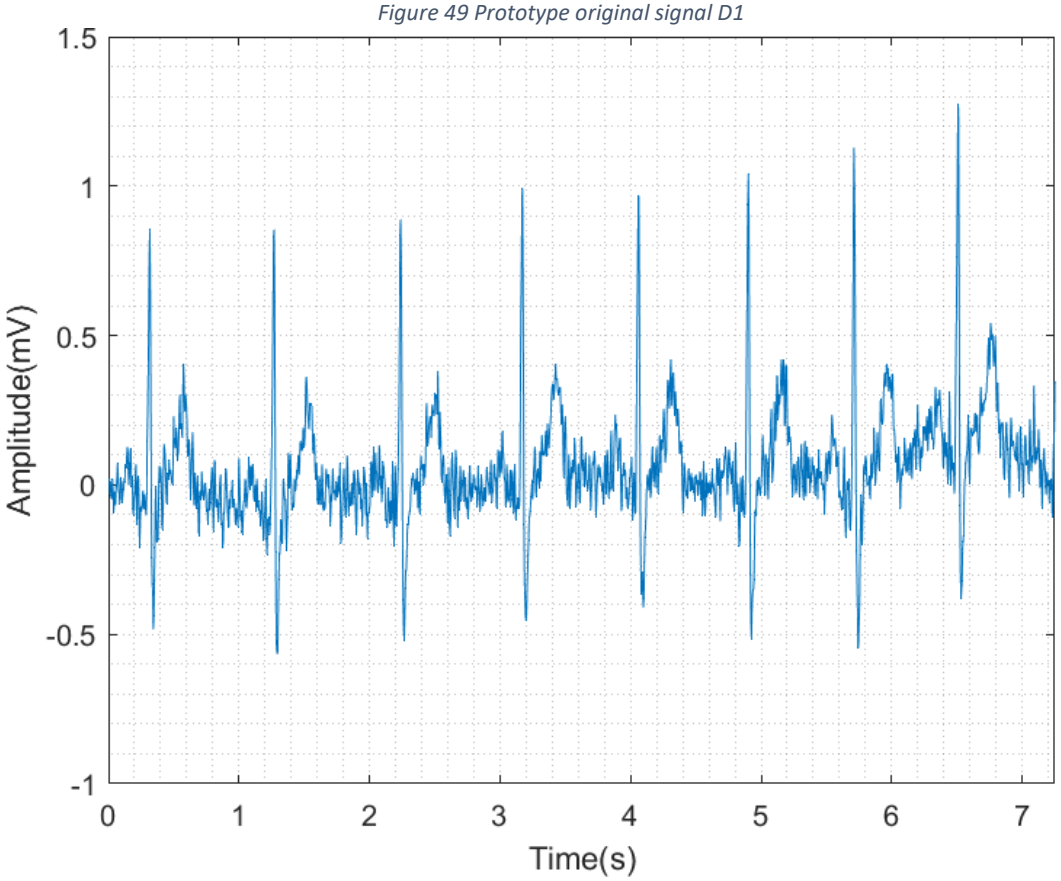

Figure 50 Prototype original signal V1

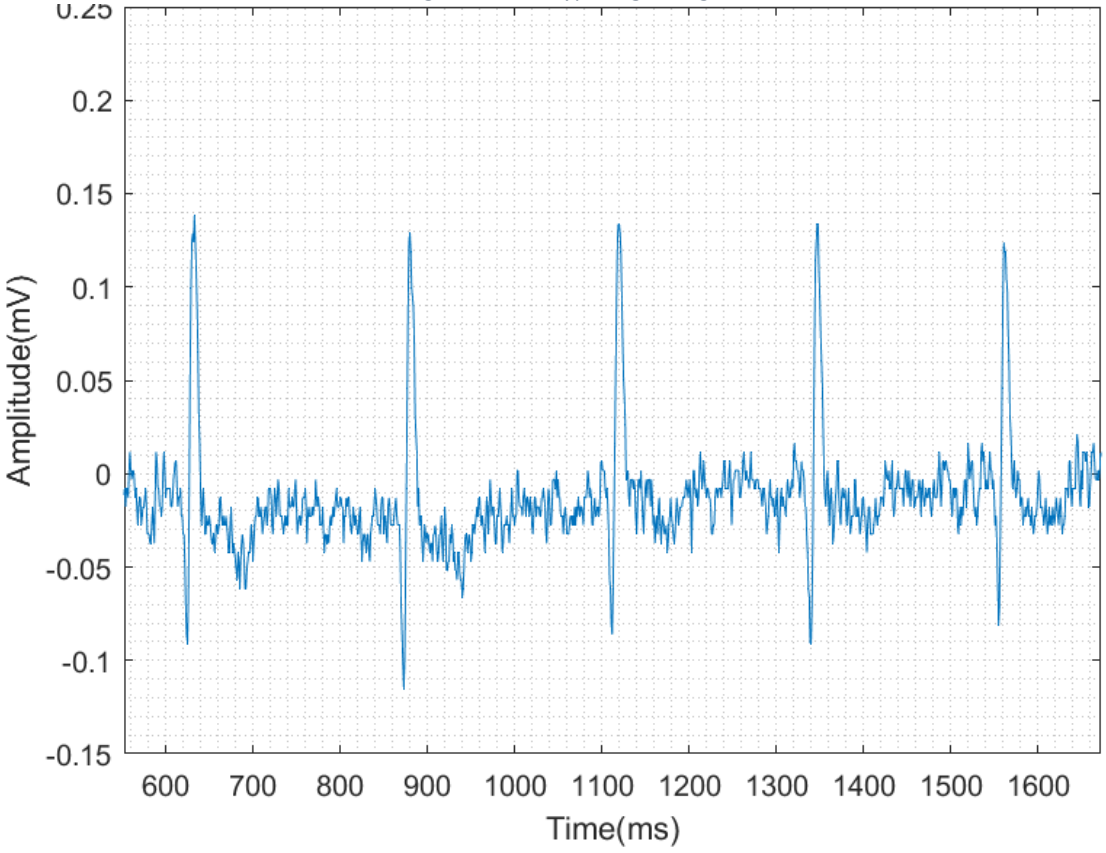

Figure 51 Prototype original signal V2

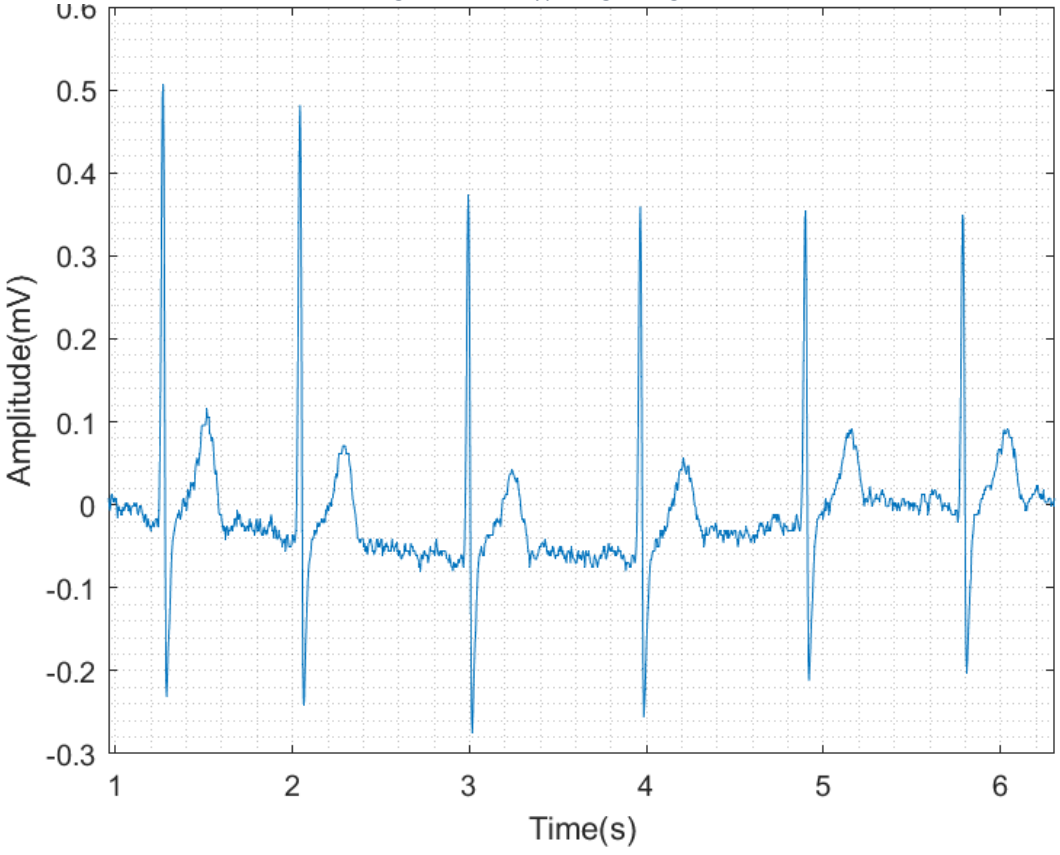

Figure 52 Ambulatory original signals

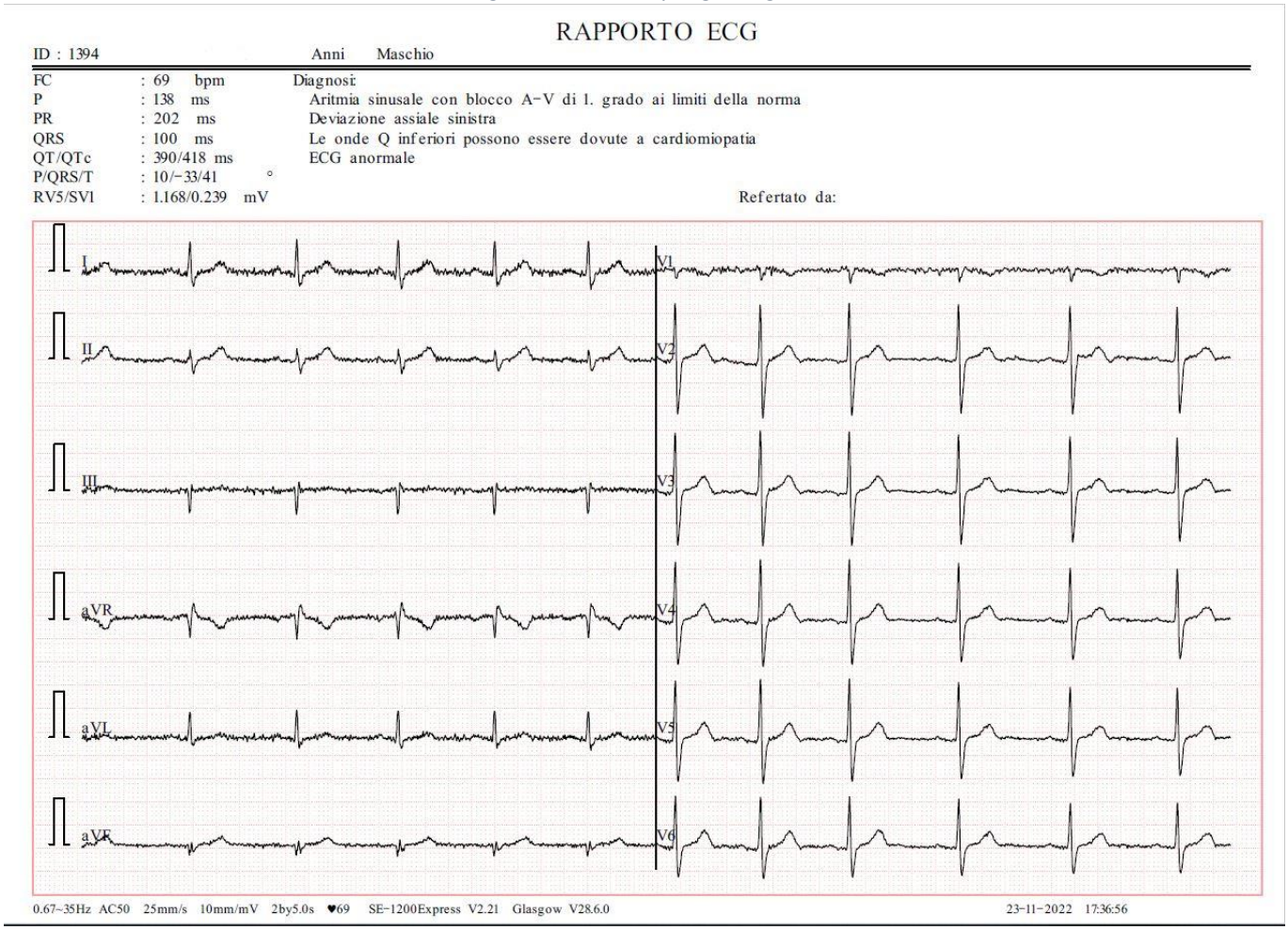

Figure 53 Ambulatory signals reconstructed

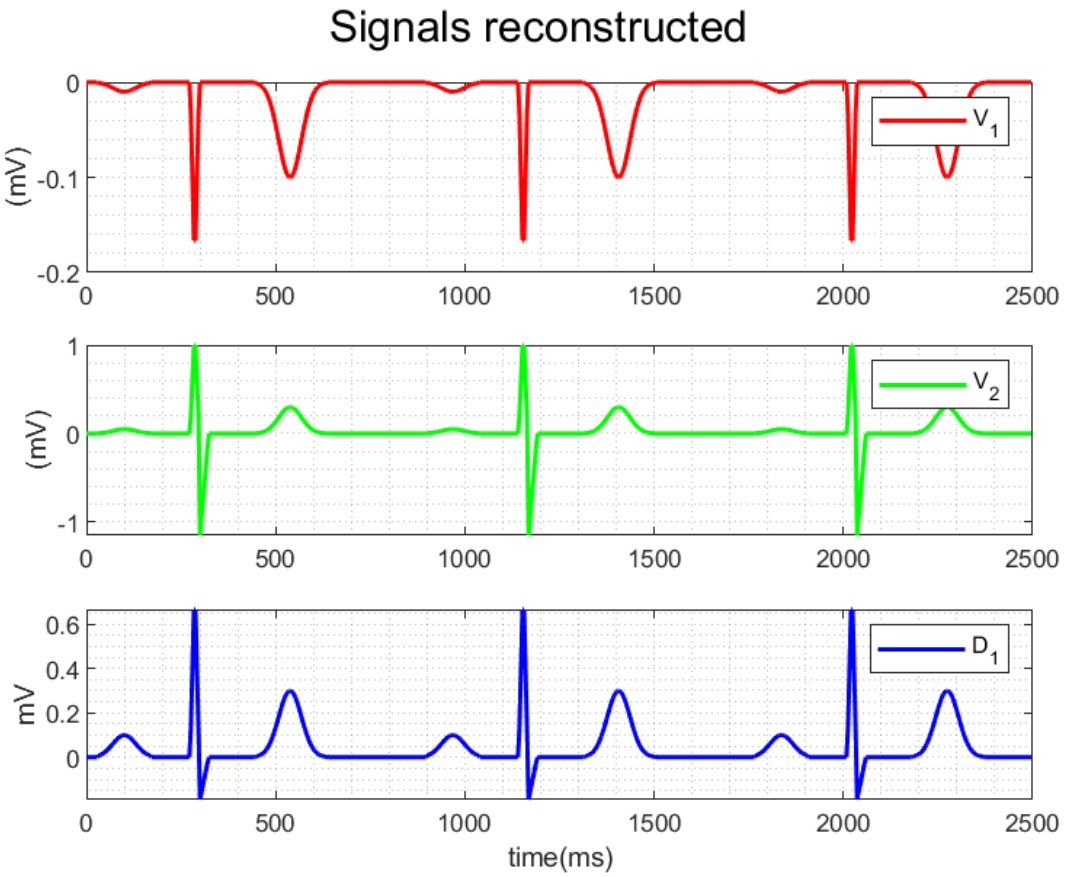

Figure 54 Comparison V1

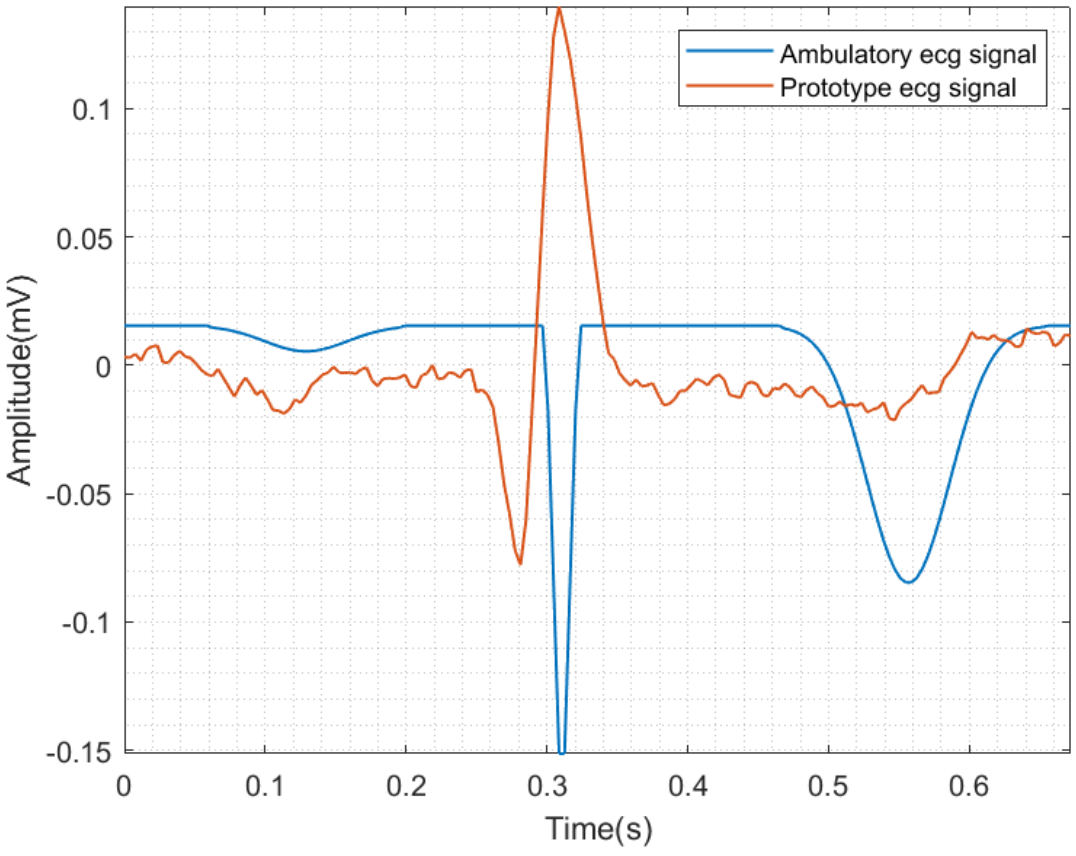

Figure 55 Comparison D1

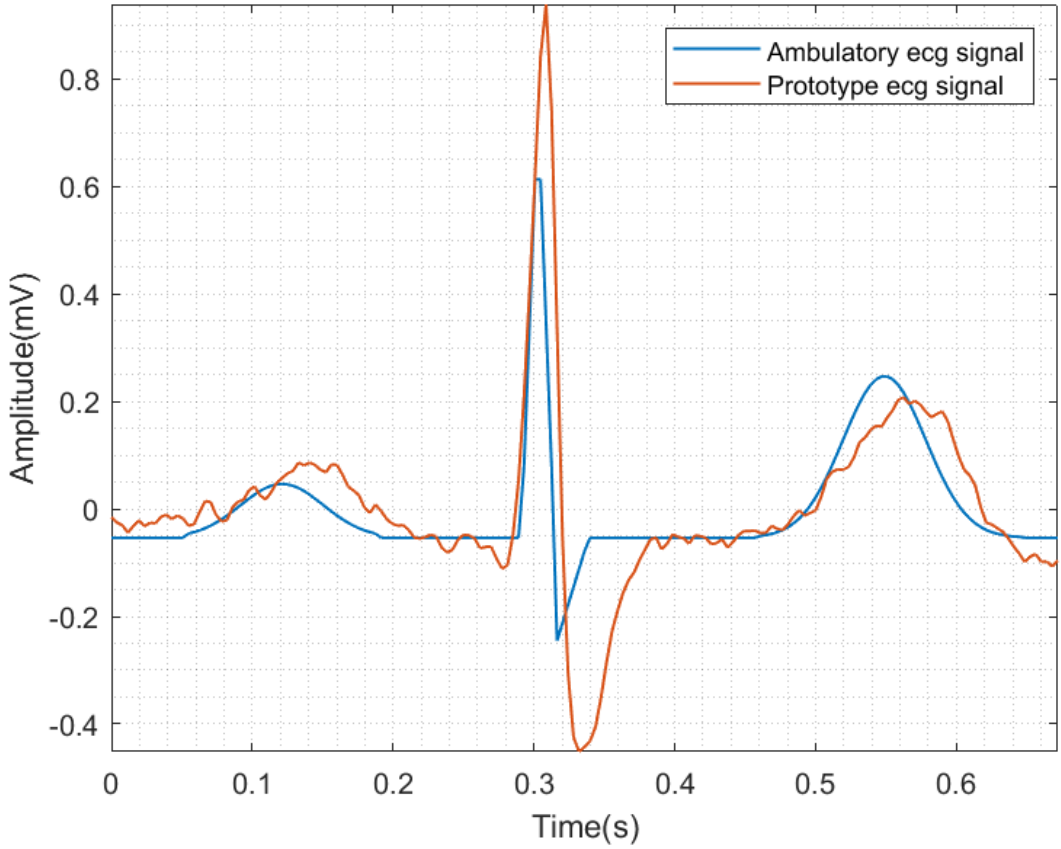

Figure 56 Comparison V2

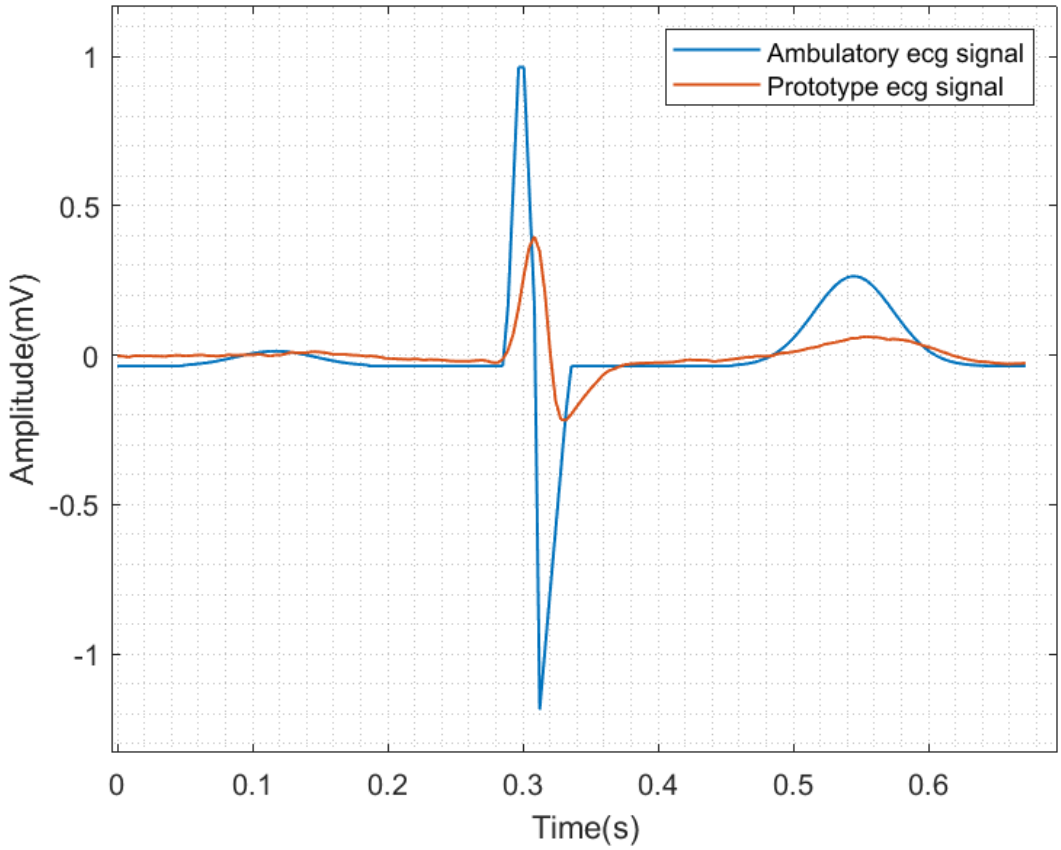

Patient #2:

Female 55 years old

BP 116/82

Figure 57 Prototype original signal V1

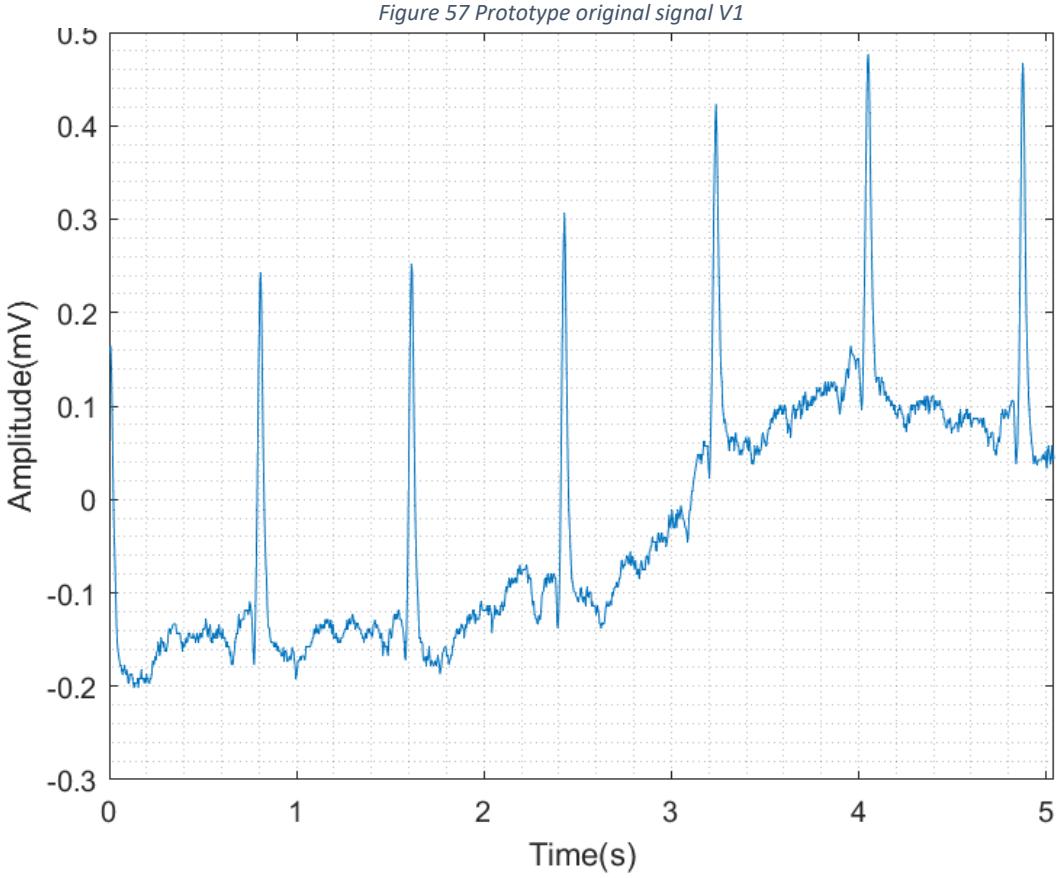

Figure 58 Prototype original signal D1

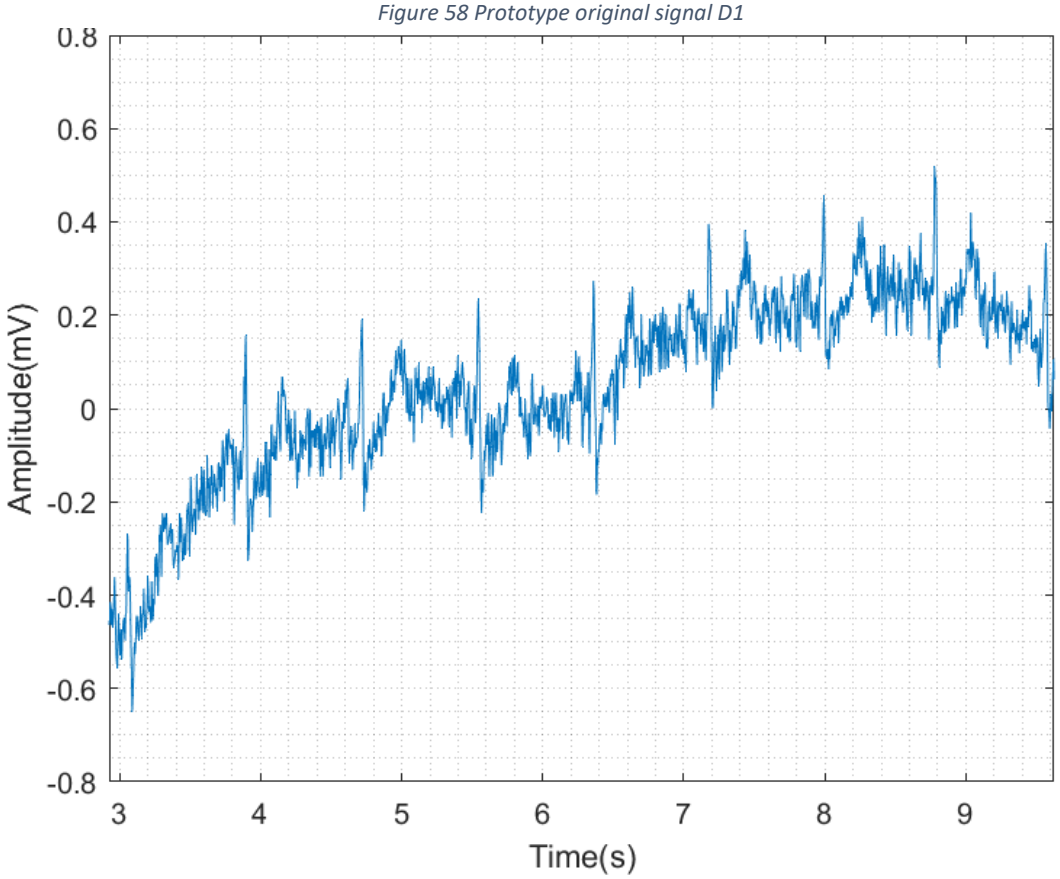

Figure 59 Prototype original signal V2

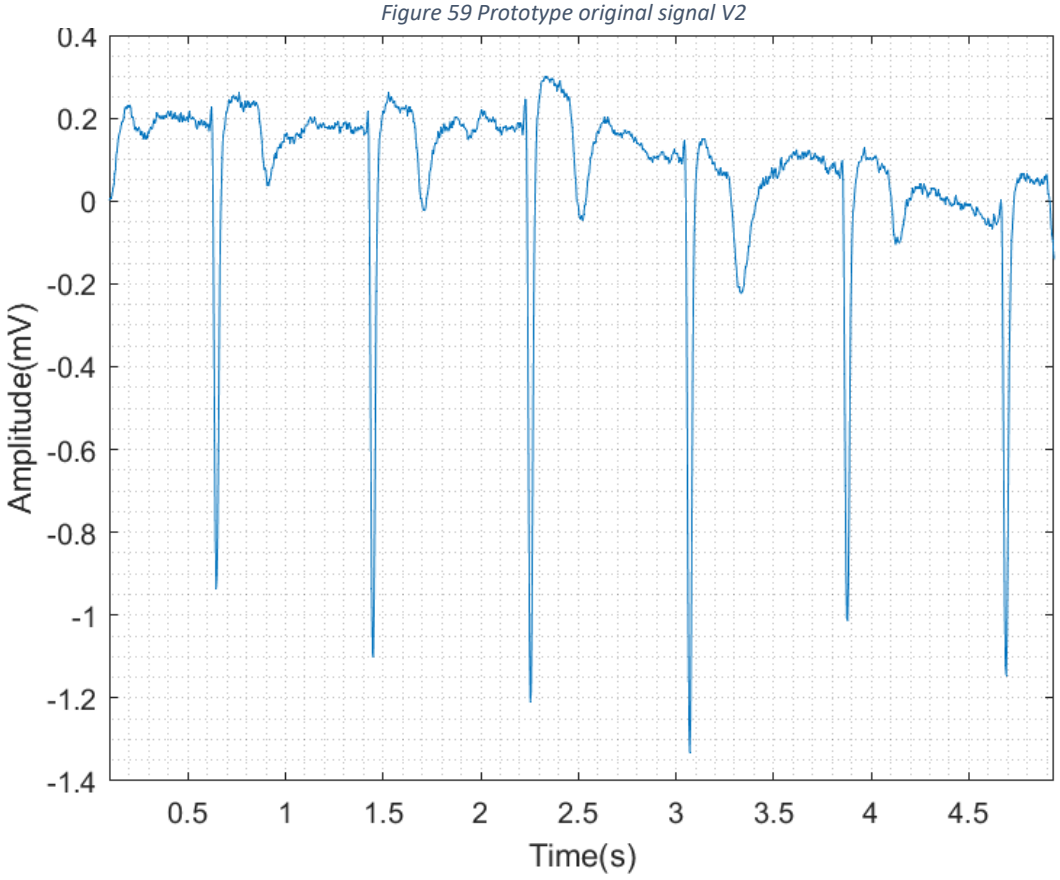

Figure 60 Ambulatory original signals

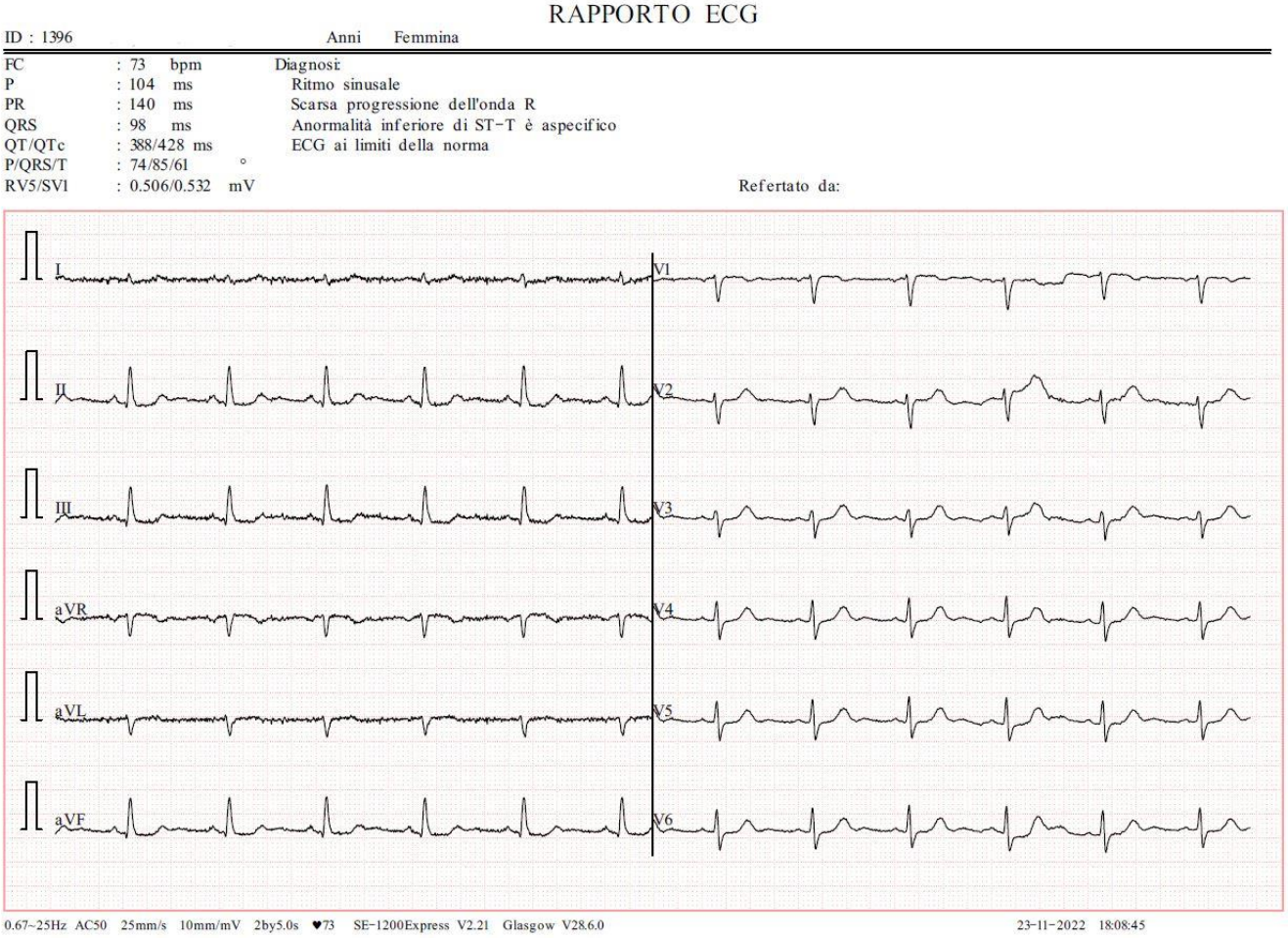

Figure 61 Ambulatory signals reconstructed

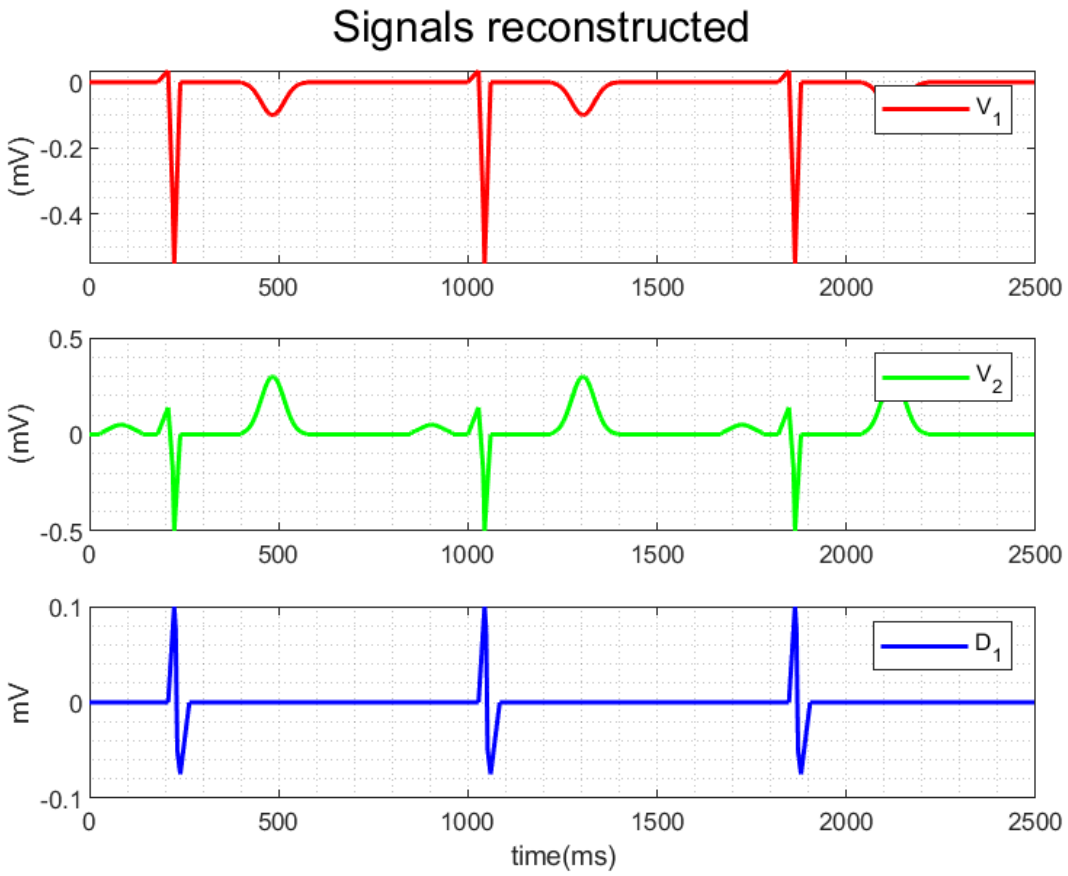

Figure 62 Comparison V2

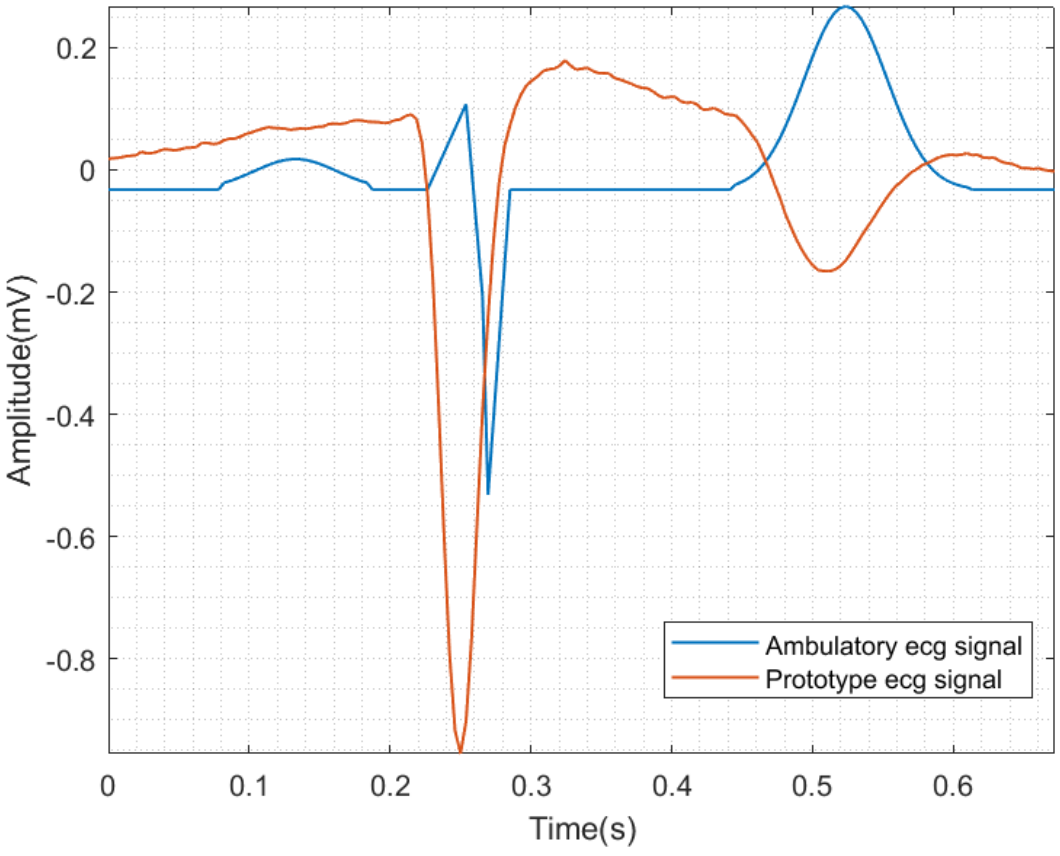

Figure 63 Comparison V1

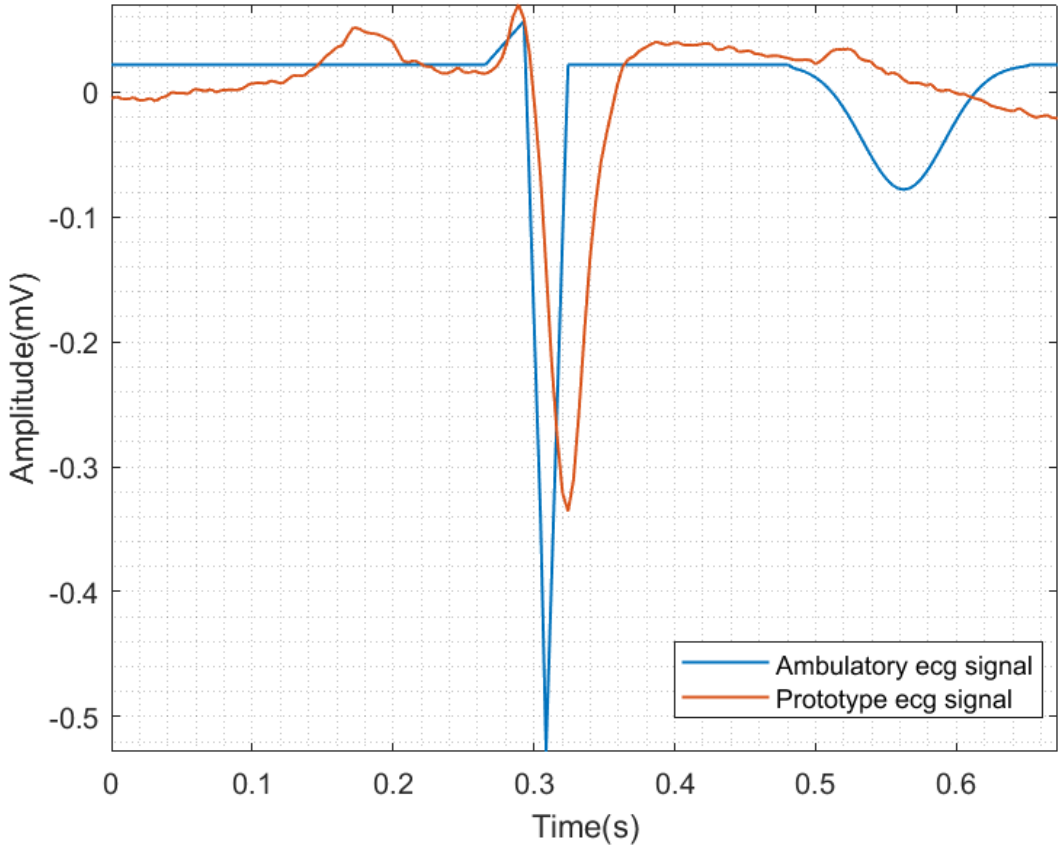

Figure 64 Comparison D1

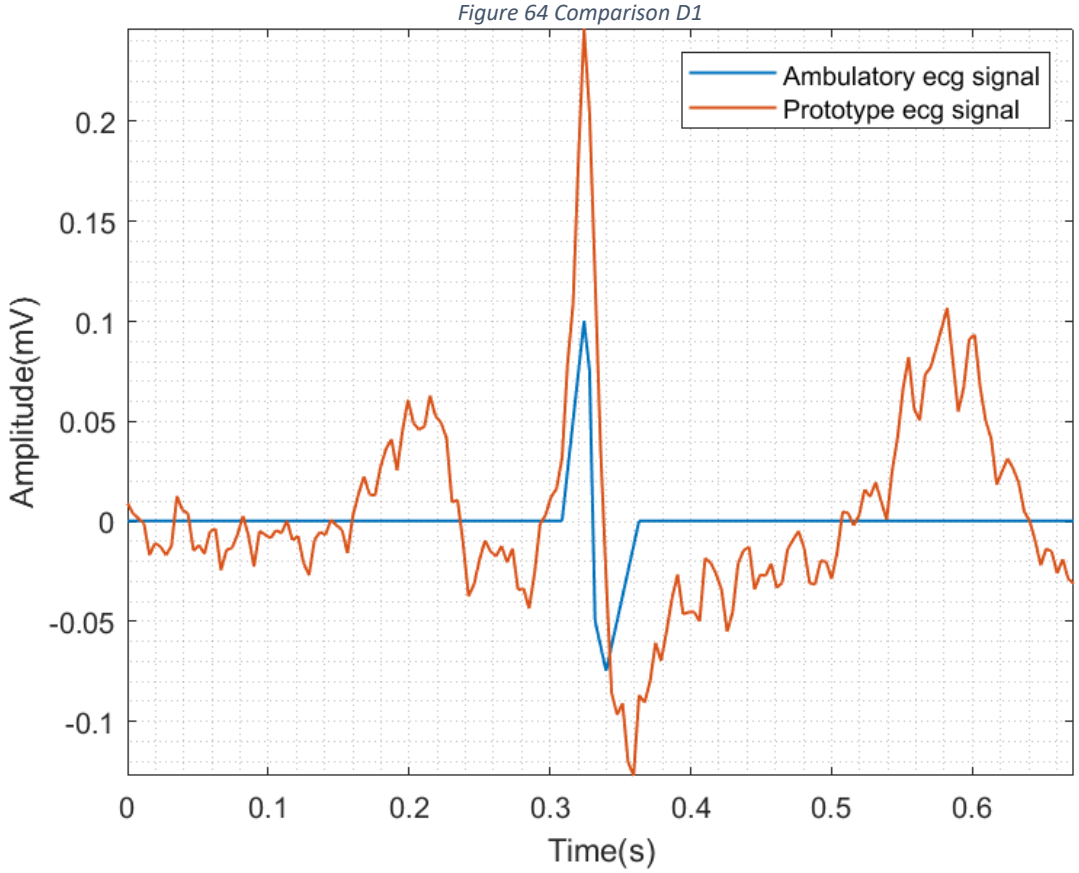

Patient #3:

Male 54 years old

BP 160/110

Figure 65 Prototype original signal V1

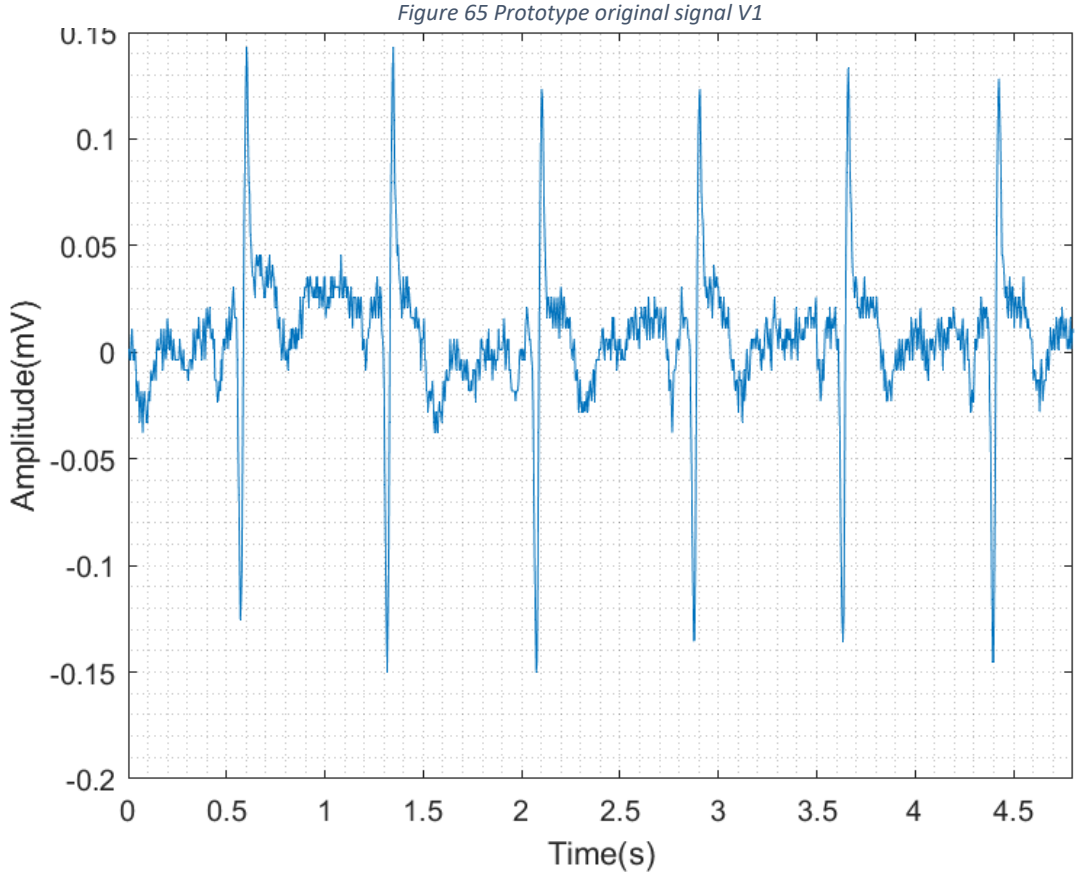

Figure 66 Prototype original signal D1

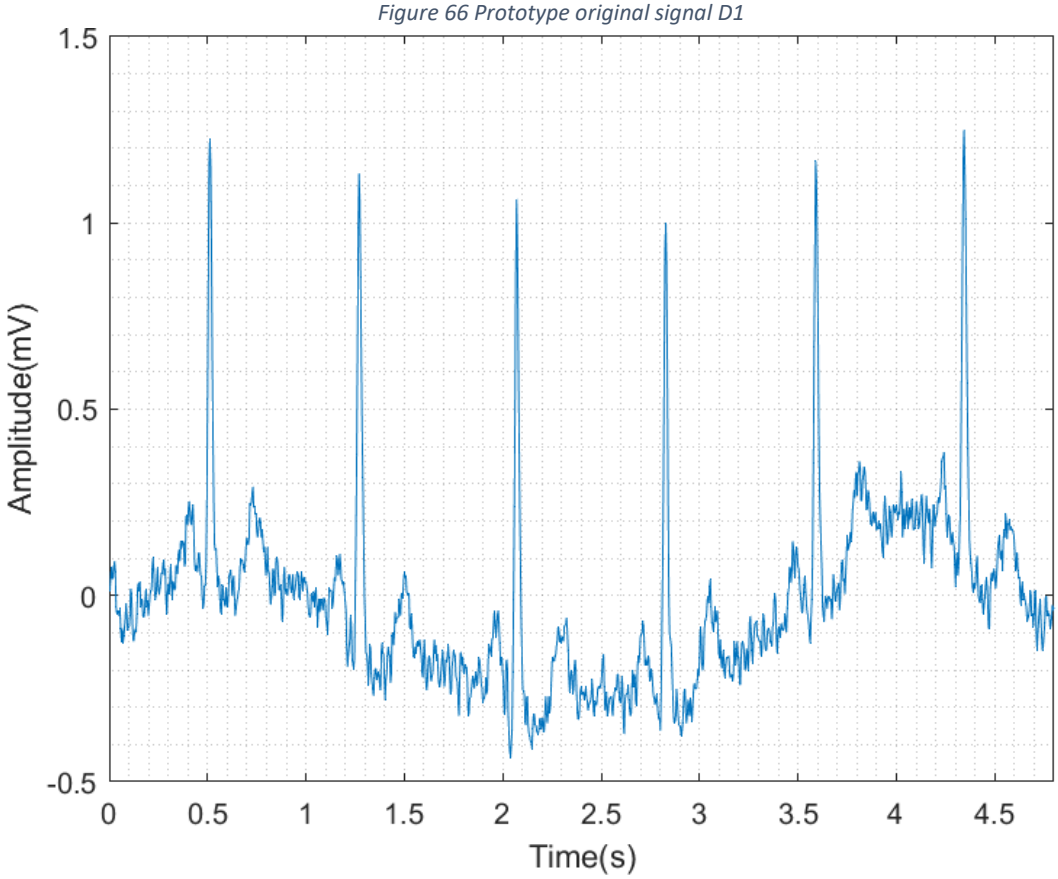

Figure 67 Prototype original signal V2

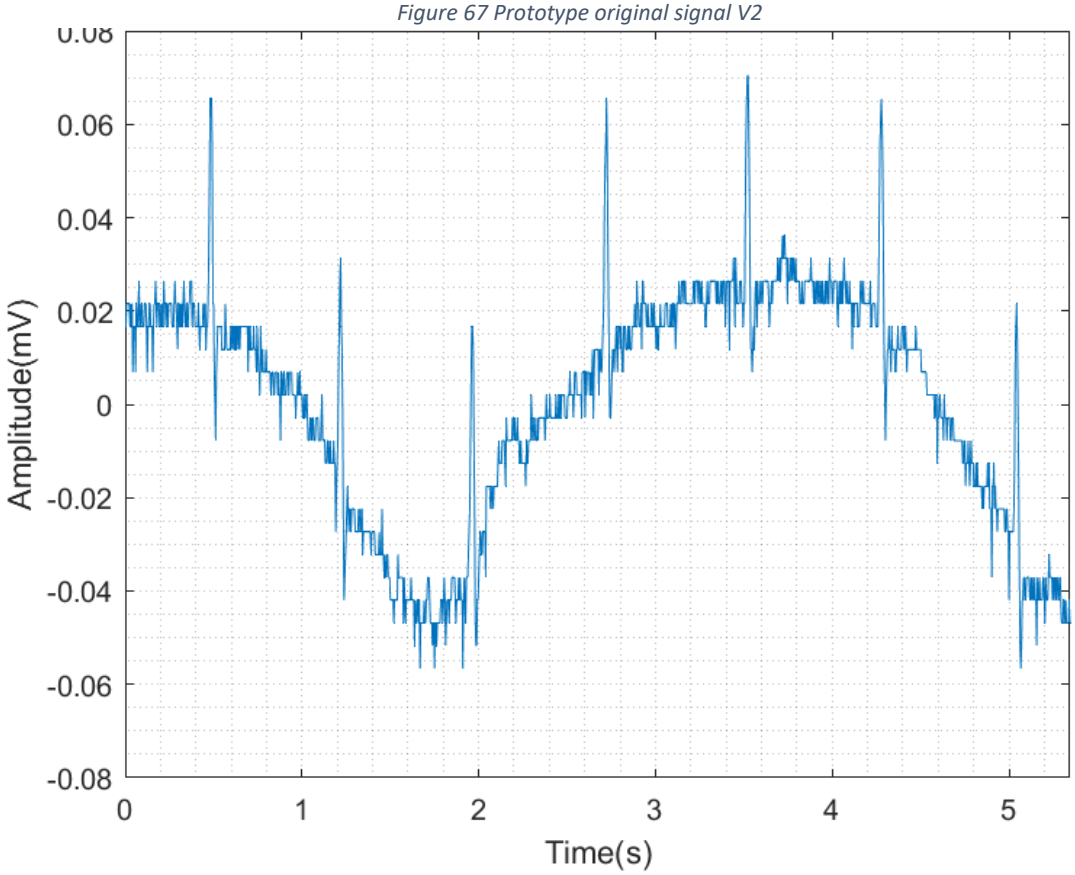

Figure 68 Ambulatory original signals

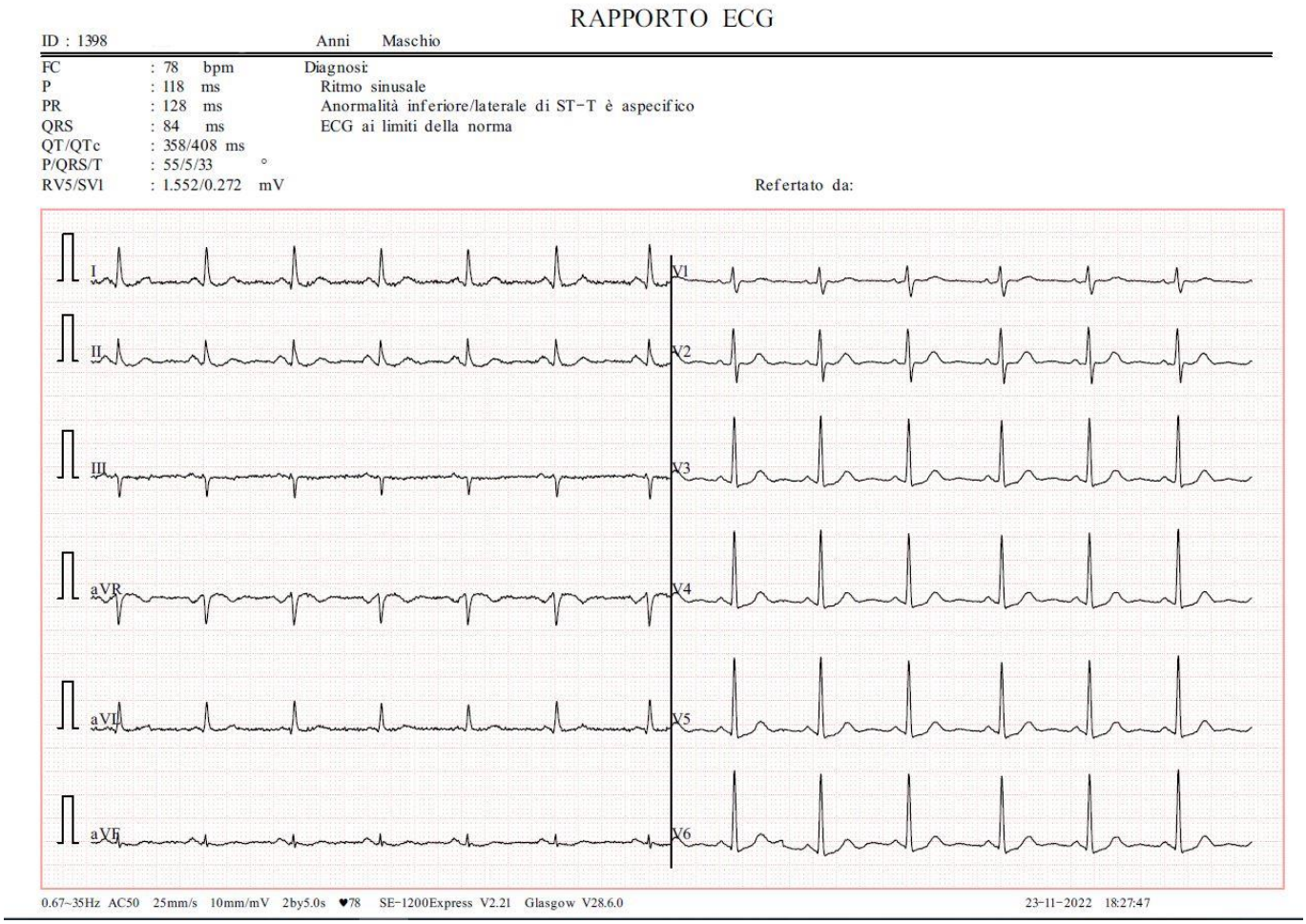

Figure 69 Ambulatory signals reconstructed

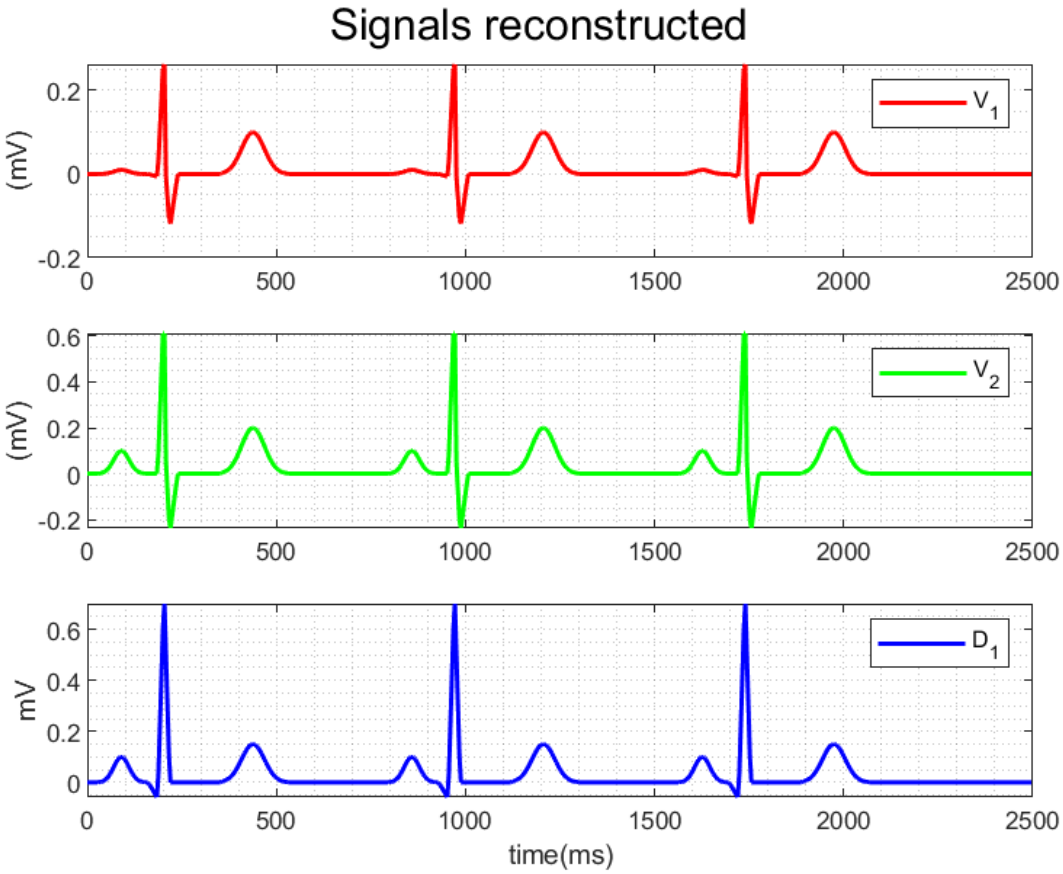

Figure 70 Comparison V1

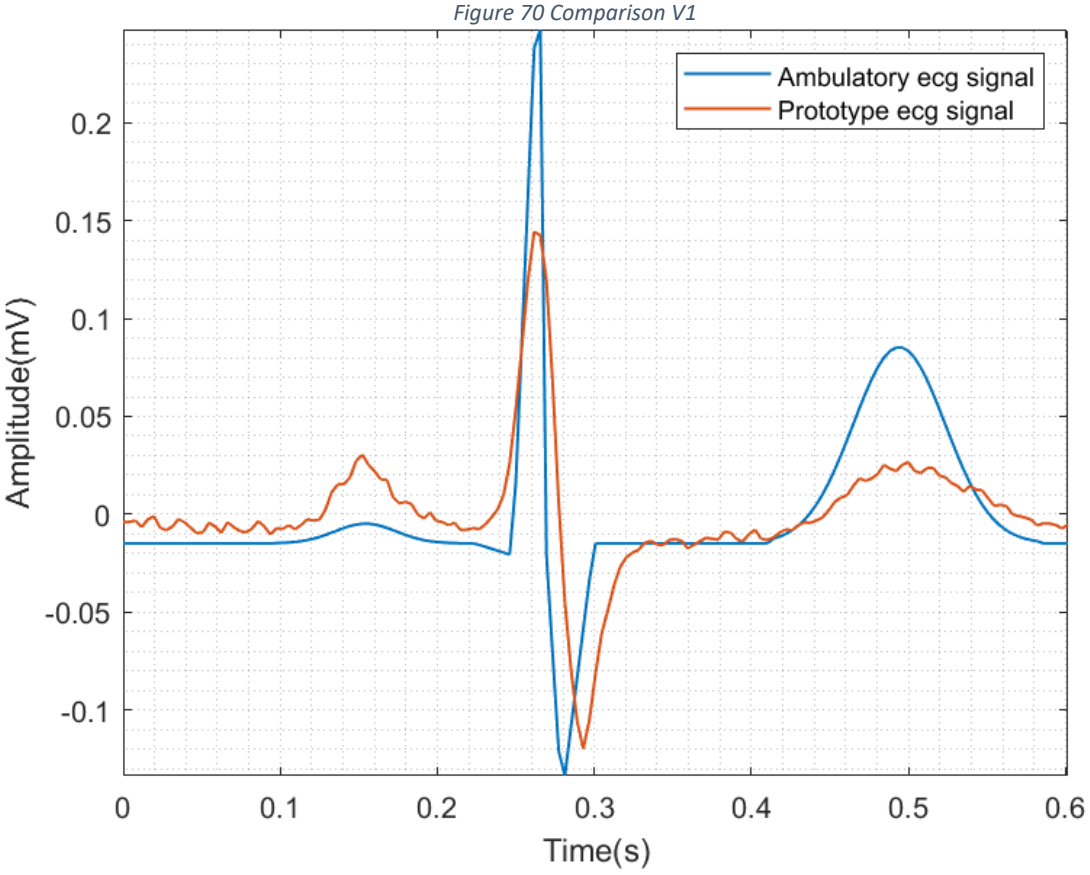

Figure 71 Comparison V2

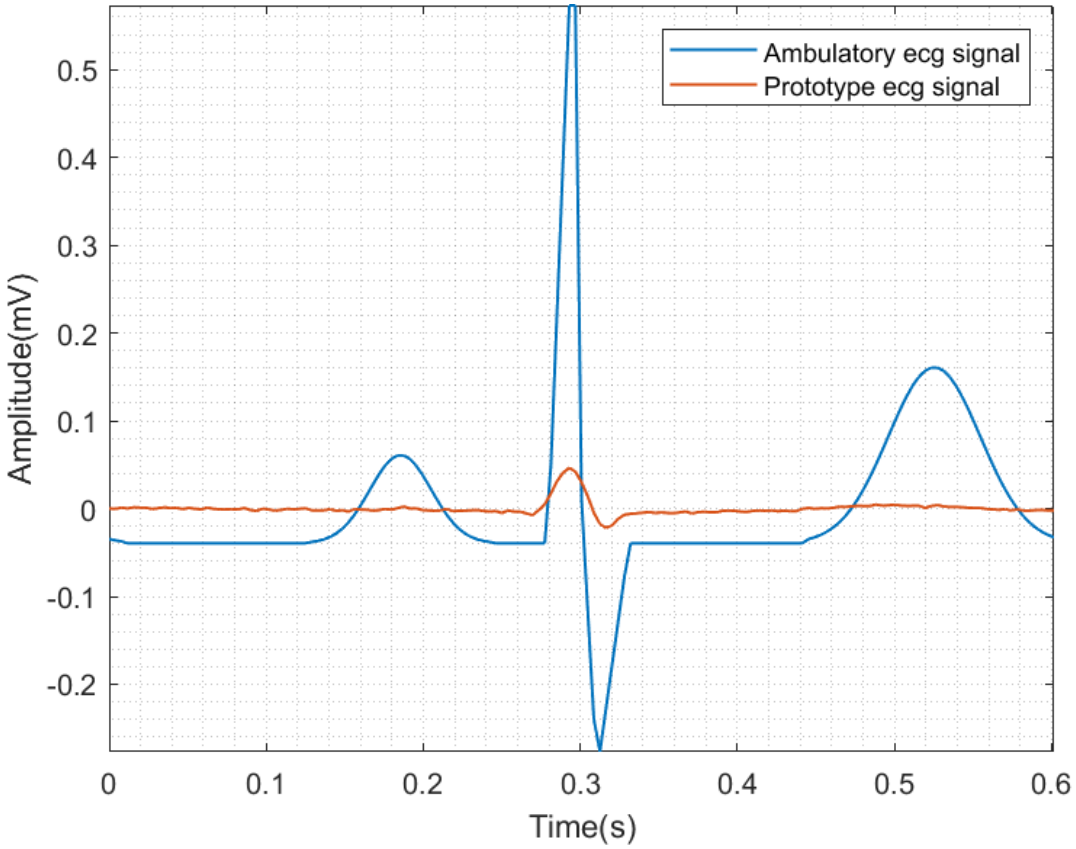

Patient #4:

Male 35 years old

BP 121/81

Figure 72 Prototype original signal V1

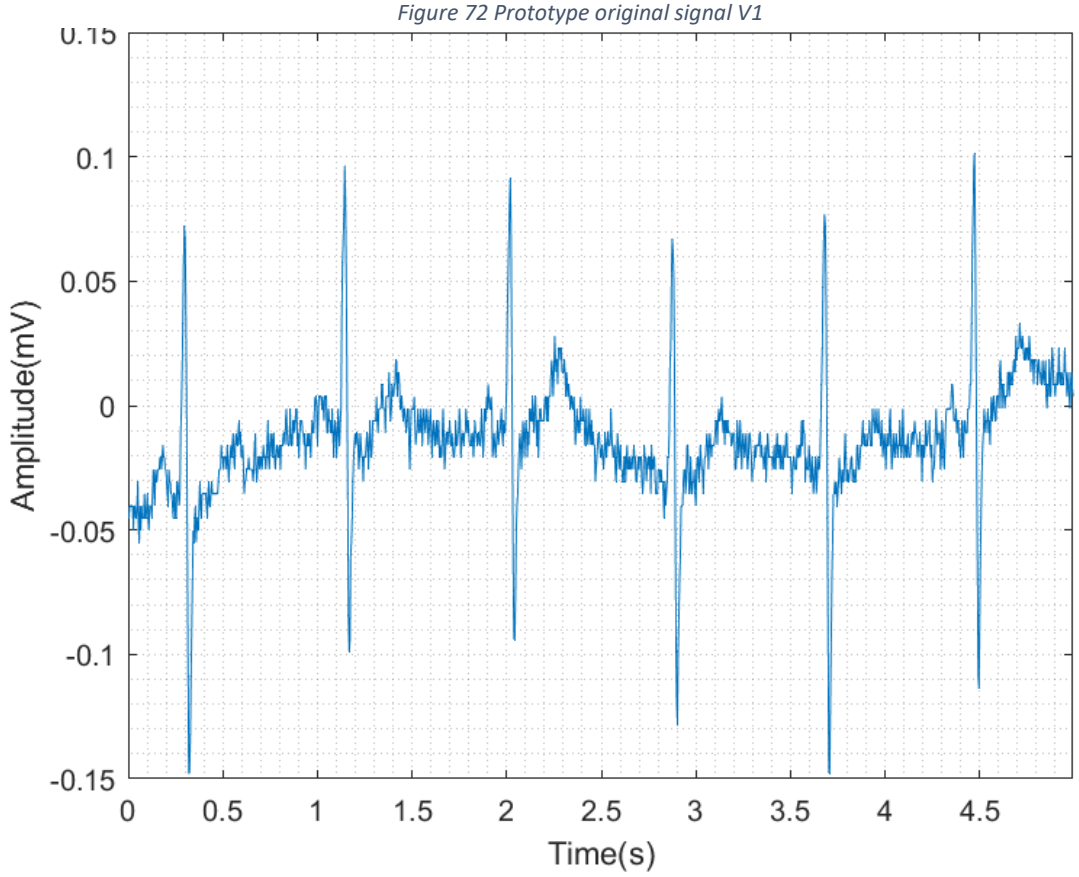

Figure 73 Prototype original signal D1

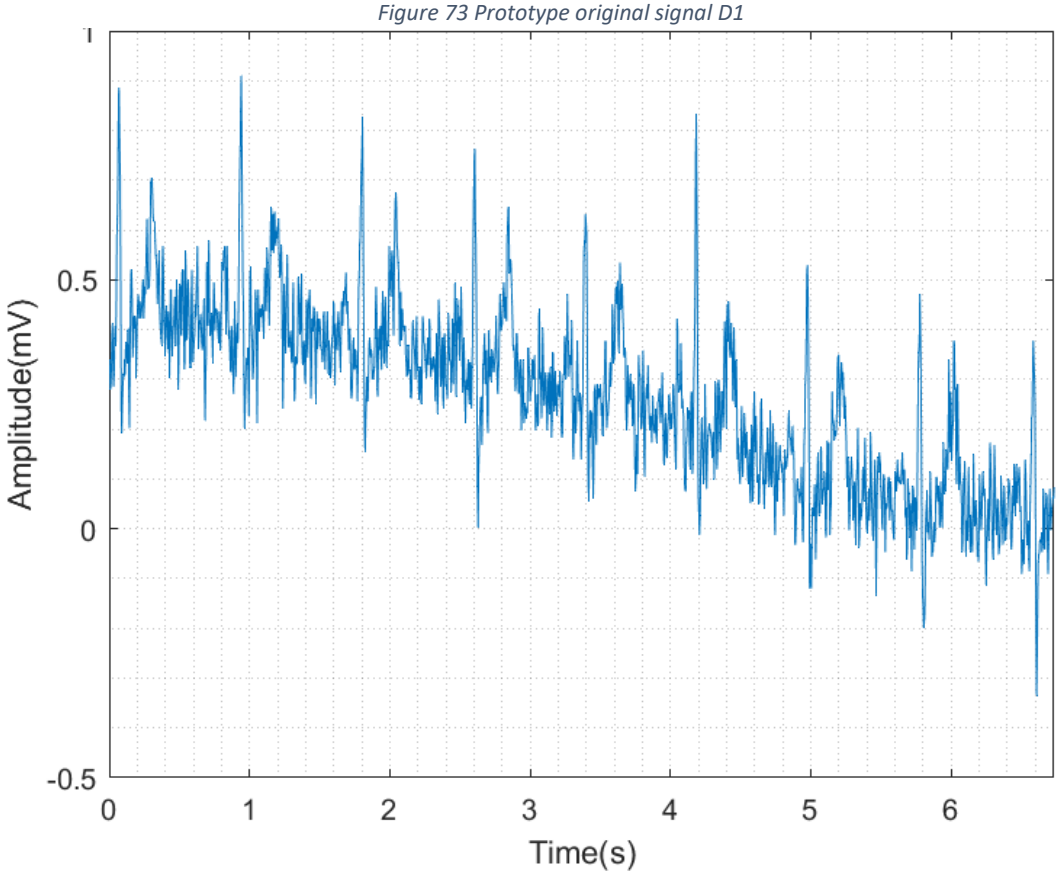

Figure 74 Prototype original signal V2

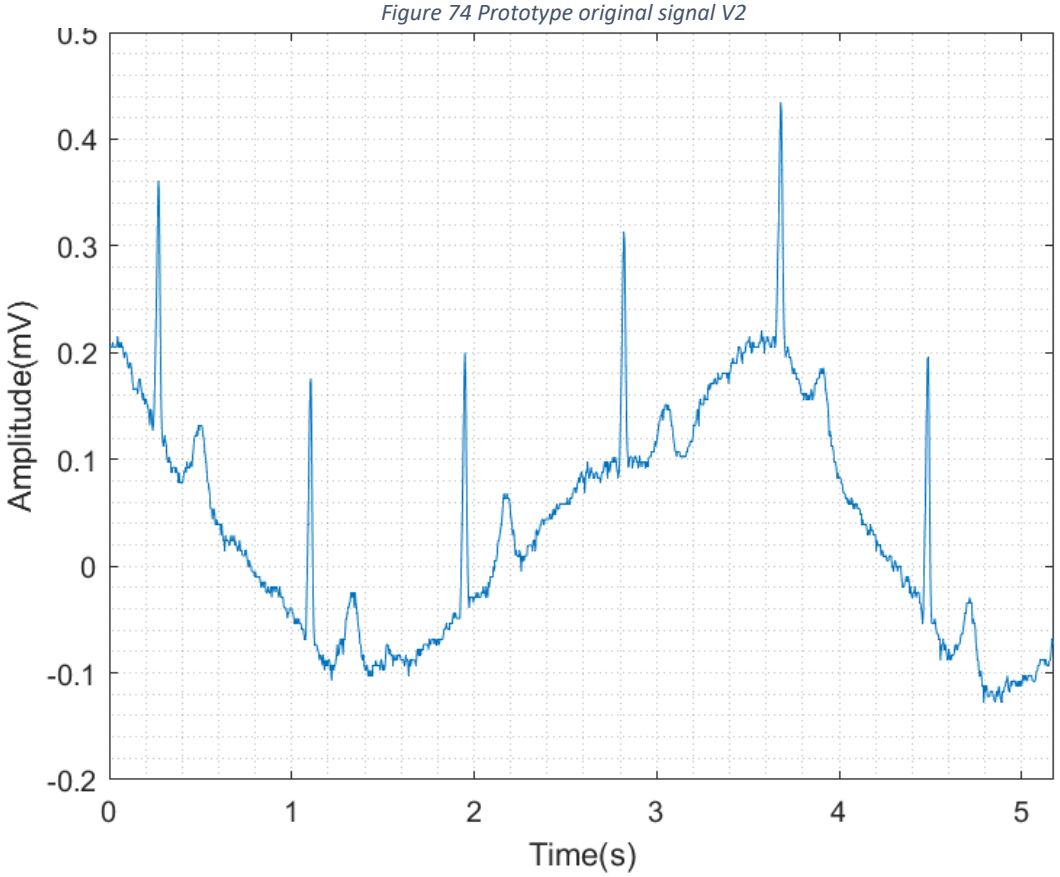

Figure 75 Ambulatory original signals

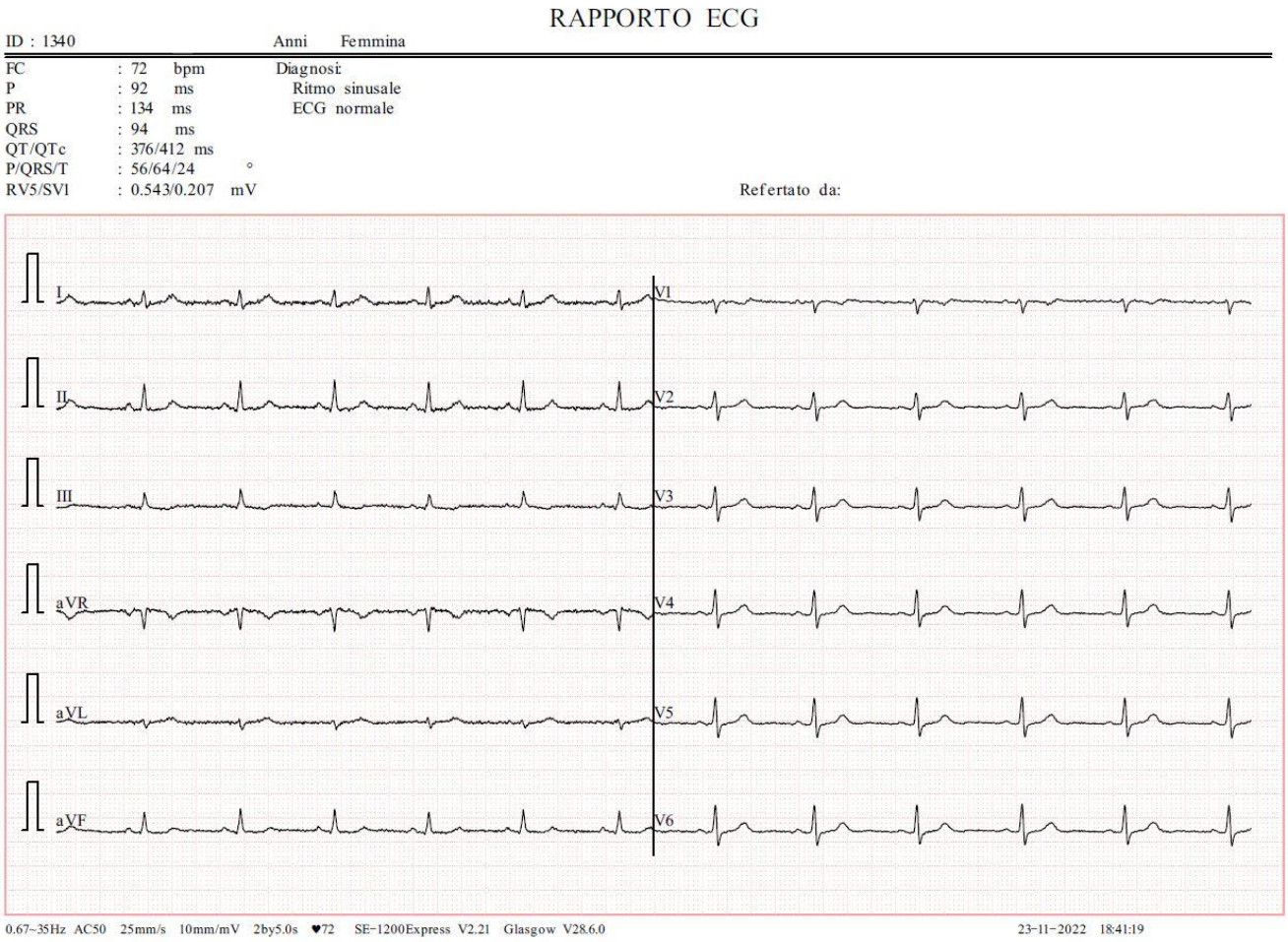

Figure 76 Ambulatory signals reconstructed

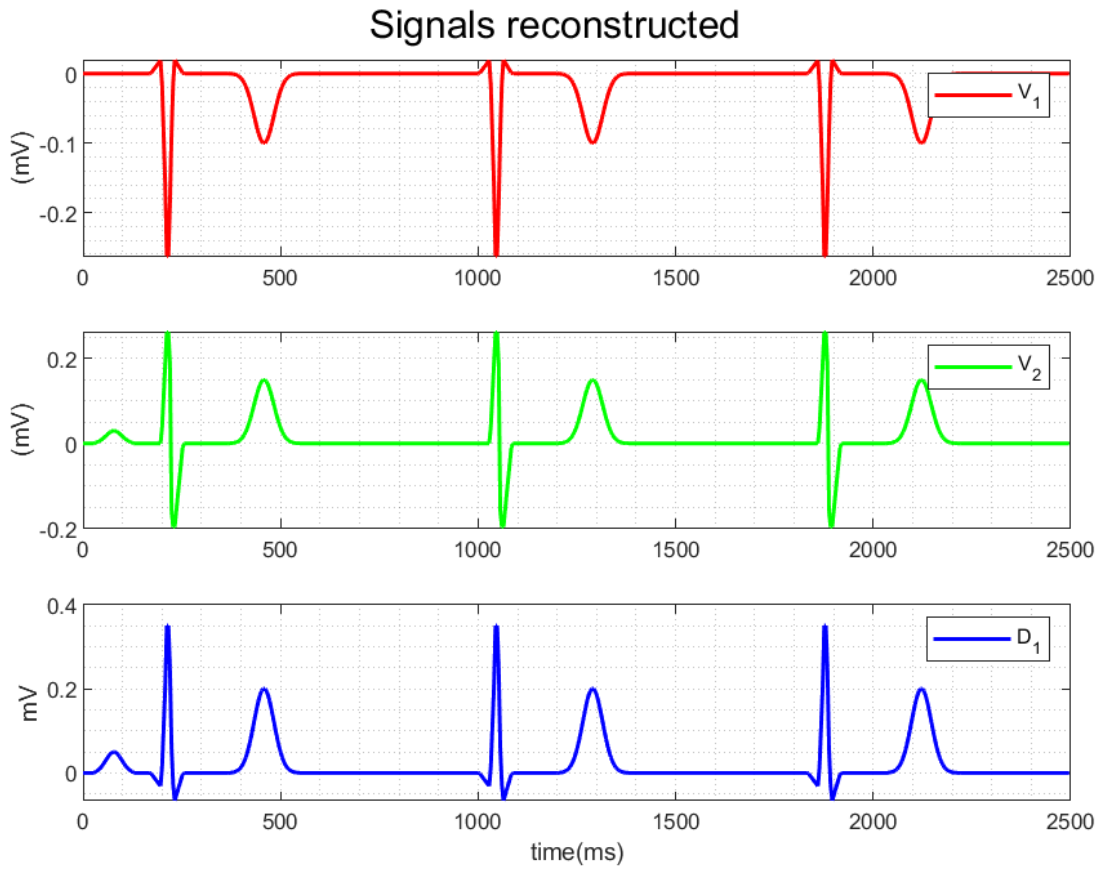

Figure 77 Comparison V2

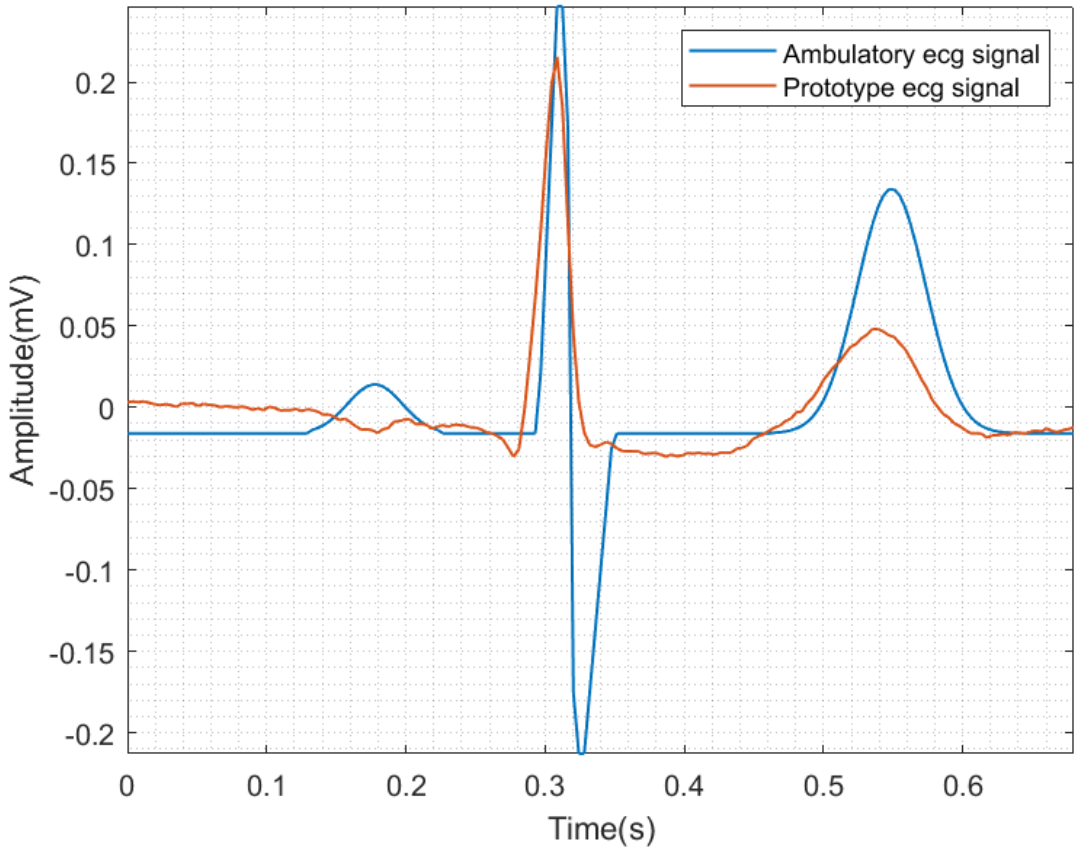

Figure 78 Comparison V1

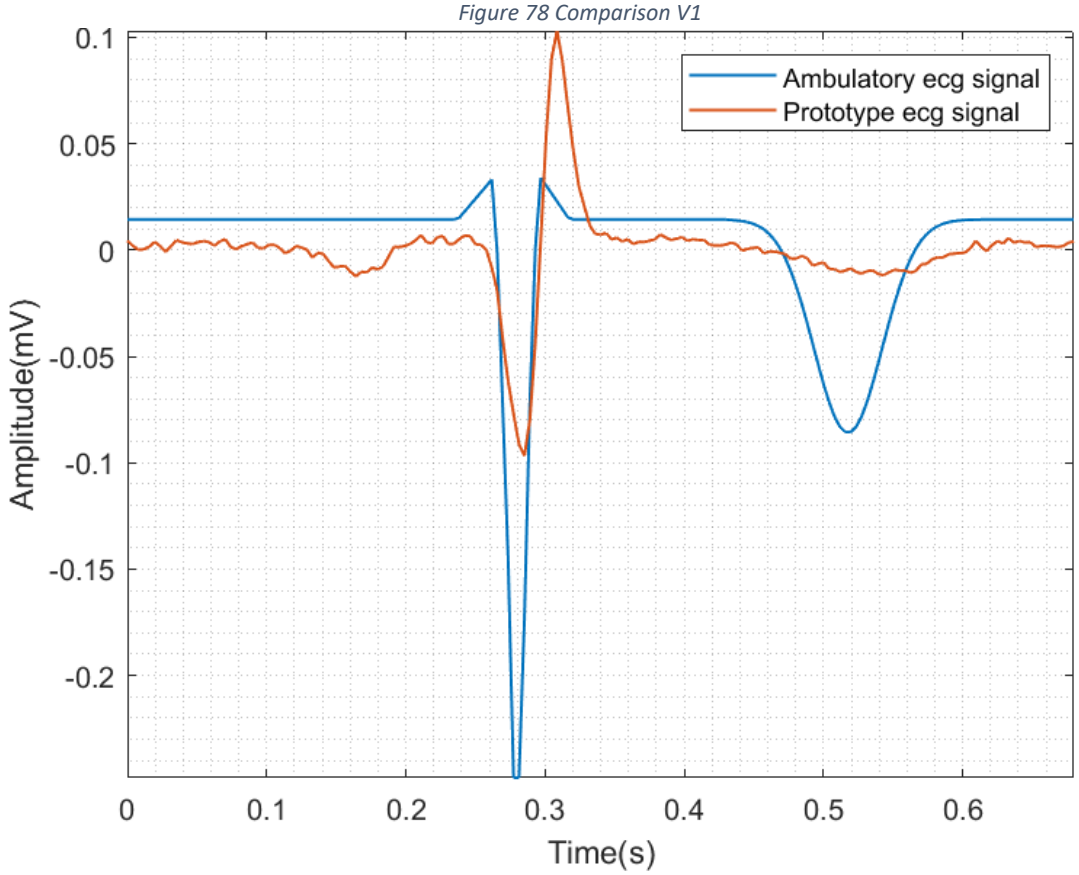

Figure 79 Comparison D1

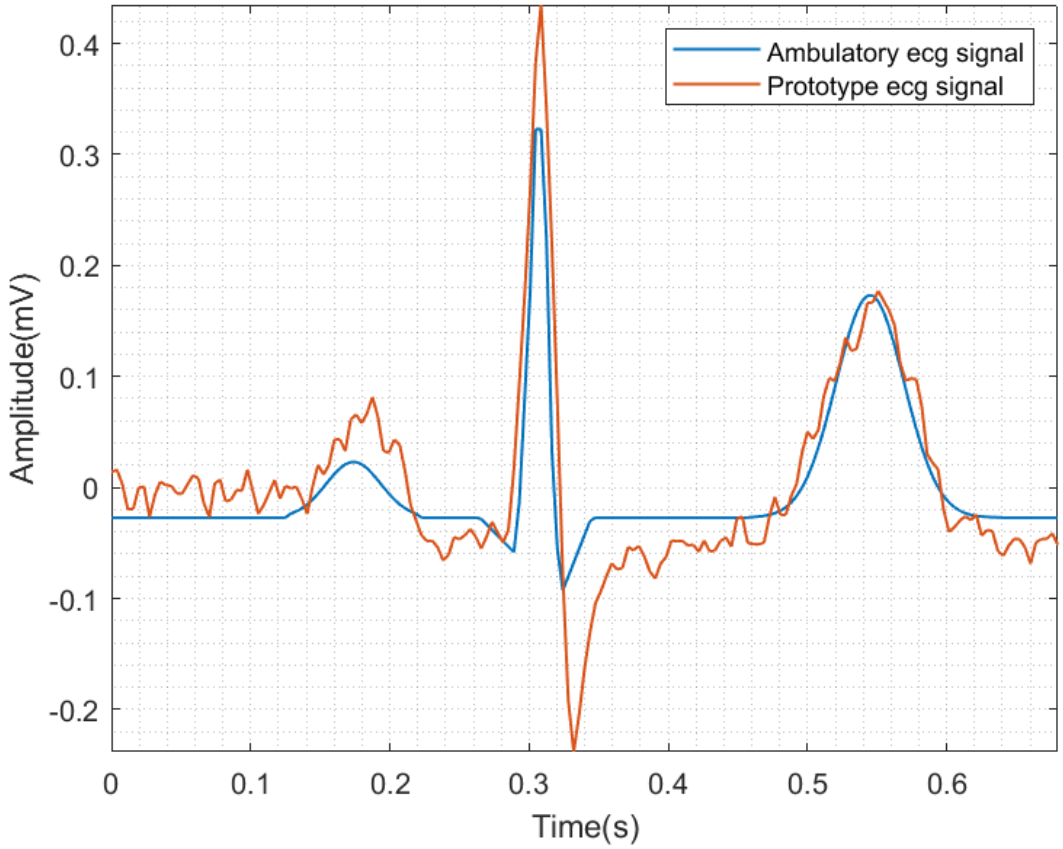

Patient #5:

Male 37 years old

BP 142/97

Figure 80 Prototype original signal V1

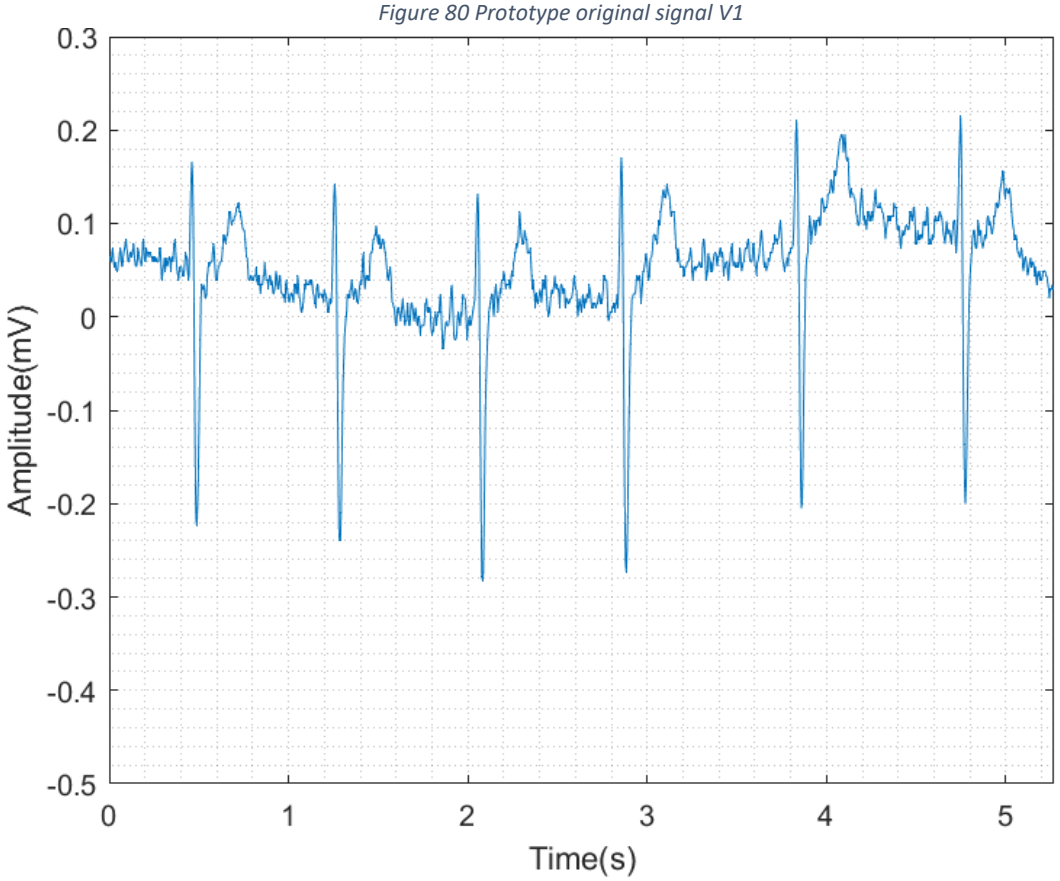

Figure 81 Prototype original signal D1

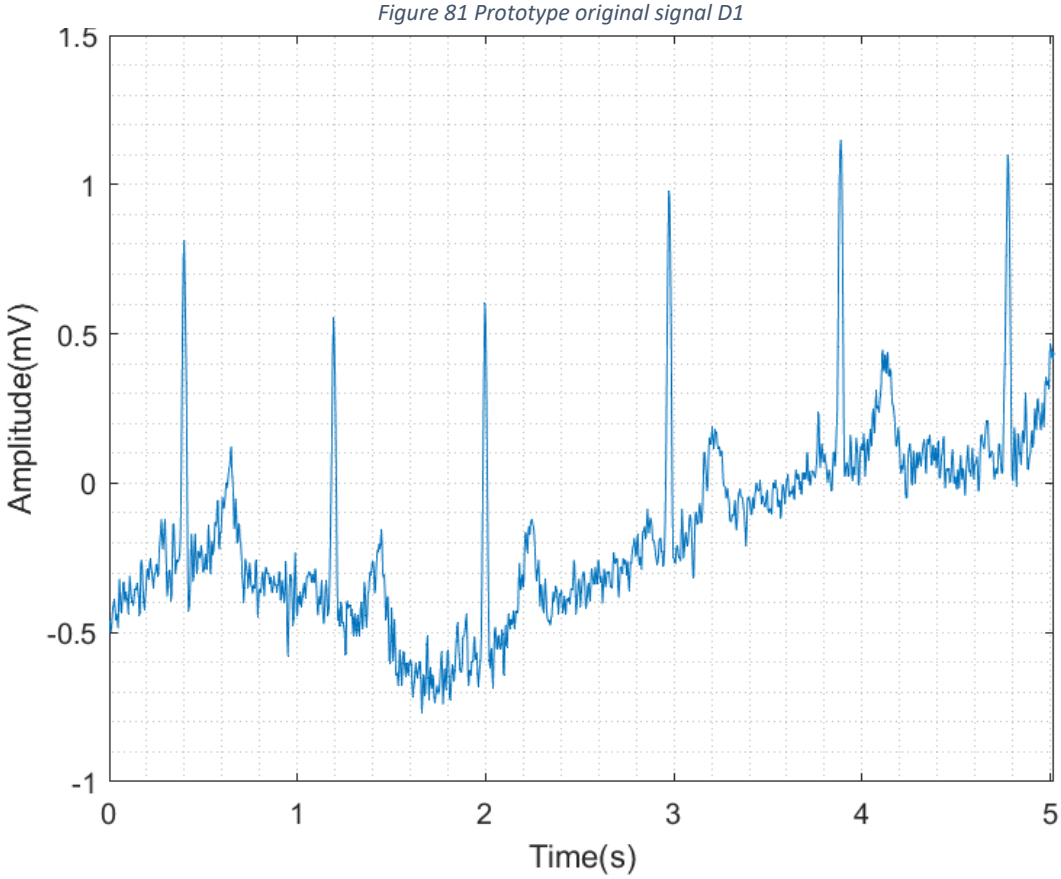

Figure 82 Prototype original signal V2

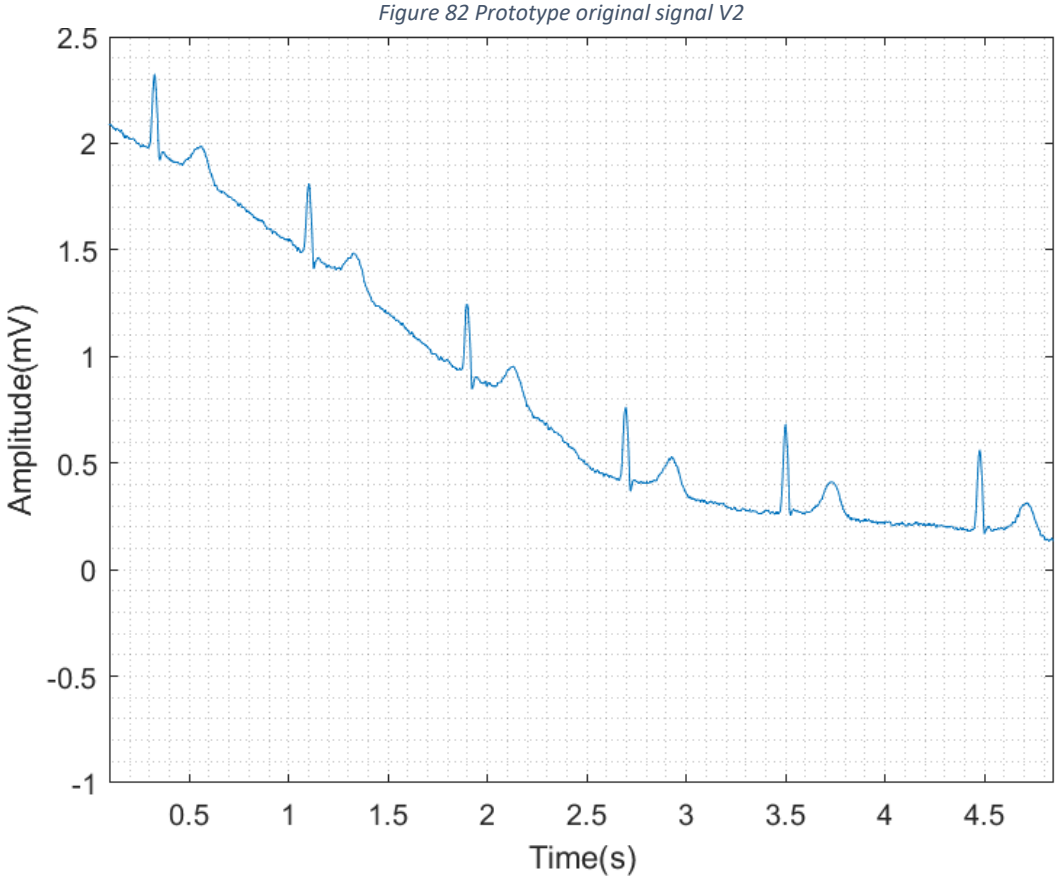

Figure 83 Ambulatory original signals

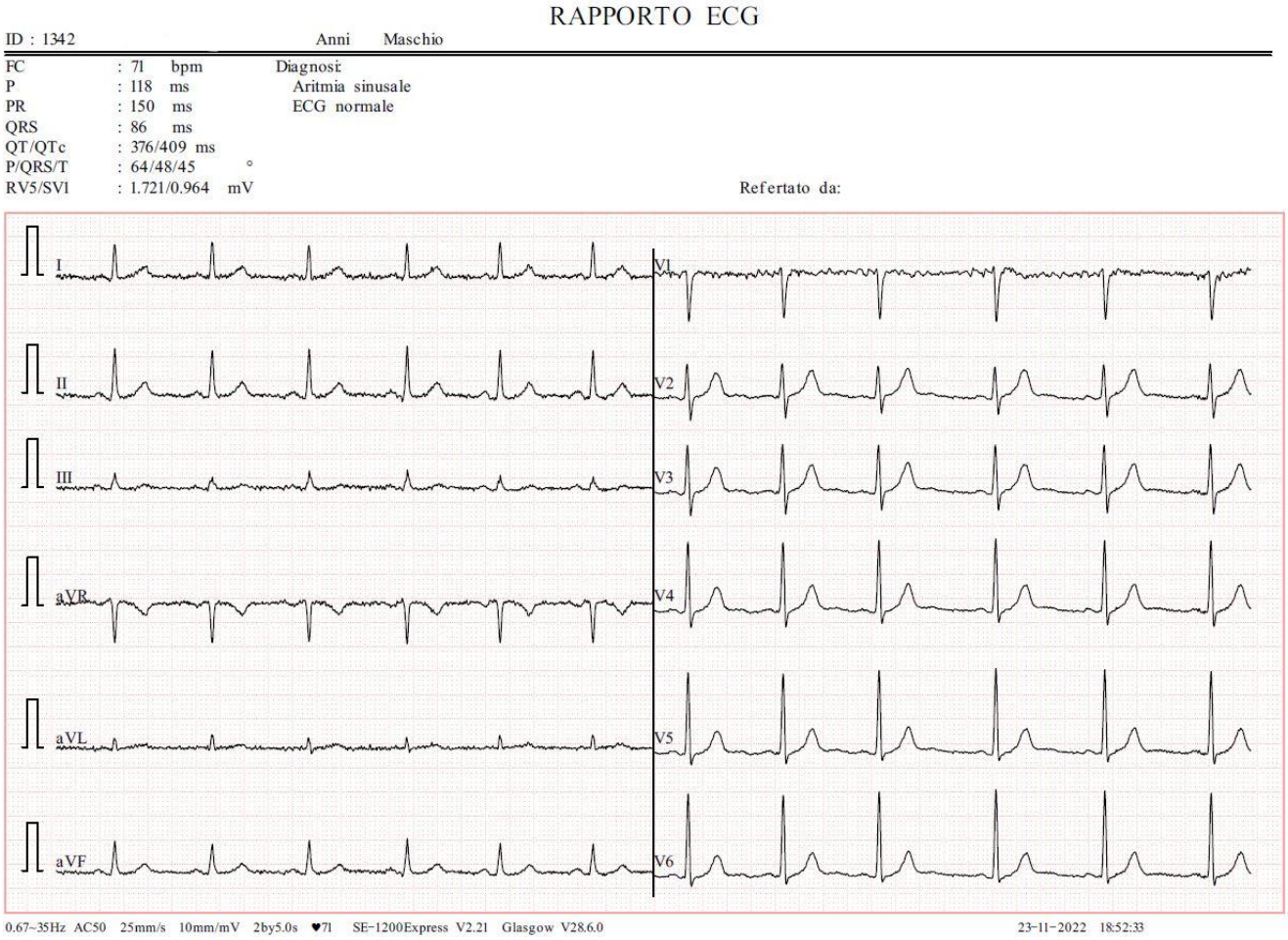

Figure 84 Ambulatory signals reconstructed

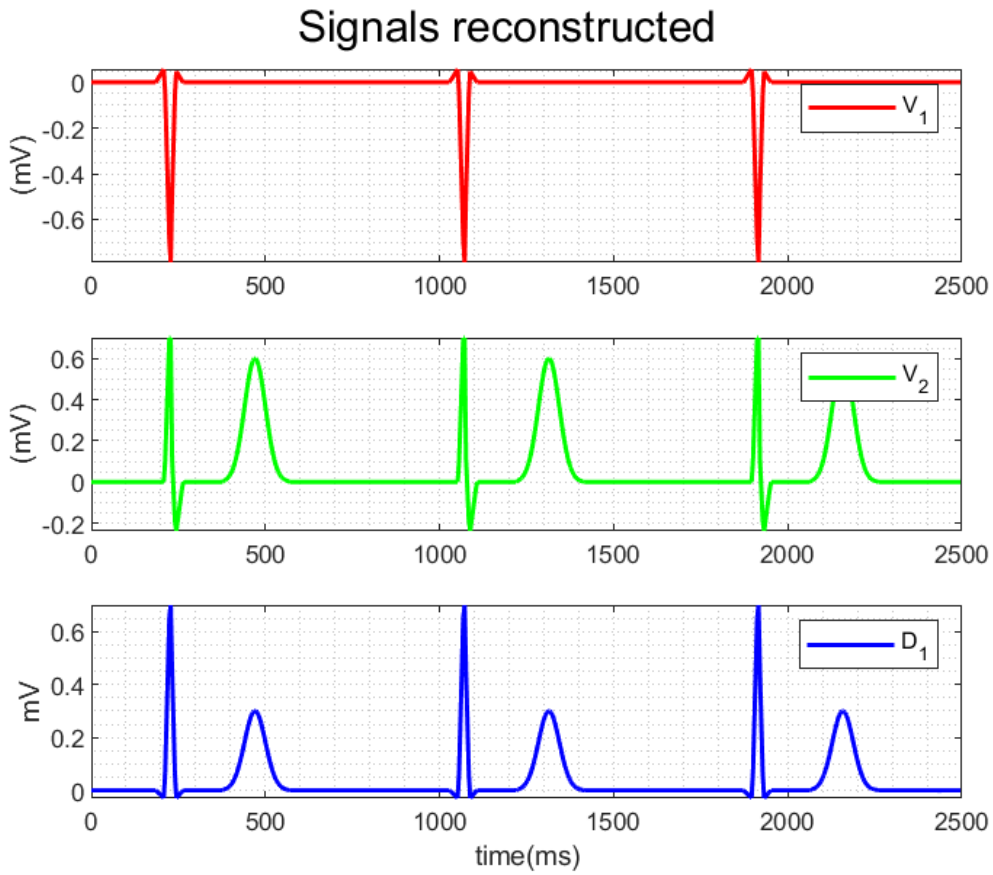

Figure 85 Comparison V2

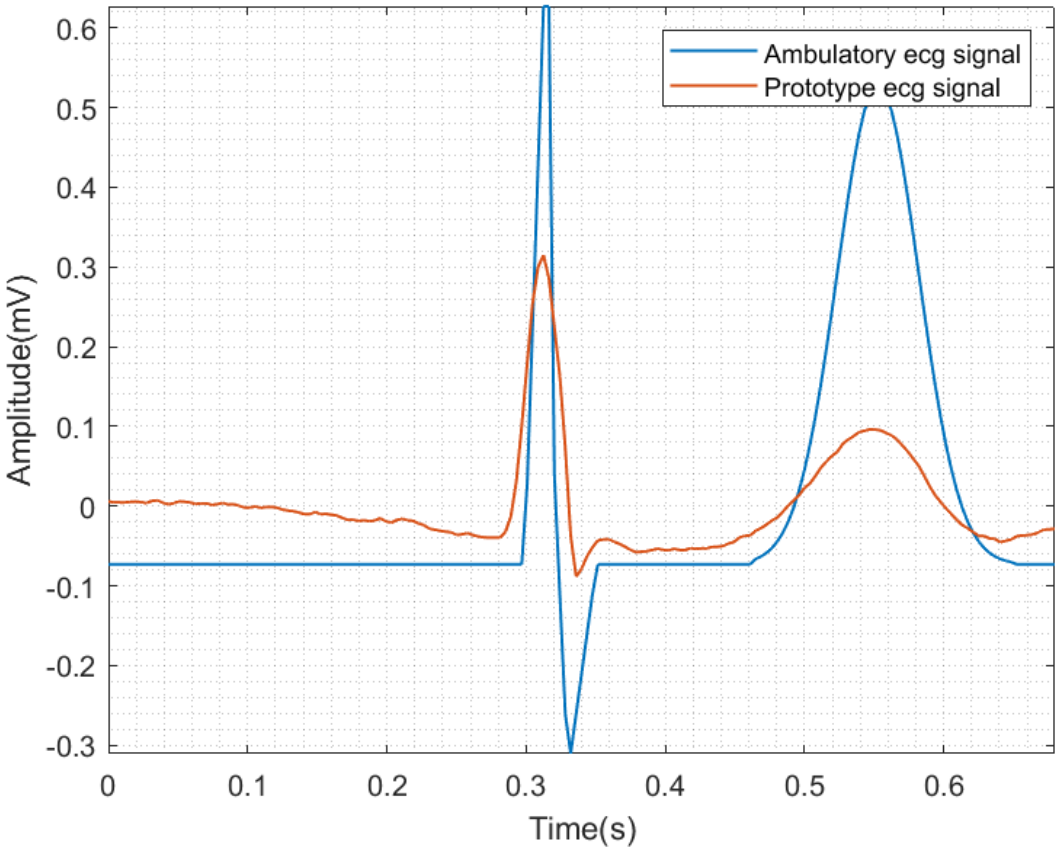

Figure 86 Comparison V1

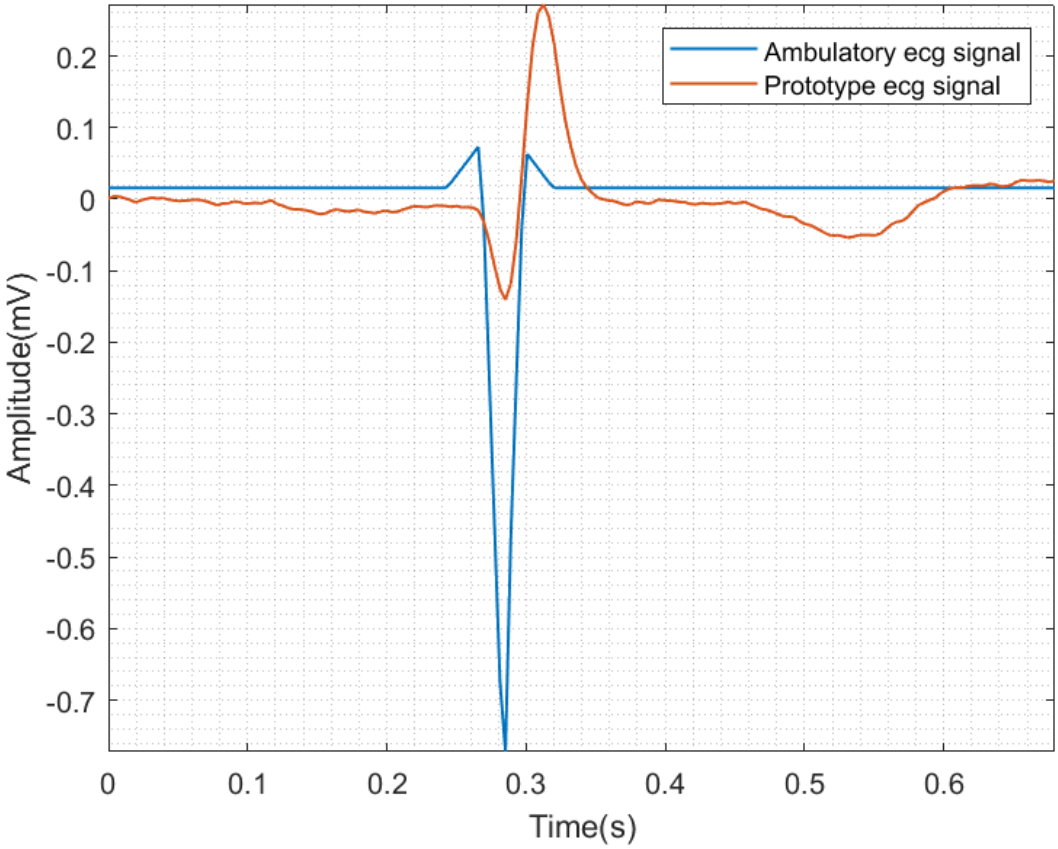

Figure 87 Comparison D1

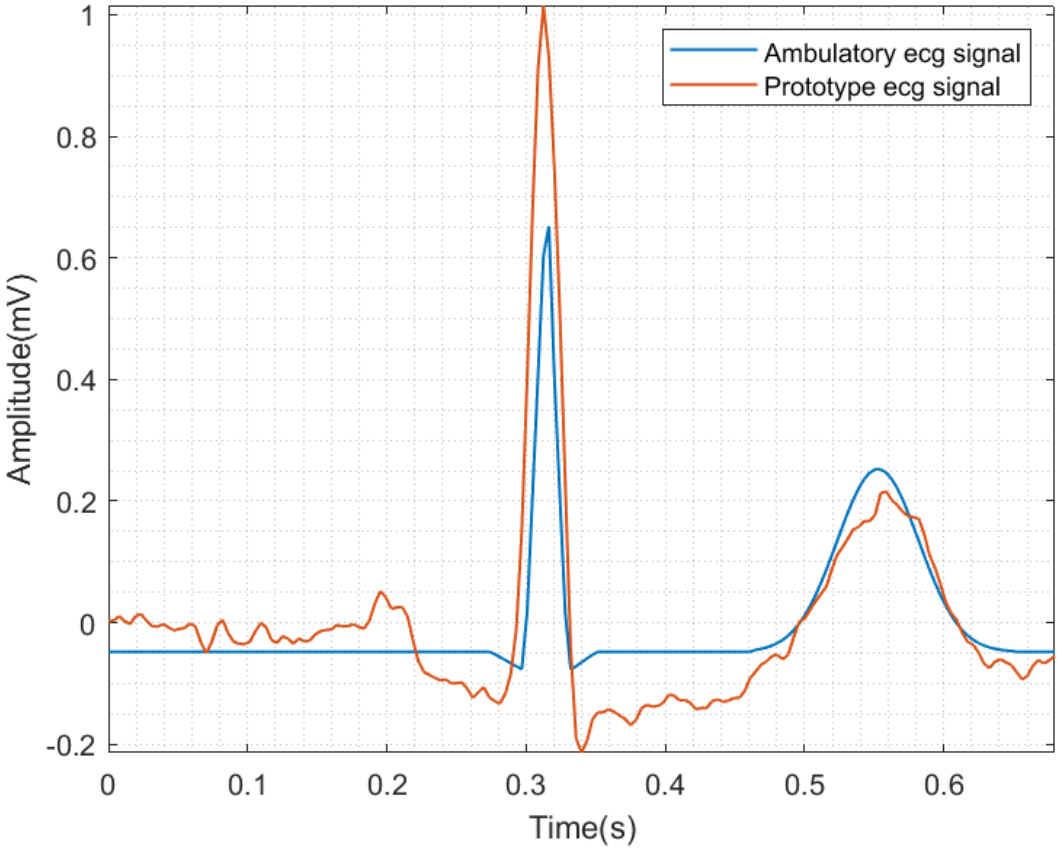

Patient #6:

Male 45 years old

BP 106/63

Figure 87 Prototype original signal V1

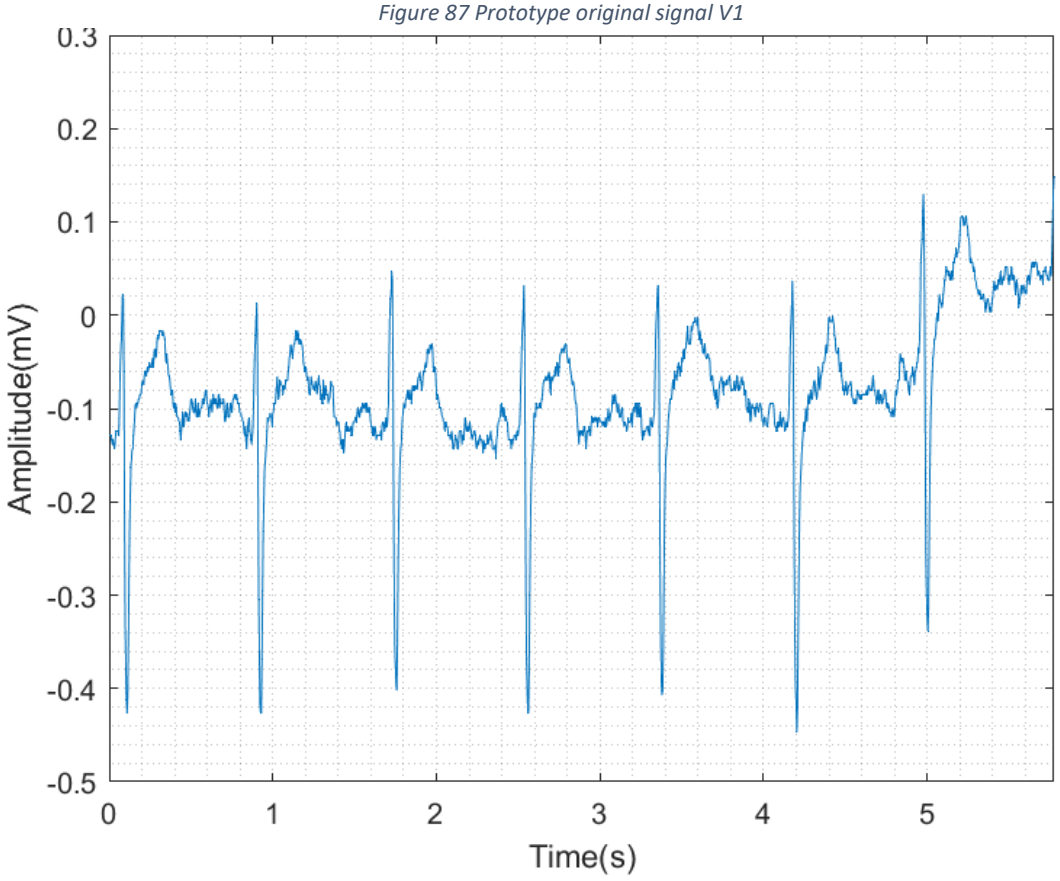

Figure 88 Prototype original signal D1

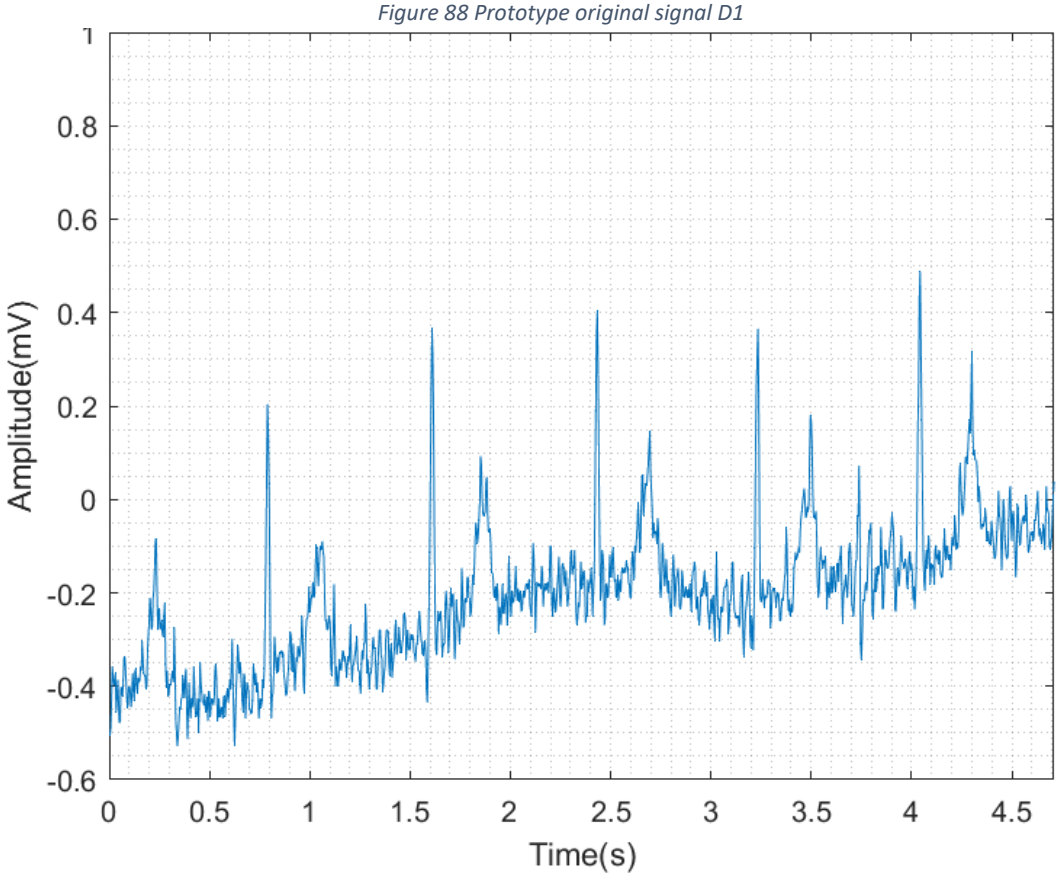

Figure 89 Prototype original signal V2

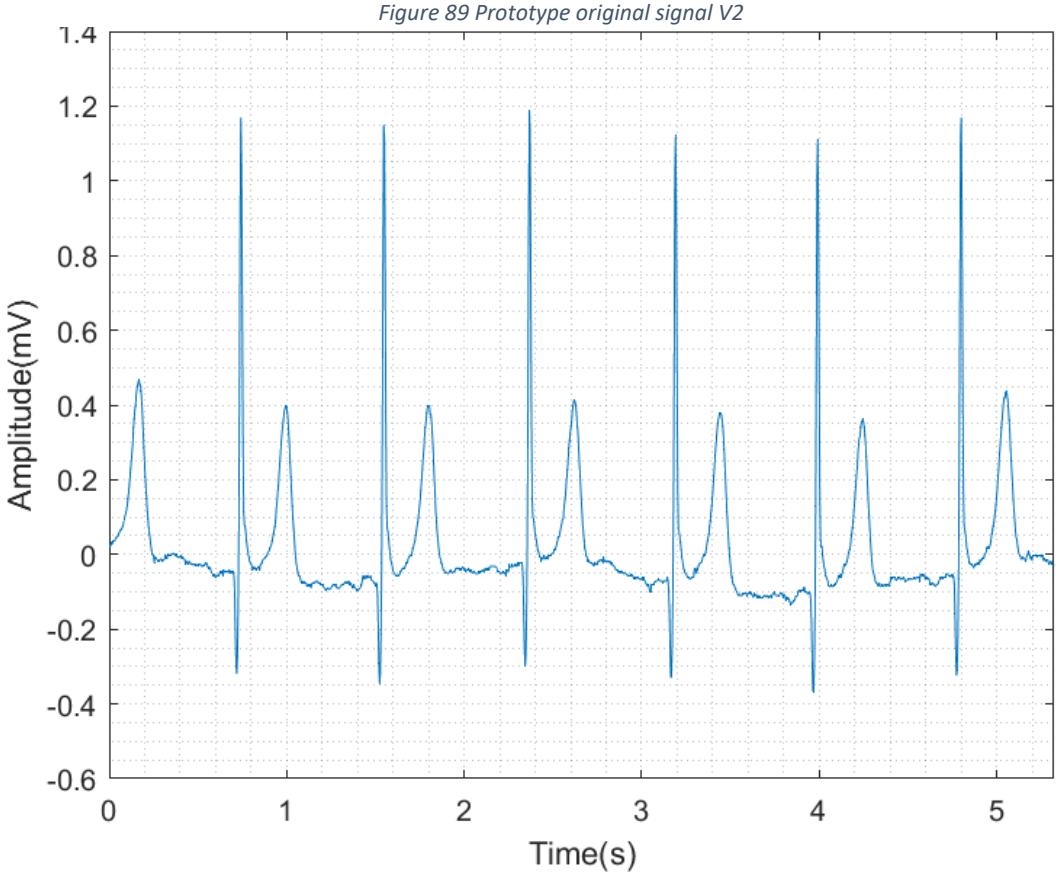

Figure 90 Ambulatory original signals

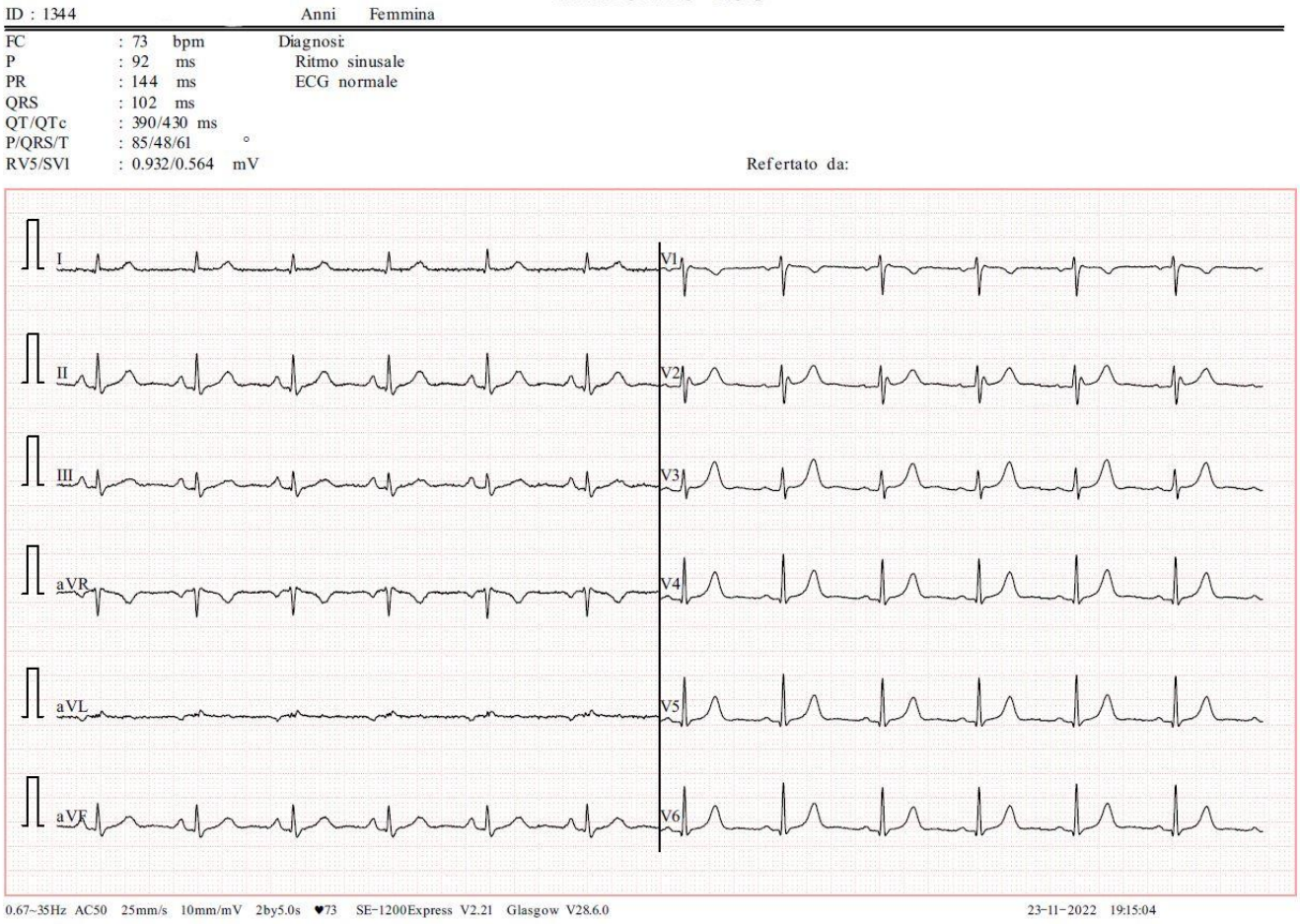

Figure 91 Ambulatory signals reconstructed

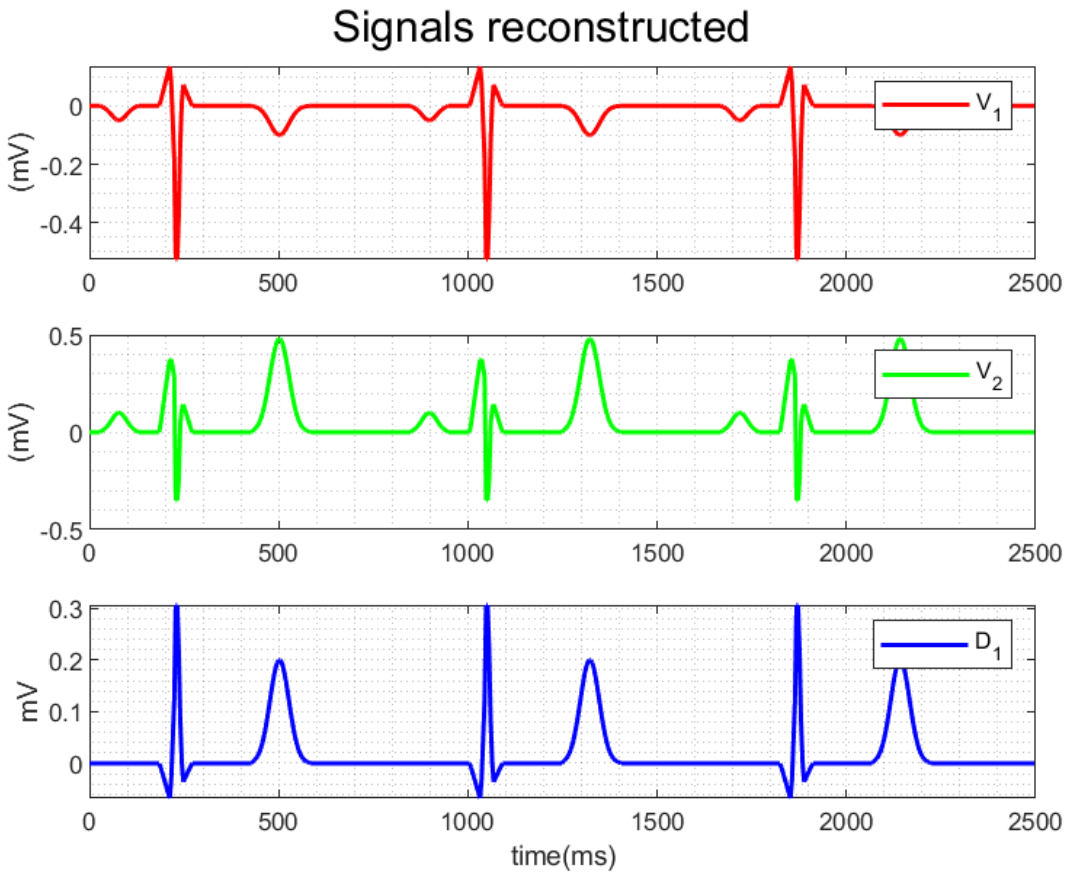

Figure 92 Comparison V2

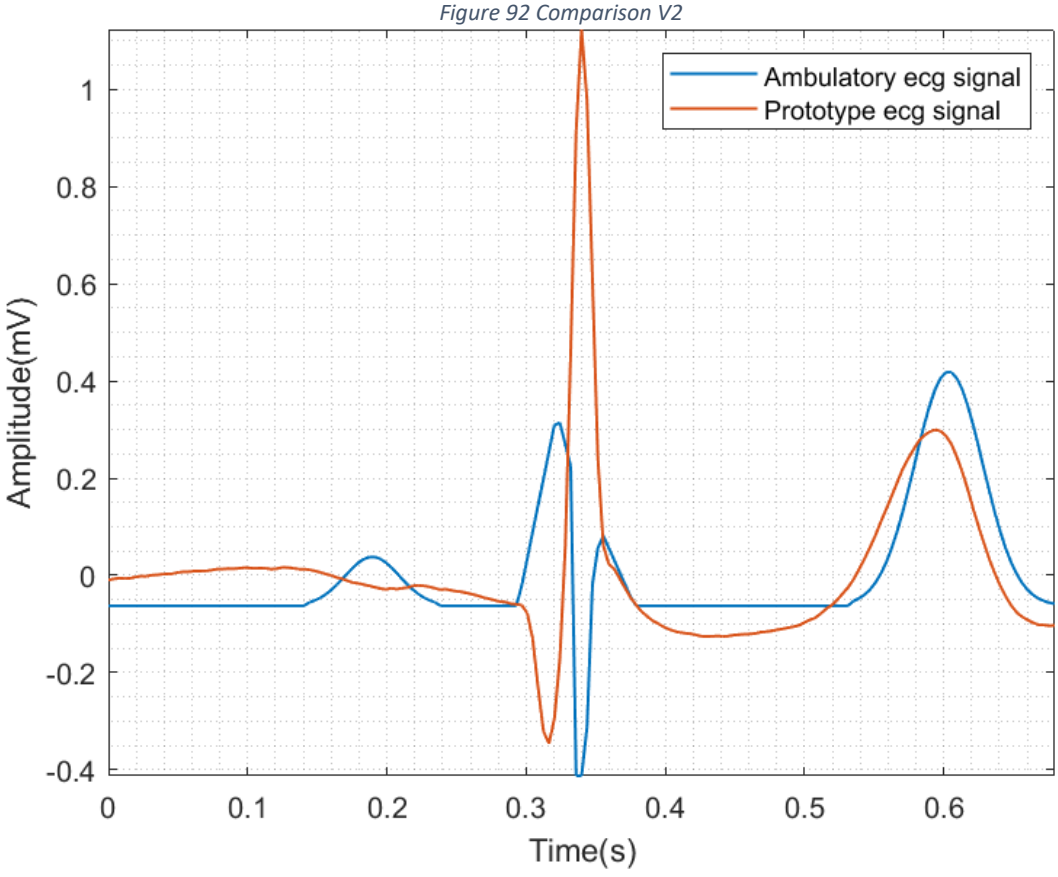

Figure 93 Comparison V1

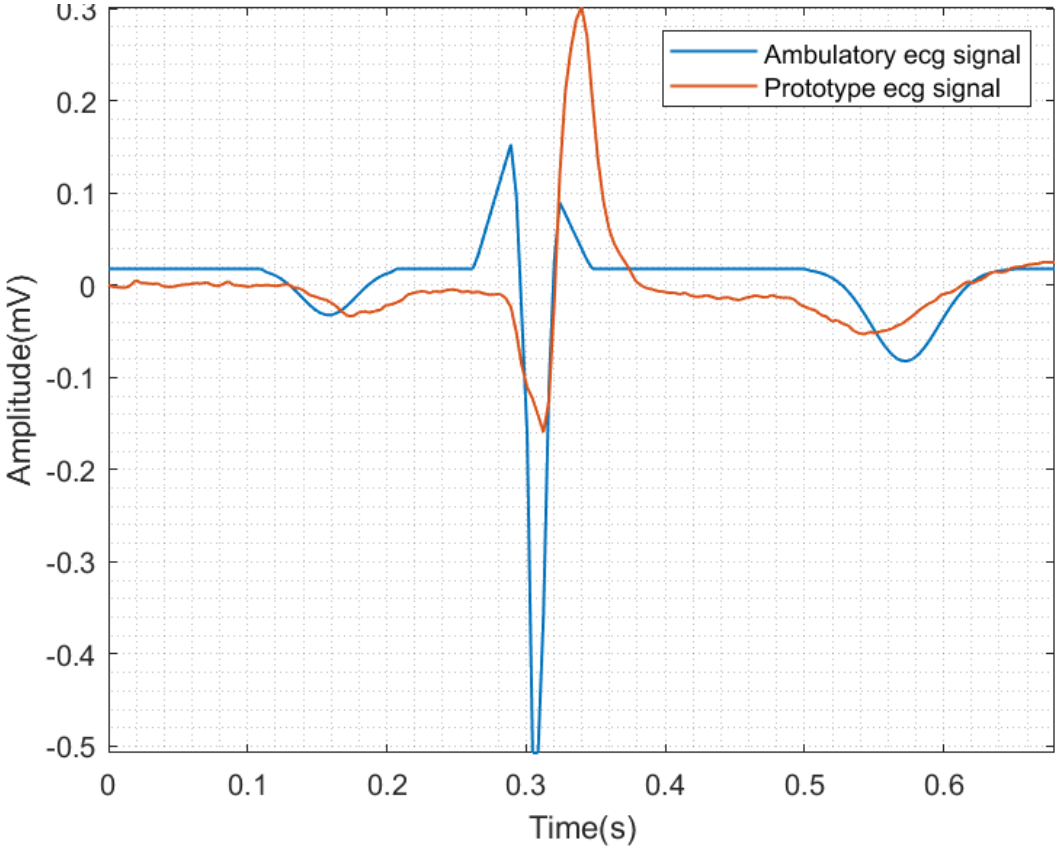

Figure 94 Comparison D1

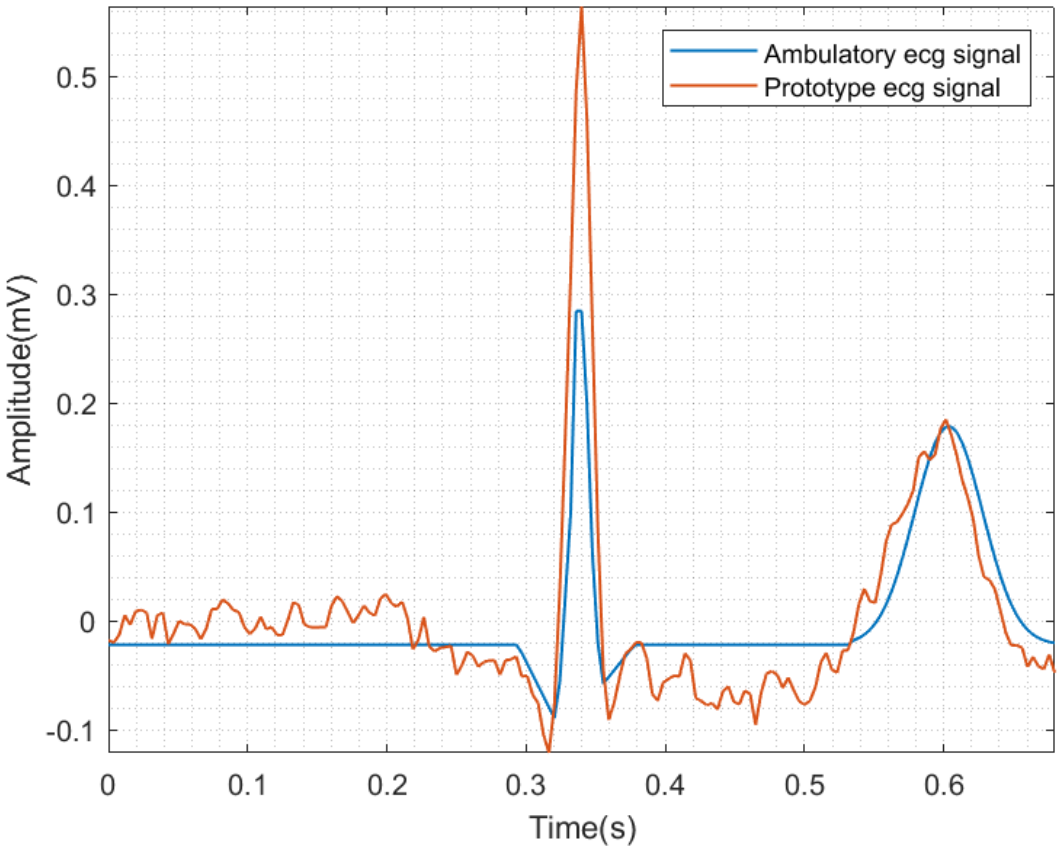

Patient #7:

Male 57 years old

BP 150/96

Figure 95 Prototype original signal V1

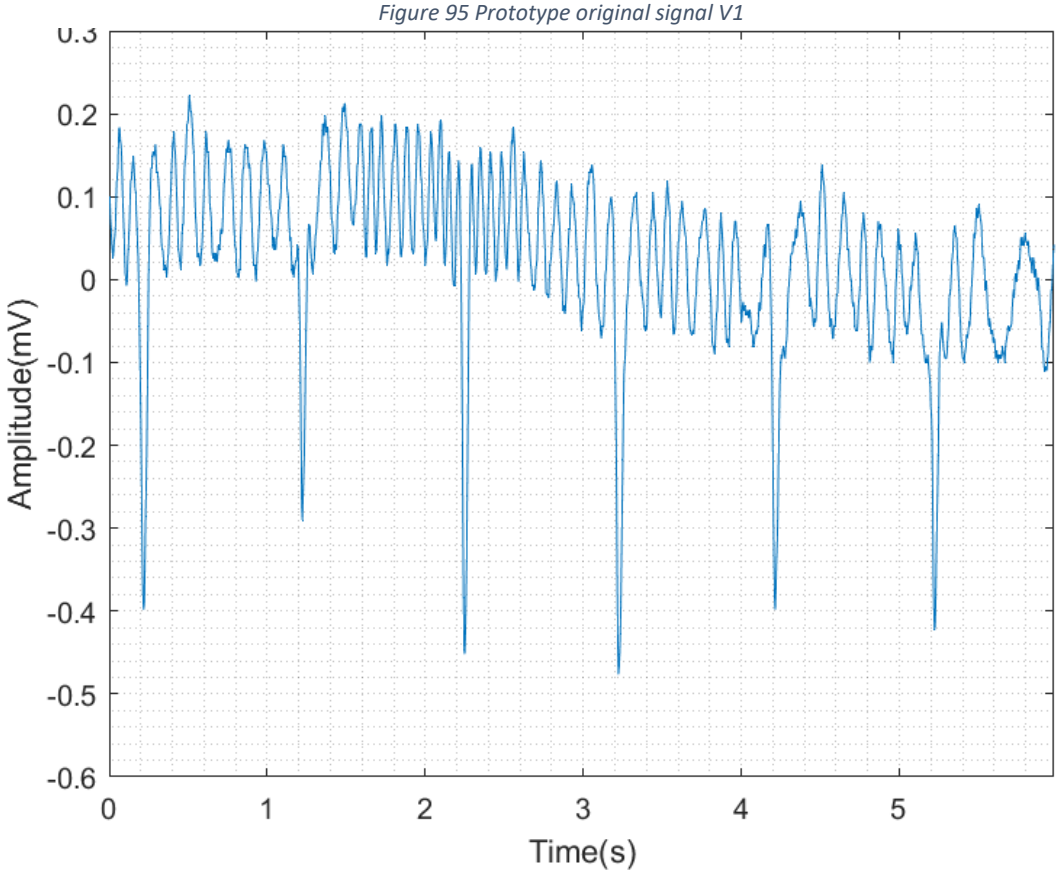

Figure 96 Prototype original signal D1

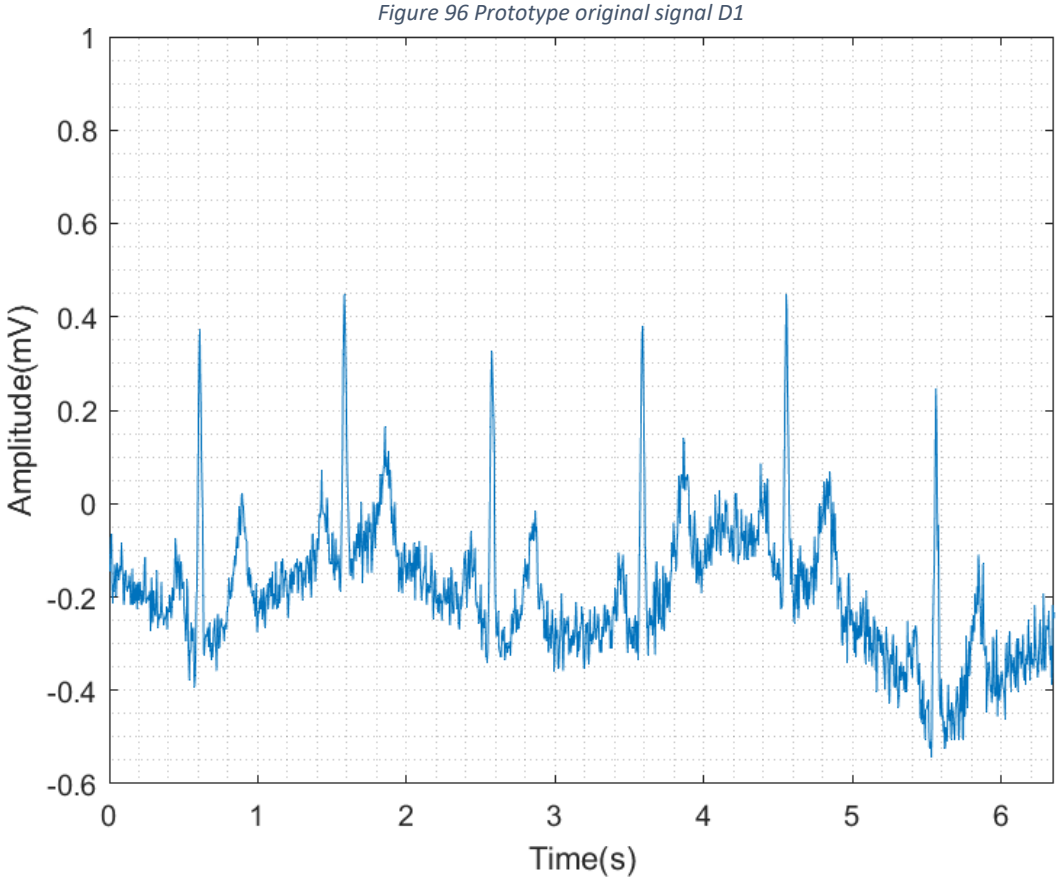

Figure 97 Prototype original signal V2

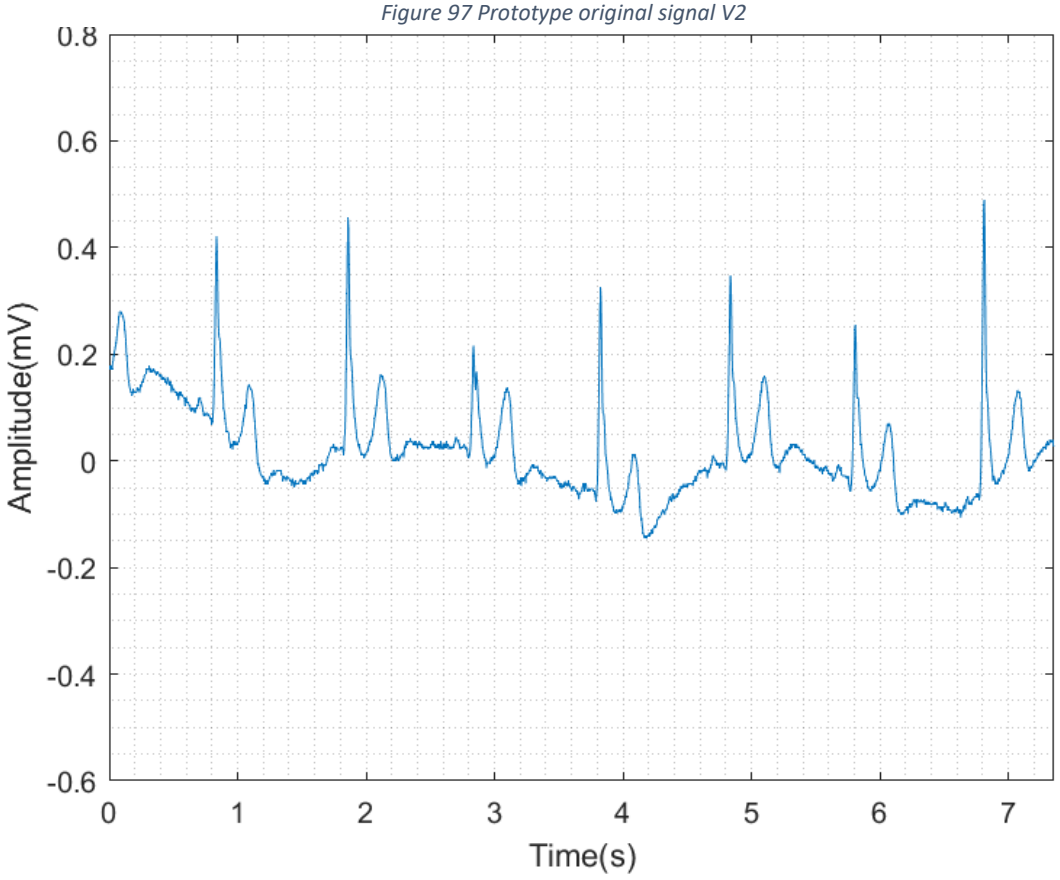

Figure 98 Ambulatory original signals

RAPPORTO ECG

ID : 1346 Anni Maschio

FC	: 60 bpm	Diagnosi:
P	: 120 ms	Ritmo sinusale
PR	: 170 ms	Emiblocco anteriore sinistro
QRS	: 118 ms	Possibile infarto antero-settale - epoca indeterminata
QT/QTc	: 426/426 ms	Ipertrofia ventricolare sinistra
P/QRS/T	: 58/-60/66 °	ECG anormale
RV5/SV1	: 1.119/0.511 mV	Refertato da:

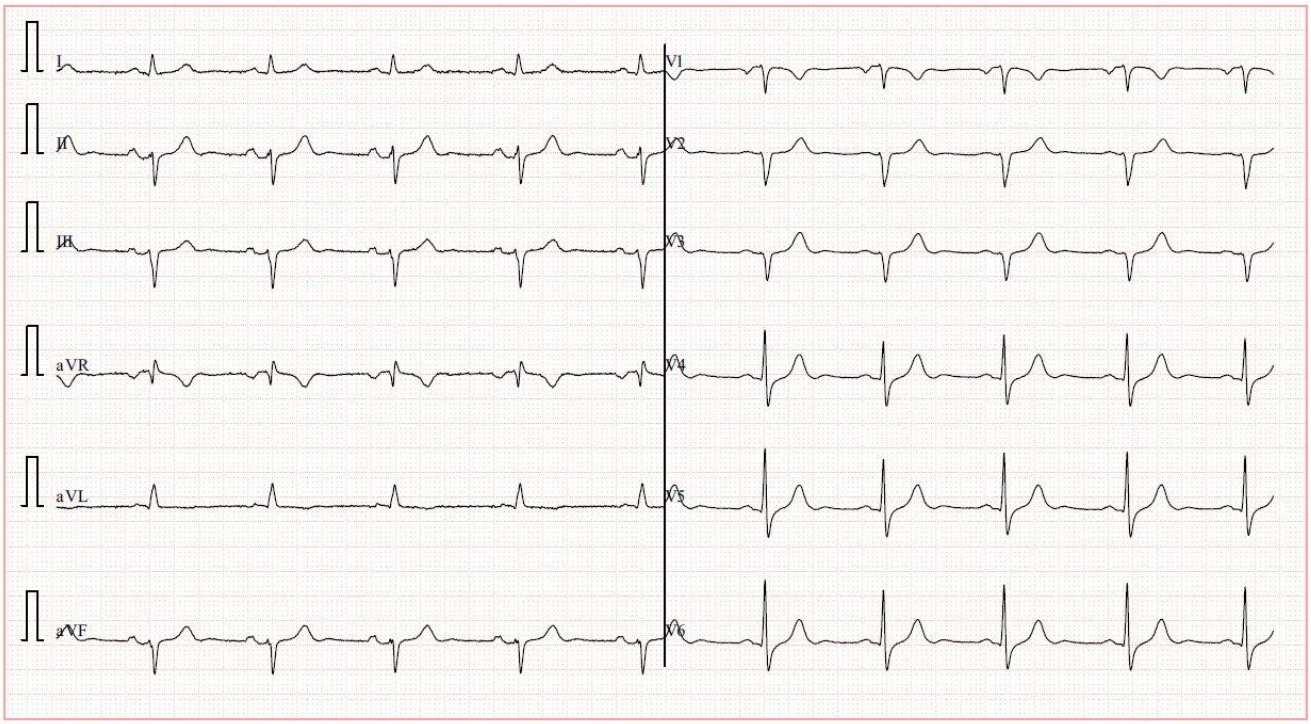

0.67-35Hz AC50 25mm/s 10mm/mV 2by5.0s ♥60 SE-1200Express V2.21 Glasgow V28.6.0 23-11-2022 19:30:15

Figure 99 Ambulatory signals reconstructed

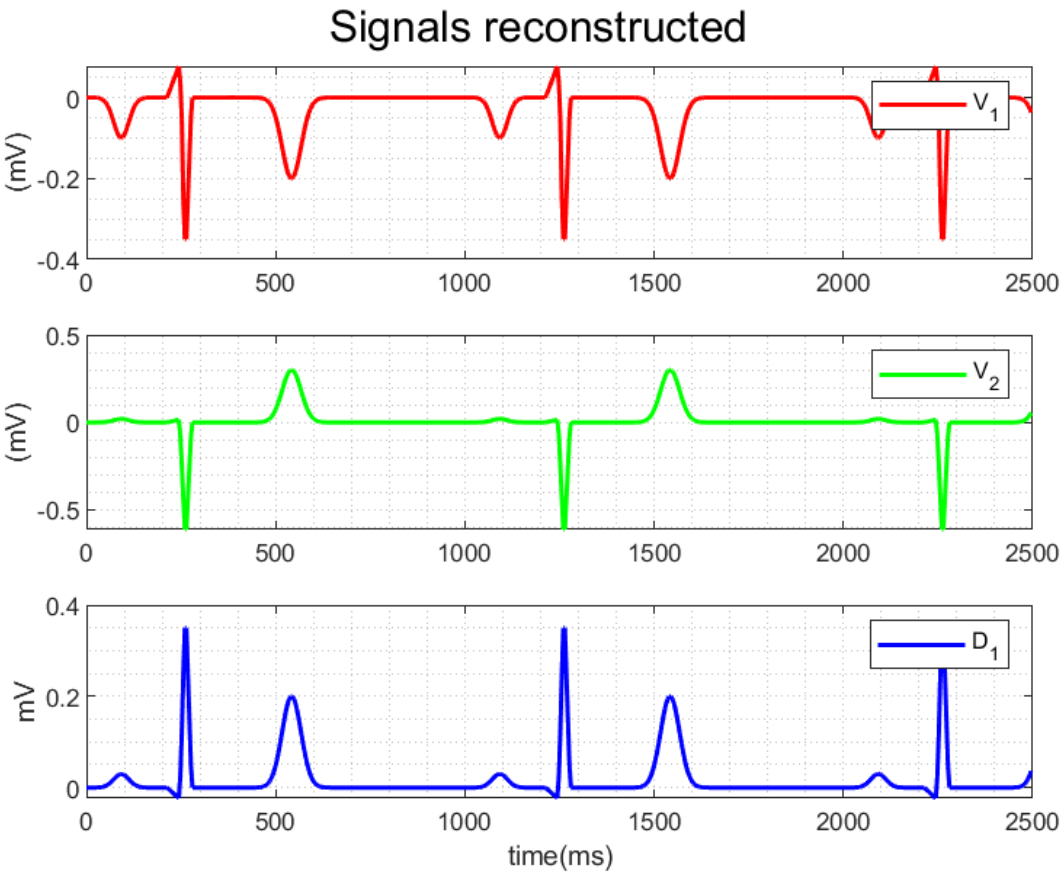

Figure 100 Comparison V2

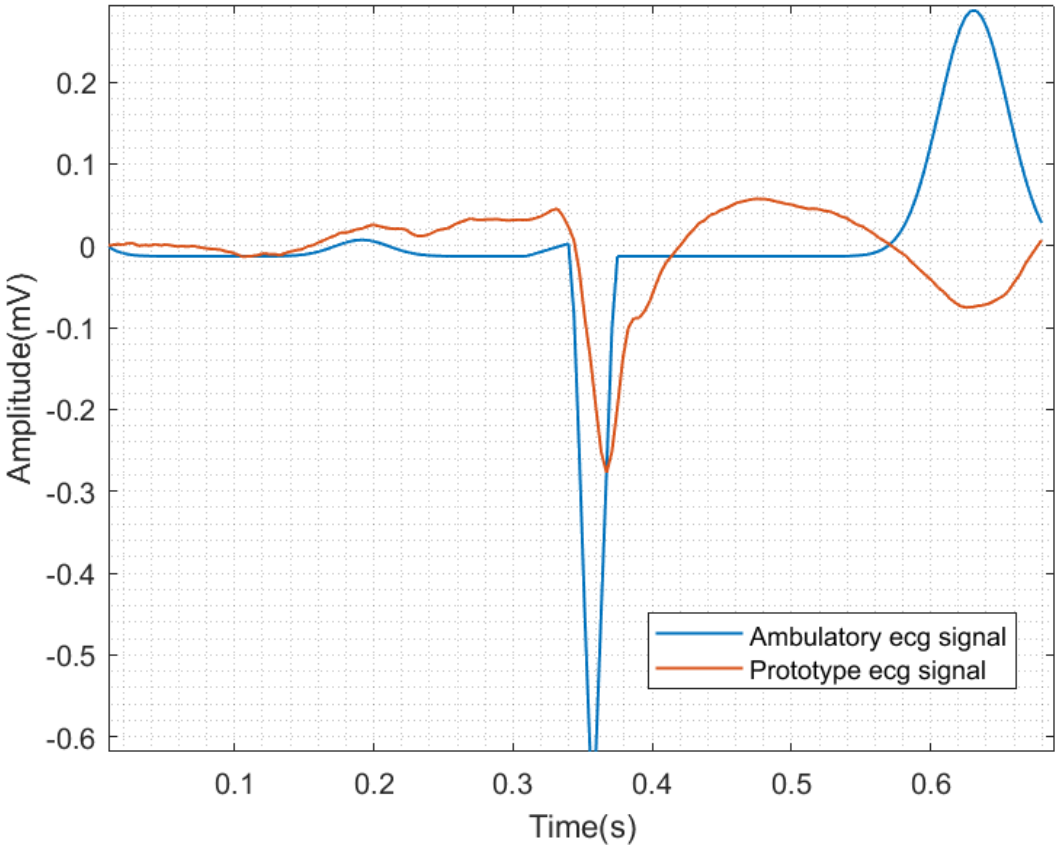

Figure 101 Comparison D1

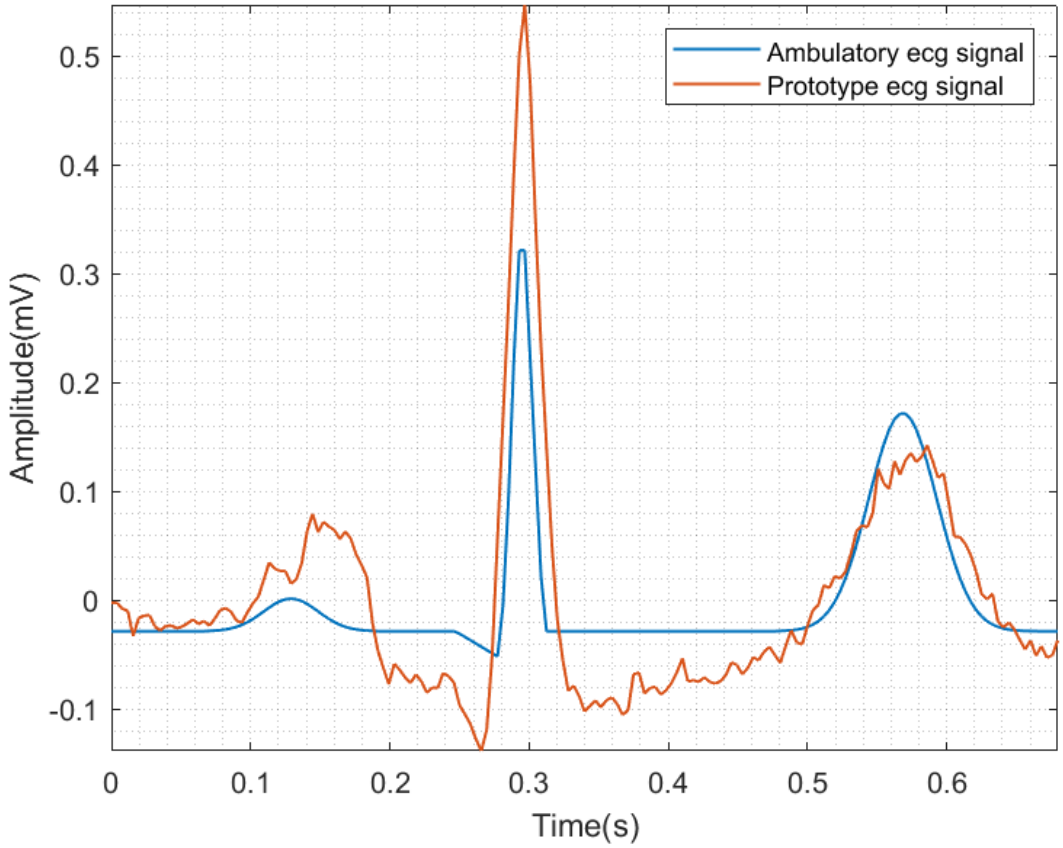

Figure 102 Comparison V1

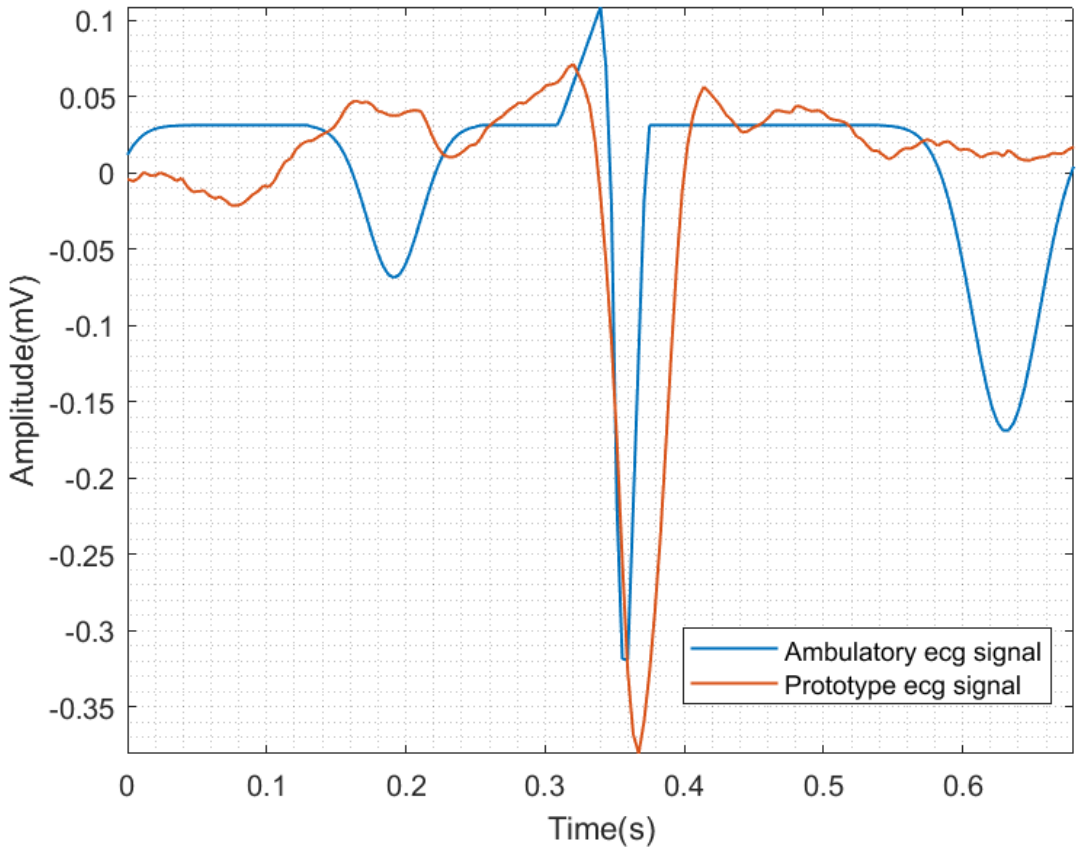

Patient #8:

Female 35 years old

BP 122/77

Figure 103 Prototype original signal V1

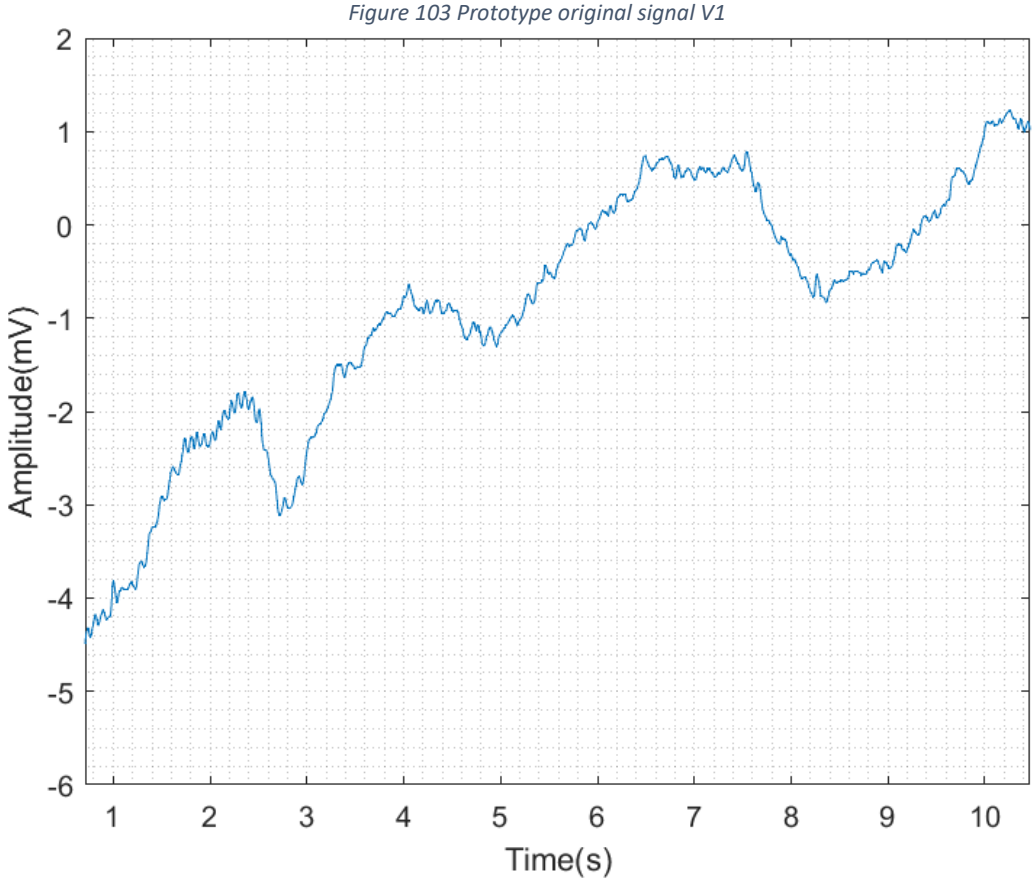

Figure 104 Prototype original signal D1

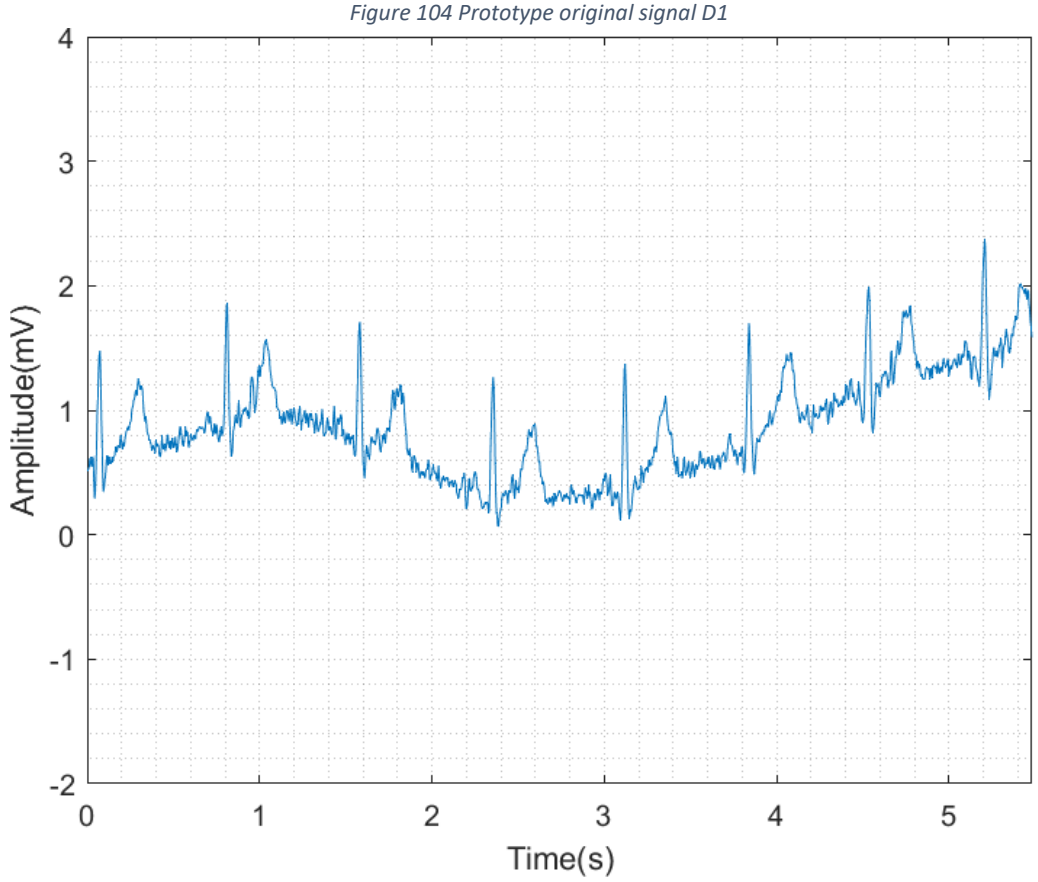

Figure 105 Prototype original signal V2

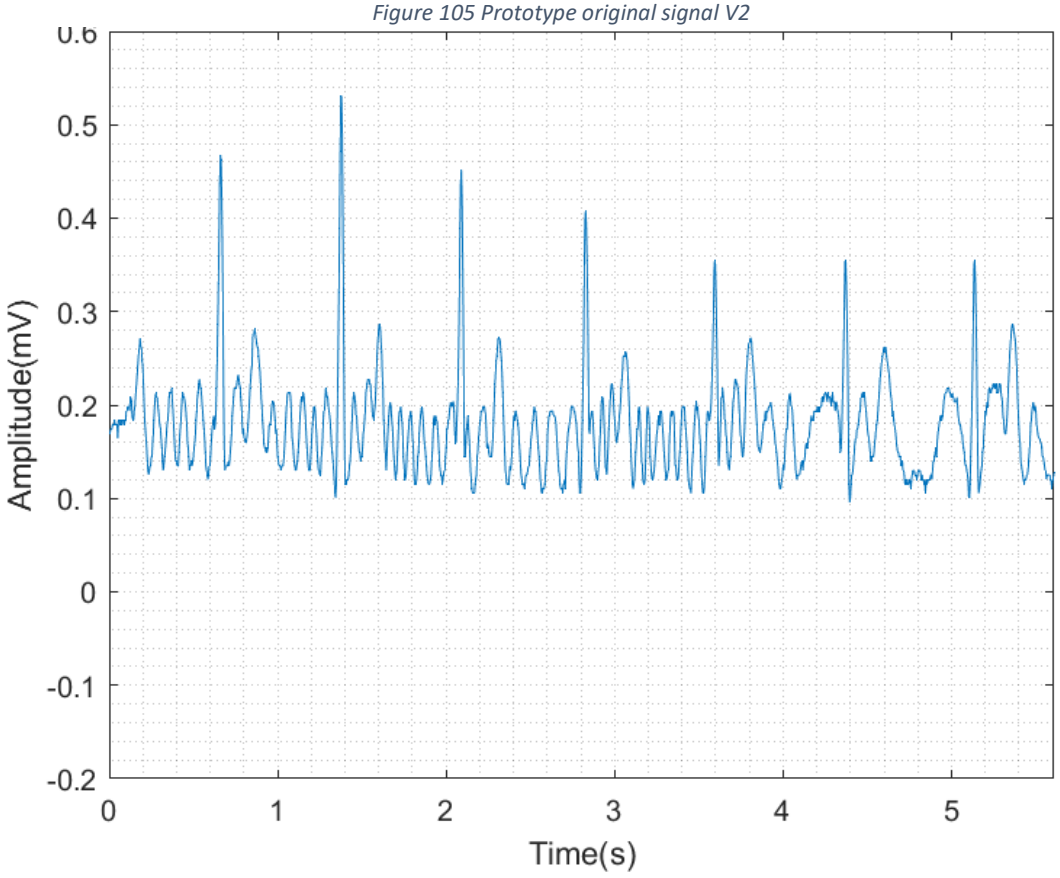

Figure 106 Ambulatory original signals

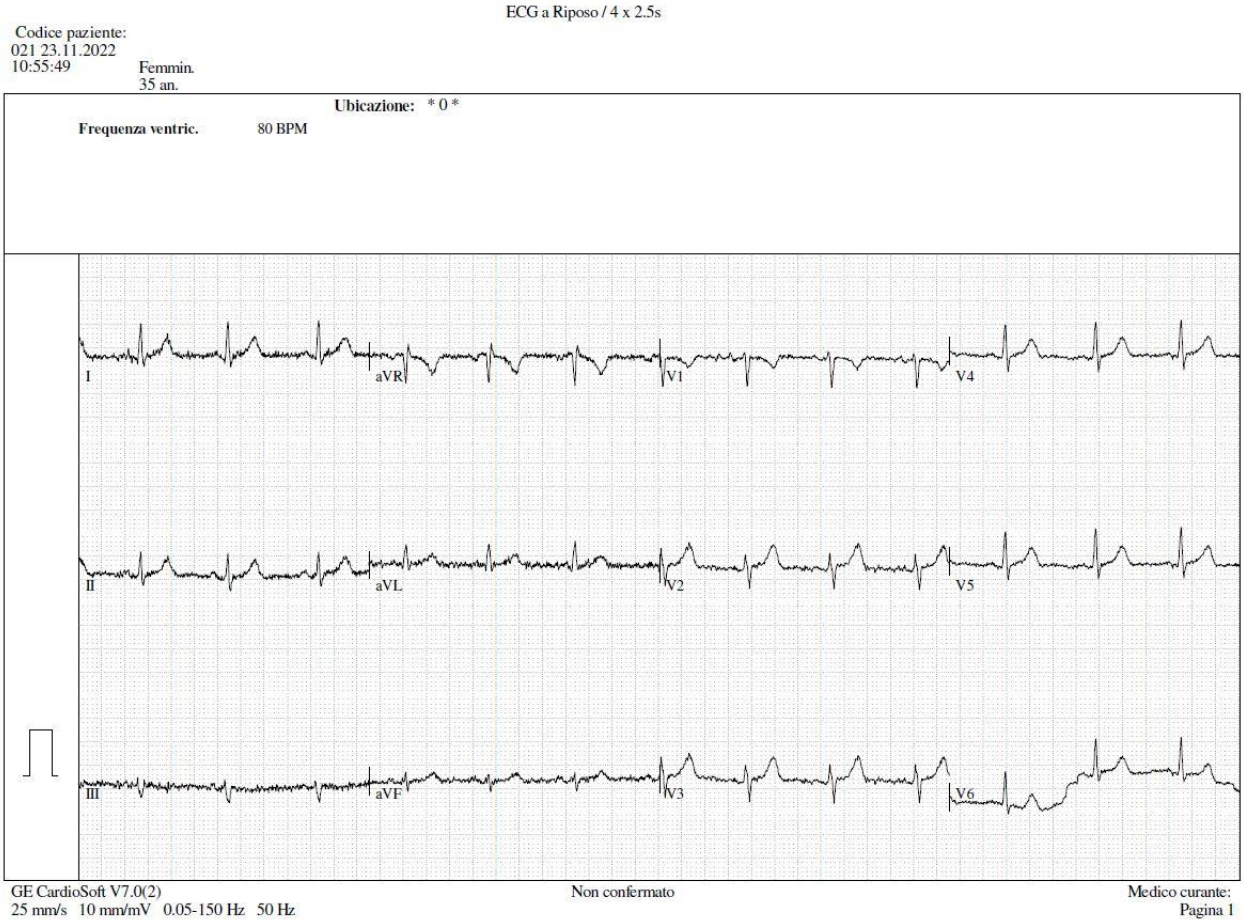

Figure 107 Ambulatory signals reconstructed

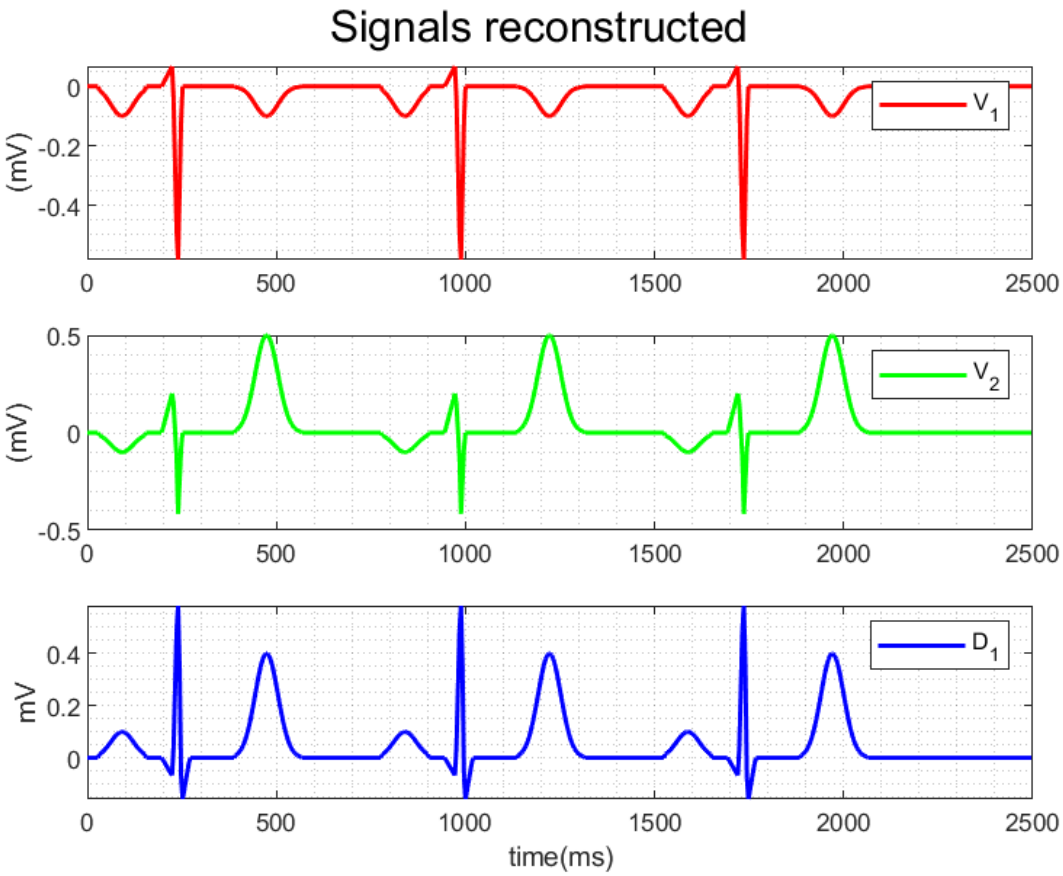

Figure 108 Comparison V1

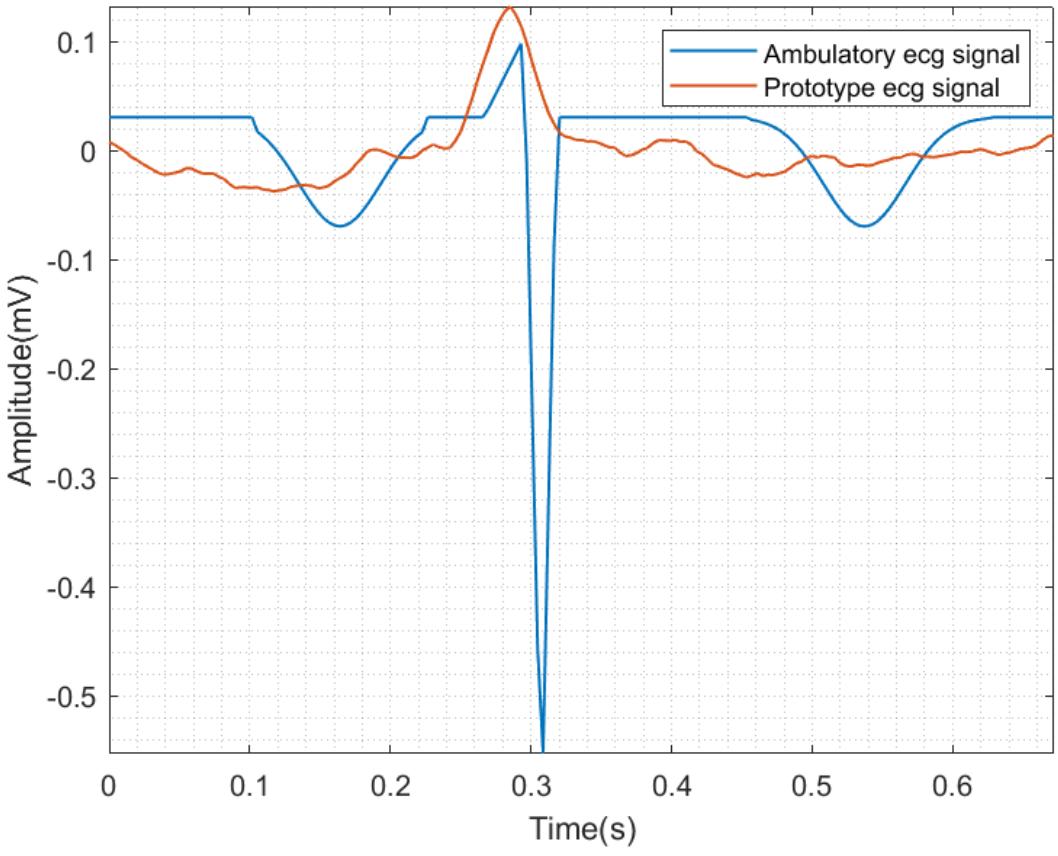

Figure 109 Comparison D1

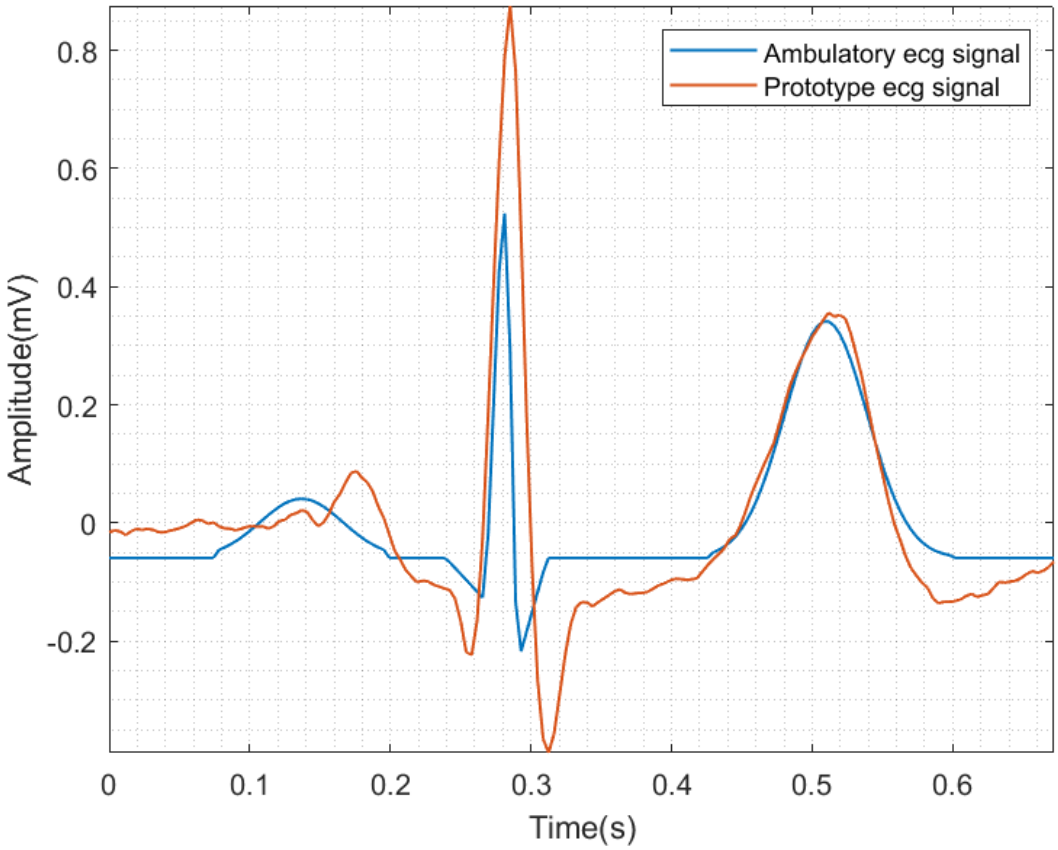

Figure 110 Comparison V2

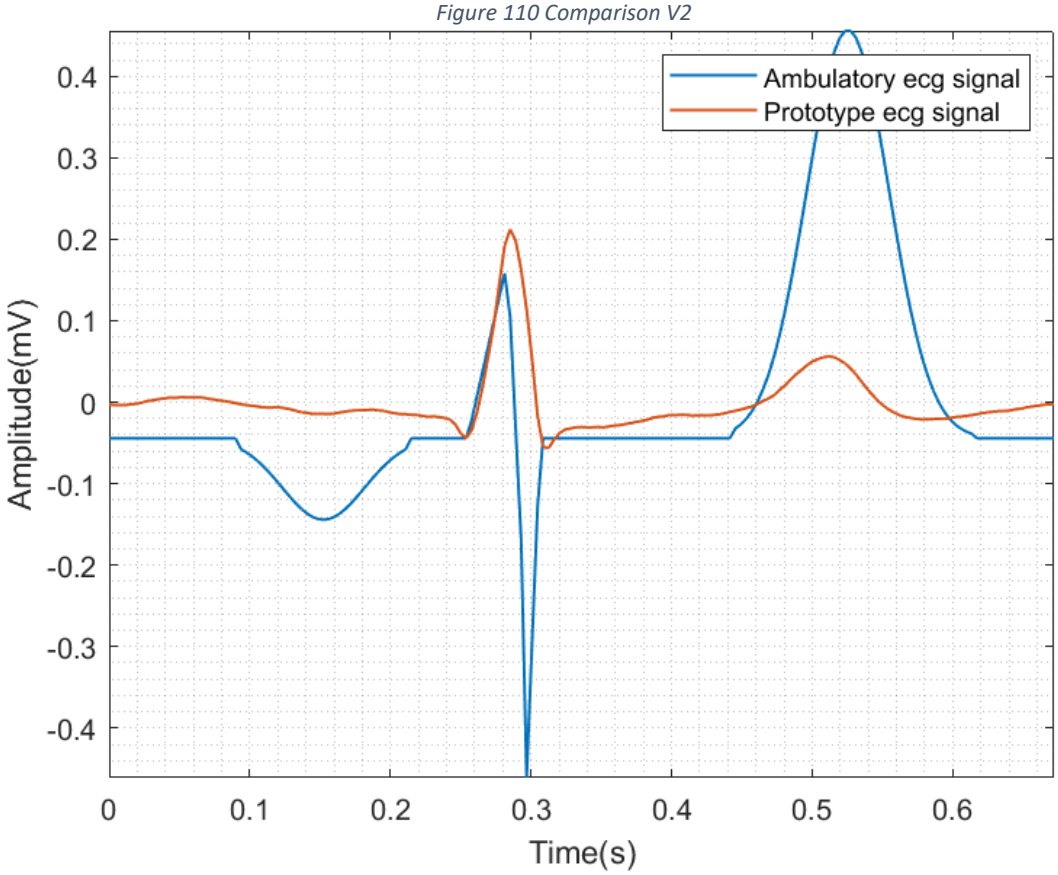

Patient #9:

Female 23 years old

BP 119/74

Figure 111 Prototype original signal V1

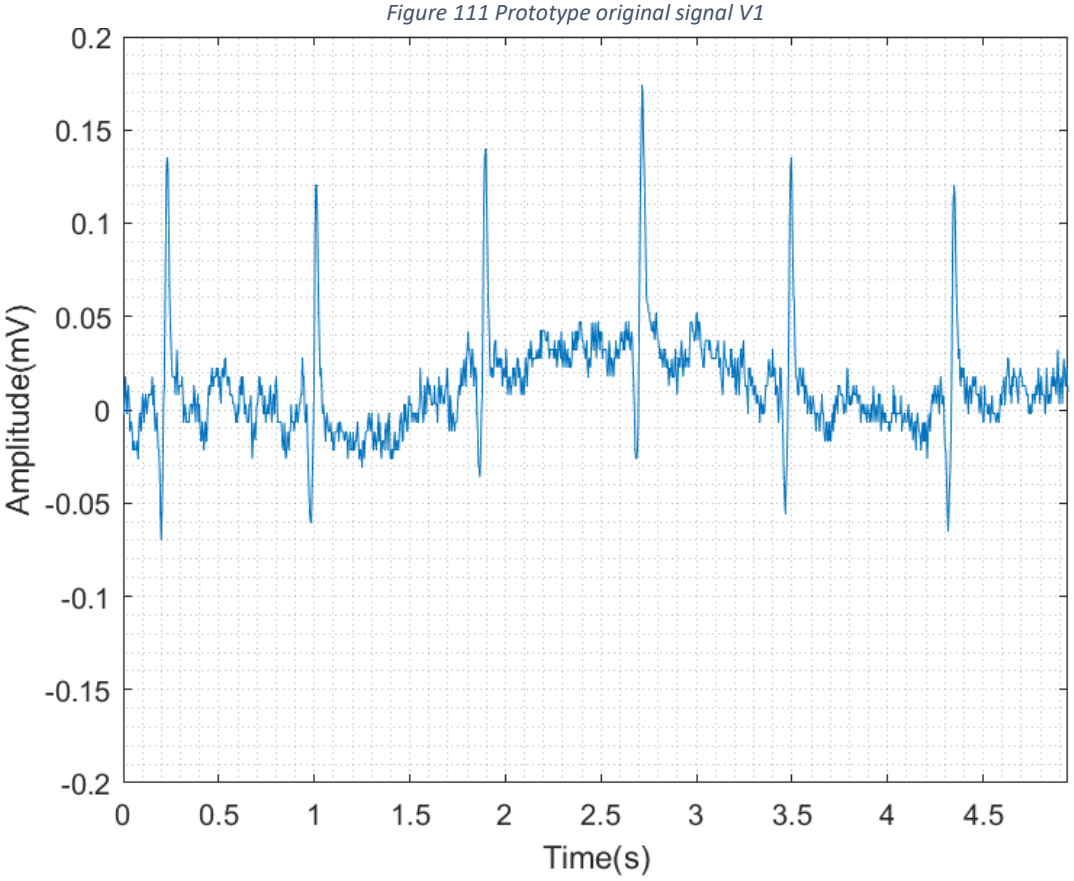

Figure 112 Prototype original signal D1

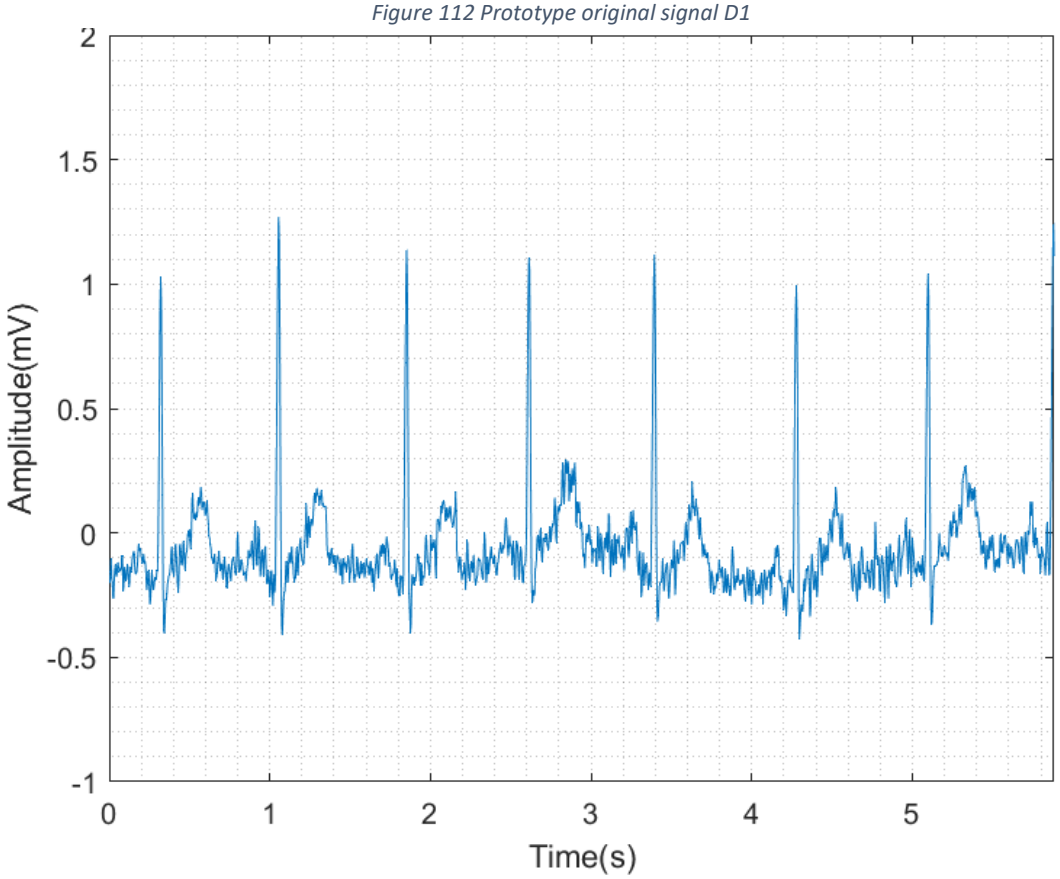

Figure 113 Prototype original signal V2

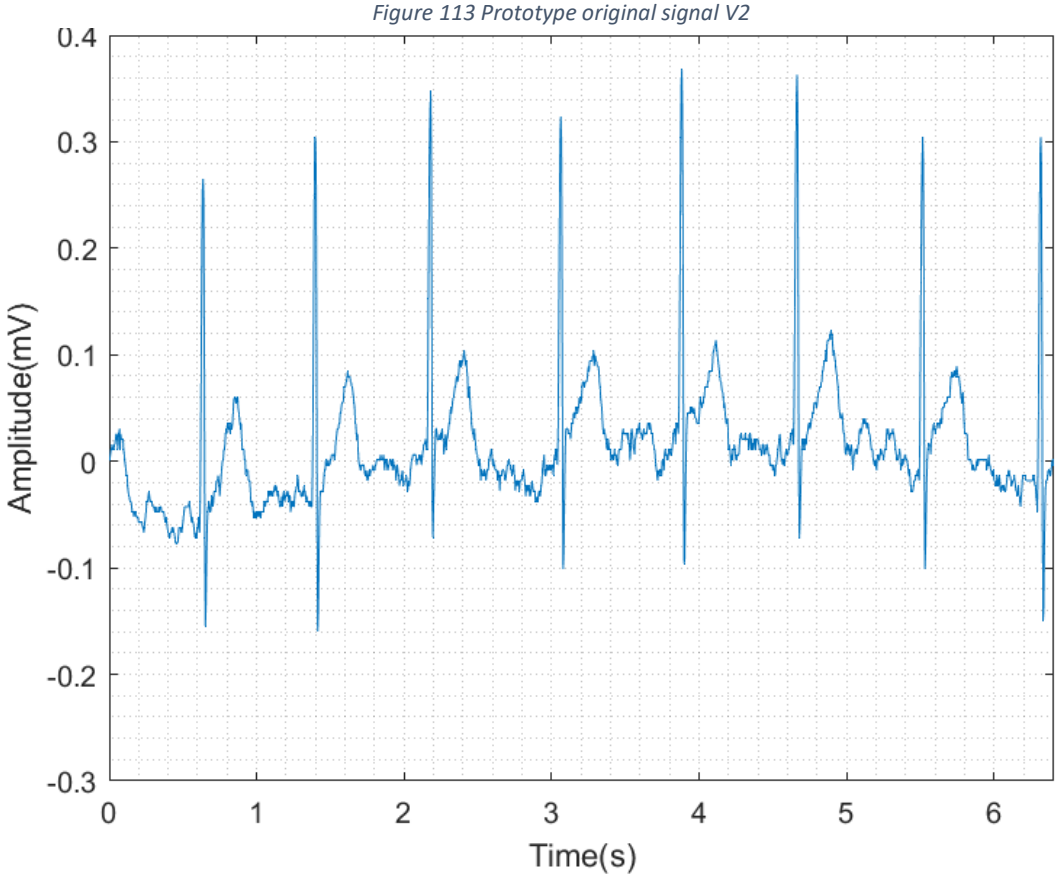

Figure 114 Ambulatory original signals

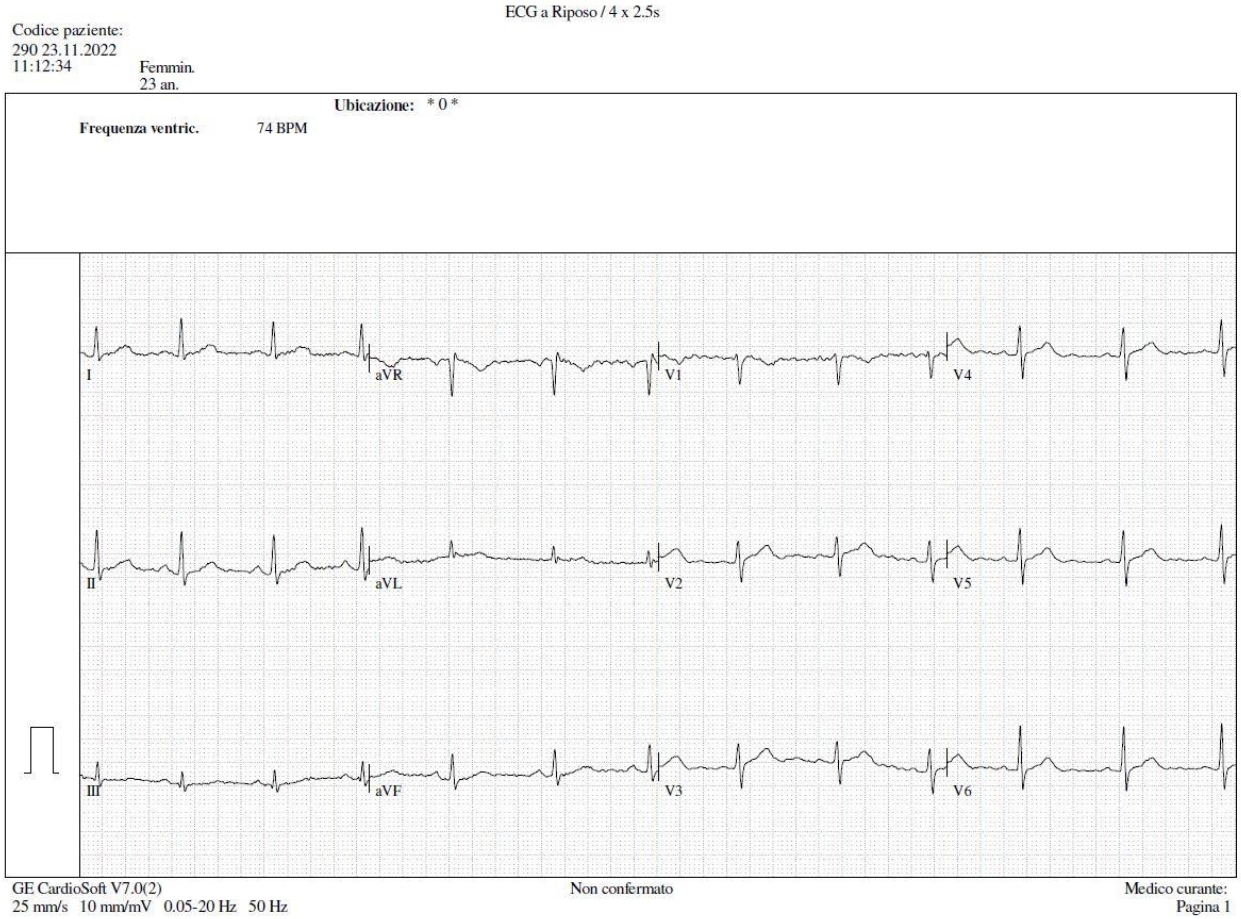

Figure 115 Ambulatory signals reconstructed

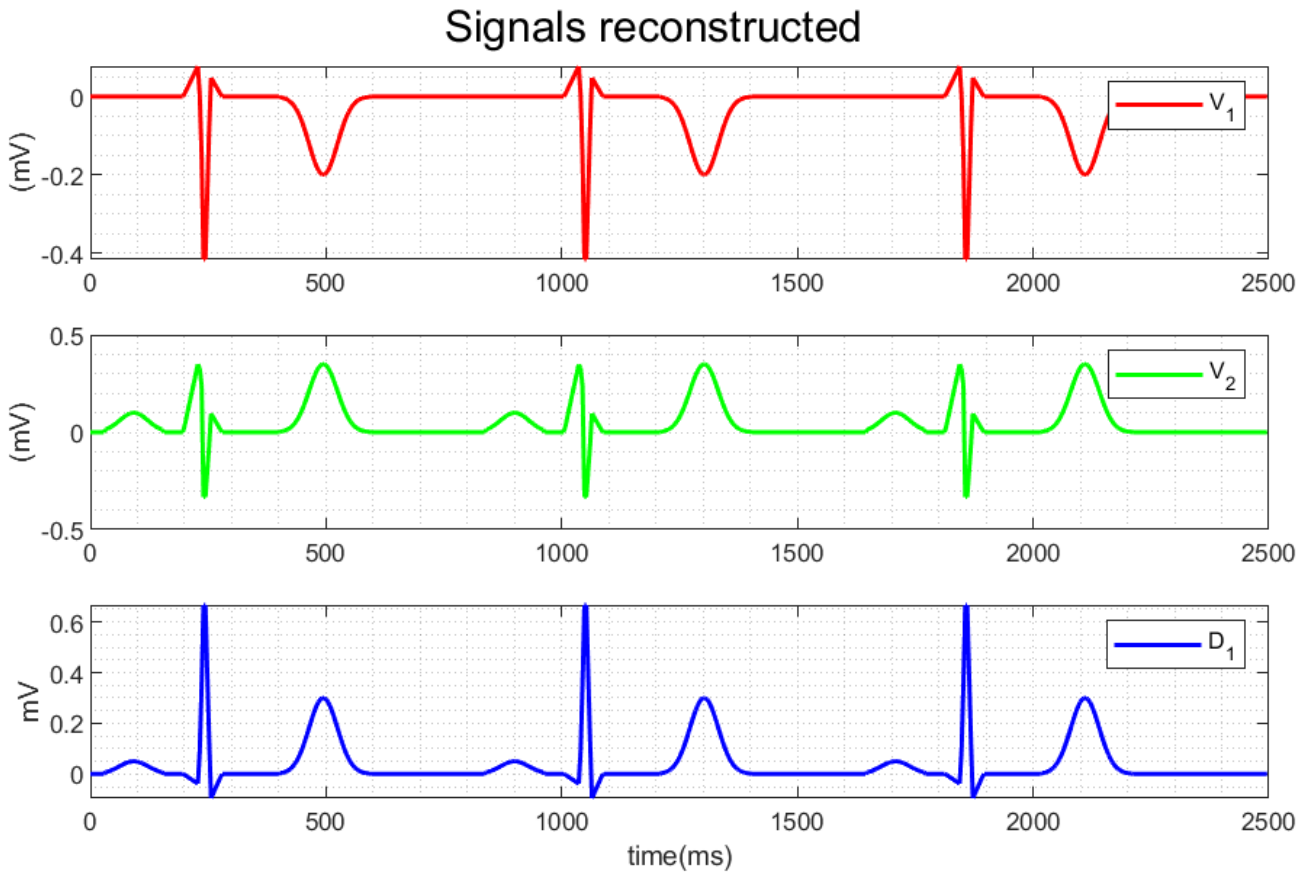

Figure 116 Comparison V1

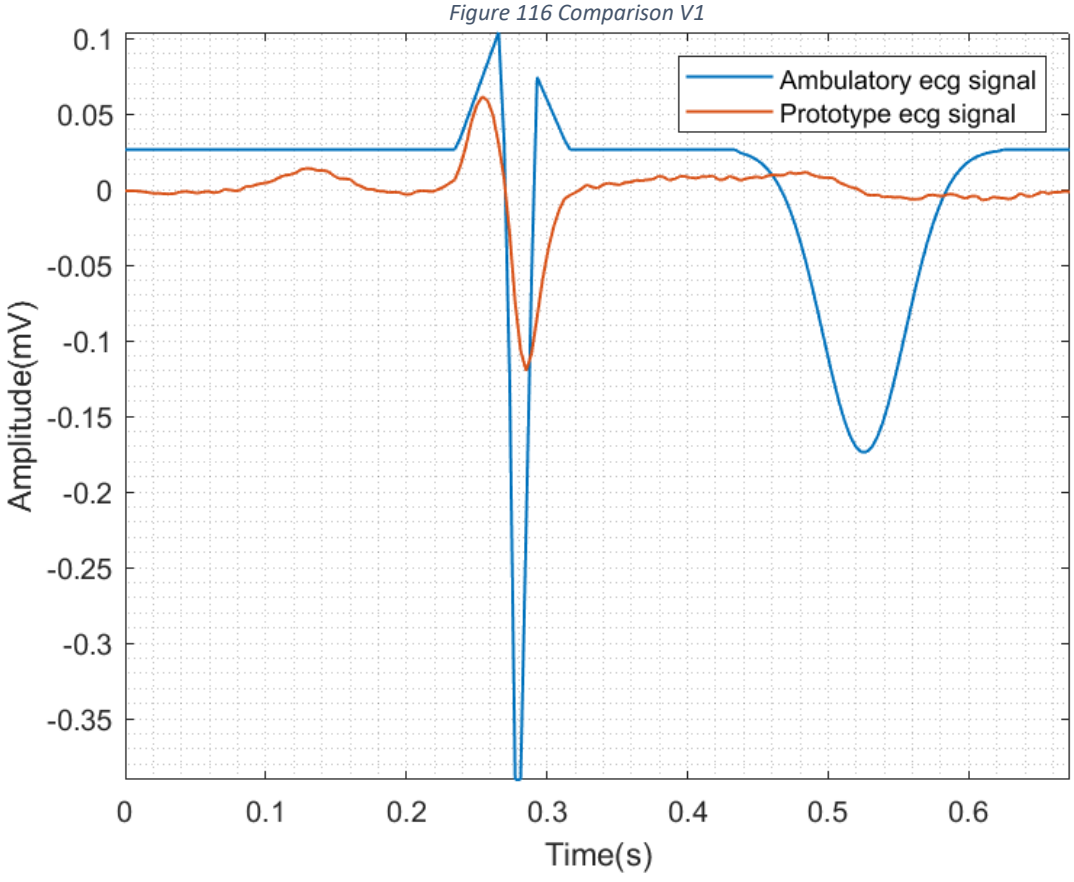

Figure 117 Comparison D1

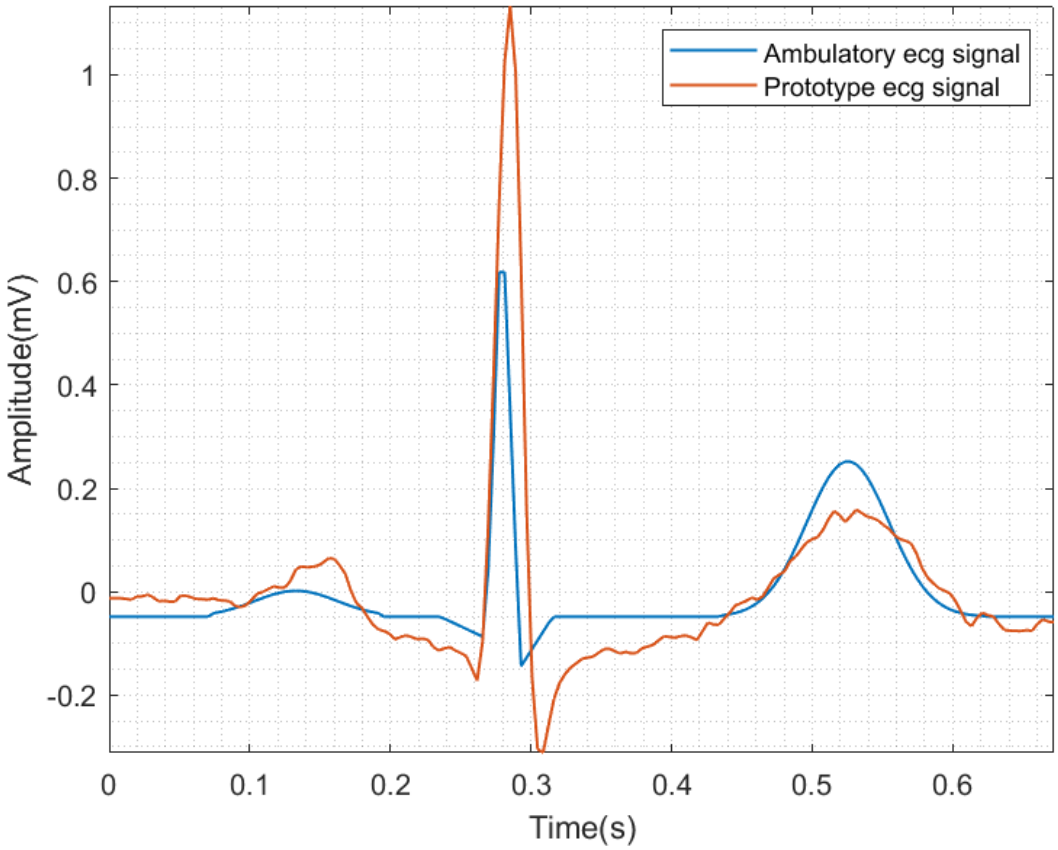

Figure 118 Comparison V2

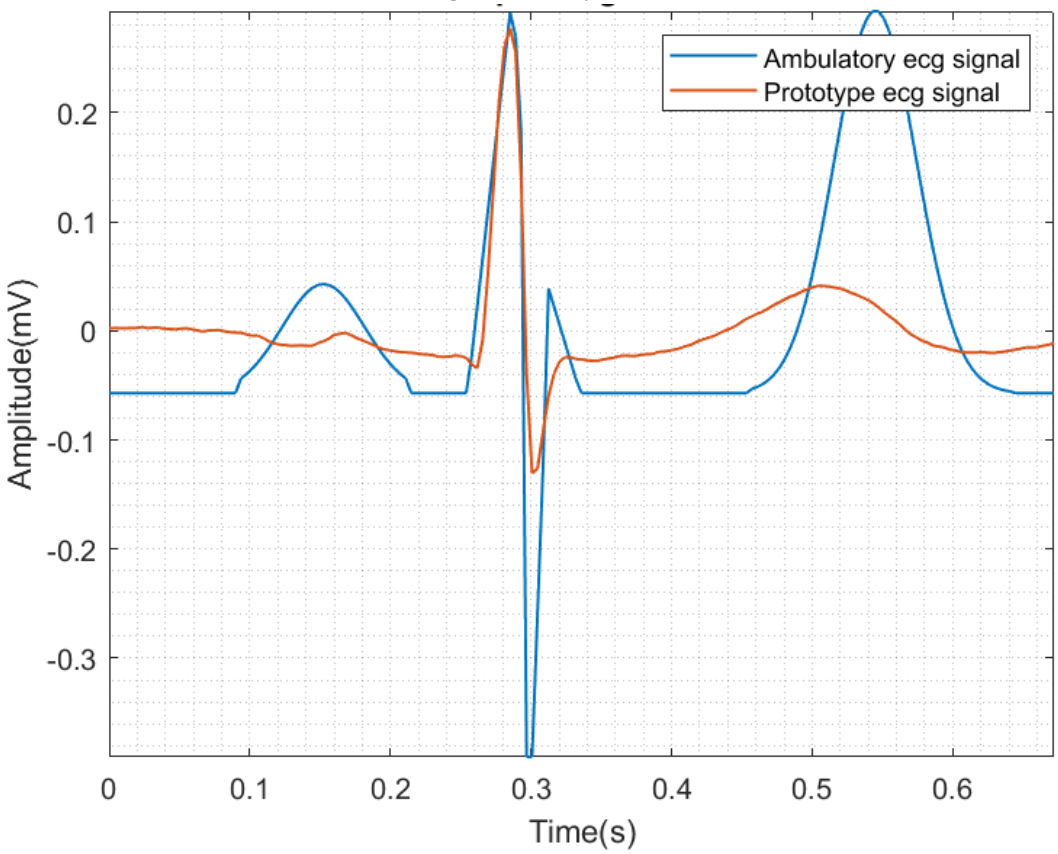

Patient #10:

Male 50 years old

BP 131/80

Figure 119 Prototype original signal V1

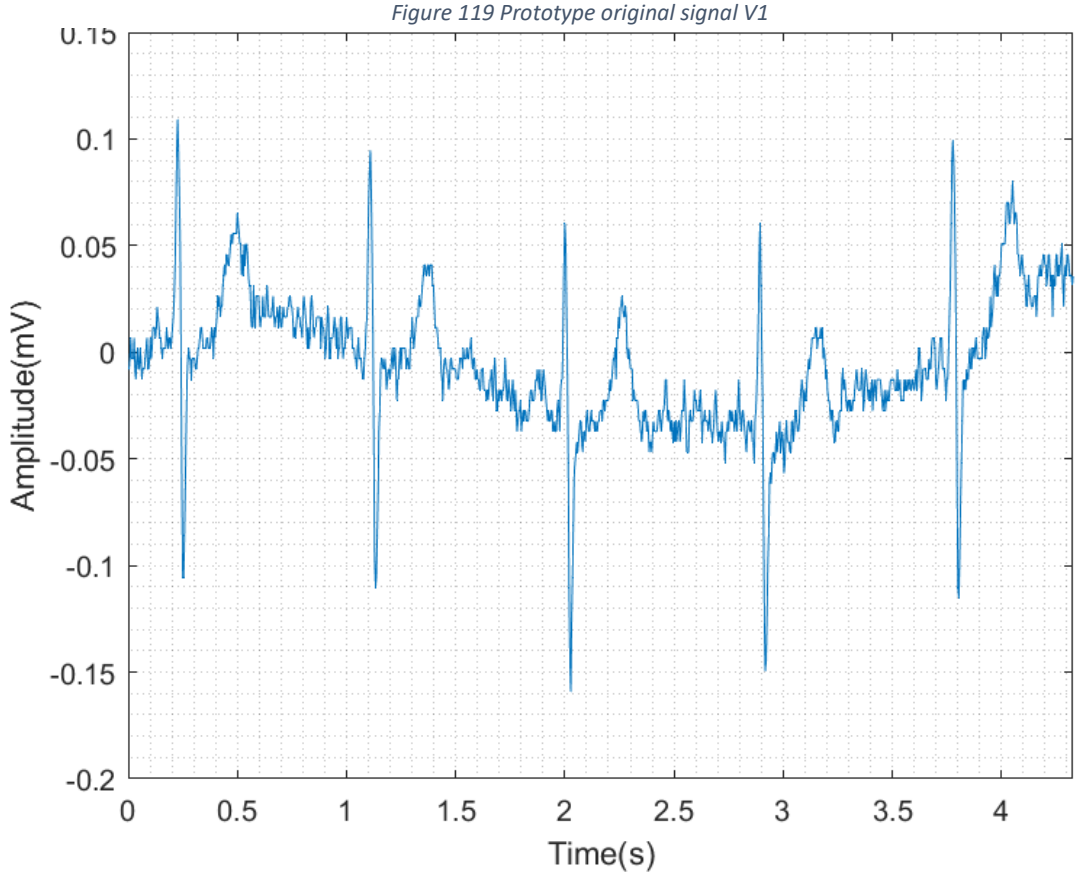

Figure 120 Prototype original signal D1

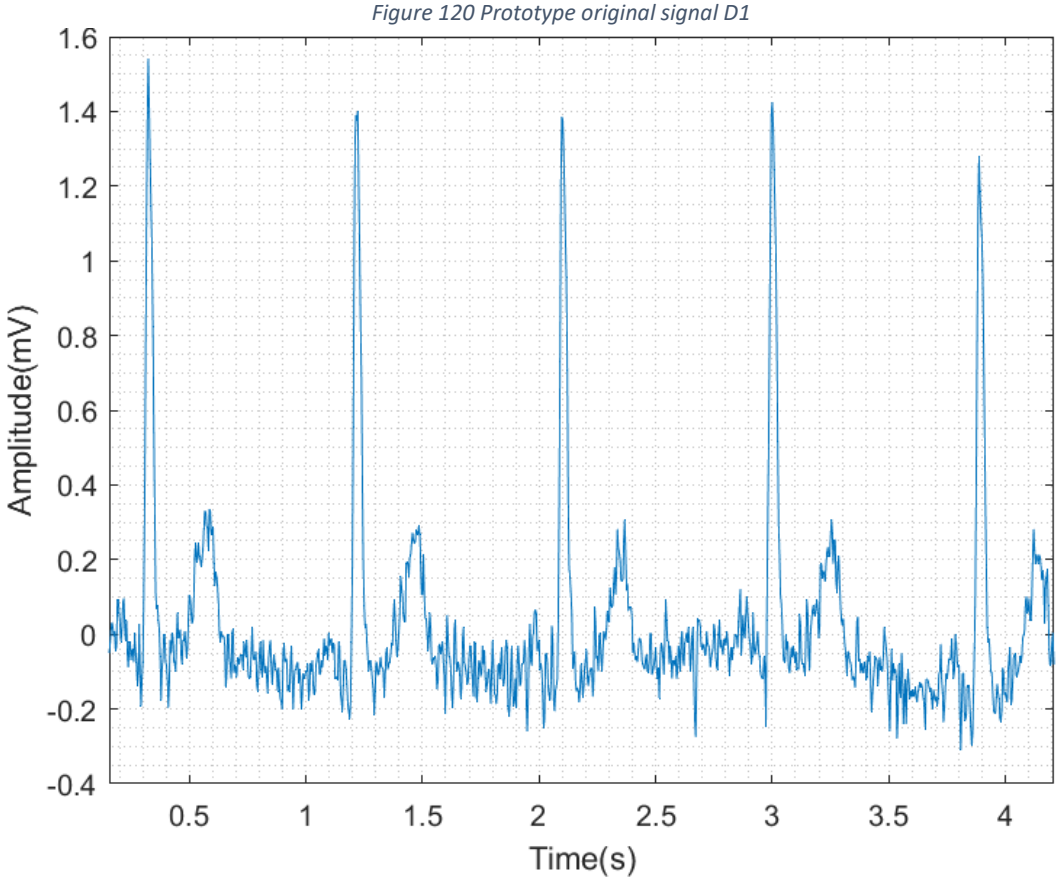

Figure 121 Prototype original signal V2

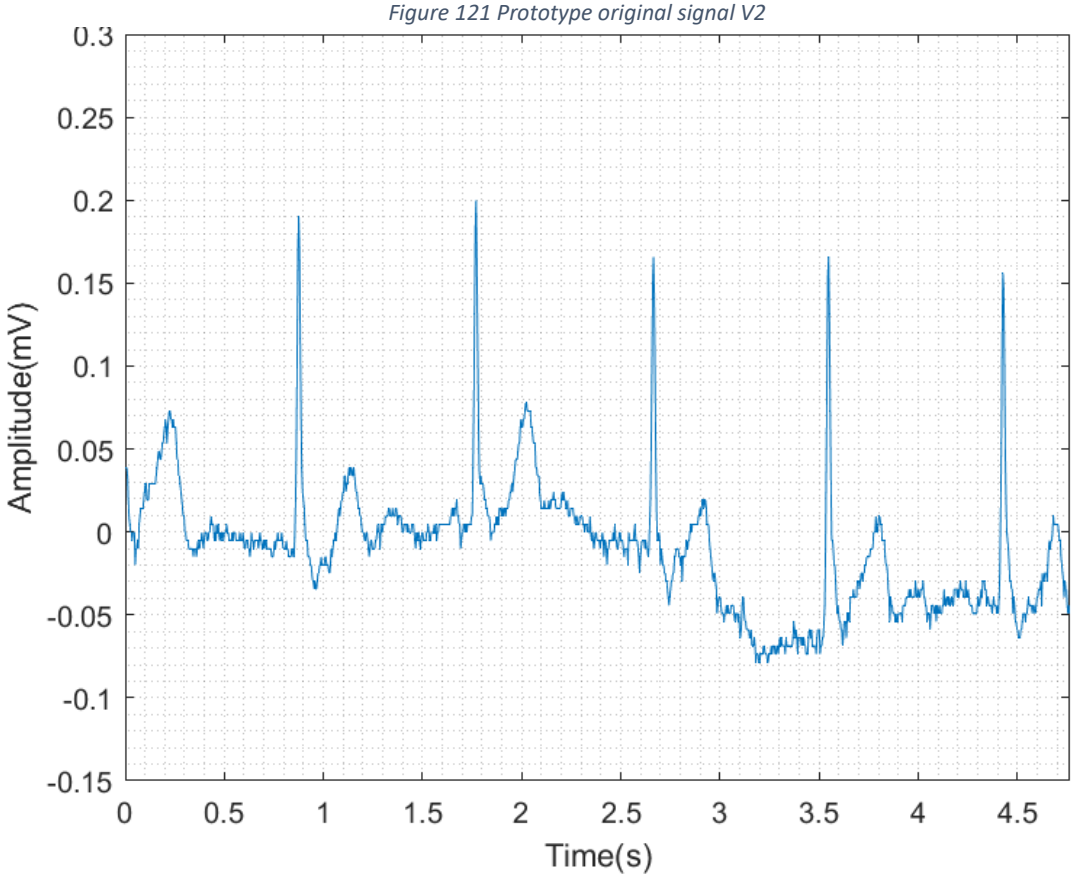

Figure 122 Ambulatory original signals

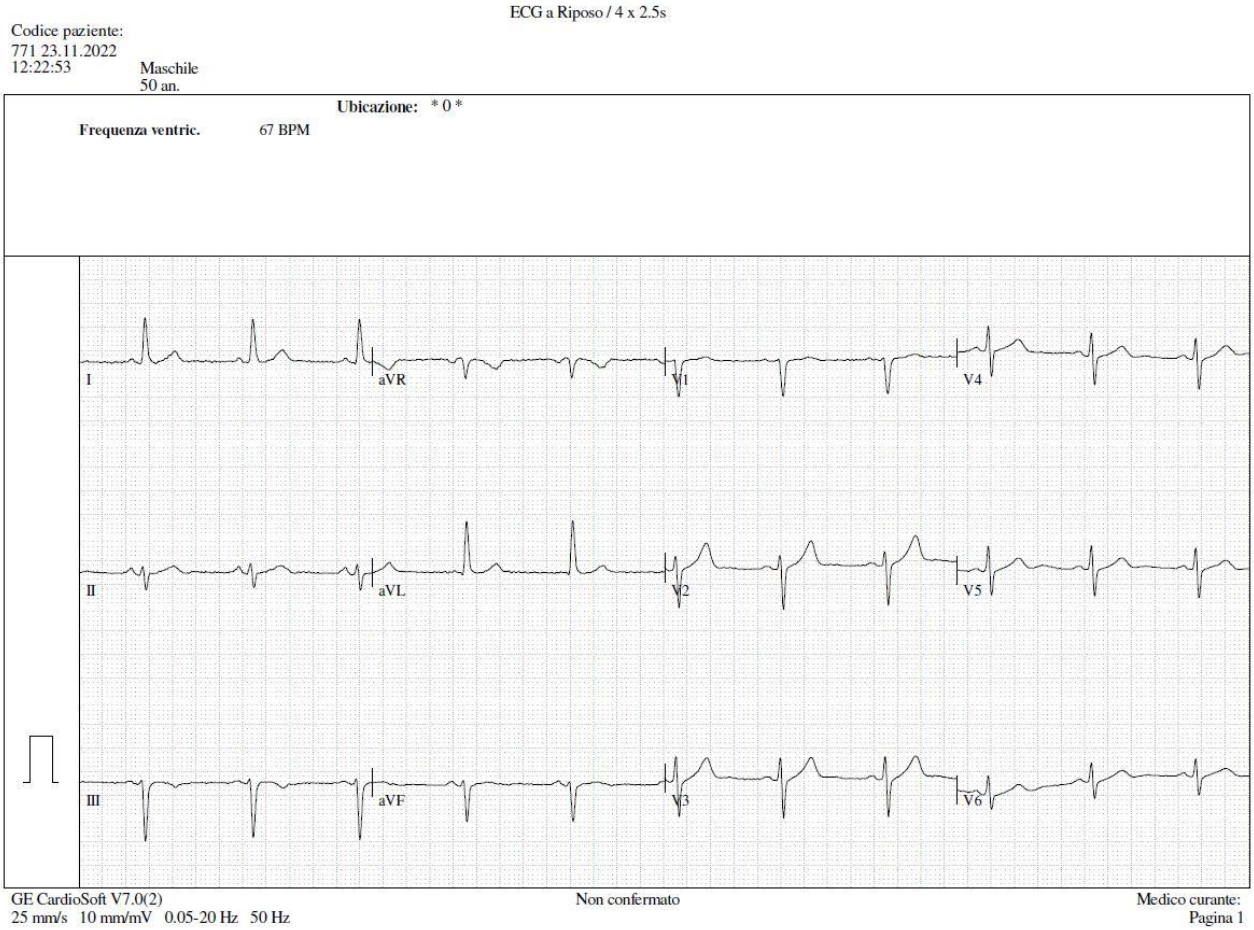

Figure 123 Ambulatory signals reconstructed

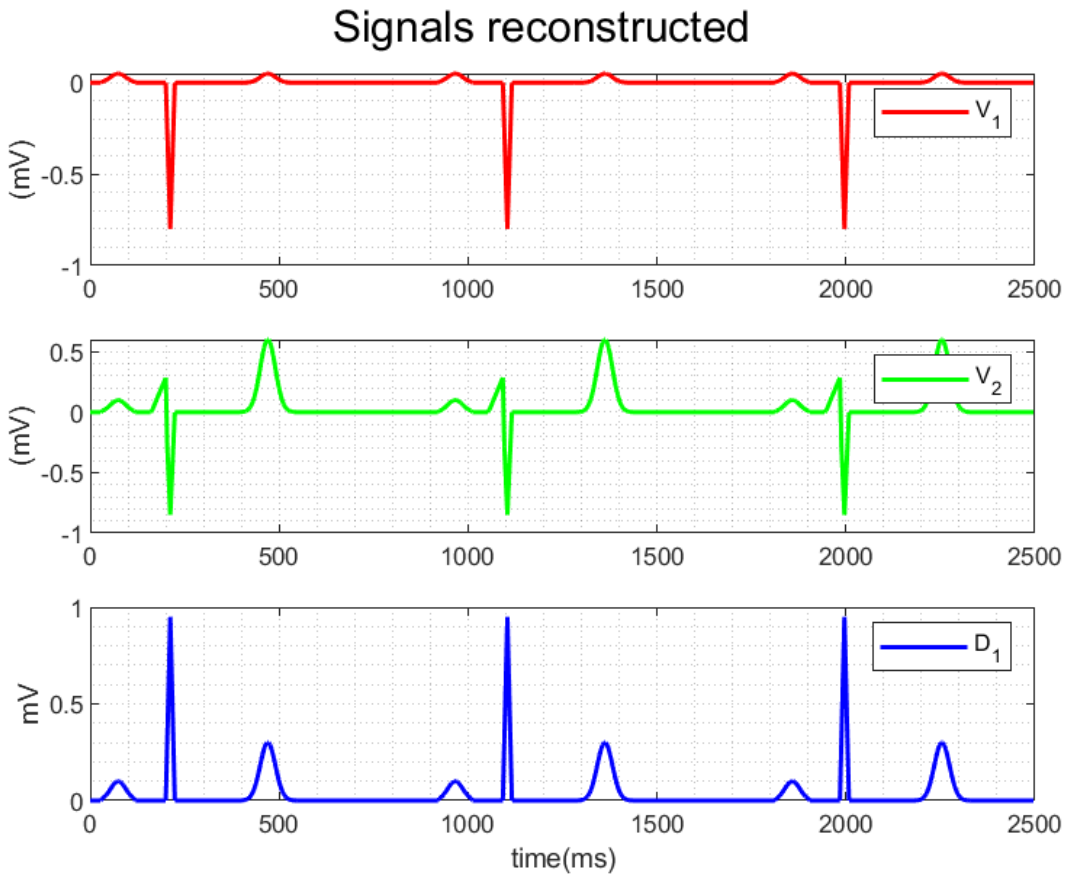

F

Figure 124 Comparison V1

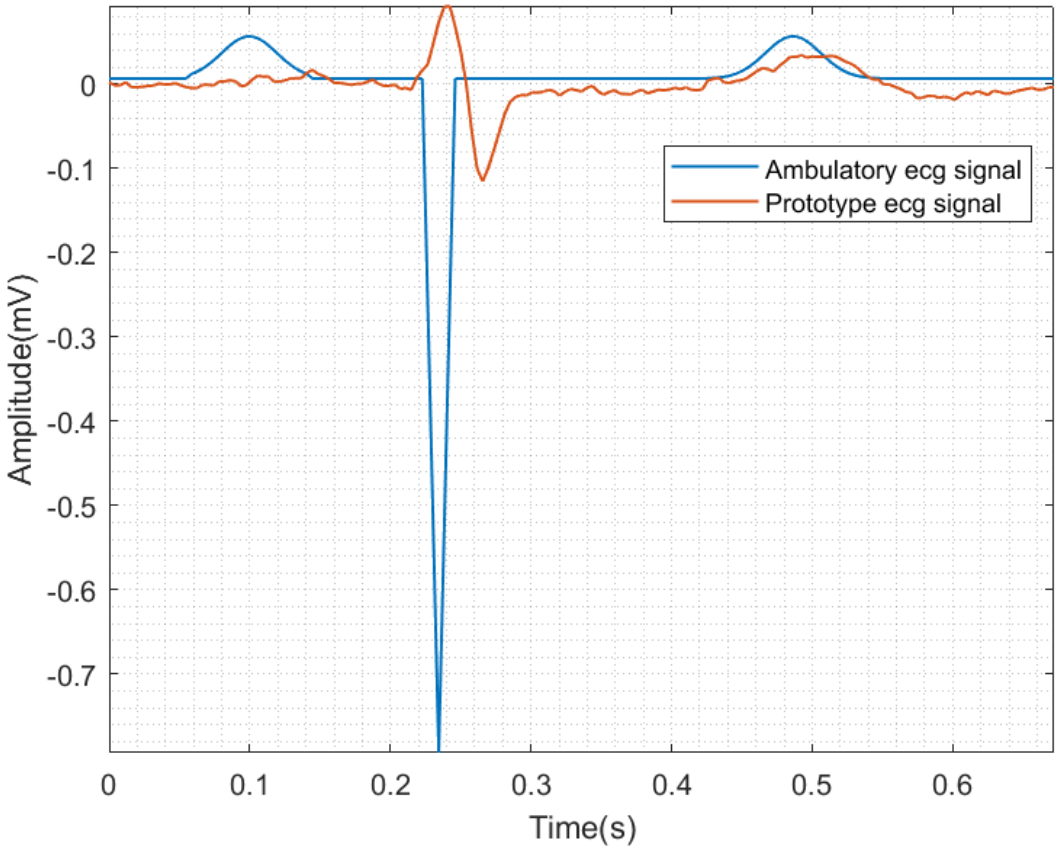

Figure 125 Comparison D1

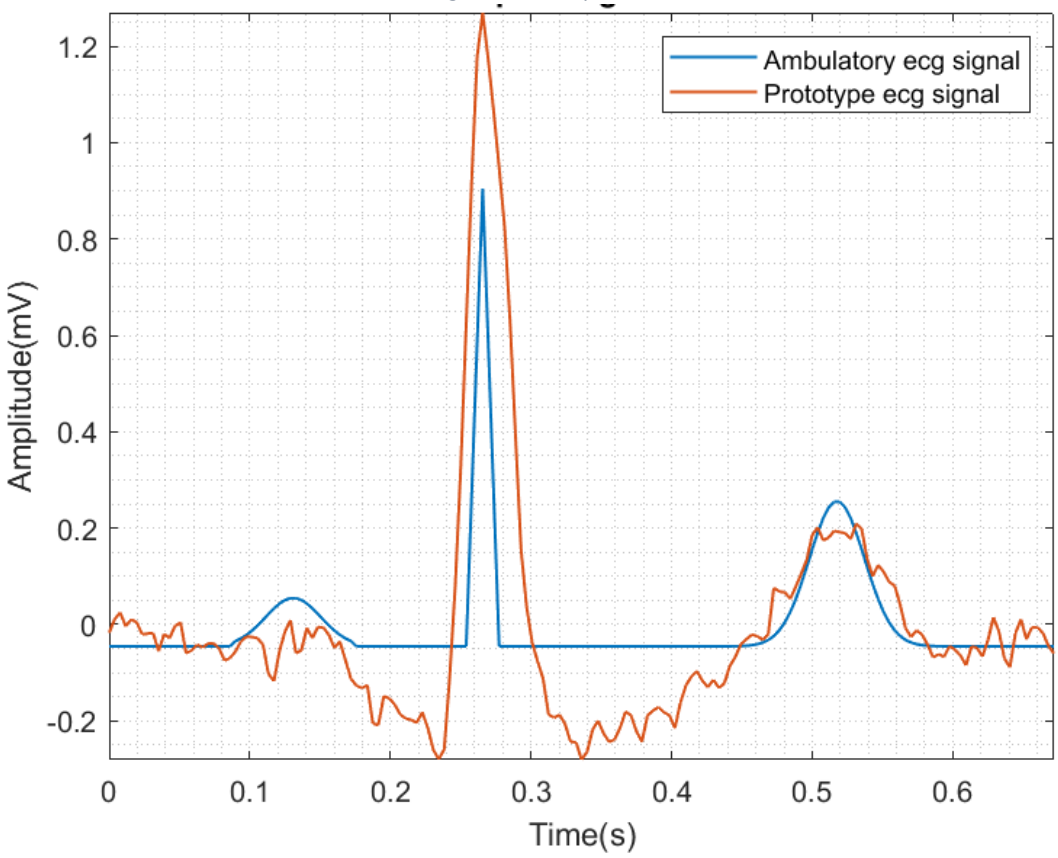

Figure 126 Comparison V2

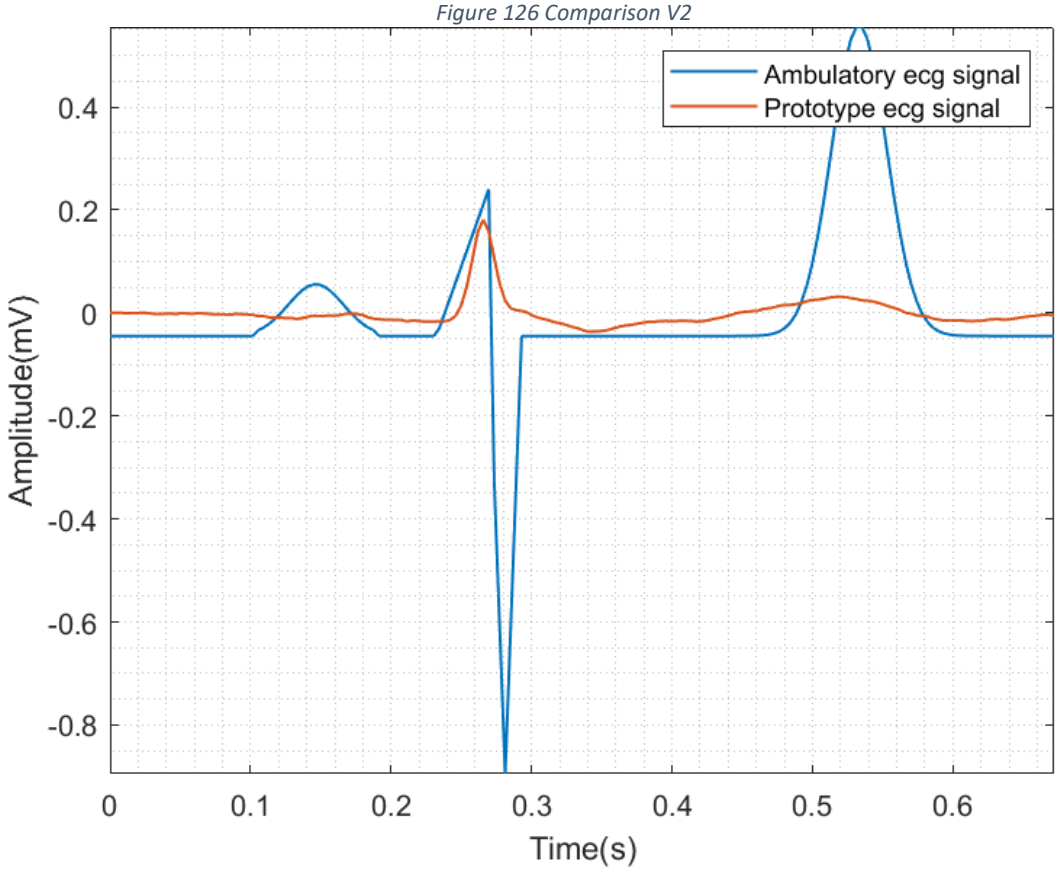

Patient #11:

Male 52 years old

BP 108/67

Figure 127 Prototype original signal V1

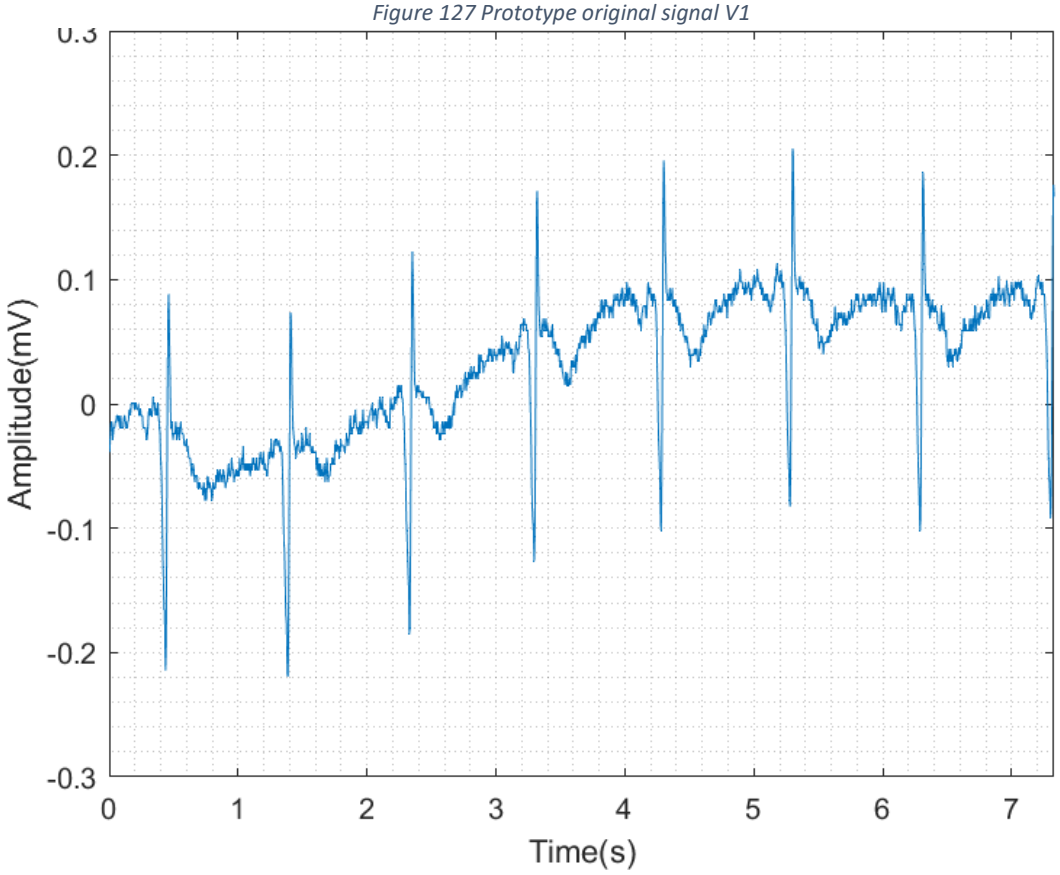

Figure 128 Prototype original signal D1

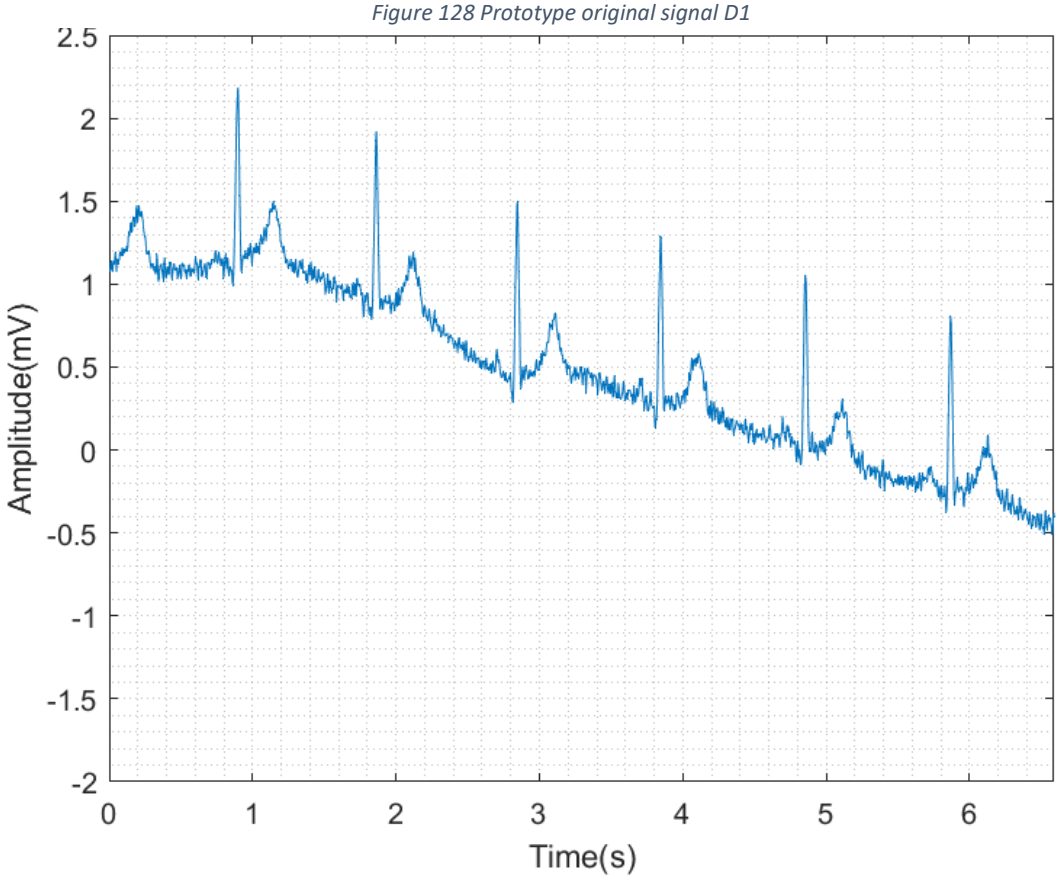

Figure 129 Prototype original signal V2

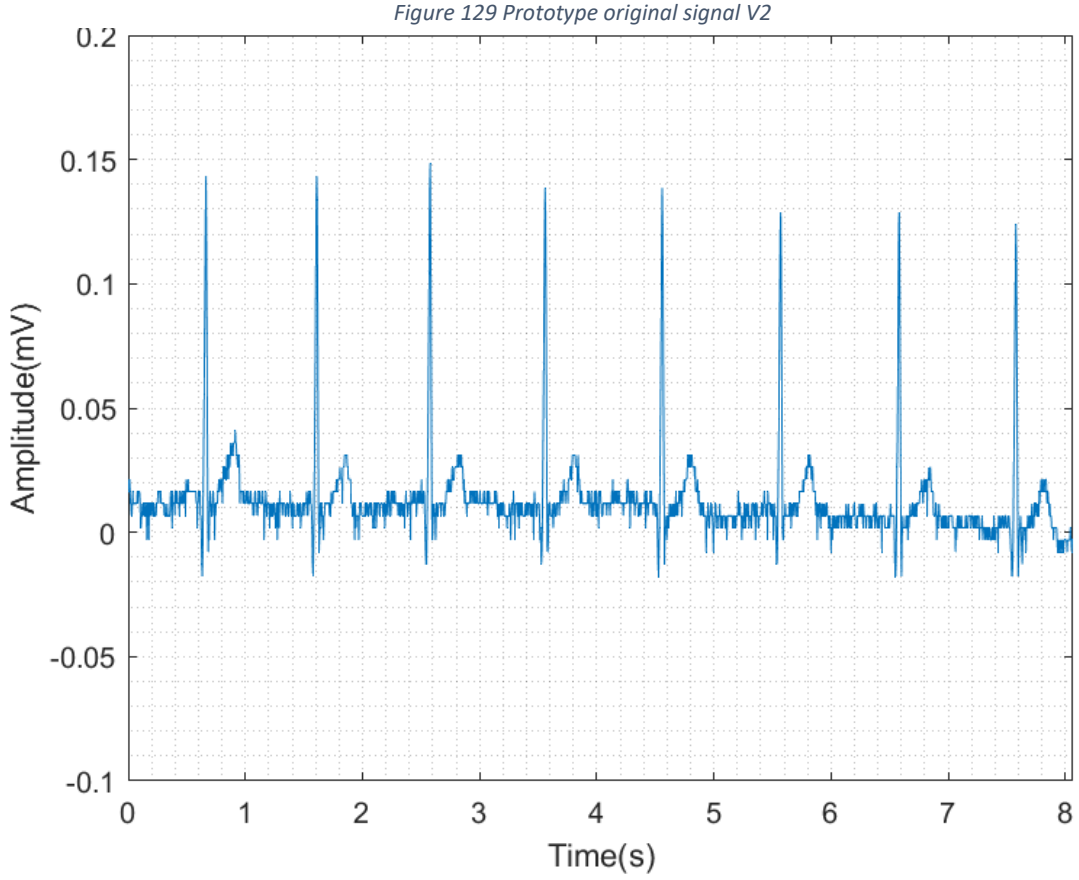

Figure 130 Ambulatory original signals

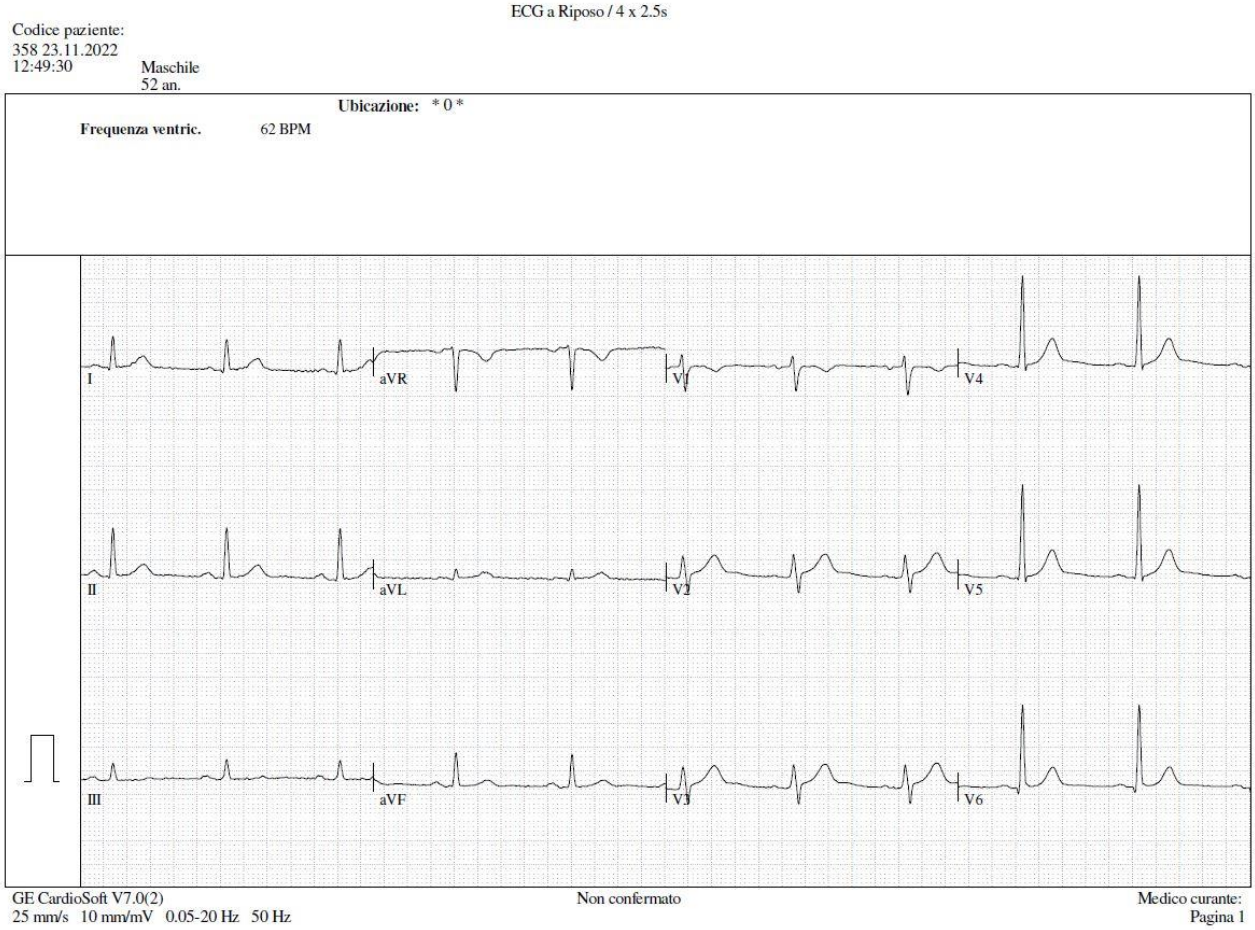

Figure 131 Ambulatory signals reconstructed

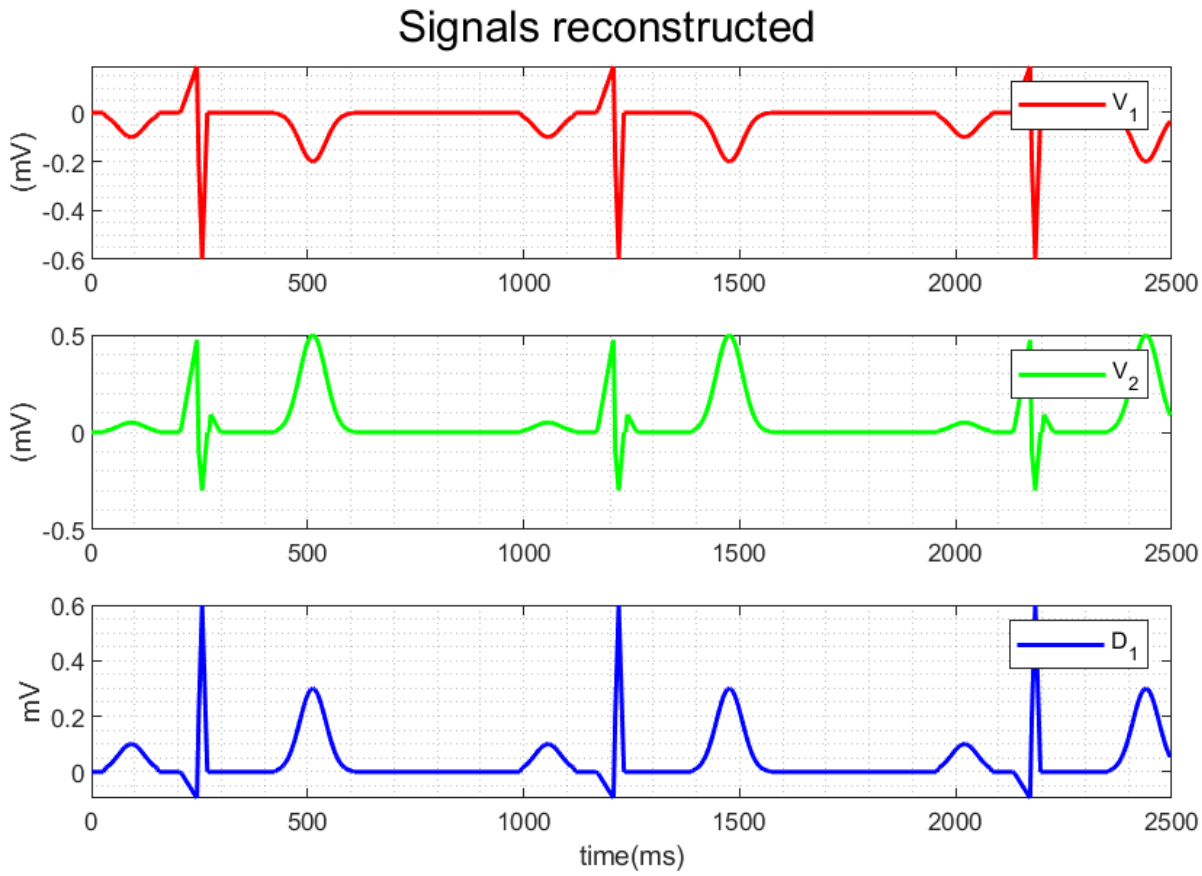

Figure 132 Comparison V1

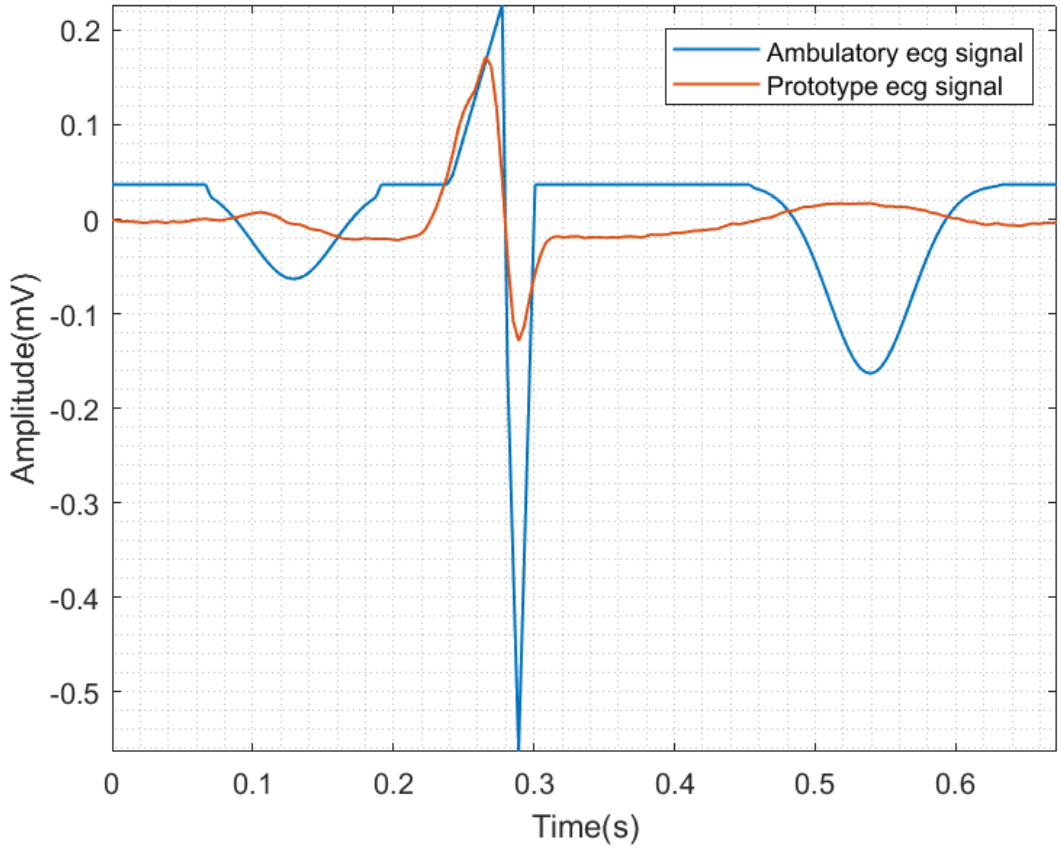

Figure 133 Comparison D1

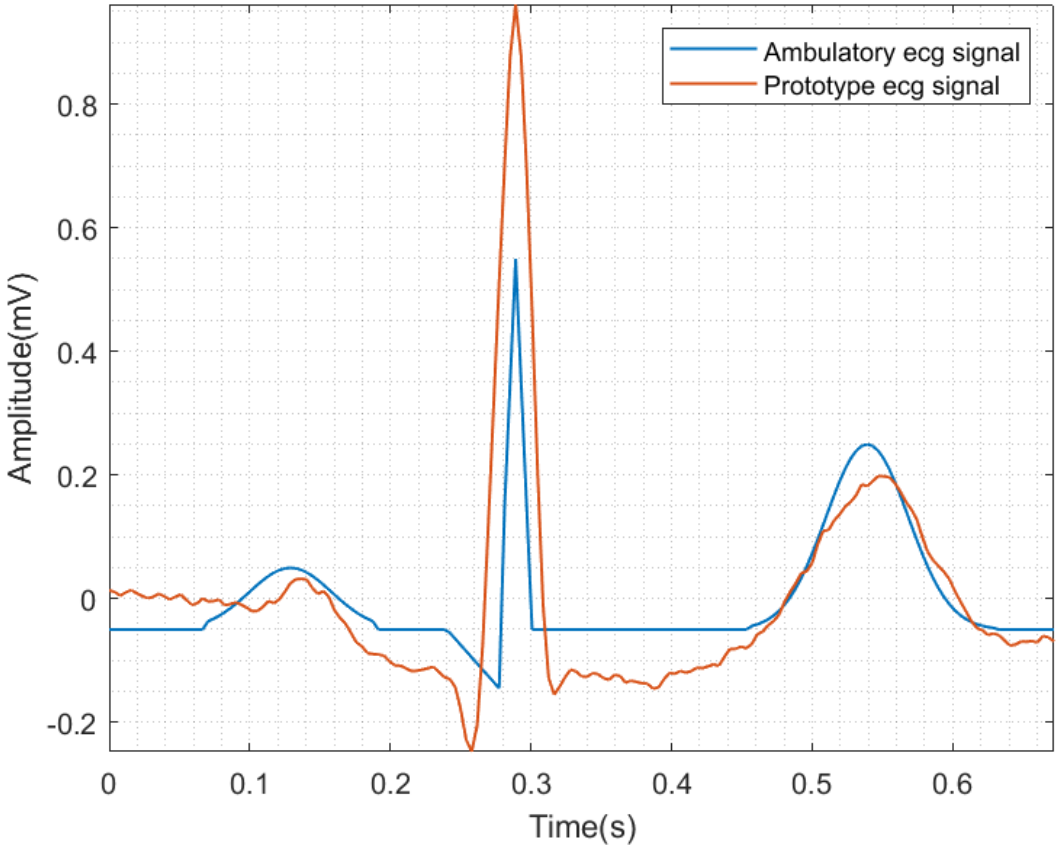

Figure 134 Comparison V2

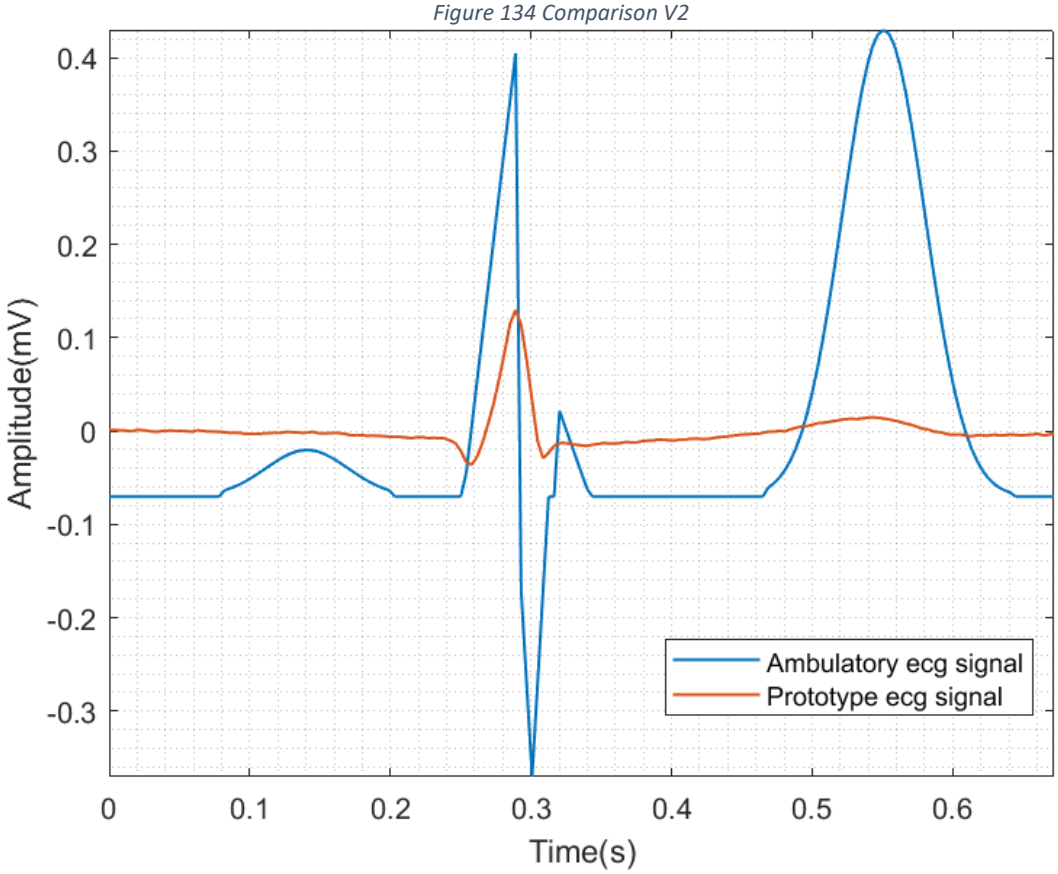

Patient #12:

Female 48 years old

BP 118/68

Figure 135 Prototype original signal V1

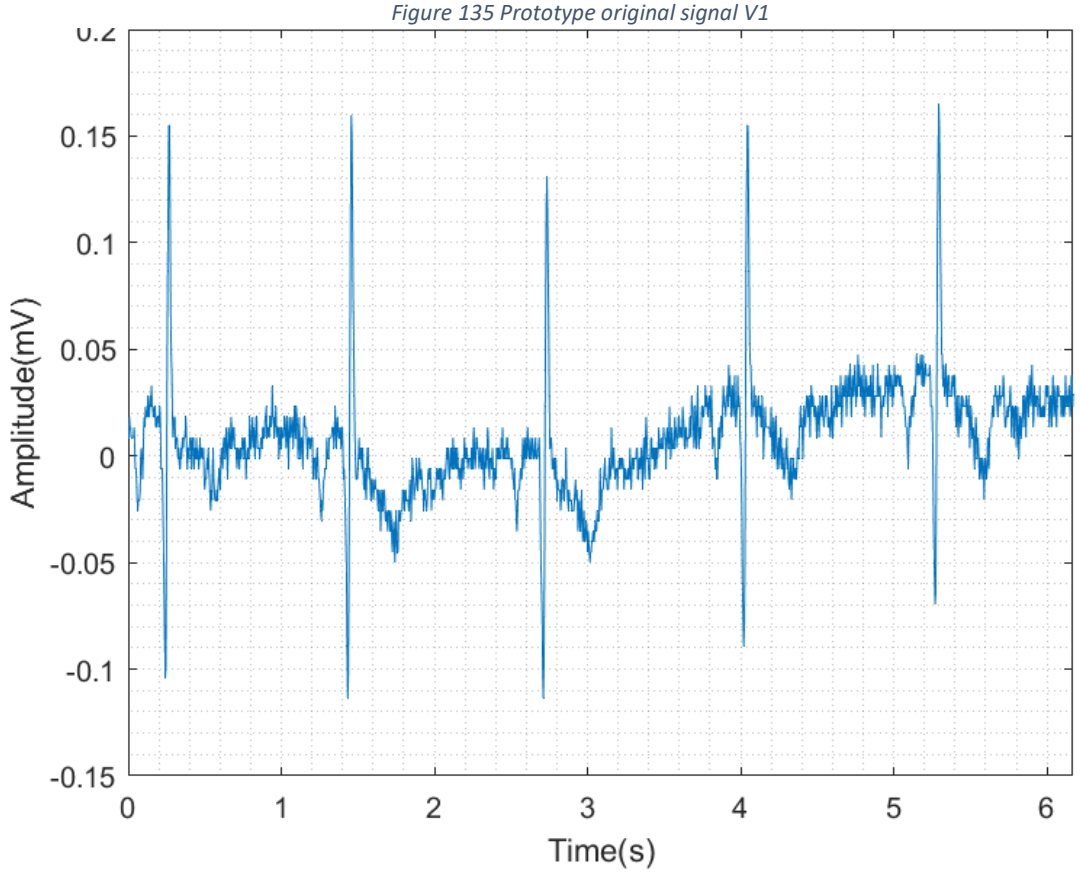

Figure 136 Prototype original signal D1

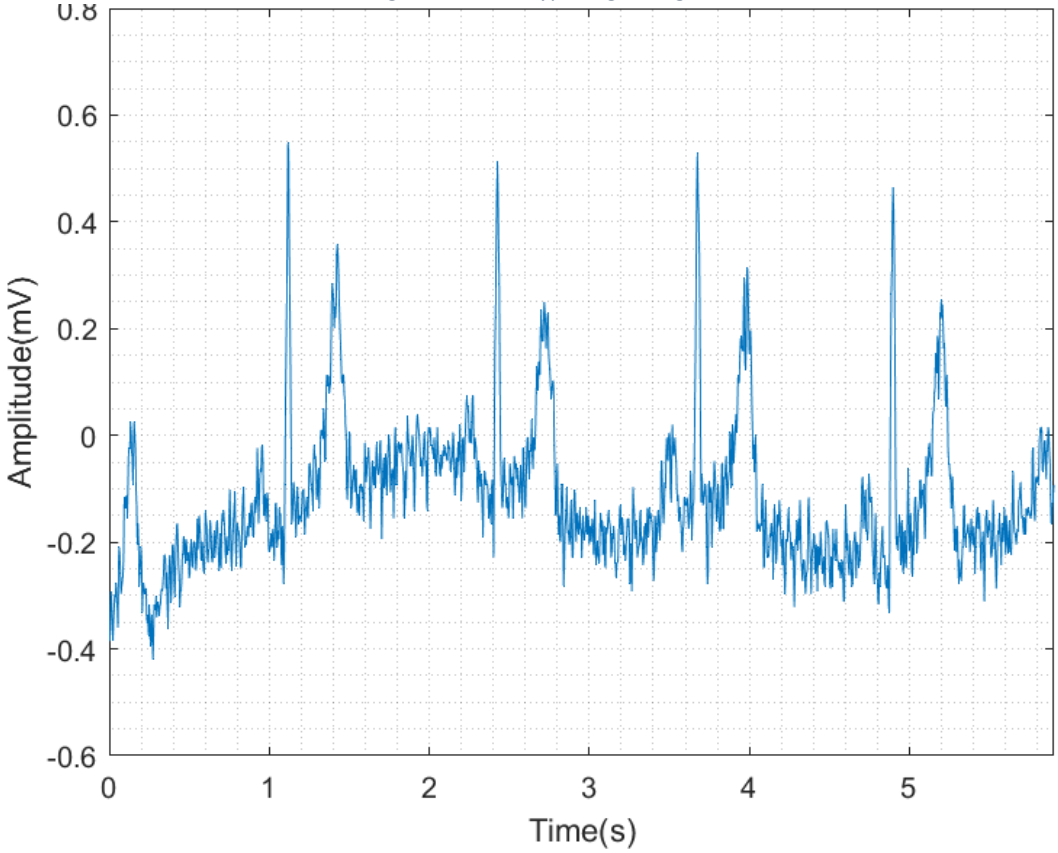

Figure 137 Prototype original signal V2

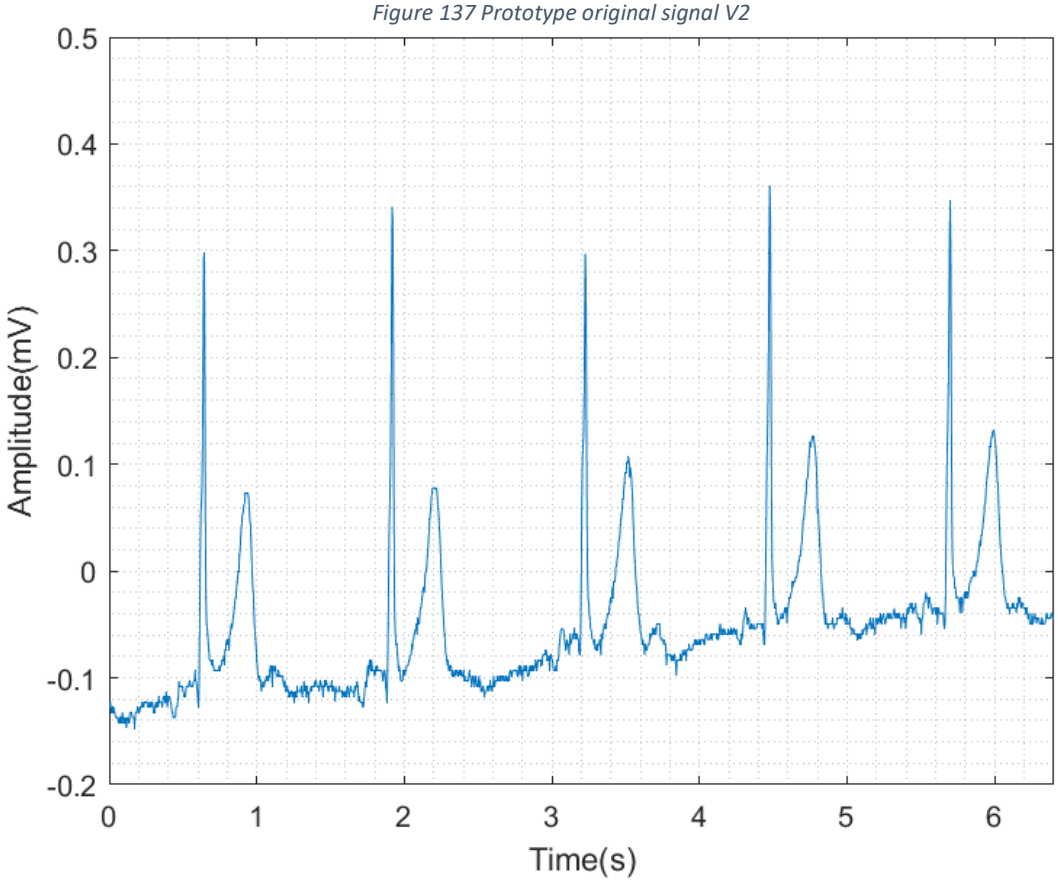

Figure 138 Ambulatory original signals

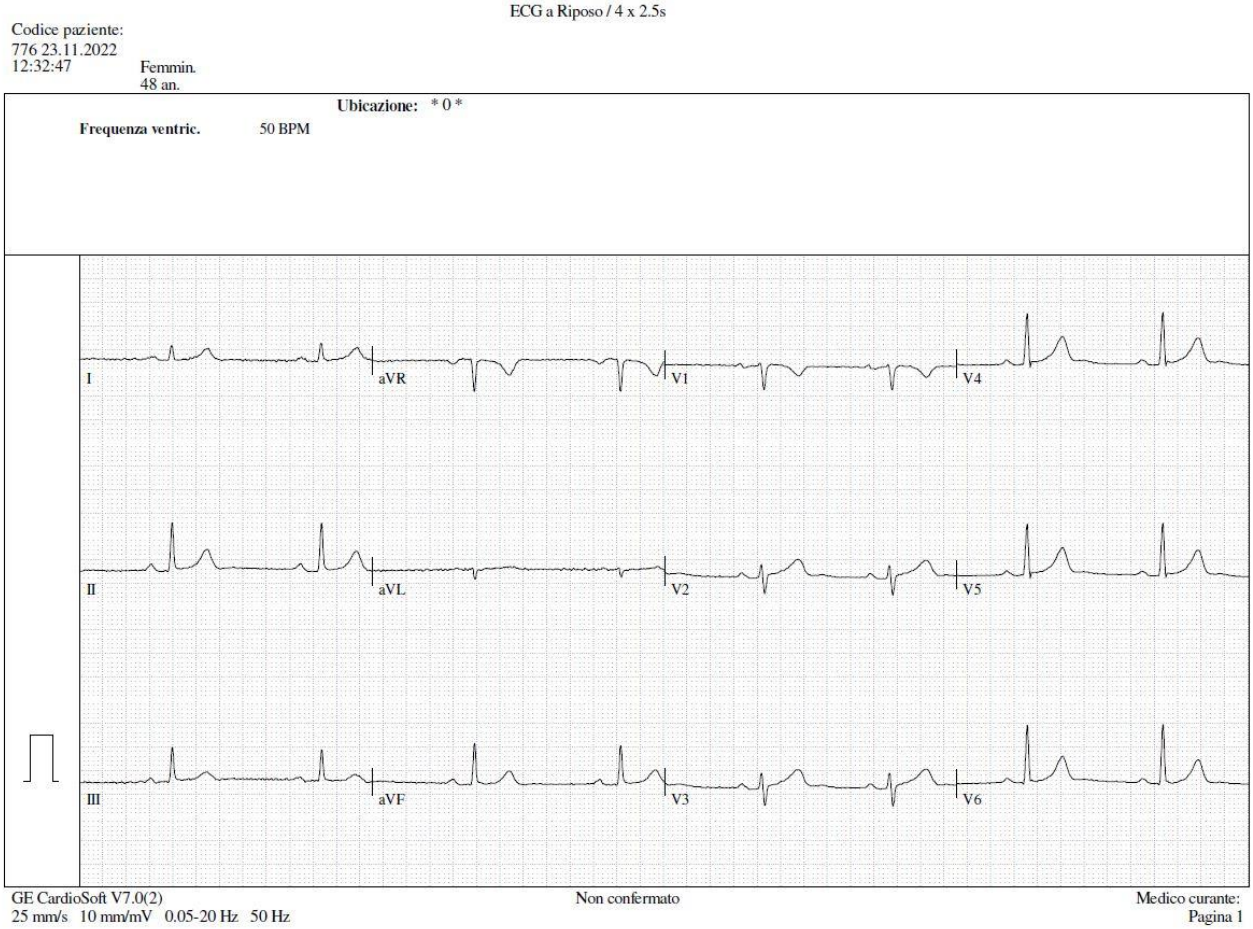

Figure 139 Ambulatory signals reconstructed

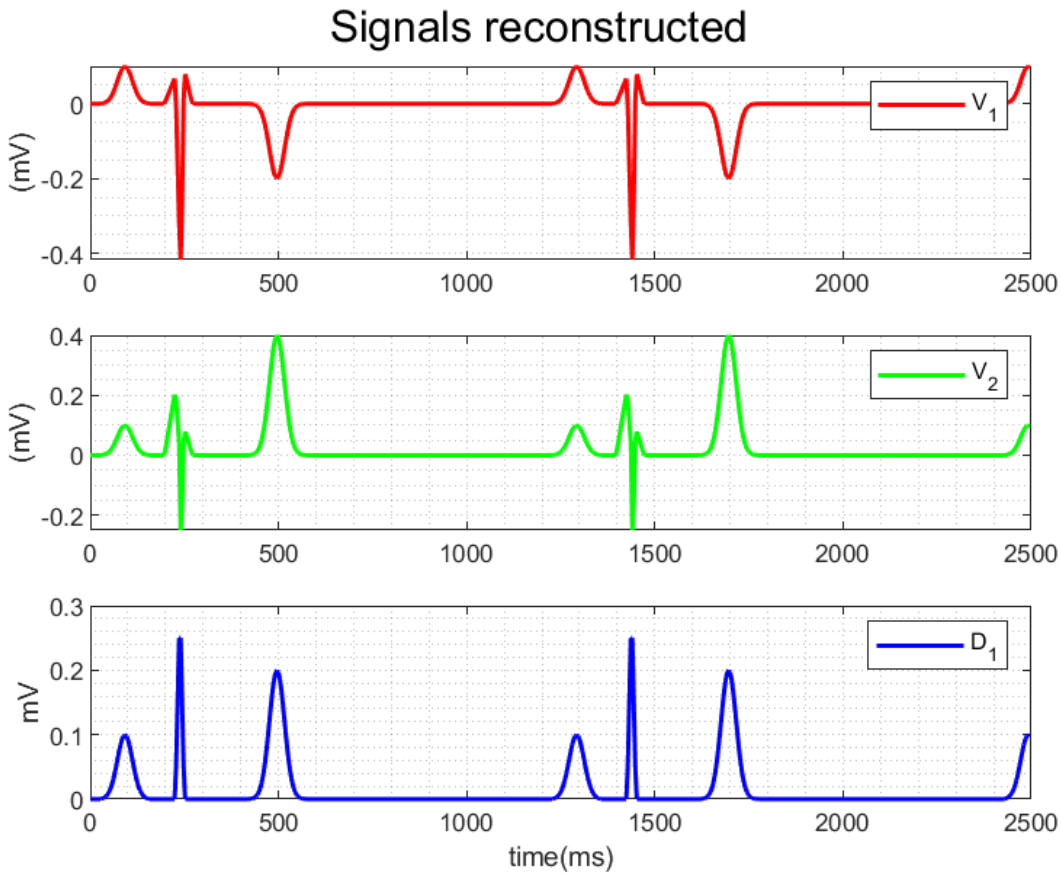

Figure 140 Comparison V1

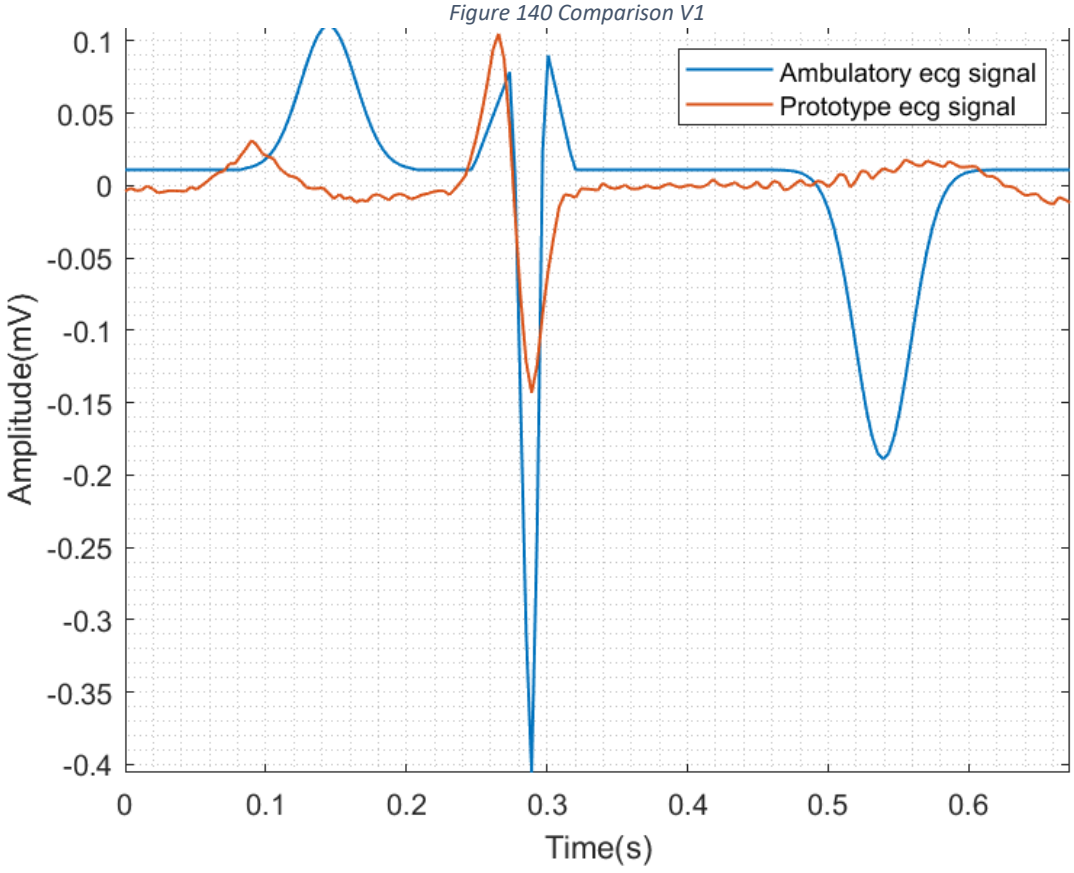

Figure 141 Comparison D1

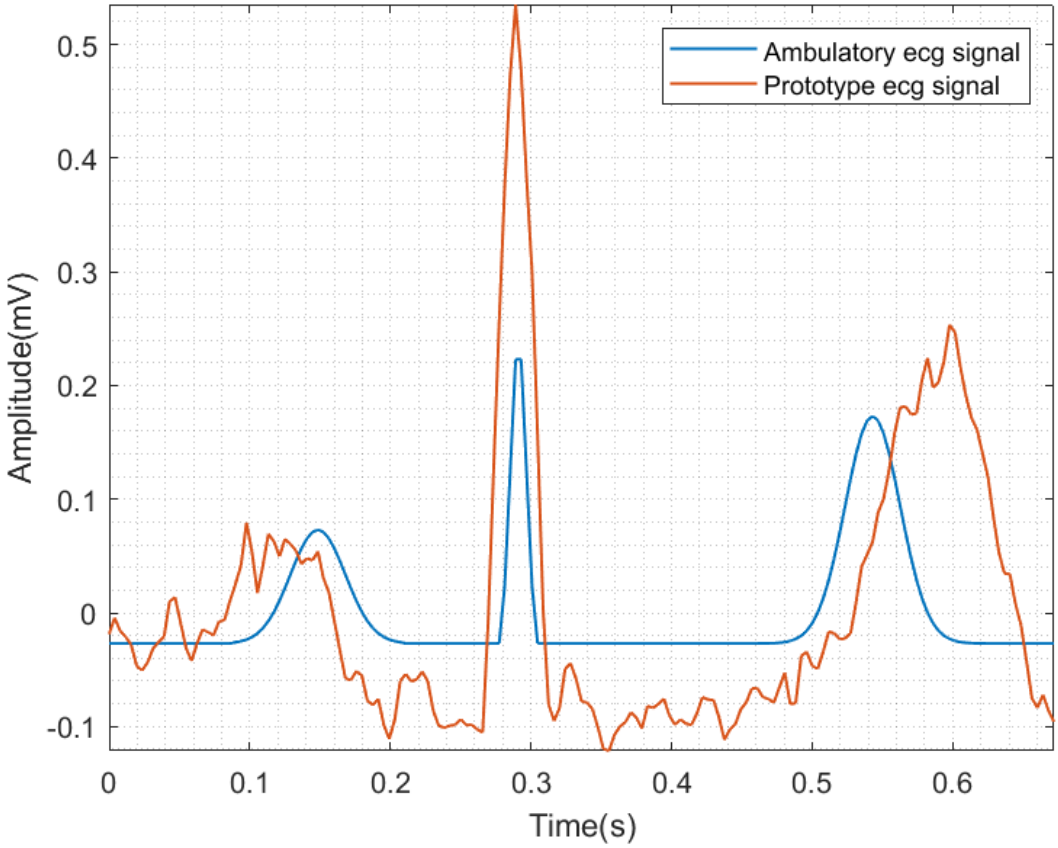

Figure 142 Comparison V2

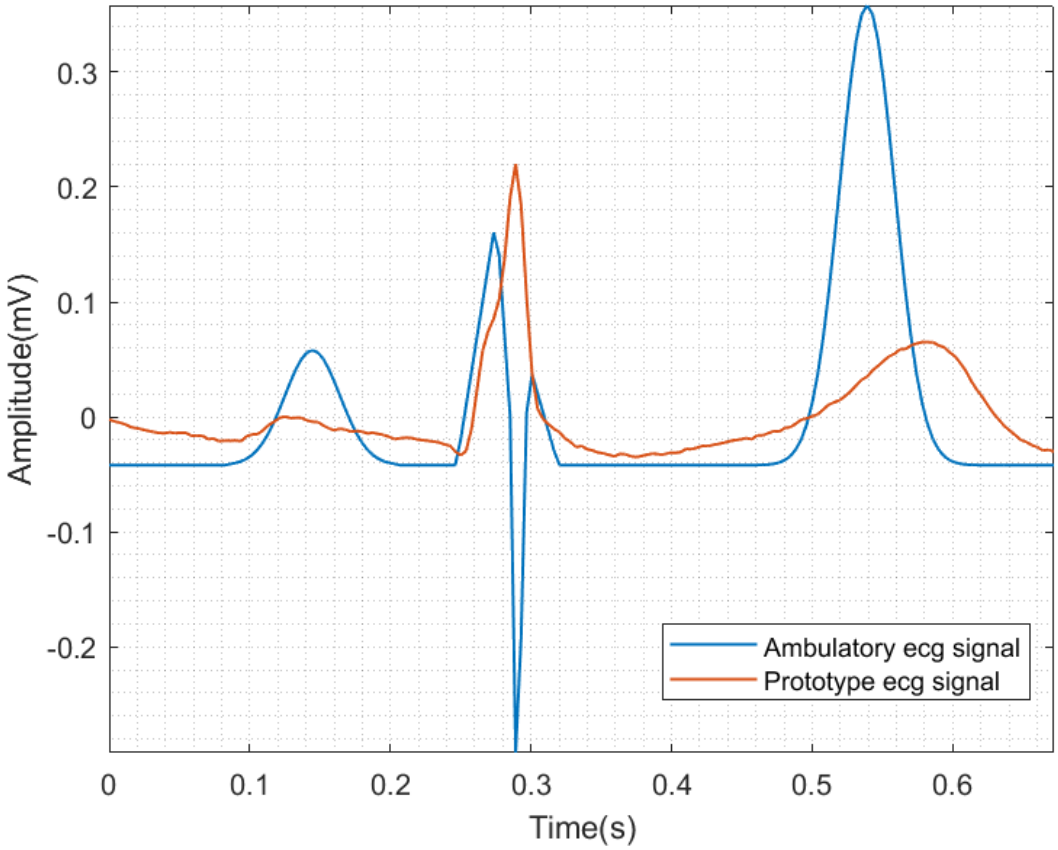

Patient #13:

Male 29 years old

BP 119/74

Figure 143 Prototype original signal V1

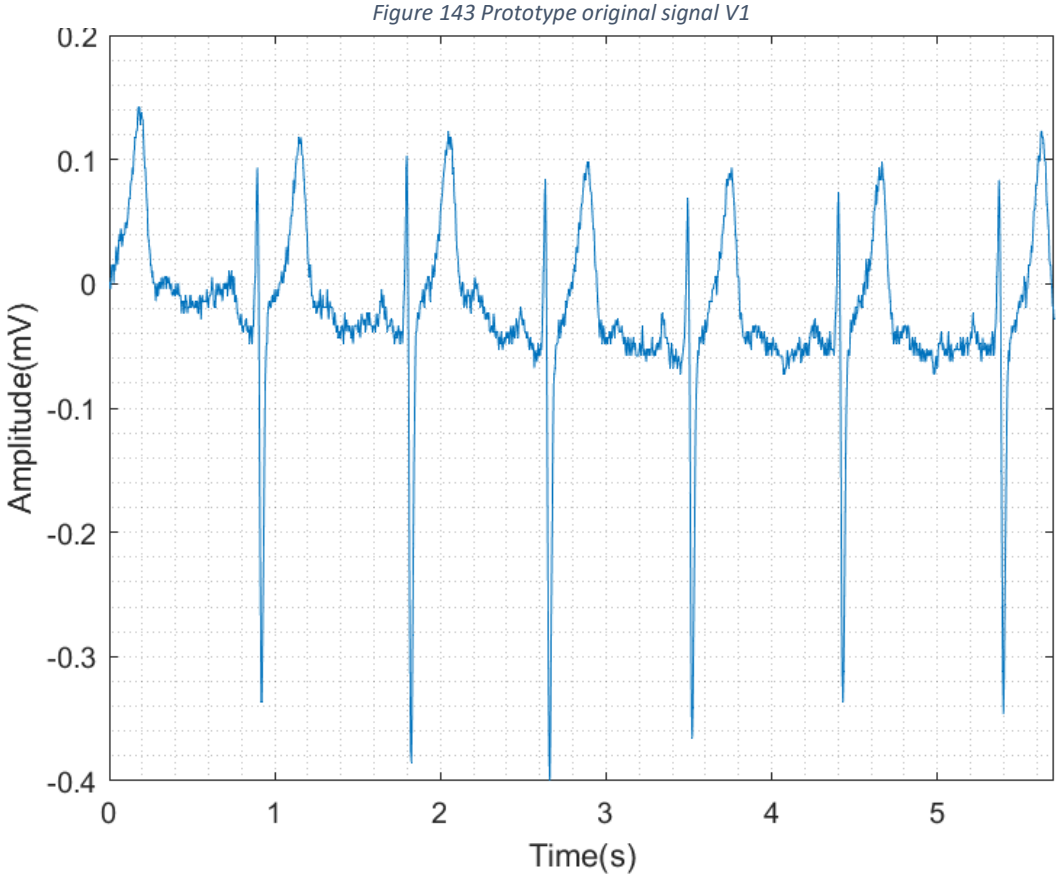

Figure 144 Prototype original signal D1

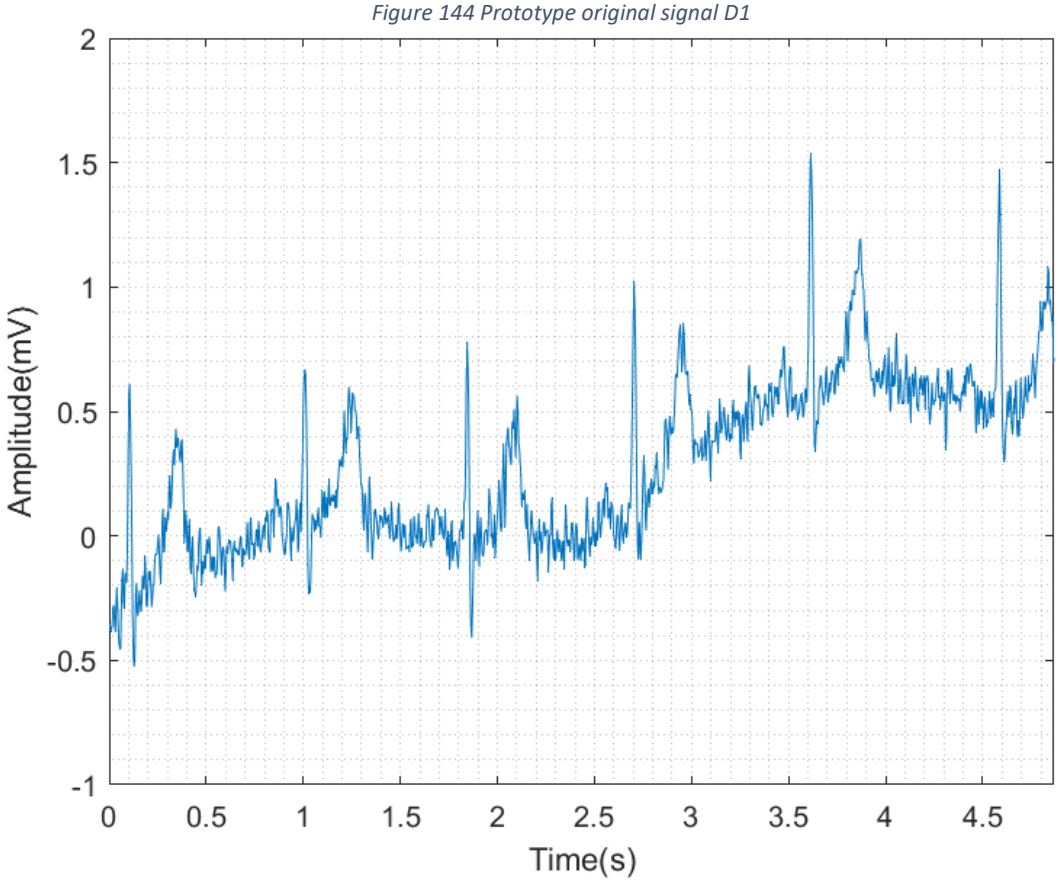

Figure 145 Prototype original signal V2

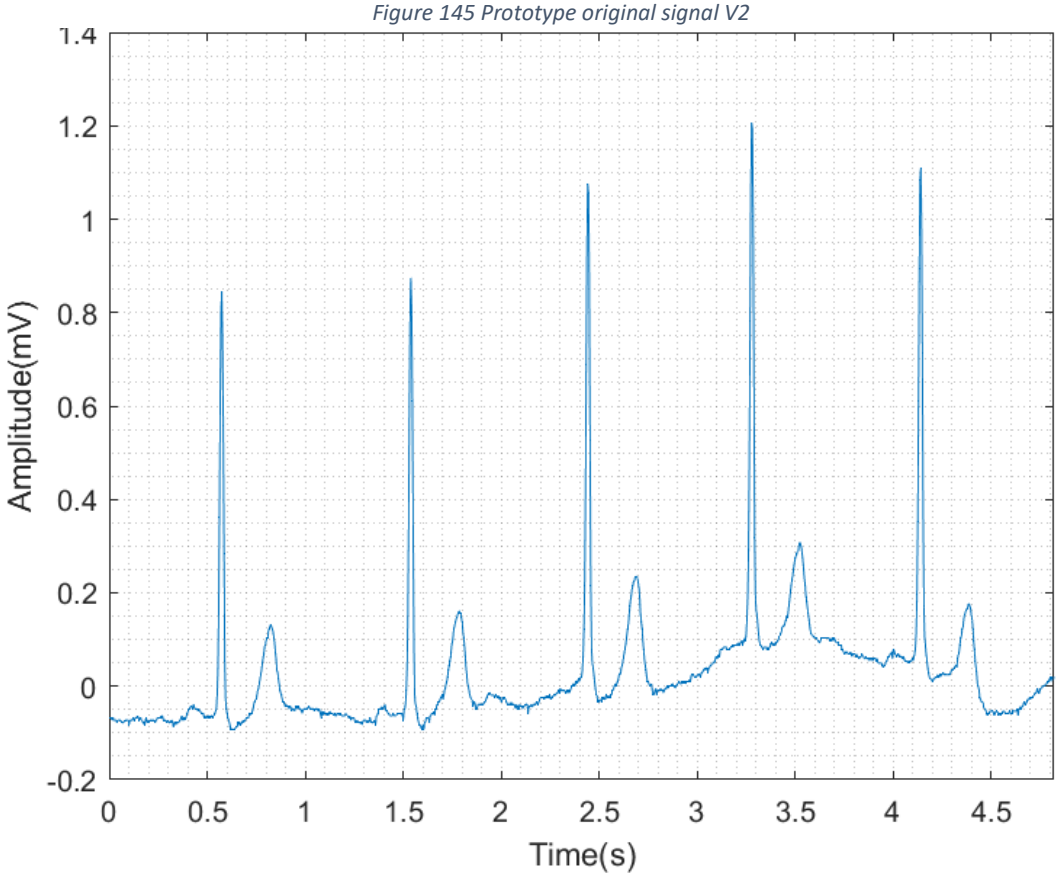

Figure 146 Ambulatory original signals

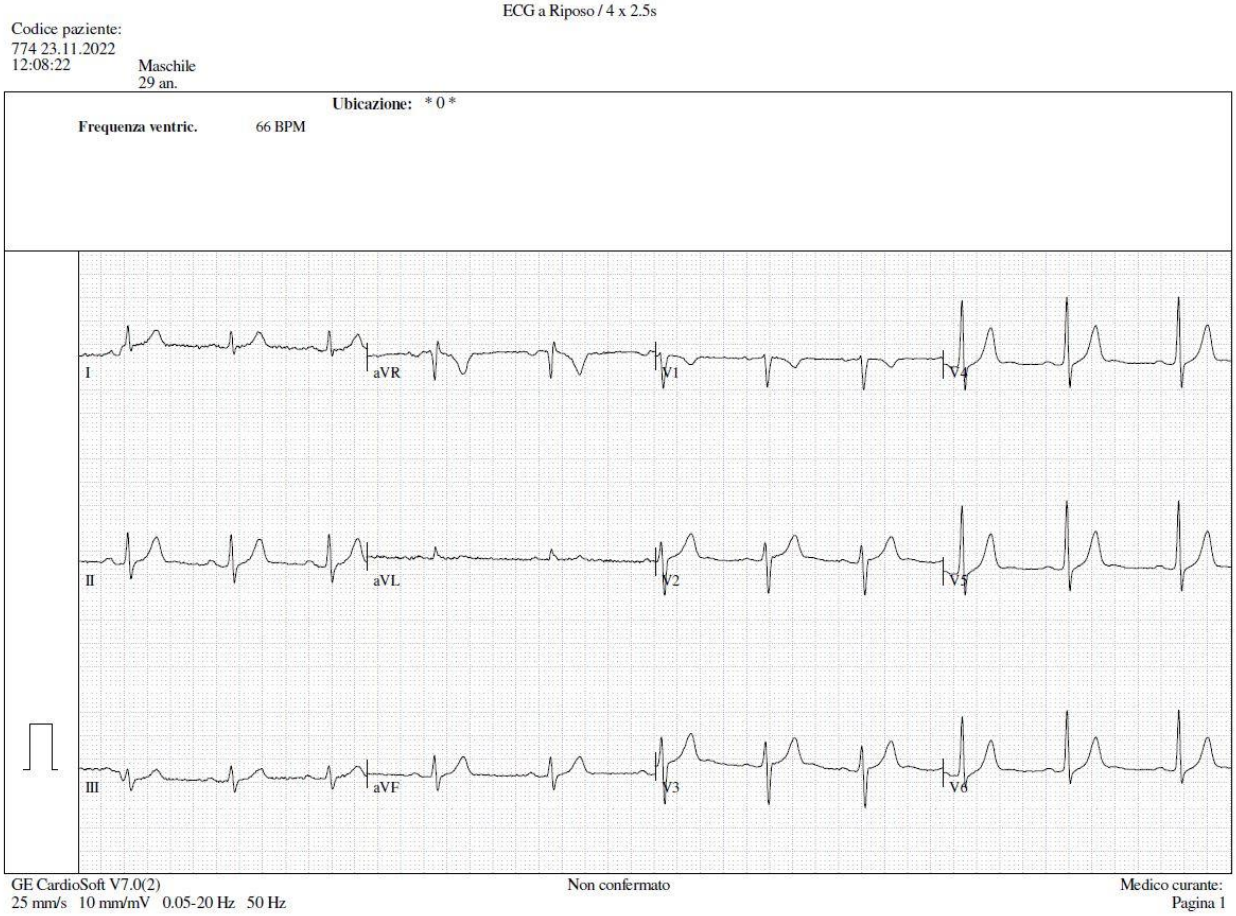

Figure 147 Ambulatory signals reconstructed

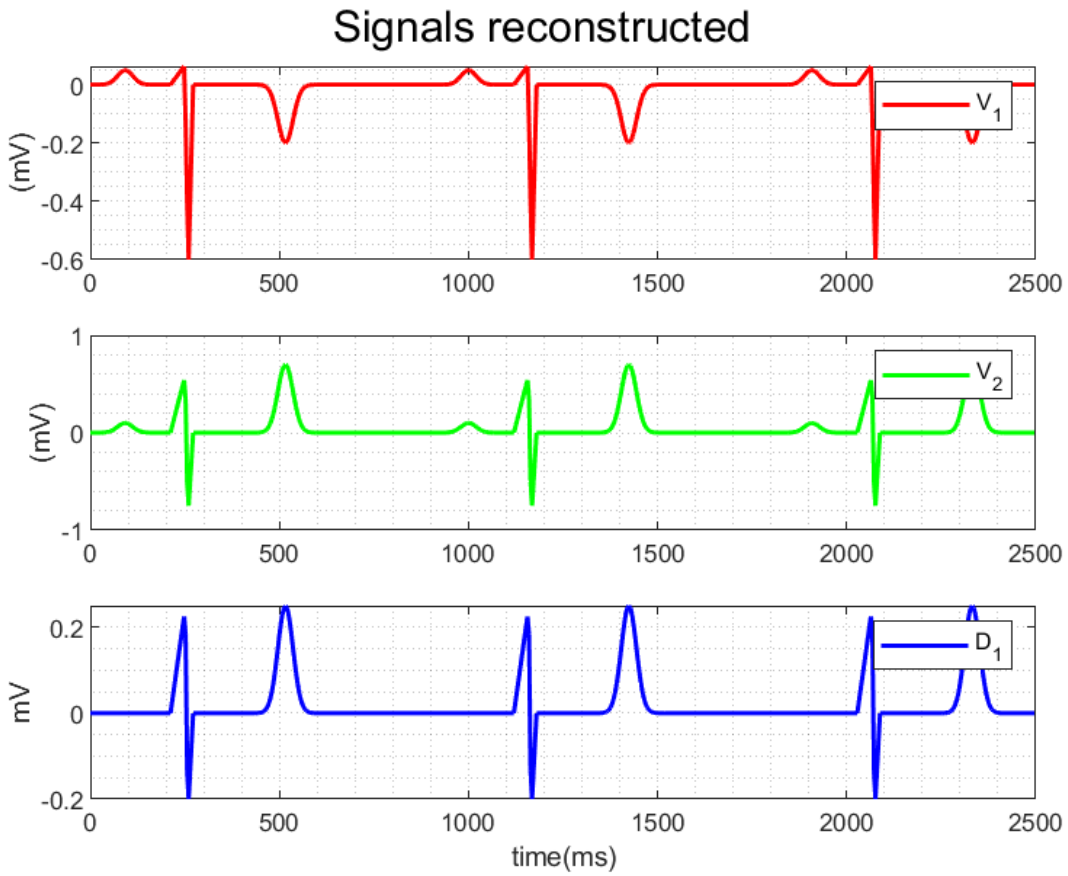

Figure 148 Comparison D1

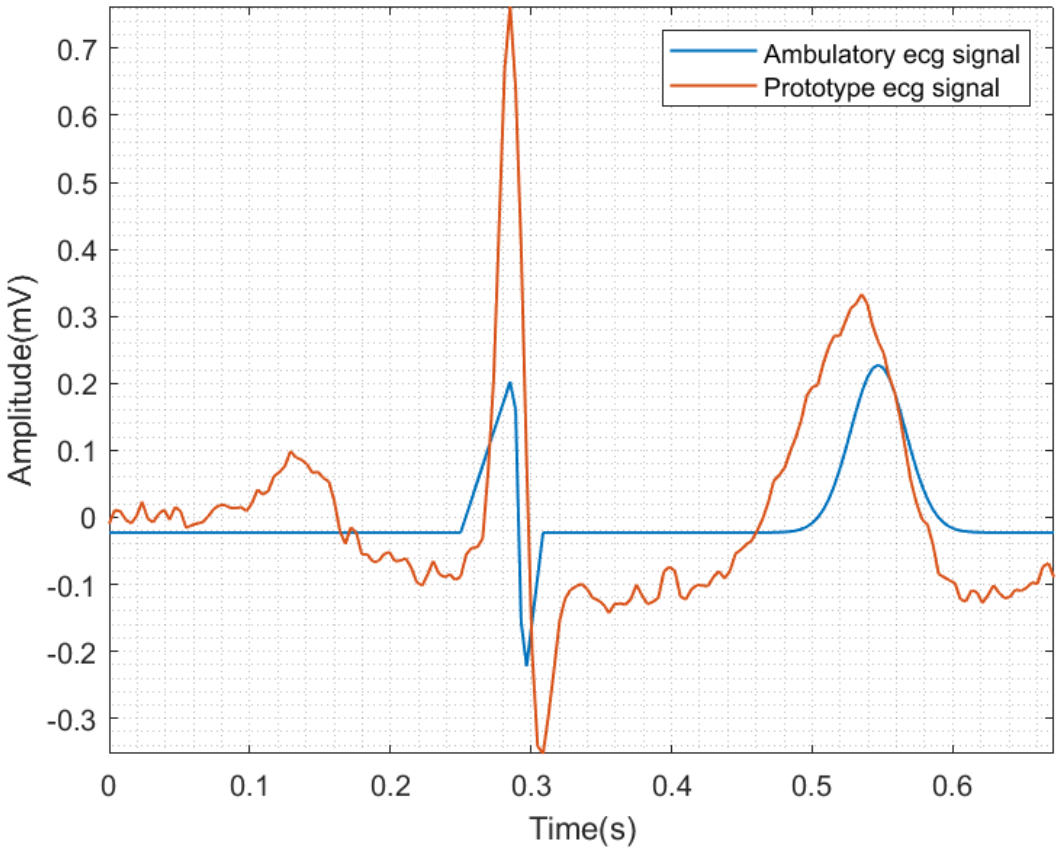

Figure 149 Comparison V1

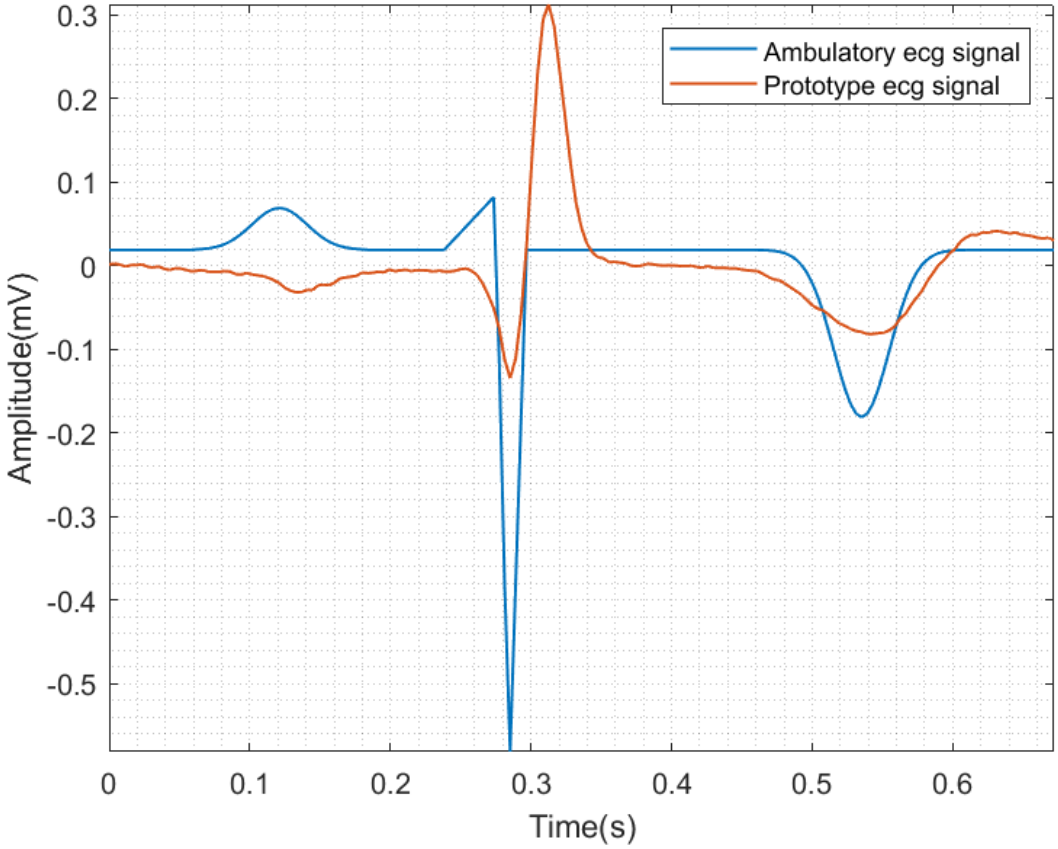

Figure 150 Comparison V2

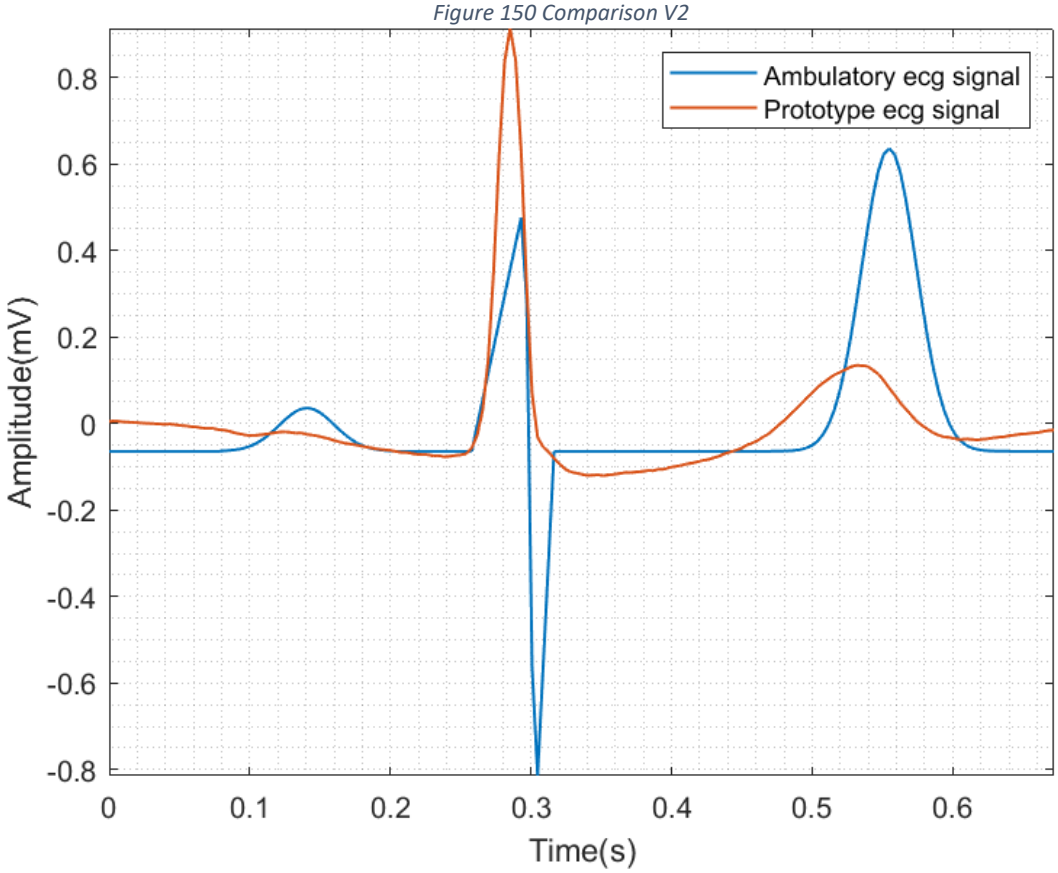

Patient #14:

Female 53 years old

BP 140/100

Figure 151 Prototype original signal V1

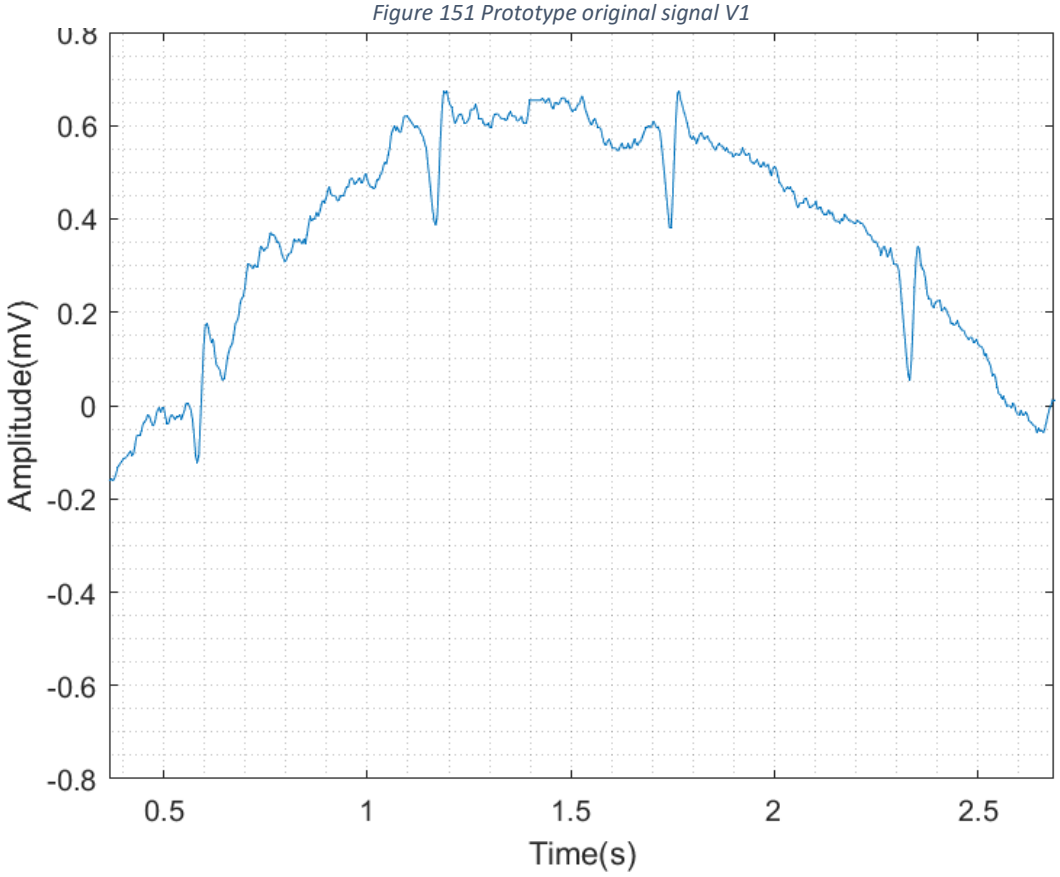

Figure 152 Prototype original signal D1

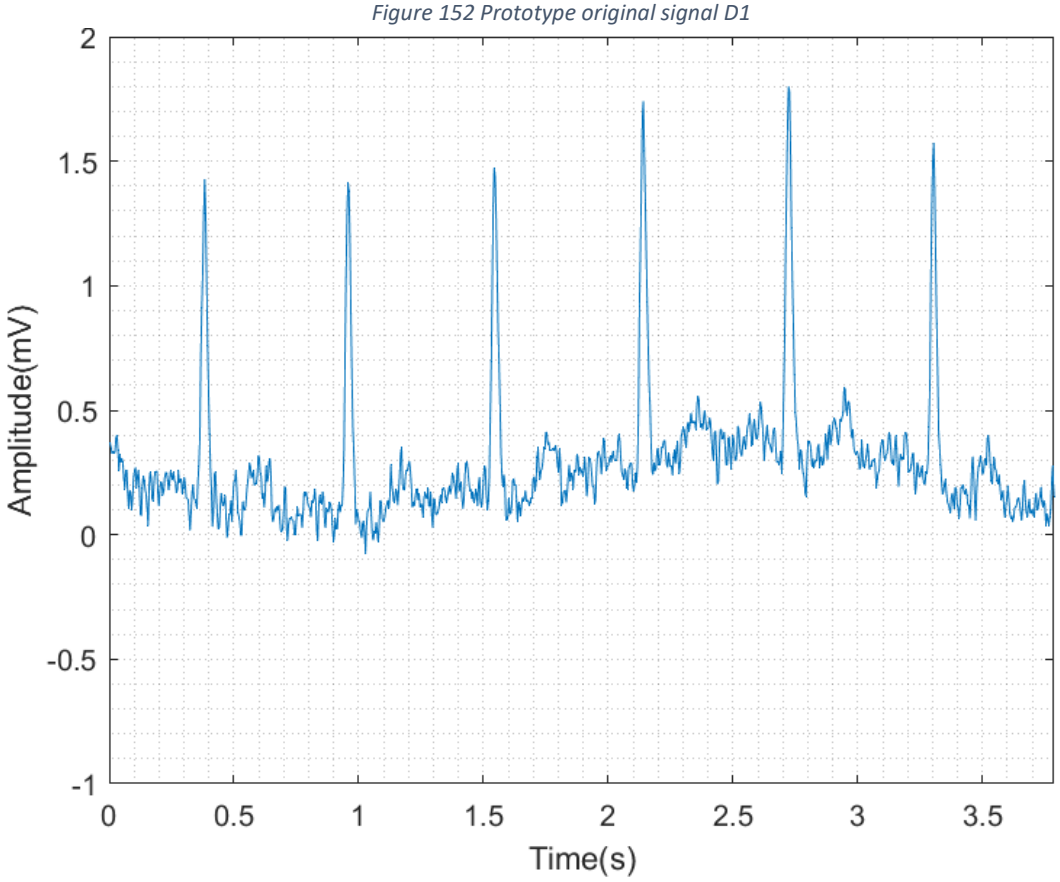

Figure 153 Prototype original signal V2

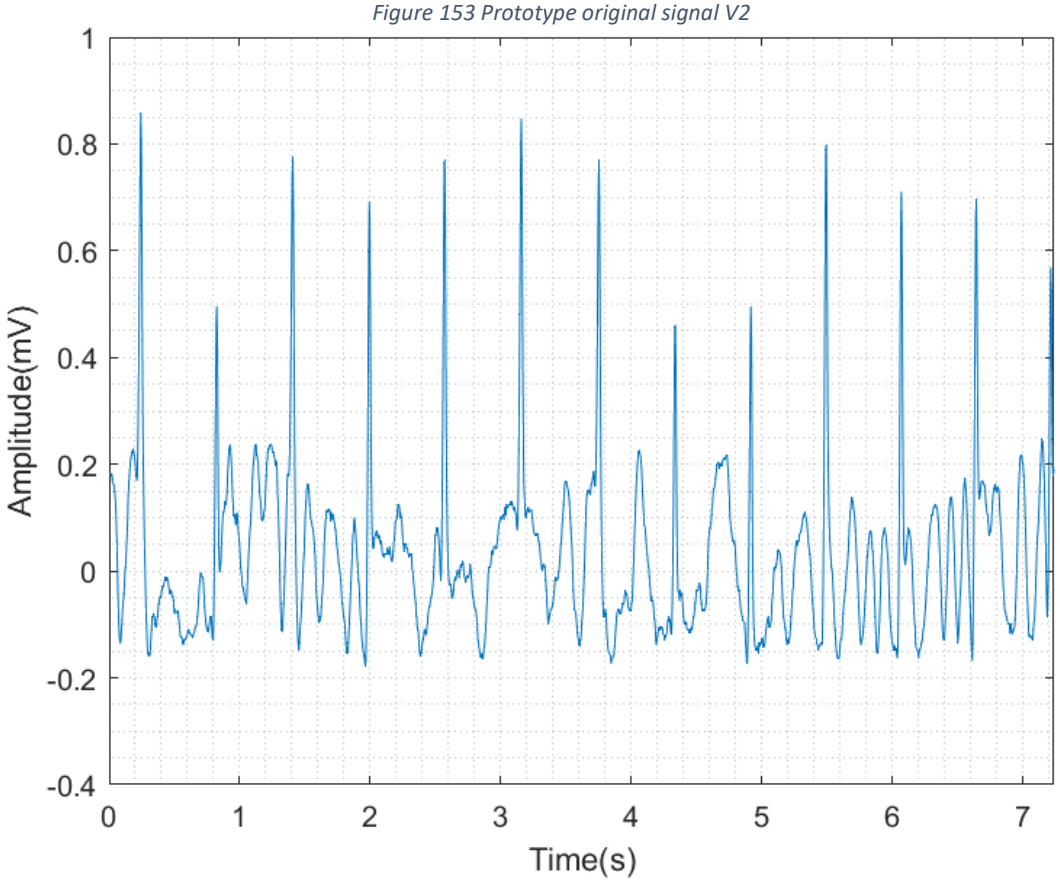

Figure 154 Ambulatory original signals

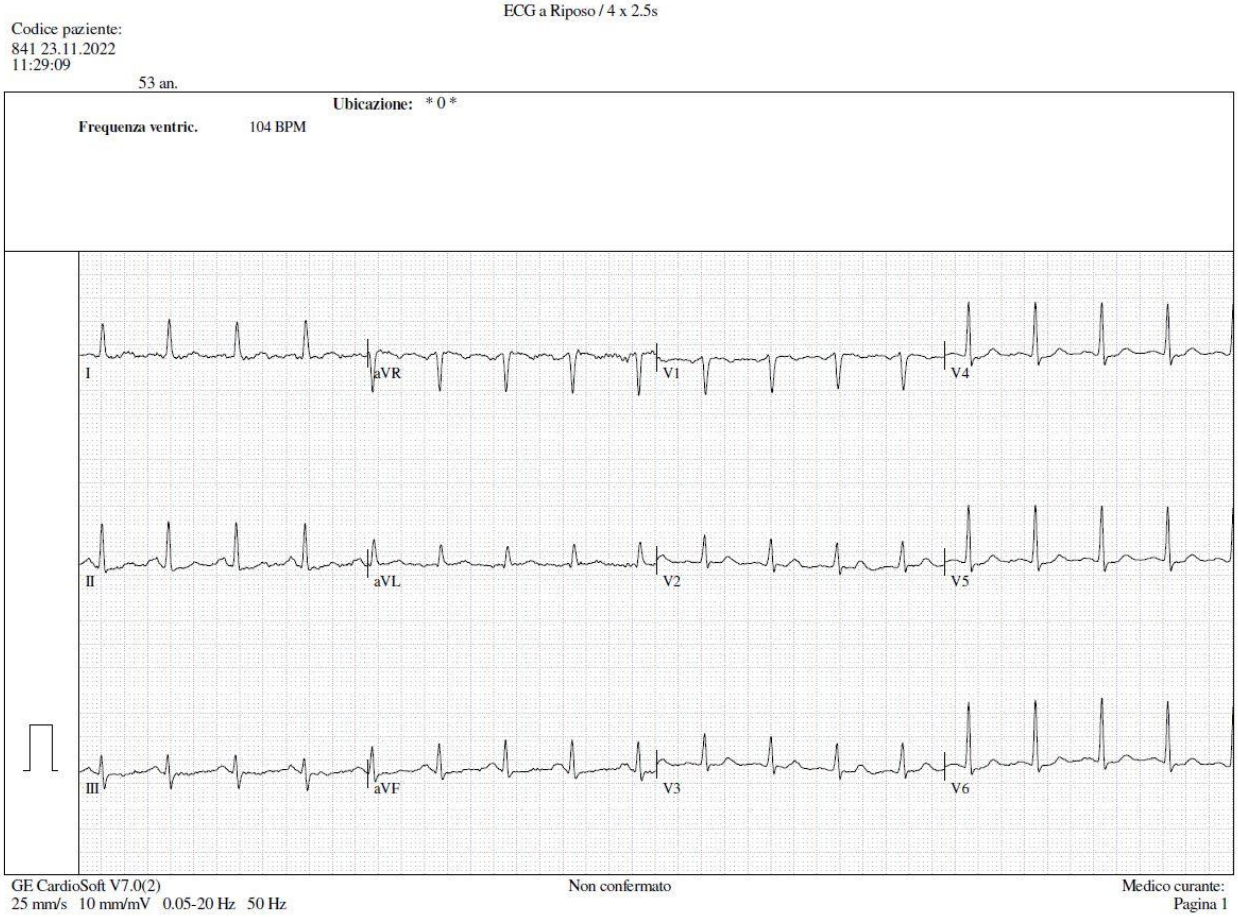

Figure 155 Ambulatory signals reconstructed

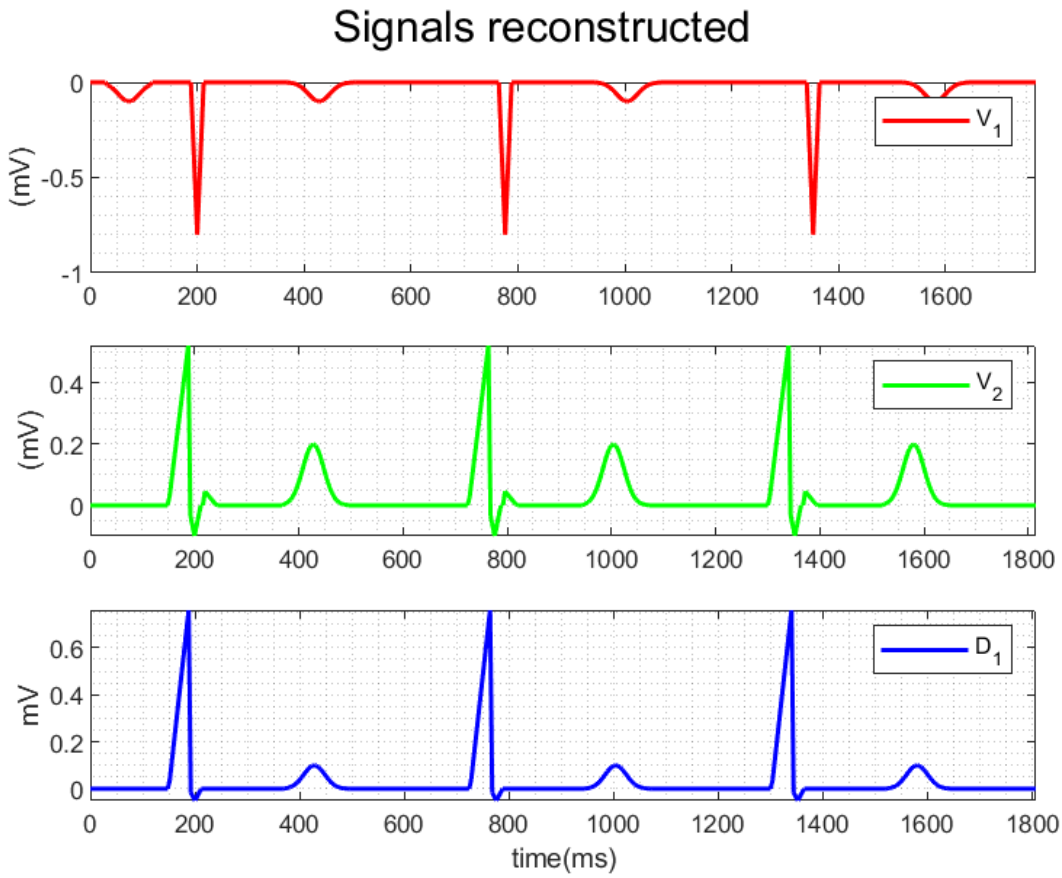

Figure 156 Comparison V1

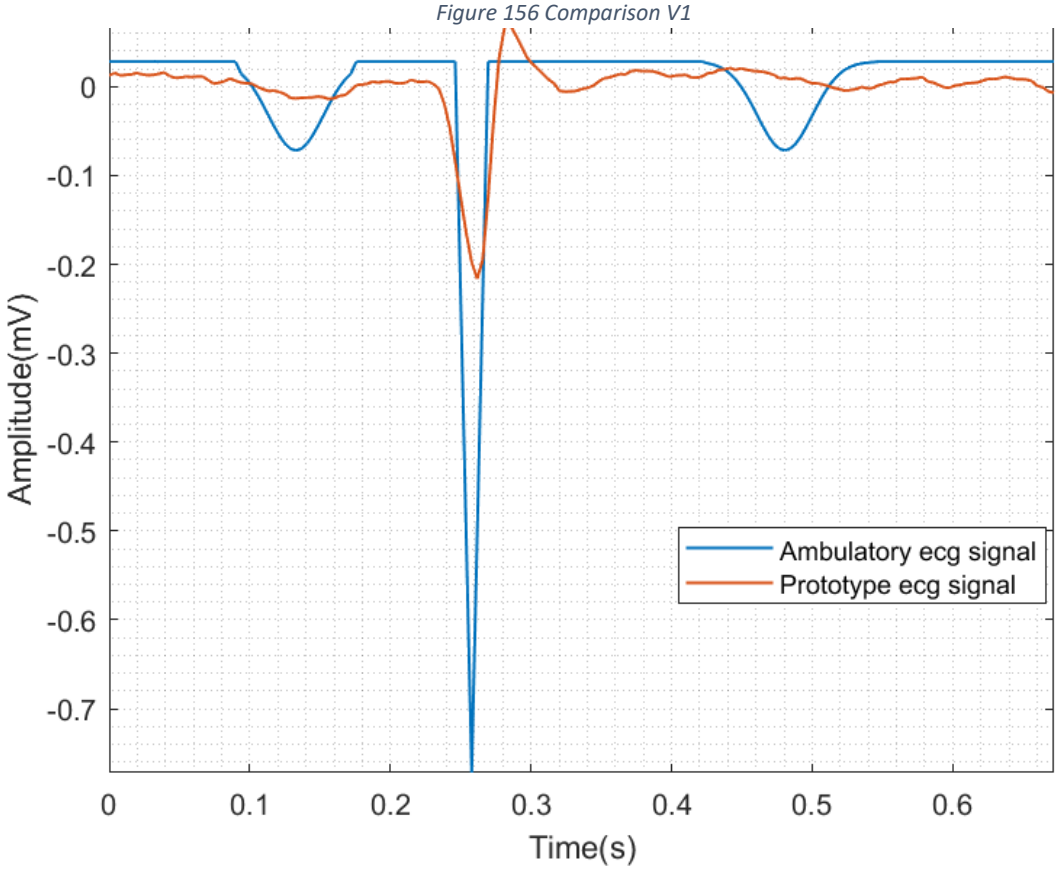

Figure 157 Comparison D1

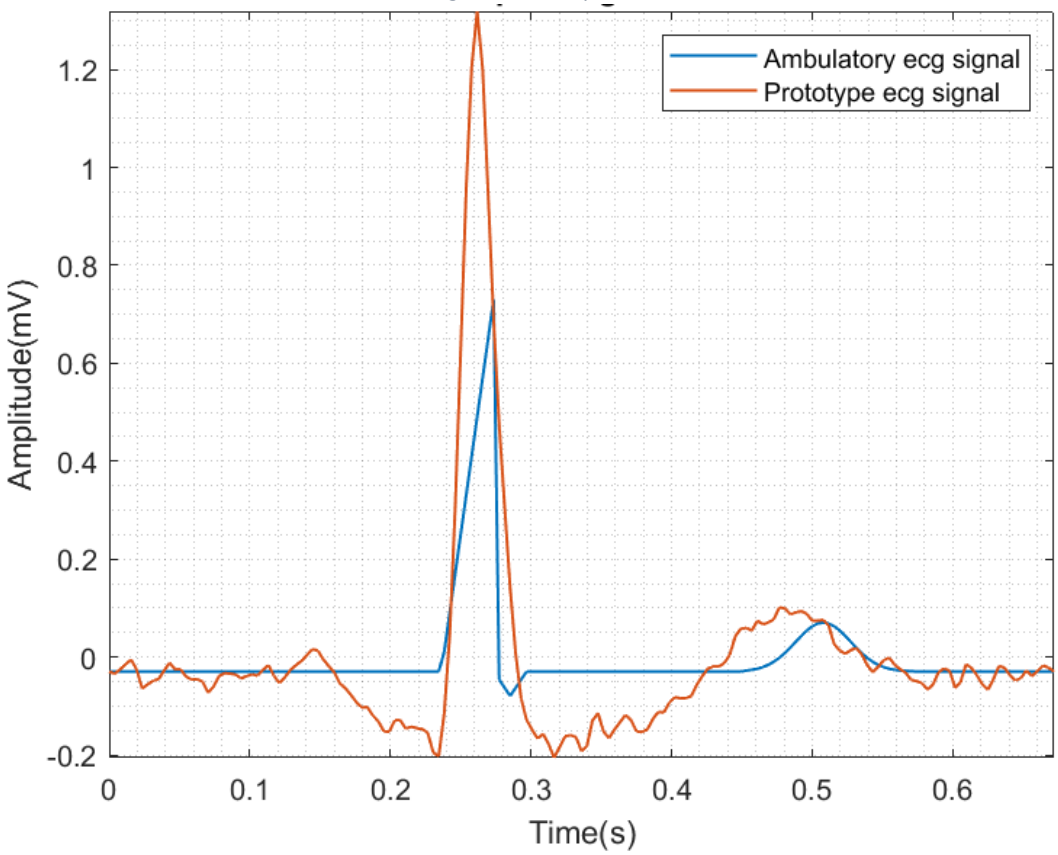

Figure 158 Comparison V2

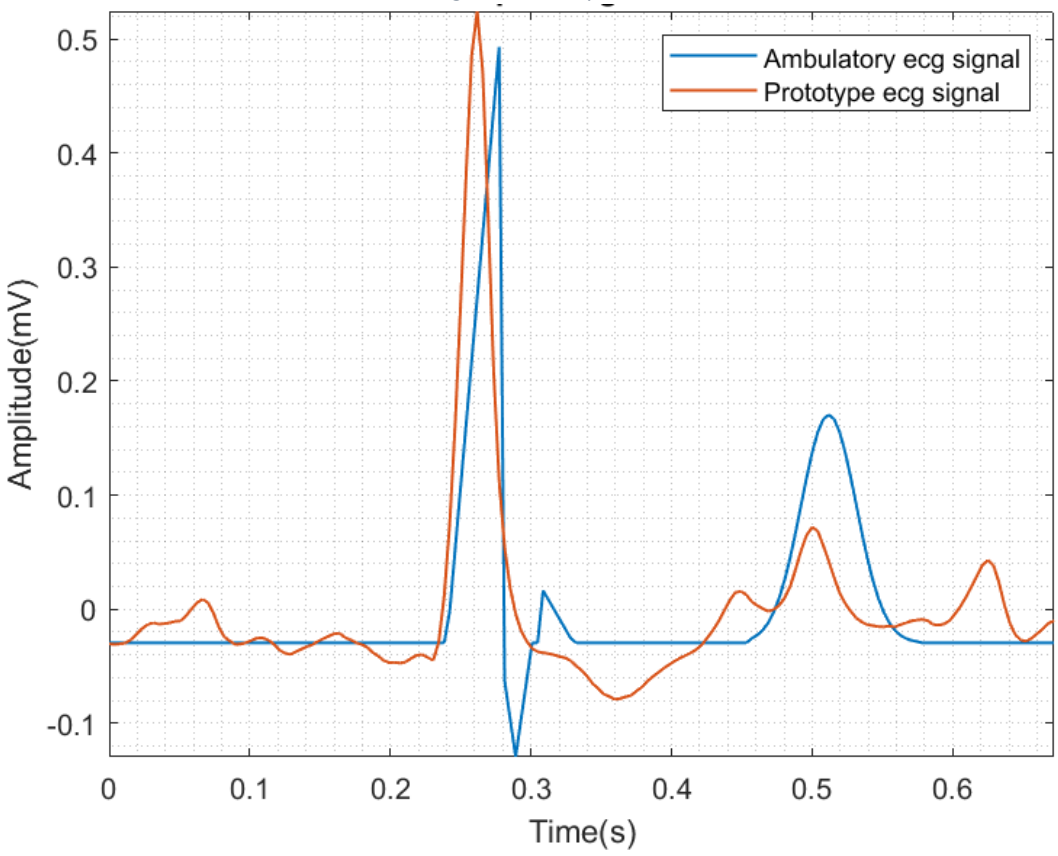

Patient #15:

Female 47 years old

BP 119/77

Figure 159 Prototype original signal V1

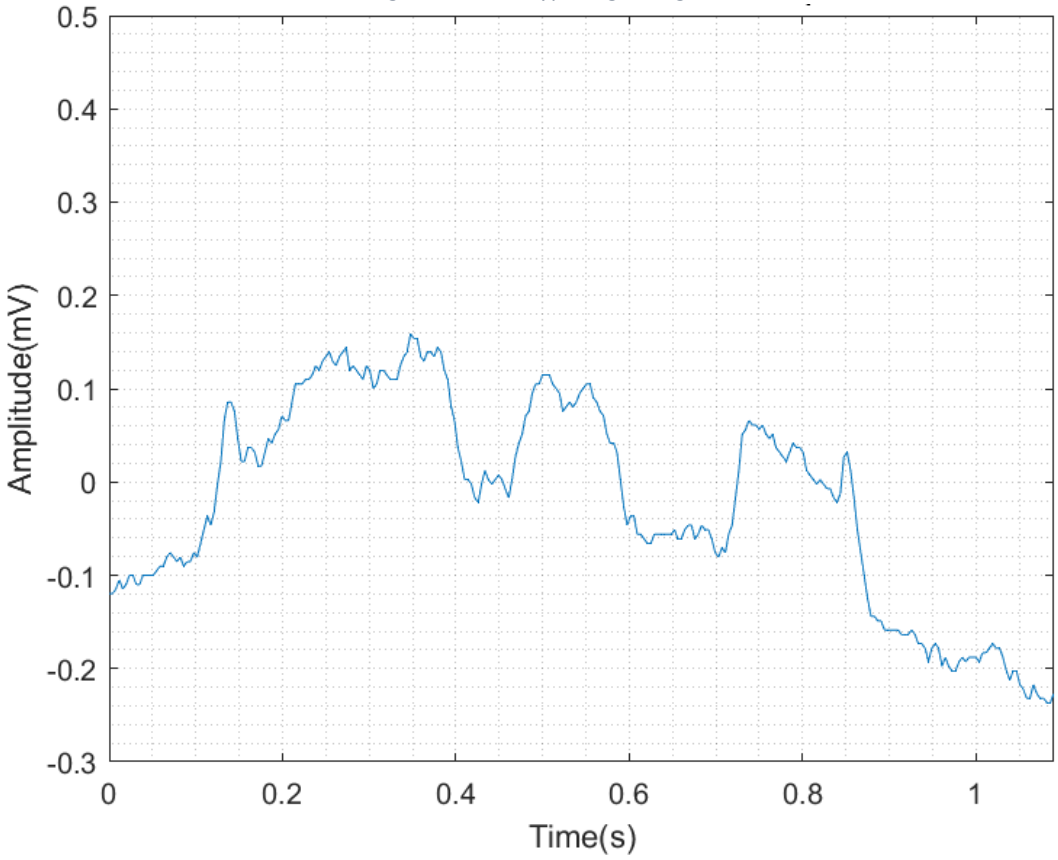

Figure 160 Prototype original signal D1

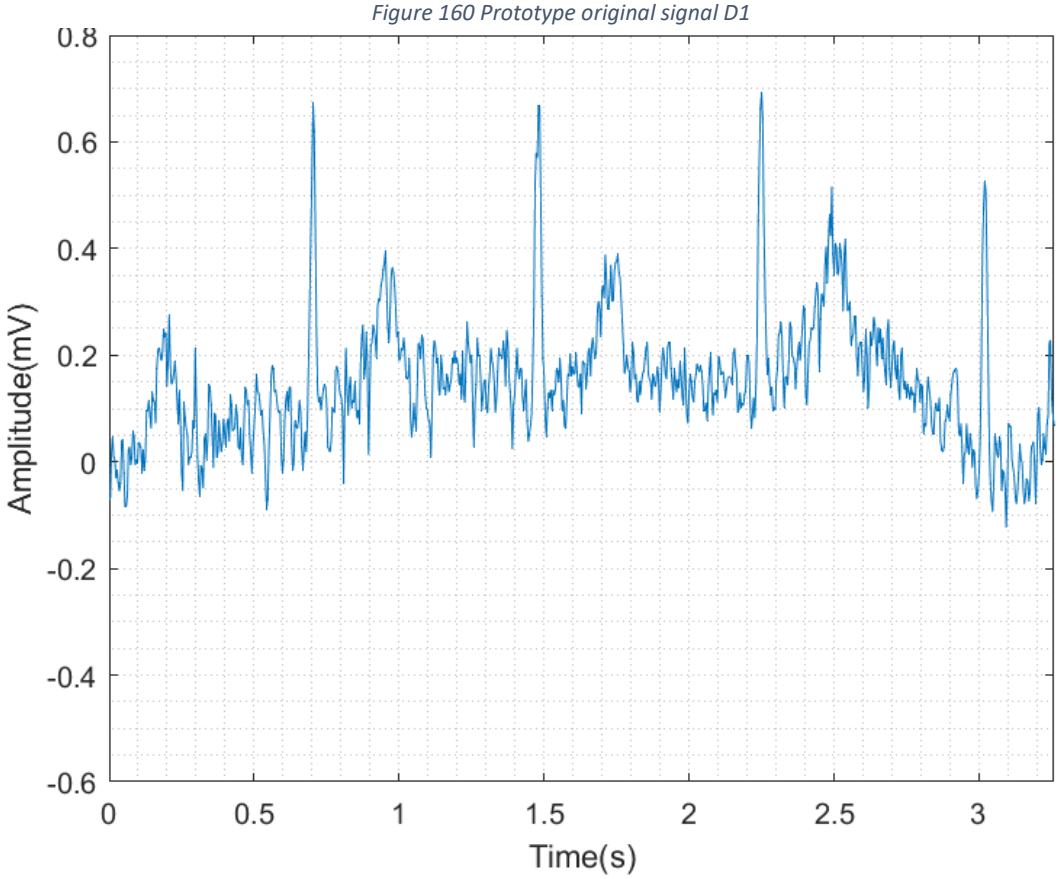

Figure 161 Prototype original signal V2

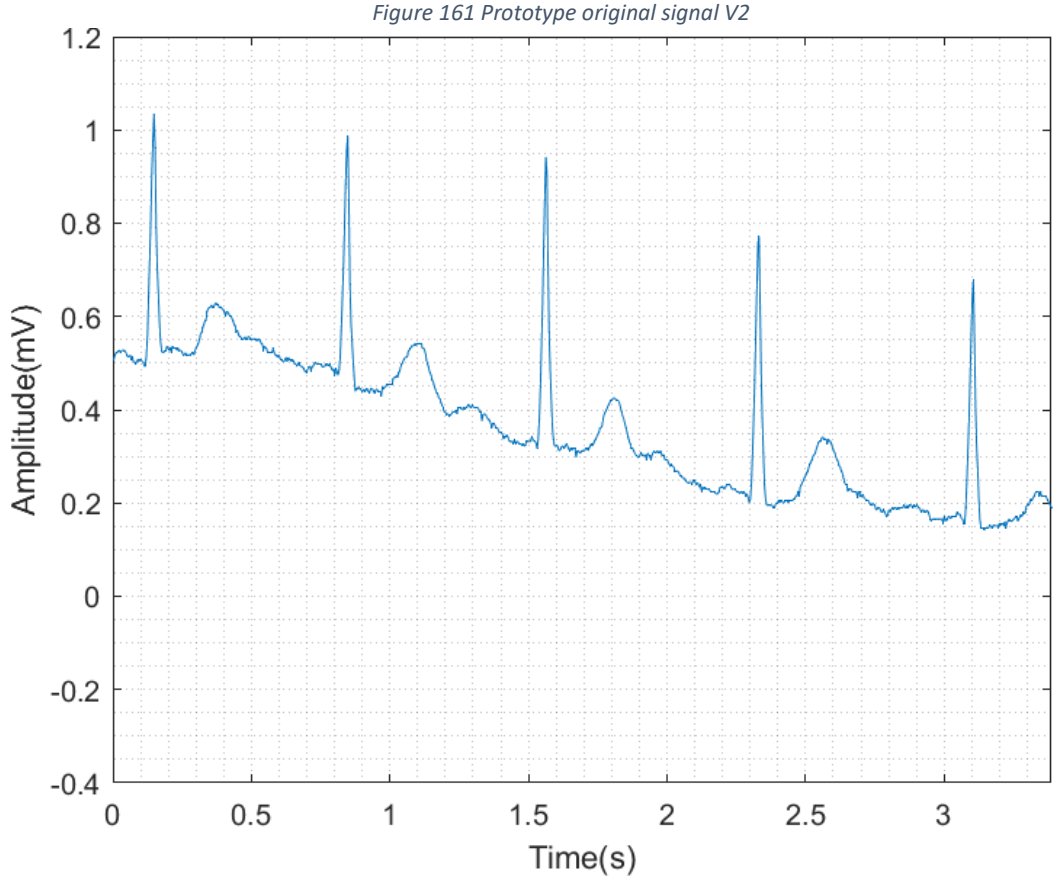

Figure 162 Ambulatory original signals

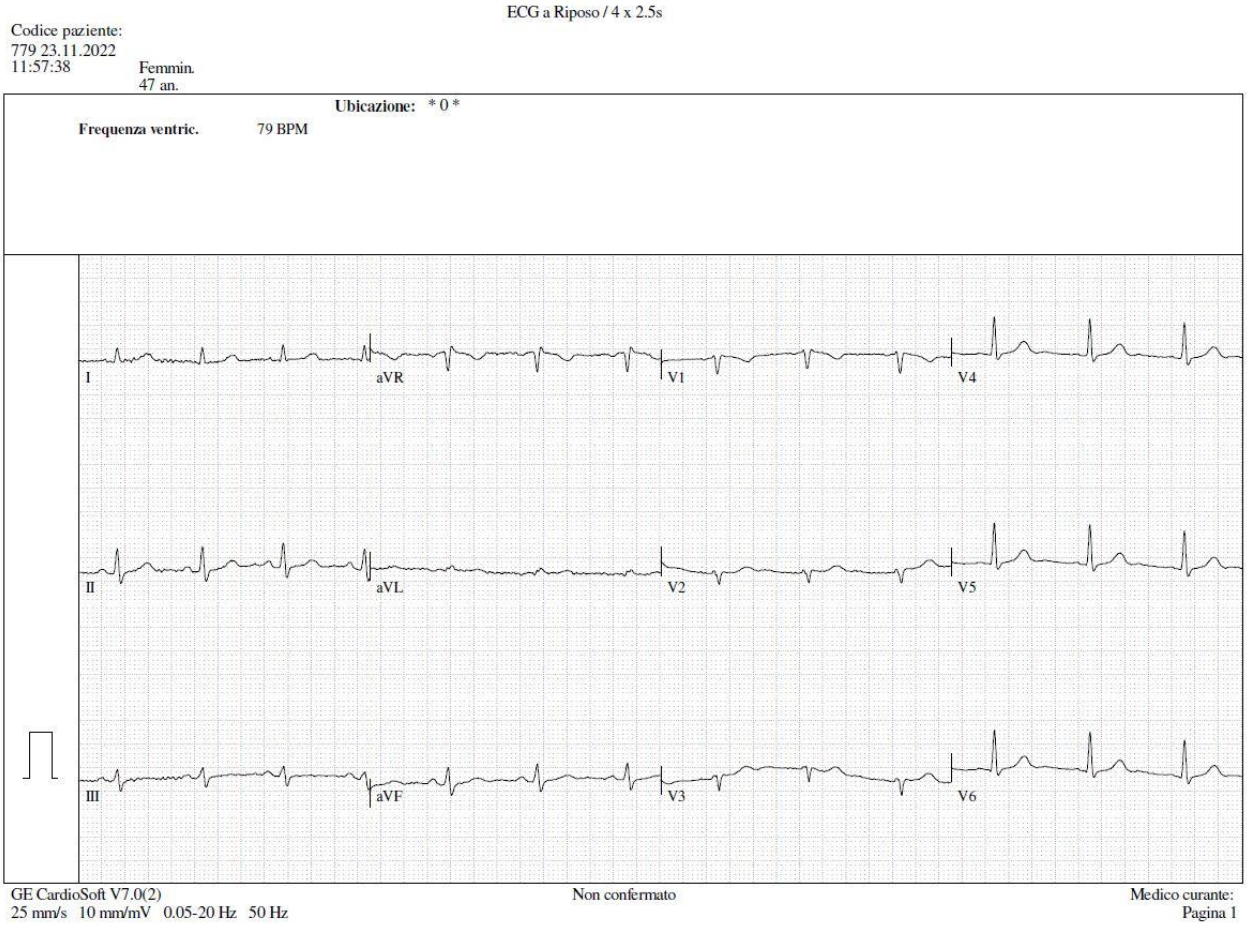

Figure 163 Ambulatory signals reconstructed

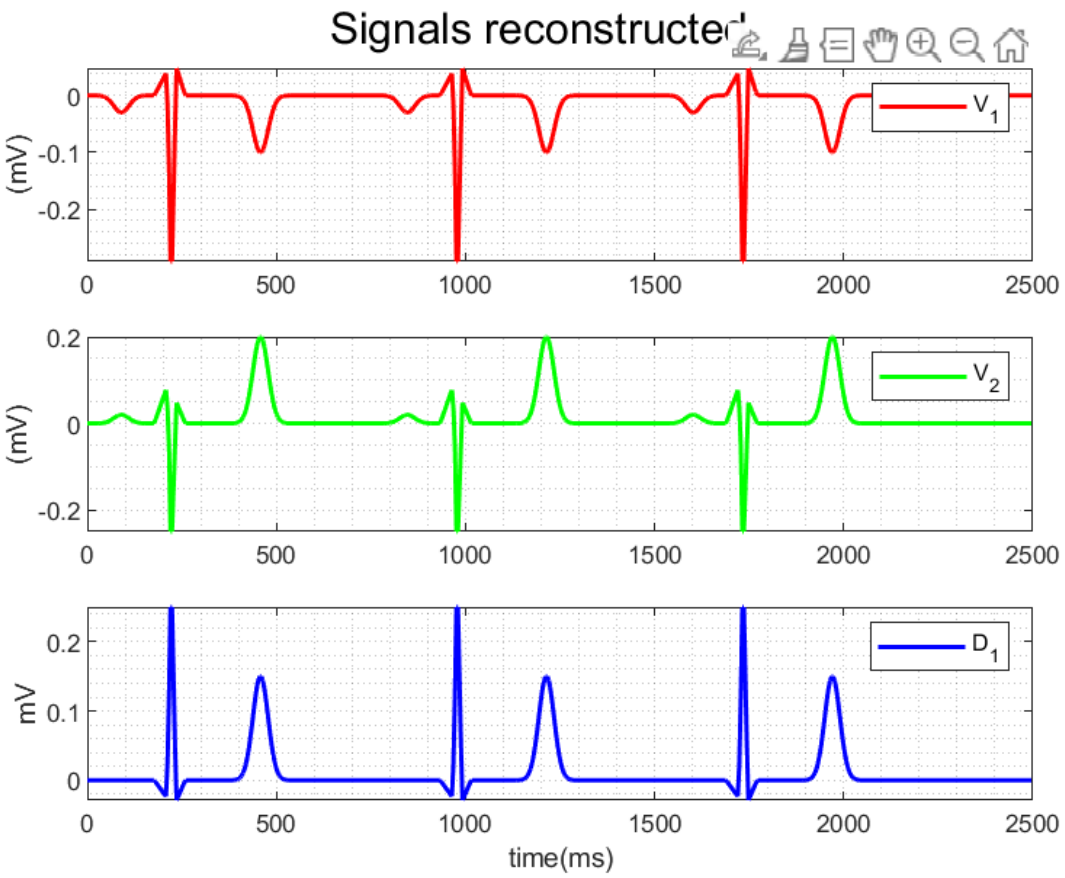

Figure 164 Comparison D1

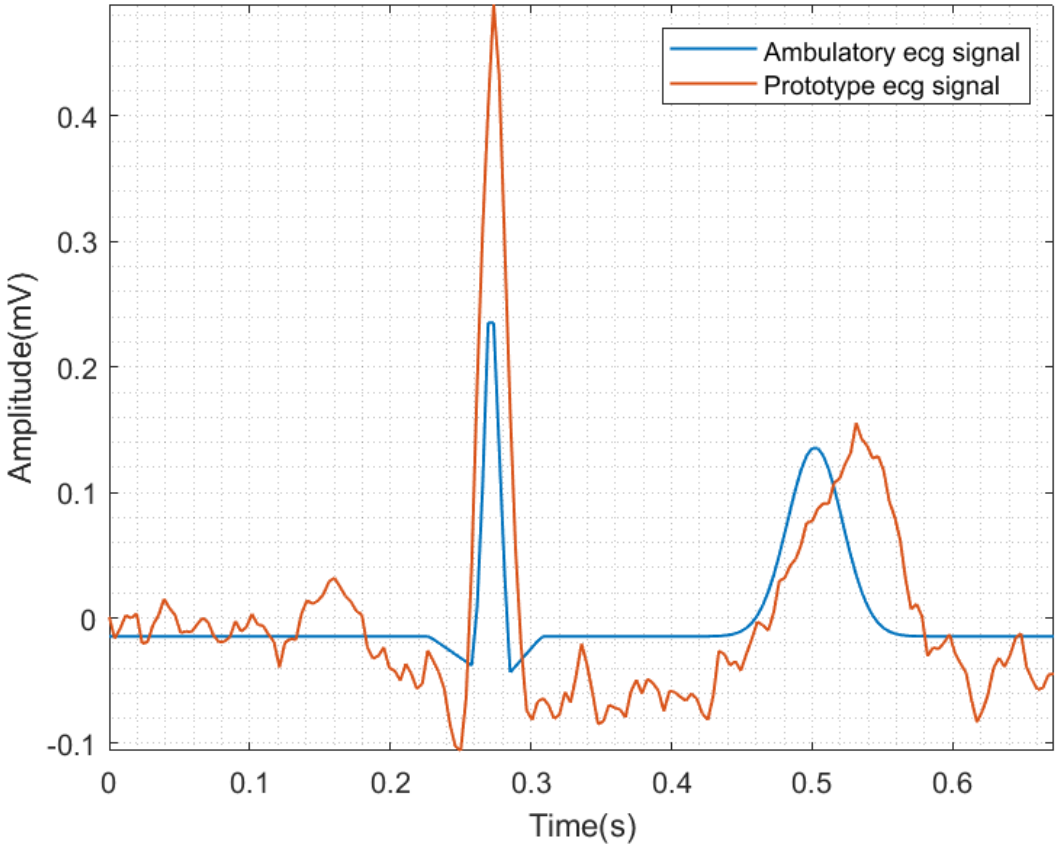

Patient #16:

Male years old

BP 124/80

Figure 165 Prototype original signal V1

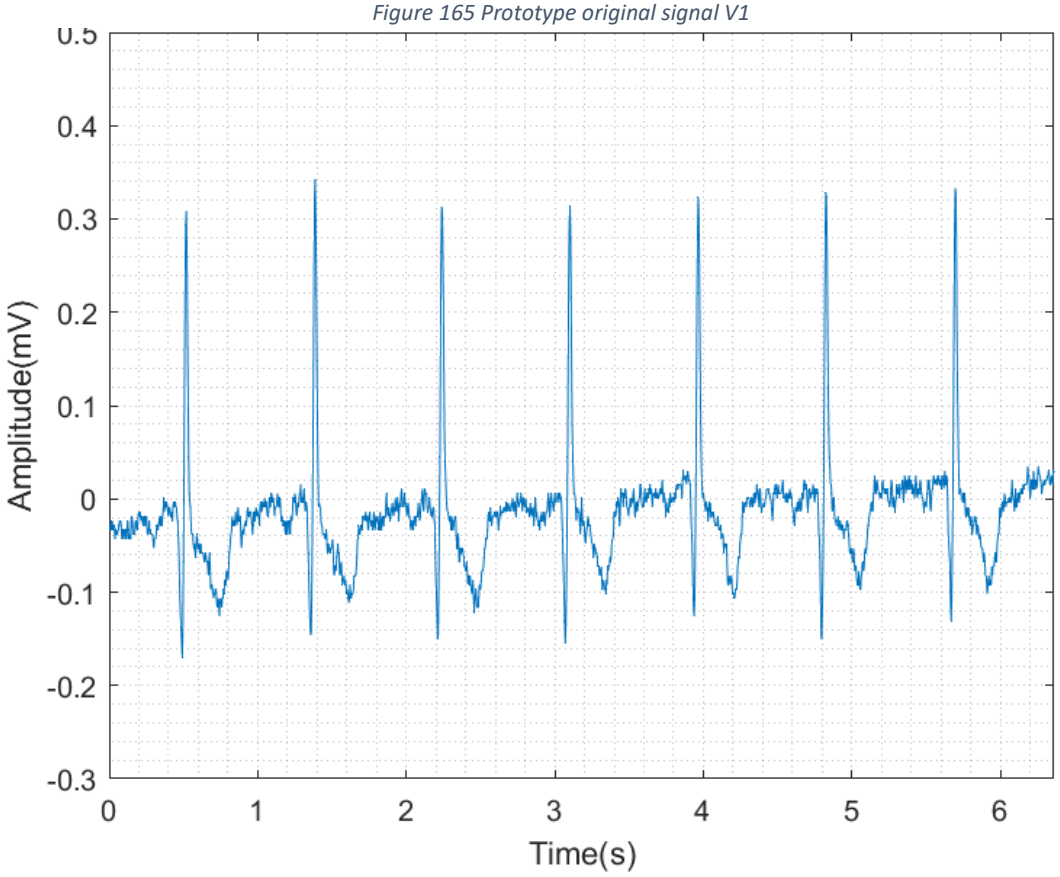

Figure 166 Prototype original signal D1

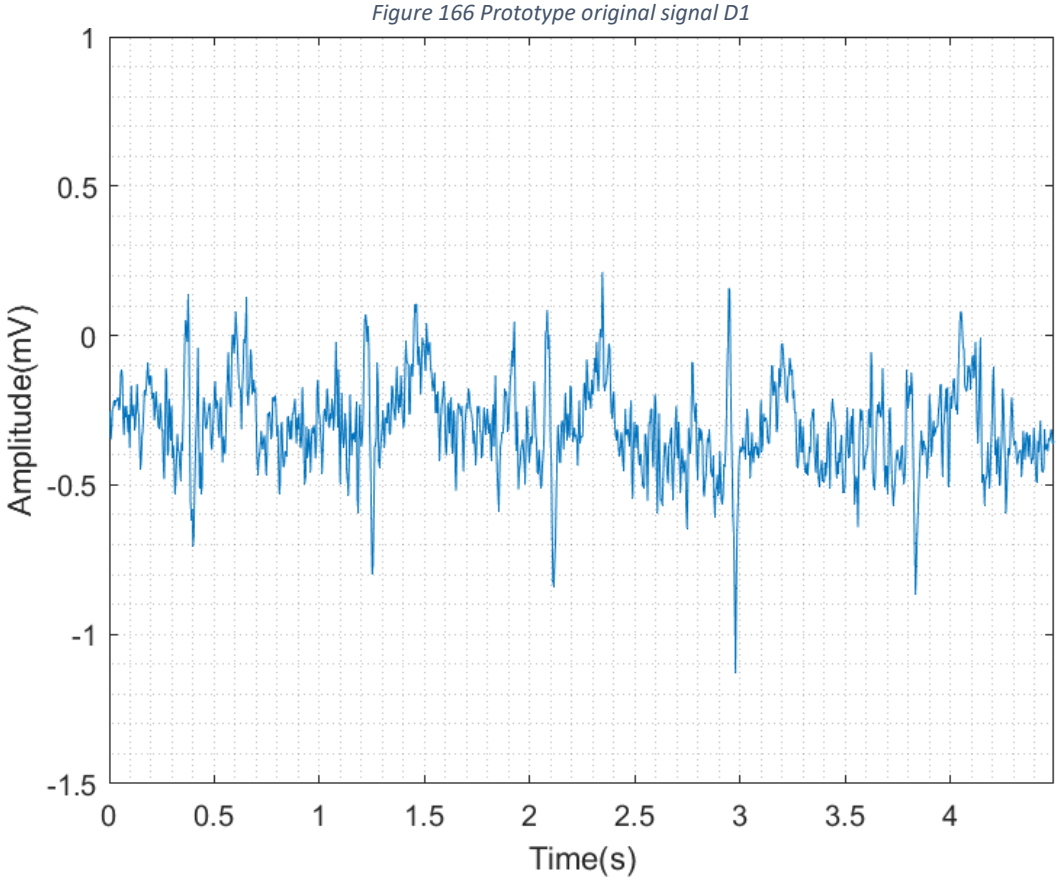

Figure 167 Prototype original signal V2

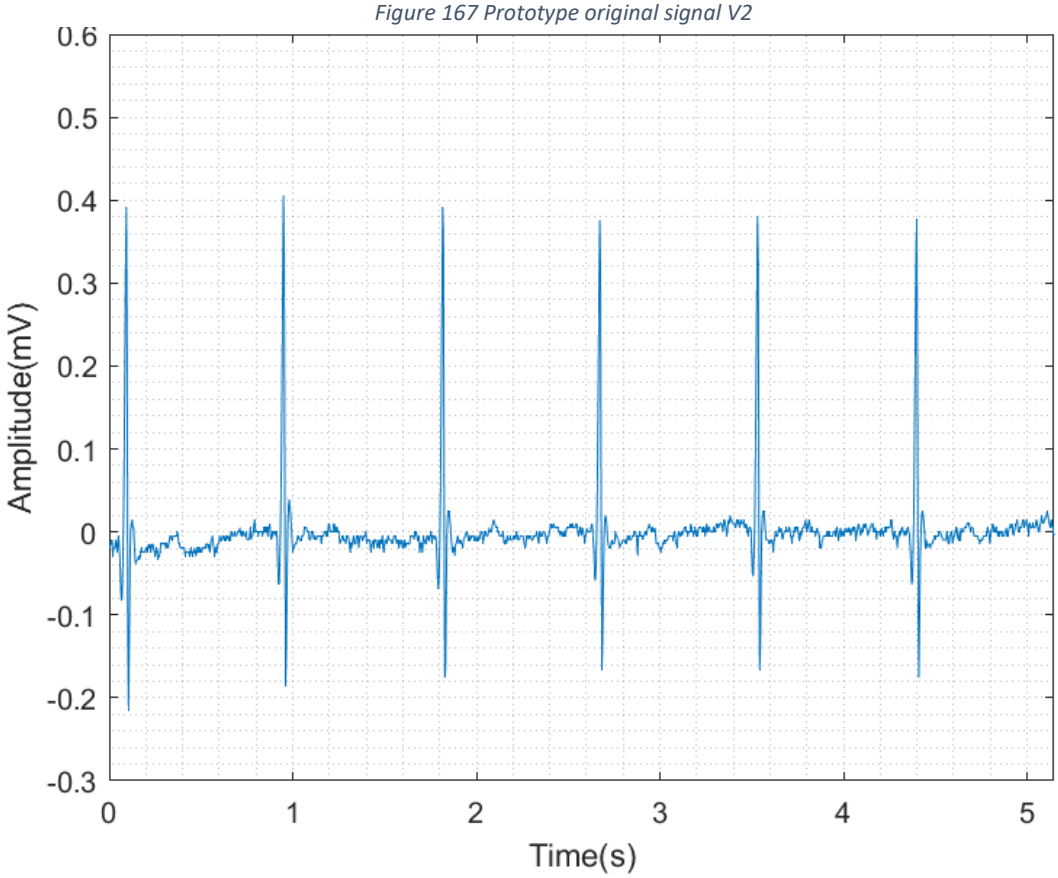

Figure 168 Ambulatory original signals

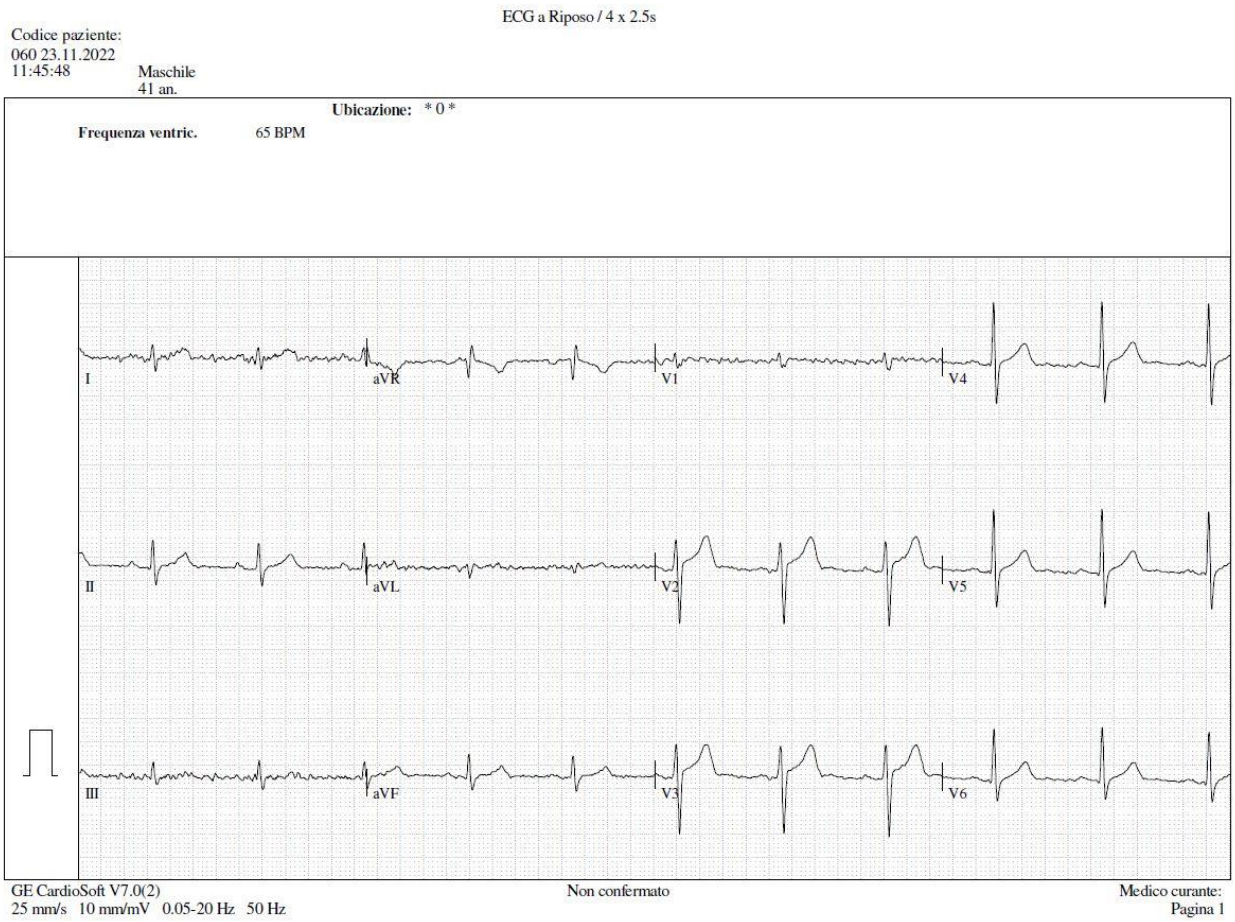

Figure 169 Ambulatory signals reconstructed

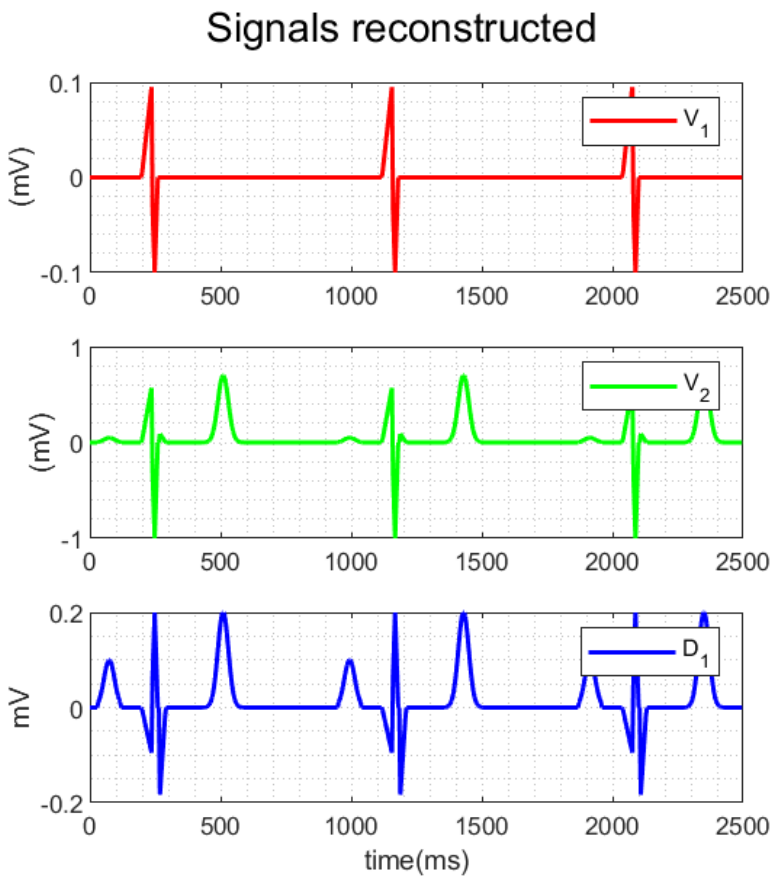

Figure 170 Prototype original signal V1

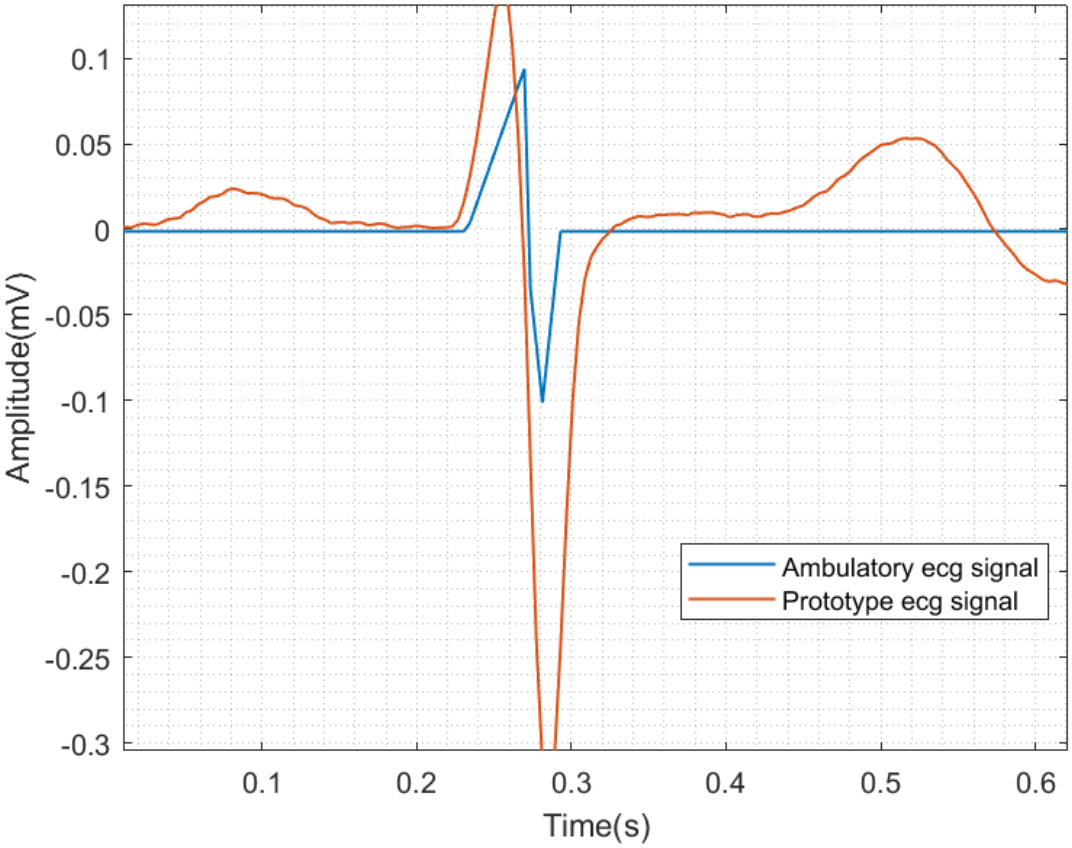

Figure 171 Prototype original signal D1

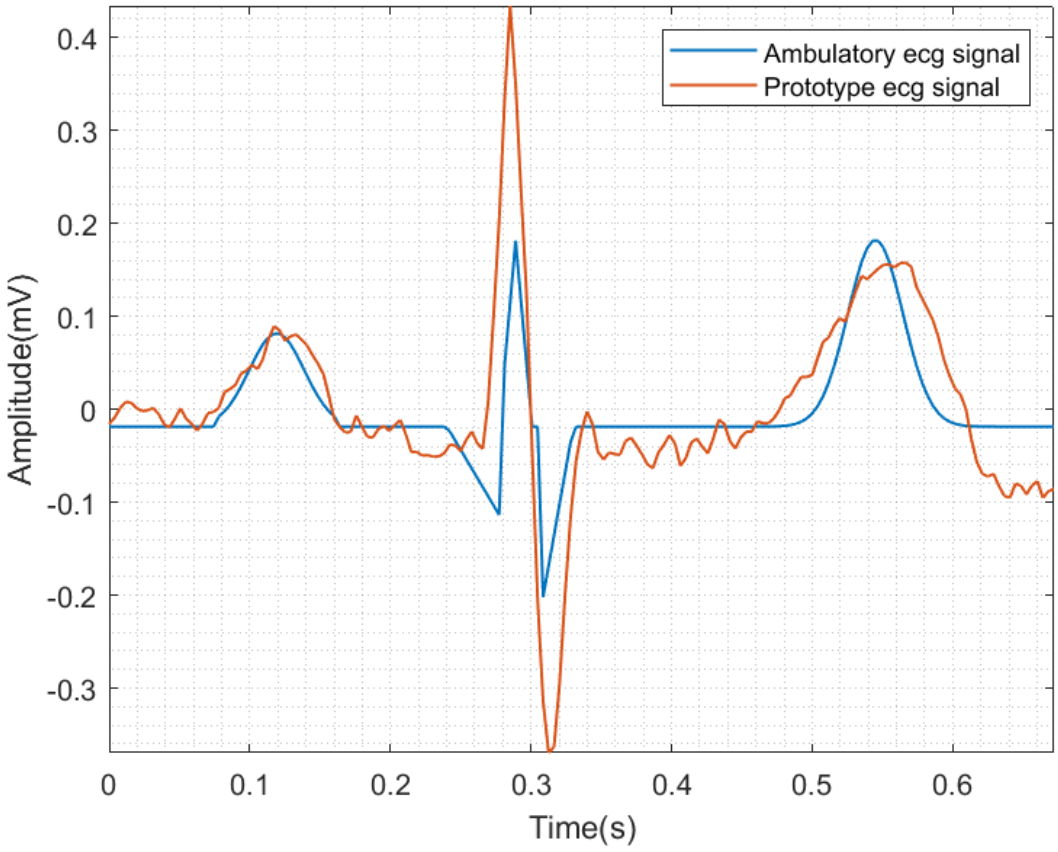

Figure 172 Prototype original signal V2

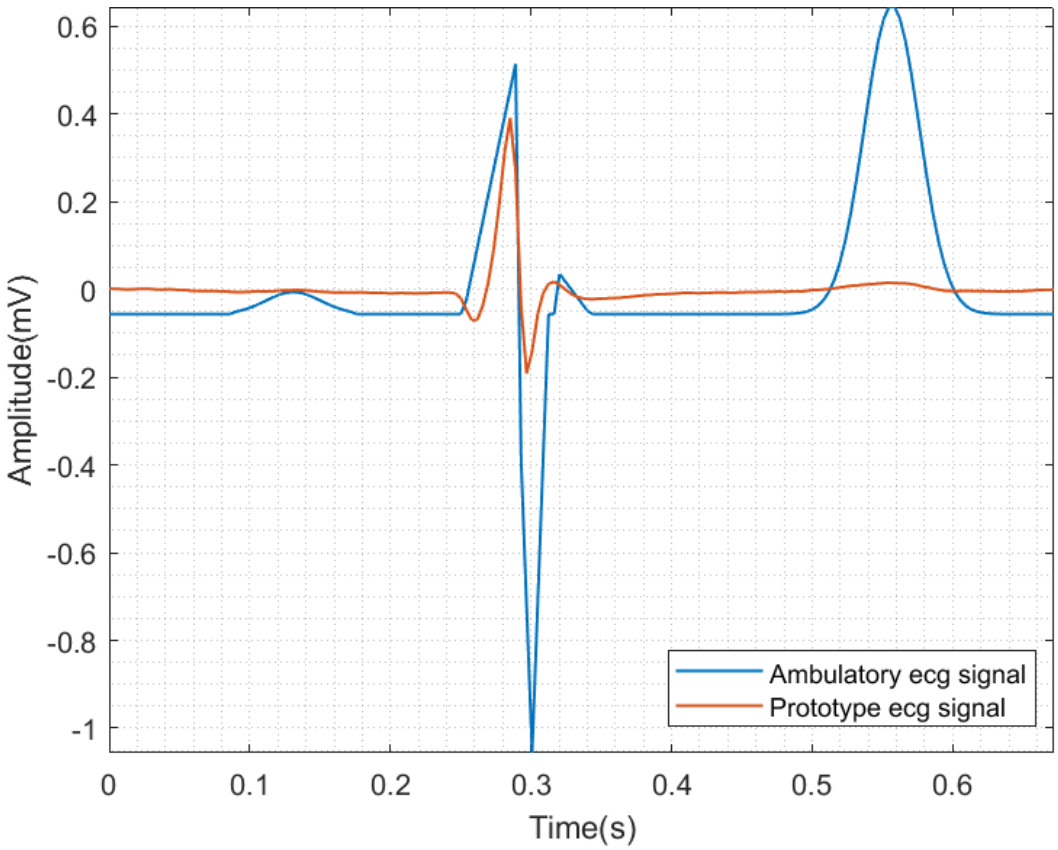

Results

After having carried out the comparison of the signals, the analysis turned to the validation of the calculable parameters. The ambulatory system outputs the following numerical values:

- P;
- P-R;
- QRS;
- QT;
- HR.

The same values were determined manually by analyzing the waveforms obtained from the prototype:

Figure 173 Prototype waveform analysis

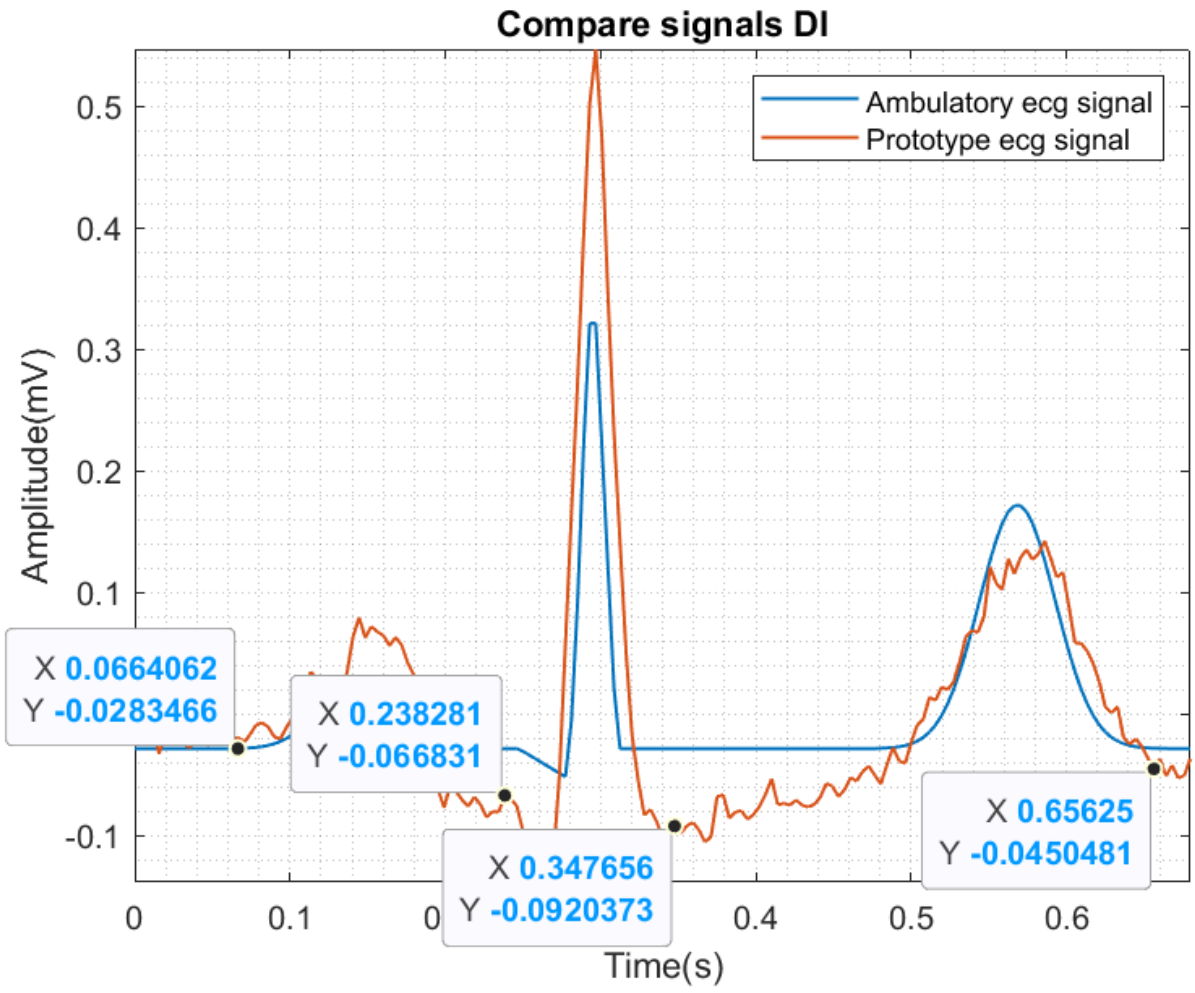

The data were then acquired and compared to start a statistical analysis of the sample, in order to obtain a precise quality indicator, named **sigma score (Z)**, typical of Six Sigma analysis.

Six Sigma is a management strategy developed in 1986 by Motorola in the USA and that has been applied in many business sectors. Six Sigma tries to improve the quality of the results of business processes by identifying and eliminating the causes of defects and errors and in doing so reducing variation in the processes. A Six Sigma process is a process in which 99.9966% of all products is flawless (3.4 defects per million).[69]

Six Sigma is a set of methodologies and tools used to improve business processes by reducing defects and errors, minimizing variation, and increasing quality and efficiency. The term implies high-quality performance: in fact, the goal of Six Sigma is to achieve a level of quality that is nearly perfect, with only 3.4 defects per million opportunities.

Basically, a sigma score shows how many standard deviations can fit between the mean and specification limit of any process or specification.

The central tendency of the performance distribution is defined by its **mean ($\bar{x}$)**. The amount of variation in the performance, or the width of the distribution, is defined by its **standard deviation (σ)**. The specifications of the outcome of a characteristic have a **Lower Control Limit (LCL)** and an **Upper Control Limit (UCL)**.

Figure 174 Lower and Upper Control Limit

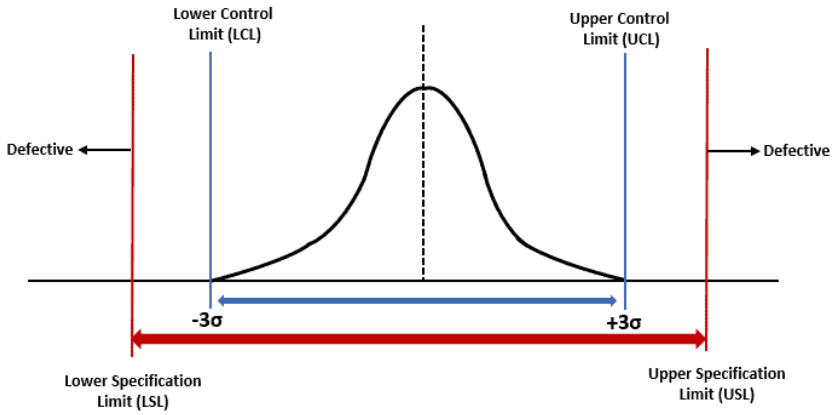

$$Z_{ST} = \frac{|\text{ nearest CL} - \bar{x}|}{\sigma}$$

A low short-term sigma (Z_{ST}) score means that a significant part of the tail of the distribution extends past the specification limit. So, the higher the sigma score, the fewer the defects. A process or characteristic gets

69 Rijk Schildmeijer, Paul Suijkrbuijk, "Six Sigma in practice", 2020 Published by The Lean Six Sigma Company.

a good sigma score when the variation distribution is safely away from the edge of the specification cliff. A sigma score can change in one of three ways:

1. The location of the central tendency of the distribution — the mean — moves either closer or farther from the specification limit.
2. The width of the distribution, as defined by the standard deviation σ changes.
3. The location of the specification limit SL moves either closer or farther from the characteristic or process variation.

Short-term variation performance, as quantified by the short-term sigma score Z_{ST}, represents the best variation performance that you can expect out of your currently configured process. This sigma score is communicated in terms of defects per million opportunities, DPMO.

The Six Sigma scale shows how well a vital feature performs compared to its requirements. The higher the sigma score, the more efficient the feature is.

This table shows the universal Six Sigma scale:

Figure 175 Universal Six Sigma scale

Z	DPMO	Percent Defects (%)	Percent Success (Yield %)
1	691,462	69	31
2	308,538	31	69
3	66,807	6.7	93.3
4	6,21	0.62	99.38
5	233	0.023	99.977
6	3.4	0.00034	9.999.966

Following the approach described above, the values relating to the five parameters measured (P, PR, QRS, QT, HR) were analyzed.

The purpose of the analysis was the calculation of the Z score for each parameter and for each patient, bearing in mind that the values shown in the following table (Figure 176) represents the average of the values recorded on **eight heart beats** detected by the prototype.

Figure 176 Values recorded average

	PARAMETERS MEASURED									
	P	**P Prototype**	**PR**	**PR Prototype**	**QRS**	**QRS Prototype**	**QT**	**QT Prototype**	**HR**	**HR Prototype**
Patient #1	138	140	202	204	100	102	390	392	69	72
Patient #2	104	107	140	143	98	101	388	391	73	76
Patient #3	118	117	128	127	84	83	358	357	78	78
Patient #4	92	90	134	132	94	92	376	374	72	71
Patient #5	118	116	150	148	86	84	376	374	71	72
Patient #6	92	94	144	146	102	104	390	392	73	74
Patient #7	120	124	170	174	118	122	426	430	60	63
Patient #8	120	115	162	161	86	85	360	359	80	83
Patient #9	122	125	158	161	100	103	390	393	74	78
Patient #10	85	86	120	121	120	121	400	401	67	67
Patient #11	120	122	163	166	120	123	398	401	62	61
Patient #12	123	125	164	166	87	89	405	407	50	50
Patient #13	122	121	170	168	115	111	400	398	66	68
Patient #14	82	83	110	111	120	121	340	341	104	107
Patient #15	116	114	136	134	102	100	360	358	79	77
Patient #16	85	86	154	156	120	122	410	412	65	65

So, for example, considering Patient#1 and the parameter P, 138 was assumed as nominal value, which represents the value of the parameter measured by the outpatient device.

The acceptable tolerance limit has been defined equal to ±5 ms: therefore, the specification limits are respectively equal to 133 (LSL) and 143 (USL).

The mean and standard deviation of the eight recorded heartbeats were calculated.

Figure 177 Mean and standard deviation calculation – P parameter Patient#1

Patient #1 - P	
HB #1	140
HB #2	140
HB #3	140
HB #4	140
HB #5	140
HB #6	139
HB #7	140
HB #8	141

Mean	**140**
Std deviation	**0,53**

Sigma score	**5,66**

The table below contains all the values calculated for each parameter and for each patient:

Figure 178 Z score for each parameter and for each patient

	Z score				
	P	**PR**	**QRS**	**QT**	**HR**
Patient #1	5,66	2,65	2,81	3,97	3,74
Patient #2	2,65	3,74	3,74	3,74	3,74
Patient #3	5,29	5,48	4,69	5,66	4,68
Patient #4	2,81	3,97	5,61	5,61	5,29
Patient #5	3,24	3,24	3,97	5,61	5,29
Patient #6	2,81	5,61	5,61	5,02	4,32
Patient #7	5,61	3,74	3,74	3,74	3,74
Patient #8	2,65	5,38	5,29	4,69	3,74
Patient #9	2,65	2,69	1,87	3,74	2,65
Patient #10	4,99	5,29	5,48	5,69	4,68
Patient #11	5,61	3,74	3,74	3,35	5,29
Patient #12	3,97	5,61	5,61	4,03	5,72
Patient #13	3,35	5,61	3,74	4,03	5,61
Patient #14	4,32	5,29	3,86	5,48	3,74
Patient #15	3,97	3,24	3,97	5,61	3,97
Patient #16	4,99	3,97	5,02	5,61	5,61
Mean	**4,04**	**4,33**	**4,30**	**4,72**	**4,49**

Considering that the average Z score for each parameter is always higher than 4 and referring to the table shown in the Figure 175, we can say that the prototype is more than 99% accurate and we would expect a defect rate less than 0.6%.

Conclusions and future developments

The objective of this study is the validation of a non-implantable device for the detection of basal parameters, in particular ECG. There are various types of devices on the market, but many of them do not have the accuracy of the systems currently in use in ambulatories.

A first innovation lies in the type of analysis conducted for the statistical validation of the results. In fact, a typical parameter of the Six Sigma approach was used, which is not common in the healthcare field but has a great statistical impact.

The device analyzed demonstrated a level of accuracy comparable to the classic systems used in clinics and demonstrated high versatility as it is completely customizable.

It is possible to use from one to six precordial leads, depending on the needs of the specific patient, and a peripheral one (D_1) on request. All leads are perfectly synchronized in time with each other, allowing the physician to correctly evaluate the ECG in real time.

The device demonstrates a high ease of use as well as a high comfort of use compared to the classic holters.

Having a totally open platform, it can be integrated with BP and SpO_2 detection systems that have already been tested but not yet validated, as well as with IG detection systems.

It can also be used in the field of simulations, as demonstrated in the first phase of in vitro analysis, by reporting perfectly synchronized ECG traces on the simulation platform, and allowing operators, especially in the Electrophysiology field, to map complex arrhythmias before the patient enter the operating room.

Finally, it is important to consider how the system is totally open to integration with Telemedicine platforms. This will allow for remote monitoring of patients, the primary objective of the present study.

Bibliography

[1] A. Di Lenarda *et al.*, "The future of telemedicine for the management of heart failure patients: A Consensus Document of the Italian Association of Hospital Cardiologists (A.N.M.C.O), the Italian Society of Cardiology (S.I.C.) and the Italian Society for Telemedicine and eHealth (Digital S.I.T.)," *Eur. Hear. Journal, Suppl.*, vol. 19, pp. D113–D129, 2017, doi: 10.1093/eurheartj/sux024.

[2] G. Marazzi, F. Iellamo, M. Volterrani, and M. Lombardo, "Erratum to: Comparison of Microlife BP A200 Plus and Omron M6 Blood Pressure Monitors to Detect Atrial Fibrillation in Hypertensive Patients(Advances in Therapy, (2012) 29(1):64–70, 10.1007/s12325-011-0087-0)," *Adv. Ther.*, vol. 31, no. 12, p. 1317, 2014, doi: 10.1007/s12325-014-0172-2.

[3] K. Kearley *et al.*, "Triage tests for identifying atrial fibrillation in primary care: A diagnostic accuracy study comparing single-lead ECG and modified BP monitors," *BMJ Open*, vol. 4, no. 5, 2014, doi: 10.1136/bmjopen-2013-004565.

[4] G. Kaleschke *et al.*, "Prospective, multicentre validation of a simple, patient-operated electrocardiographic system for the detection of arrhythmias and electrocardiographic changes," *Europace*, vol. 11, no. 10, pp. 1362–1368, 2009, doi: 10.1093/europace/eup262.

[5] C. De Asmundis *et al.*, "Comparison of the patient-activated event recording system vs. traditional 24 h Holter electrocardiography in individuals with paroxysmal palpitations or dizziness," *Europace*, vol. 16, no. 8, pp. 1231–1235, 2014, doi: 10.1093/europace/eut411.

[6] R. Jaafar and A. S. Abdul Salam, "Portable electrocardiography with cloud based features: A review of current technologies," *2019 Int. Biomed. Instrum. Technol. Conf. IBITeC 2019*, pp. 118–122, 2019, doi: 10.1109/IBITeC46597.2019.9091683.

[7] M. Shao, Z. Zhou, G. Bin, Y. Bai, and S. Wu, "A wearable electrocardiogram telemonitoring system for atrial fibrillation detection," *Sensors (Switzerland)*, vol. 20, no. 3, 2020, doi: 10.3390/s20030606.

[8] I. Voiculescu, F. Li, G. Kowach, K. L. Lee, N. Mistou, and R. Kastberg, "Stretchable piezoelectric power generators based on ZnO thin films on elastic substrates," *Micromachines*, vol. 10, no. 10, 2019, doi: 10.3390/mi10100661.

[9] W. Tong, C. Kan, and H. Yang, "Sensitivity analysis of wearable textiles for ECG sensing," *2018 IEEE EMBS Int. Conf. Biomed. Heal. Informatics, BHI 2018*, vol. 2018-Janua, no. March, pp. 157–160, 2018, doi: 10.1109/BHI.2018.8333393.

[10] R. Castrillón, J. J. Pérez, and H. Andrade-Caicedo, “Electrical performance of PEDOT: PSS-based textile electrodes for wearable ECG monitoring: A comparative study,” *Biomed. Eng. Online*, vol. 17, no. 1, pp. 1–23, 2018, doi: 10.1186/s12938-018-0469-5.

[11] X. An, O. Tangsirinaruenart, and G. K. Stylios, “Investigating the performance of dry textile electrodes for wearable end-uses,” *J. Text. Inst.*, vol. 110, no. 1, pp. 151–158, 2019, doi: 10.1080/00405000.2018.1508799.

[12] K. Arquilla, A. K. Webb, and A. P. Anderson, “Textile electrocardiogram (Ecg) electrodes for wearable health monitoring,” *Sensors (Switzerland)*, vol. 20, no. 4, pp. 1–13, 2020, doi: 10.3390/s20041013.

[13] Y. T. Tsukada *et al.*, “Validation of wearable textile electrodes for ECG monitoring,” *Heart Vessels*, vol. 34, no. 7, pp. 1203–1211, 2019, doi: 10.1007/s00380-019-01347-8.

[14] X. An and G. K. Stylios, “A hybrid textile electrode for electrocardiogram (ECG) measurement and motion tracking,” *Materials (Basel).*, vol. 11, no. 10, 2018, doi: 10.3390/ma11101887.

[15] N. Wu, H. Liu, S. Wan, S. Su, H. Huang, and L. Sun, “Ultrahigh Skin-Conformal and Biodegradable Graphene-based Flexible Sensor for Measuring ECG Signal,” *Int. J. Inf. Electron. Eng.*, vol. 10, no. 2, pp. 52–56, 2020, doi: 10.18178/ijiee.2020.10.2.720.

[16] A. Villegas, D. McEneaney, and O. Escalona, “Arm-ECG wireless sensor system for wearable long-term surveillance of heart arrhythmias,” *Electron.*, vol. 8, no. 11, pp. 1–26, 2019, doi: 10.3390/electronics8111300.

[17] J. W. Ahn, Y. Ku, and H. C. Kim, “A novel wearable EEG and ECG recording system for stress assessment,” *Sensors (Switzerland)*, vol. 19, no. 9, 2019, doi: 10.3390/s19091991.

[18] N. Huda, S. Khan, R. Abid, S. B. Shuvo, M. M. Labib, and T. Hasan, “A Low-cost, Low-energy Wearable ECG System with Cloud-Based Arrhythmia Detection,” *2020 IEEE Reg. 10 Symp. TENSYMP 2020*, pp. 1840–1843, 2020, doi: 10.1109/TENSYMP50017.2020.9230619.

[19] J. Lazaro, N. Reljin, Y. Noh, P. Laguna, and K. H. Chon, “Feasibility of Long-Term Daily Life Electrocardiogram Monitoring Based on a Wearable Armband Device,” *Proc. Annu. Int. Conf. IEEE Eng. Med. Biol. Soc. EMBS*, pp. 4314–4317, 2019, doi: 10.1109/EMBC.2019.8857219.

[20] Y. Tada, Y. Amano, T. Sato, S. Saito, and M. Inoue, “A smart shirt made with conductive ink and conductive foam for the measurement of electrocardiogram signals with unipolar precordial leads,” *Fibers*, vol. 3, no. 4, pp. 463–477, 2015, doi: 10.3390/fib3040463.

[21] A. Boehm, X. Yu, W. Neu, S. Leonhardt, and D. Teichmann, “A novel 12-lead ECG T-shirt with active electrodes,” *Electron.*, vol. 5, no. 4, 2016, doi: 10.3390/electronics5040075.

[22] C. Steinberg *et al.*, “A novelwearable device for continuous ambulatory ECG recording: Proof of concept and assessment of signal quality,” *Biosensors*, vol. 9, no. 1, pp. 1–13, 2019, doi: 10.3390/bios9010017.

[23] W. Y. Lin, H. L. Ke, W. C. Chou, P. C. Chang, T. H. Tsai, and M. Y. Lee, “Realization and technology acceptance test of a wearable cardiac health monitoring and early warning system with multi-channel MCGs and ECG,” *Sensors (Switzerland)*, vol. 18, no. 10, 2018, doi: 10.3390/s18103538.

[24] M. P. Turakhia *et al.*, “Rationale and design of a large-scale, app-based study to identify cardiac arrhythmias using a smartwatch: The Apple Heart Study,” *Am. Heart J.*, vol. 207, pp. 66–75, 2019, doi: 10.1016/j.ahj.2018.09.002.

[25] D. Fuller *et al.*, “Using machine learning methods to predict physical activity types with Apple Watch and Fitbit data using indirect calorimetry as the criterion.,” pp. 1–16, 2020, doi: 10.21203/rs.3.rs-17022/v1.

[26] A. Samol, K. Bischoff, B. Luani, D. Pascut, M. Wiemer, and S. Kaese, “Recording of bipolar multichannel ECGs by a smartwatch: Modern ECG diagnostic 100 years after Einthoven,” *Sensors (Switzerland)*, vol. 19, no. 13, 2019, doi: 10.3390/s19132894.

[27] N. Isakadze and S. S. Martin, “How useful is the smartwatch ECG?,” *Trends Cardiovasc. Med.*, vol. 30, no. 7, pp. 442–448, 2020, doi: 10.1016/j.tcm.2019.10.010.

[28] M. Strik *et al.*, “Validating QT-Interval measurement using the apple watch ecg to enable remote monitoring during the COVID-19 pandemic,” *Circulation*, vol. 142, no. 4, pp. 416–418, 2020, doi: 10.1161/CIRCULATIONAHA.120.048253.

[29] I. L. Goldenthal *et al.*, “Recurrent atrial fibrillation/flutter detection after ablation or cardioversion using the AliveCor KardiaMobile device: iHEART results,” *J. Cardiovasc. Electrophysiol.*, vol. 30, no. 11, pp. 2220–2228, 2019, doi: 10.1111/jce.14160.

[30] M. Karacan, “Validation of a smartphone based electrocardiography in the screening of QT intervals in children,” *North. Clin. Istanbul*, vol. 6, no. 1, pp. 48–52, 2018, doi: 10.14744/nci.2018.44452.

[31] J. M. Bumgarner *et al.*, “Smartwatch Algorithm for Automated Detection of Atrial Fibrillation,” *J. Am. Coll. Cardiol.*, vol. 71, no. 21, pp. 2381–2388, 2018, doi: 10.1016/j.jacc.2018.03.003.

[32] V. Randazzo, J. Ferretti, and E. Pasero, “A wearable smart device to monitor multiple vital parameters—VITAL ECG,” *Electron.*, vol. 9, no. 2, pp. 1–13, 2020, doi: 10.3390/electronics9020300.

[33] S. S. Thomas *et al.*, “BioWatch - A wrist watch based signal acquisition system for physiological signals including blood pressure,” *2014 36th Annu. Int. Conf. IEEE Eng. Med. Biol. Soc. EMBC 2014*, pp. 2286–2289, 2014, doi: 10.1109/EMBC.2014.6944076.

[34] H. Lee *et al.*, “Toward all-day wearable health monitoring: An ultralow-power, reflective organic pulse oximetry sensing patch,” *Sci. Adv.*, vol. 4, no. 11, pp. 1–9, 2018, doi: 10.1126/sciadv.aas9530.

[35] B. R. Bloem *et al.*, “The Personalized Parkinson Project: Examining disease progression through broad biomarkers in early Parkinson’s disease,” *BMC Neurol.*, vol. 19, no. 1, 2019, doi: 10.1186/s12883-019-1394-3.

[36] J. Hernandez, D. McDuff, and R. W. Picard, “Biowatch: Estimation of heart and breathing rates from wrist motions,” *Proc. 2015 9th Int. Conf. Pervasive Comput. Technol. Heal. PervasiveHealth 2015*, pp. 169–176, 2015, doi: 10.4108/icst.pervasivehealth.2015.259064.

[37] A. Stojanova, S. Koceski, and N. Koceska, “Continuous Blood Pressure Monitoring as a Basis for Ambient Assisted Living (AAL) – Review of Methodologies and Devices,” *J. Med. Syst.*, vol. 43, no. 2, 2019, doi: 10.1007/s10916-018-1138-8.

[38] A. Chandrasekhar, C. S. Kim, M. Naji, K. Natarajan, J. O. Hahn, and R. Mukkamala, “Smartphone-based blood pressure monitoring via the oscillometric finger-pressing method,” *Sci. Transl. Med.*, vol. 10, no. 431, pp. 1–12, 2018, doi: 10.1126/scitranslmed.aap8674.

[39] Q. Zhang, D. Zhou, and X. Zeng, “Highly wearable cuff-less blood pressure and heart rate monitoring with single-arm electrocardiogram and photoplethysmogram signals,” *Biomed. Eng. Online*, vol. 16, no. 1, pp. 1–20, 2017, doi: 10.1186/s12938-017-0317-z.

[40] J. H. Moon, M. K. Kang, C. E. Choi, J. Min, H. Y. Lee, and S. Lim, “Validation of a wearable cuff-less wristwatch-type blood pressure monitoring device,” *Sci. Rep.*, vol. 10, no. 1, pp. 1–9, 2020, doi: 10.1038/s41598-020-75892-y.

[41] H. Lin, W. Xu, N. Guan, D. Ji, Y. Wei, and W. Yi, “Continuous Blood.”

[42] Q. Zhang, X. Zeng, W. Hu, and D. Zhou, “A Machine Learning-Empowered System for Long-Term Motion-Tolerant Wearable Monitoring of Blood Pressure and Heart Rate with Ear-ECG/PPG,” *IEEE Access*, vol. 5, pp. 10547–10561, 2017, doi: 10.1109/ACCESS.2017.2707472.

[43] A. M. Carek, J. Conant, A. Joshi, H. Kang, and O. T. Inan, "SeismoWatch," *Proc. ACM Interactive, Mobile, Wearable Ubiquitous Technol.*, vol. 1, no. 3, pp. 1–16, 2017, doi: 10.1145/3130905.

[44] S. S. Thomas, V. Nathan, C. Zong, K. Soundarapandian, X. Shi, and R. Jafari, "BioWatch: A Noninvasive Wrist-Based Blood Pressure Monitor That Incorporates Training Techniques for Posture and Subject Variability," *IEEE J. Biomed. Heal. Informatics*, vol. 20, no. 5, pp. 1291–1300, 2016, doi: 10.1109/JBHI.2015.2458779.

[45] J. P. Sirkia, T. Panula, and M. Kaisti, "Multi-Wavelength Photoplethysmography Device for the Measurement of Pulse Transit Time in the Skin Microvasculature," *Comput. Cardiol. (2010).*, vol. 2020-Septe, 2020, doi: 10.22489/CinC.2020.179.

[46] P. Yousefian *et al.*, "The Potential of Wearable Limb Ballistocardiogram in Blood Pressure Monitoring via Pulse Transit Time," *Sci. Rep.*, vol. 9, no. 1, pp. 1–11, 2019, doi: 10.1038/s41598-019-46936-9.

[47] V. P. Rachim and W. Y. Chung, "Multimodal Wrist Biosensor for Wearable Cuff-less Blood Pressure Monitoring System," *Sci. Rep.*, vol. 9, no. 1, pp. 1–9, 2019, doi: 10.1038/s41598-019-44348-3.

[48] B. Ibrahim and R. Jafari, "Cuffless Blood Pressure Monitoring from an Array of Wrist Bio-impedance Sensors using Subject-Specific Regression Models: Proof of Concept," *IEEE Trans. Biomed. Circuits Syst.*, vol. 13, no. 6, pp. 1723–1735, 2019, doi: 10.1109/TBCAS.2019.2946661.

[49] T. W. Wang and S. F. Lin, "Wearable piezoelectric-based system for continuous beat-to-beat blood pressure measurement," *Sensors (Switzerland)*, vol. 20, no. 3, pp. 1–12, 2020, doi: 10.3390/s20030851.

[50] T. Arakawa, "Recent research and developing trends of wearable sensors for detecting blood pressure," *Sensors (Switzerland)*, vol. 18, no. 9, 2018, doi: 10.3390/s18092772.

[51] J. Nawrocki *et al.*, "Validation of a Portable Blood Gas Analyzer for Use in Challenging Field Conditions at High Altitude," *Front. Physiol.*, vol. 11, no. January, pp. 1–6, 2021, doi: 10.3389/fphys.2020.600551.

[52] M. Kramer, A. Lobbestael, E. Barten, J. Eian, and G. Rausch, "Wearable pulse oximetry measurements on the torso, arms, and legs: A proof of concept," *Mil. Med.*, vol. 182, pp. 92–98, 2017, doi: 10.7205/MILMED-D-16-00129.

[53] P. Singh, F. Shaik, P. Eunice, I. Luther, R. S. Deepthi, and Y. A. Nath, "A Novel Method for

Monitoring SpO2 in Wearable Health Monitoring Applications," *Int. J. Eng. Adv. Technol.*, vol. 9, no. 1S5, pp. 272–274, 2019, doi: 10.35940/ijeat.a1043.1291s52019.

[54] Y. Zhang *et al.*, "Poster abstract: Breathing disorder detection using wearable electrocardiogram and oxygen saturation," *SenSys 2018 - Proc. 16th Conf. Embed. Networked Sens. Syst.*, pp. 313–314, 2018, doi: 10.1145/3274783.3275159.

[55] M. Peng, S. A. Imtiaz, and E. Rodriguez-Villegas, "Pulse oximetry in the neck - A proof of concept," *Proc. Annu. Int. Conf. IEEE Eng. Med. Biol. Soc. EMBS*, pp. 877–880, 2017, doi: 10.1109/EMBC.2017.8036964.

[56] T. E. Morey, M. J. Rice, T. Vasilopoulos, D. M. Dennis, and R. J. Melker, "Feasibility and accuracy of nasal alar pulse oximetry," *Br. J. Anaesth.*, vol. 112, no. 6, pp. 1109–1114, 2014, doi: 10.1093/bja/aeu095.

[57] S. Seifi, A. Khatony, G. Moradi, A. Abdi, and F. Najafi, "Accuracy of pulse oximetry in detection of oxygen saturation in patients admitted to the intensive care unit of heart surgery: Comparison of finger, toe, forehead and earlobe probes," *BMC Nurs.*, vol. 17, no. 1, pp. 1–8, 2018, doi: 10.1186/s12912-018-0283-1.

[58] O. Senn, C. F. Clarenbach, V. Kaplan, M. Maggiorini, and K. E. Bloch, "Monitoring carbon dioxide tension and arterial oxygen saturation by a single earlobe sensor in patients with critical illness or sleep apnea," *Chest*, vol. 128, no. 3, pp. 1291–1296, 2005, doi: 10.1378/chest.128.3.1291.

[59] G. Tajkia, M. Shirin, M. M. Hossain, and M. A. A. Mamun, "Accuracy of SpO2 measurements by placing probes on newborns' wrist and ankle," *Bangladesh Med. Res. Counc. Bull.*, vol. 45, no. 3, pp. 191–196, 2019, doi: 10.3329/BMRCB.V45I3.44651.

[60] R. R. Adiputra, S. Hadiyoso, and Y. Sun Hariyani, "Internet of things: Low cost and wearable SpO2 device for health monitoring," *Int. J. Electr. Comput. Eng.*, vol. 8, no. 2, pp. 939–945, 2018, doi: 10.11591/ijece.v8i2.pp939-945.

[61] A. T. Ayance, H. S. Ramírez, J. M. R. Pérez, and C. G. T. Palacios, "Wireless heart rate and oxygen saturation monitor," *AIP Conf. Proc.*, vol. 2090, no. April, pp. 1–5, 2019, doi: 10.1063/1.5095913.

[62] P. P. Banik, S. Hossain, T. H. Kwon, H. Kim, and K. D. Kim, "Development of a wearable reflection-type pulse oximeter system to acquire clean ppg signals and measure pulse rate and spo2 with and without finger motion," *Electron.*, vol. 9, no. 11, pp. 1–26, 2020, doi: 10.3390/electronics9111905.

[63] M. Niswar, M. Nur, A. A. Ilham, and I. Mappangara, "A low cost wearable medical device for vital

signs monitoring in low-resource settings," *Int. J. Electr. Comput. Eng.*, vol. 9, no. 4, pp. 2321–2327, 2019, doi: 10.11591/ijece.v9i4.pp2321-2327.

[64] C. Phillips, D. Liaqat, M. Gabel, and E. De Lara, "WristO2: Reliable Peripheral Oxygen Saturation Readings from Wrist-Worn Pulse Oximeters," *2021 IEEE Int. Conf. Pervasive Comput. Commun. Work. other Affil. Events, PerCom Work. 2021*, pp. 623–629, 2021, doi: 10.1109/PerComWorkshops51409.2021.9430986.

[65] A. F. P. Aleixo, E. G. Lima, É. C. Leite, A. V. M. Inocêncio, L. T. Lins, and M. A. B. Rodrigues, *Wearable device for acquisition of spo2 and Heart Rate*, vol. 70, no. 1. Springer Singapore, 2019.

[66] A. Guber, G. Epstein Shochet, S. Kohn, and D. Shitrit, "Wrist-Sensor Pulse Oximeter Enables Prolonged Patient Monitoring in Chronic Lung Diseases," *J. Med. Syst.*, vol. 43, no. 7, 2019, doi: 10.1007/s10916-019-1317-2.

[67] G. Pang and C. Ma, "A Neo-Reflective Wrist Pulse Oximeter," *IEEE Access*, vol. 2, pp. 1562–1567, 2014, doi: 10.1109/ACCESS.2014.2382179.

[68] D. Jarchi, D. Salvi, C. Velardo, A. Mahdi, L. Tarassenko, and D. A. Clifton, "Estimation of HRV and SpO2 from wrist-worn commercial sensors for clinical settings," *2018 IEEE 15th Int. Conf. Wearable Implant. Body Sens. Networks, BSN 2018*, vol. 2018-Janua, no. March, pp. 144–147, 2018, doi: 10.1109/BSN.2018.8329679.

[69] Rijk Schildmeijer, Paul Suijkrbuijk, "Six Sigma in practice", 2020 Published by The Lean Six Sigma Company.

Acknowledgements

I would like to thank Prof. Andrea Fausto Piana for his assistance at every stage of the research project and for his insightful comments and suggestions.

I would like to thank Ing. Leonardo Fiore for his ideas and contribution in finalizing this work, for his tireless enthusiasm and for believing in me.

I would like to extend my sincere thanks to Dr. Pierfranco Terrosu for offering his time and his precious experience in order to produce valuable data and statistics which I used in my project.

I would like to thank Dr. Sonia Albanese for her contribution to the project and for her patience in explaining medical concepts to me.

I would like to express my sincere gratitude to Marcella Angei, Giulia Bottoni, Annalisa Minoia, Leonardo Napoli, Domenico Ruggieri, Valentina Lopez Suarez for their contribution to this project and their brilliant ideas. Working with them made everything better!

I am deeply grateful to my colleagues Gianluca Ara, Mariangela Chighine, Antonello Codinas, Gianni Demelas, Matteo Fadda, Leonardo Fiore, Francesco Marino, Francesca Masala, Leonardo Napoli, Domenico Ruggieri, Alessia Salis, Chiara Sanna, Valentina Lopez Suarez, Grazia Stara, Alessandra Tiloca for their contribution to the research and for their enthusiastic approach to the project.

I would like to thank as usual, my husband, my family and my friends for their unwavering support and belief in me.